CARBON OXIDATION REACTIONS AT HIGH TEMPERATURES.

A Thesis submitted for the degree of

DOCTOR OF PHILOSOPHY

in the University of London

by

JULIAN ROBERT EGERTON. M.Sc

Department of Chemical Engineering and
Chemical Technology,
Imperial College of Science and Technology,
London, S.W.7.

April, 1968.

ABSTRACT.

A study of the reaction of oxygen with pyrolytic carbon filaments at 50μ pressure showed a well defined maximum in the rate and the hysterecis effect, in the temperature range 900-2000°C. The hysteresis changed sense at high temperatures, about 1500°C, giving hysteresis above in the same sense as found earlier at 0.76μ. This change over in the hysteresis was shown to occur at lower temperatures for lower pressures. It was also shown that differences in the quantities of carbon reacted and in filaments used were not responsible for different hysteresis effects observed previously.

The Nagle Strickland-Constable theory was found to give a considerably better prediction of the maximum and minimum if account was taken of the variation of active sites as found by the hysteresis results. A simple mechanism is proposed based on annealing and creation of active sites which gives a good fit to the hysteresis data at 50 and 0.76μ.

Reaction in N_2O was not found to affect subsequent reaction in O_2 and vice versa, suggesting different active sites are involved.

Various additives were added to the filament. Boron and Silicon were found to be without effect, while Fe, W, Zr, U, Mo and Pt all catalysed the reaction. The basic mechanism of the reaction did not appear to be changed fundamentally by catalysis, maxima in the rates still being evident. There was also a strong suggestion of hysteresis.

The oxygen balances suggested in most cases that lower oxides still existed on the surface, but at the carbon-metal interface it was thought likely free metal or carbides were the active agents. The experimental evidence strongly suggests an electronic mode of catalysis.

ACKNOWLEDGEMENTS.

The author wishes to thank Dr.R.F.Strickland-Constable for his invaluable supervision and advice throughout this research, and Professor R.V.H.Sargent, and his predecessor Professor K.G.Denbigh in whose Department the work was carried out.

During this work the author has been supported by the Courtauls Trust Fund and the United Kingdom Atomic Energy Authority, Harwell, for which he is very grateful, particularly to the latter who also supplied an apparatus grant.

CONTENTS.

NOMENCLATURE.

UNTREATED FILAMENT: Carbon filament, coated with pyrolytic carbon but not treated with any additive.

TREATED FILAMENT: Carbon filament to which an impurity has deliberately added.

COATED FILAMENT: A filament coated with pyrolytic carbon.

LOW SENSE HYSTERESIS: Hysteresis effect such that reaction at a lower temperature, following reaction at a higher temperature, gives initially low rates of reaction, and visa versa.

HIGH SENSE HYSTERESIS: Hysteresis effect such that reaction at a lower temperature, following reaction at a higher temperature, gives initially high rates of reaction, and visa versa.

Where the letter A appears in a Graph or Table number, the relevant Graph or Table will be found in the Appendices. The first numeral, in a Graph or Table number, gives the relevant Section or Appendix.

D.L. Detection limit for Spectrographic analysis.

E. Activation Energy.

F. Frequency of reaction, as defined by Duval[3].

K. Reaction rate constant.

Oxygen Balance. % oxygen balance, as defined in Appendix 1.

P. Pressure.

R. Rate of rection. g. atoms of carbon cm^{-2}. sec^{-1}. based on geometric area.

μ. Pressure in microns of Hg. $1\mu = 10^{-3}$ mm. Hg.

Symbols used in Section 6.

A. site, B. site } Fast reaction sites.

C. site Slow reaction sites.

A/B. Either A or B site without discrimination.

n. Number of A+B sites (cm^{-2})

N. Constant 'related' to max. number of C sites.

r. (Rate of reaction)/(No. of A and B sites.) = $\frac{R}{n}$

f. $F/_n$

1. INTRODUCTION.

From the technical point of view carbon is finding increasing use as a construction material because of its good mechanical properties at elevated temperatures. Two important examples of the present use of carbon are in nuclear piles and for re-entry cones for space vehicles. Two main factors limit the upper temperature at which carbon can be used. The first is the increasing amount of chemical attack at high temperatures, and this is the subject of this work. The second, which has more relevance in the space programme, is that of mechanical erosion.

The carbon oxidation reactions are also of considerable theoretical interest, since it is one of the few reactions in which a gas reacts with a solid to give gaseous products and also to show a maximum in the variation of the rate of reaction with temperature. Recently it has been shown that tungsten and molybdenum show this same effect.[1].

Considerable work has been carried out previously on the effects of catalysts on the oxidation of graphites but almost all this previous work was limited to below 1000°C. The mechanism of the carbon oxidation reactions differ below 1000°C and above 1000°C where the rate shows a maximum. Part of the present work was carried out to see if various additives had any effect on the high temperature reactions. Filaments treated with additives will be described hereon as TREATED.

In previous studies of high temperature oxidation of carbon at low pressures so as to eliminate the effect of diffusion, not only has a maximum in the rate been found but also a hysteresis effect, such that for reaction at one temperature, following reaction at a lower or higher temperature, the rate was initially lower or higher than the final steady value. This hysteresis was found by Strickland-Constable [2] and Duval [3], but these two authors found opposite hysteresis effects for oxygen. The second part of this work was carried out to try and elucidate the apparent contradictions in these previous results.

2. REVIEW OF LITERATURE.

The literature on aspects of carbon now covers a very wide field ranging from electronic, through chemical to purely mechanical properties. As far as possible in this review the literature has been subdivided into separate sections.

2.1. Previous Filament Work.

Following the pioneer work of Langmuir [4] whose results were largely governed by the amount of oxygen adsorbed, Meyer et al [5,6,7] using a flow system found the reaction with oxygen followed two paths. The first region up to 1300°C where a maximum in the rate was evident consisted of a 1st order reaction with a CO_2/CO ratio of 1. In this region the postulated mechanism involved dissolved oxygen. Evidence to support this included change of electrical resistance of the filament, direct adsorption measurements, and analysis of electron diffraction diagrams[8]. The second region above 1500°C gave a zero order reaction with a CO_2/CO ratio of 0.5 and a Eucken [9] type mechanism based on the simultaneous adsorption of two O_2 molecules at edge atoms was assumed. It was also Eucken who first suggested that the maximum in the rate was caused by atomic rearrangement removing active edge atoms.

Strickland-Constable [2] using a static system at

about 30μ pressure found a 1st order reaction between 900°C and 2000°C with a maximum in rate at about 1150°C and the reaction was found insensitive to small quantities of impurities. No oxygen adsorption by the actual filament was found and the adsorption found by Langmuir and Meyer was attributed to absorption by the filament mounts. Other experiments showed that a zero order reaction took place when a thermionic glow discharge was present. Arthur[10] further confirmed the effect of glow discharge which was found to be associated with the secondary reaction $CO \rightarrow CO_2$. Maxima in the rates were also found by Strickland-Constable[11] for CO_2, N_2O and water vapour, with 1st order reactions above 1200°C and a tendency for fractional orders below.

The results of Duval [3] who used a flow system at 0.76μ agreed in large with those of Strickland-Constable although the order of reaction was found to be greater than one at intermediate temperatures. Using a thermionic emission technique the negligible adsorption of oxygen was confirmed. In this context Duval attributed the spread of the carbon network spacing, seen on diffraction patterns, under the action of oxygen to a decrease of crystalline fit under combustion. Duval also confirmed the effect of glow discharge which was thought to be due to mercury vapour.

In the works cited Strickland-Constable found a

hysteresis effect whereby the past history of the filament governed the reaction rate. In oxygen this hysteresis was in the high sense (see table of nomenclature), while for N_2O and H_2O it was in the opposite direction. These results and the maximum in the rate were explained qualitatively by Strickland-Constable in terms of two active sites. Only one of these sites, associated with carbon edge atoms, was considered to take part in the N_2O, CO_2 and H_2O reactions. Above 1200°C these sites were assumed to anneal out and the rate therefore started to decrease. The hysteresis effect for N_2O and H_2O being due to low temperature reaction forming fresh edges which temporarily increased the reactivity for subsequent reaction at high temperatures. On the other hand annealing of sites at high temperatures made the graphite less reactive.

To explain the oxygen results the participation of two sites was considered. At low temperatures although the reaction would be principally with the more active edge atoms, reaction would also occur by direct attack on the basal plane resulting in the formation of more edges. As for the other gases above 1200°C annealing of the active edges takes place so that by 1800°C the reaction occurs principally on the faces, which produces a large number of edges. If the temperature is lowered, edge reaction will take place at an increasing rate owing to the increased

number of edges available which more than compensate for the fact that the edges were annealed. The fact that the filament burnt black in oxygen was taken by Strickland-Constable to support the idea of attack on the basal planes.

Duval[3] also found pressure hysteresis effects in oxygen, but at his pressures the temperature hysteresis worked in the low sense, which is opposite to Strickland-Constable's results. Boulangier [12] also found hysteresis for CO_2 and H_2O to be in the low sense, ans for all three gases at near 0.76μ it was found a steady rate was achieved after a burn off of about 3 x10^{-7} gr atoms of carbon per cm^2 of geometric area. The ratio of the true area to the geometric area for O_2, CO_2 and H_2O was found to be 25, 100 and 40.

The explanation used by Duval to explain his oxygen results is in essence that given earlier to explain the N_2O hysteresis. It was found that the measured rate F could be related to the number of sites, s, and the fundamental rate on each site f; this latter factor being constant with time for constant temperature and pressure. The relationship was simply

$$F = sf.$$

The hysteresis is supposed to be caused by variation in s going from one temperature to another. Using this expression Duval obtained experimental curves for f and the

steady values of s with temperature.

Rosner et al[13] found the rate with atomic oxygen to be between 5 and 50 times greater than for O_2 with a shift in the maximum to 1600°K at 1 torr. The reaction with atomic oxygen was found to be less temperature dependent and of 1st order, compared with 0.56 order for O_2. These results, however, were possibly catalysed by the tungsten contacts pressing on the hot filament.

2.2. Other High Temperature Results.

A considerable number of the studies of high temperature oxidation were in the region of diffusion control and as a result no maximum was observed. Nagle [14] eliminated this factor by using high speed impinging oxygen at 0.23 atm. and he found that the maximum in the rate was shifted up to 2000°C with a zero order reaction below this temperature. Pyrolytic carbon was found to react about 9 times slower than reactor grade. A similar shift in the maximum was found for CO_2 by Walls [15] who also found the reaction order with oxygen to be greater than zero at very high temperatures. The rate of reaction with CO_2 was again not found to be so great as for oxygen.

Since diamond does not have the layer structure of graphite it is interesting that Evans et al [16] found a maximum in the rate at 1050°C for reaction in 0.4 mm Hg of O_2.

The diamonds initially gave low rates when new which rapidly increased to a constant value. Also hysteresis in the high sense, which is the same as the oxygen results at 50μ, was found for reaction at low temperatures after reaction at high temperatures. The importance of this work is that it shows that reaction can occur elsewhere from the edge atoms of graphite as was postulated by Strickland-Constable.

2.3. Secondary Reactions and Effect of Preheating.

Meyer[8] suggested that the differences between his results and those of later workers were due to preheating of the oxygen and secondary reactions in the micropores on the surface. With incomplete accommodation of the attacking molecules they attack several times before reaction and thereby become preheated. The lower rate of the first order reaction observed by Strickland-Constable was taken to occur by a small number of molecules trapped in micropores. Similarly reaction products hit the filament several times, in pores, or because of a static system, leading to a postulated secondary reaction converting the CO_2 to CO. Meyer [17] used his results on the decomposition of methane below 15μ to support this supposition. No decomposition was found unless the surface was first roughened, allowing the gas to be preheated in the micropores.

However, as argued by Strickland-Constable[18] for a difference in pressure of 300 times, the number of molecules

striking the surface will be considerably greater, as will be gas collisions, giving a considerable increase in gas temperature. But since the rate constant is the same it is necessary to conclude that it is independent of gas temperature and the accommodation coefficient is near unity. No effect was found by Bangham [19] for preheating between 0 and 800°C for the gasification of carbons by high velocity jets of air.

The fact that the rate of reaction with CO_2 [11,12] is less than the rate with oxygen, that Duval used a flow system to eliminate secondary reactions and still obtained predominantly CO, and that Strickland-Constable found no difference in the CO_2 produced if a cold trap was in place on the reactor are all inconsistent with Meyer's postulate. Duval attributed the larger amounts of CO_2 found by Meyer to catalytic oxidation on the Pt support wires used; a fact that glow discharge cannot explain at low temperatures.

2.4. Quantitative Theories.

(1) The first theory postulating two sites for reaction was due to Eyring et al [20]. The two sites were considered to be different types of edge atoms, one of which was associated with some type of impurity which catalysed the low temperature reaction. The processes taking part included the conversion of one site to another by reaction

and by annealing; the sum of the two sites however remaining constant with pressure and temperature. The kinetic expressions were arranged to give a zero order reaction at high temperatures, and to fit the results it was necessary to assume the relative numbers of the two sites to be independent of pressure. The theory does not therefore explain the first order reactions at high temperatures; nor explain the shift in maximum with pressure.

(2) Nagle and Strickland-Constable[19] modified Eyring's theory taking into account a first order reaction at high temperatures. [This is hereafter referred to as the Nagle theory]. The physical basis of the theory is that at high temperatures carbon atoms can migrate to heal the surface, which would otherwise be fairly reactive.

There are assumed to be two kinds of sites on the surface, reactive A sites and less reactive B sites. If x is the fraction of the surface covered by A and (1-x) the fraction covered by B, the following processes are assumed to take place.

1. Reaction of O_2 with A sites to give further A sites and 2CO; the rate being governed by a Langmuir isotherm and the oxide is formed by a first order reaction

$$\text{Rate of (1)} \quad \left[\frac{K_A P}{1 + K_T P} \right]$$

where K_A, K_T are appropriate constants.

2. O_2 reacts with B sites to give an A site + 2CO

with a first order reaction, in this case the rate $= K_B P\ (1 - x)$.

3. A sites can become B sites by thermal annealing at a rate $K_T x$. For stationary values of x

$$K_T x = K_B P\ (1 - x)$$

$$\therefore\ x = \frac{1}{1 + K_T/(K_B P)}$$

with overall rate $= \left(\frac{K_A P}{1 + K_Z P}\right) x + K_B P(1 - x)$

Besides giving a first order reaction at high temperatures for low pressures, the other main difference from Eyring's theory is that x is now pressure dependent. Strickland-Constable [21] has shown that this theory fits both high and low pressure results well, predicting the shift in the maximum with pressure and the variation of the order from greater than one at low pressures to zero at 0.23 atm. below 2100°K, and greater than zero above 2100°K as found by Walls[15].

In support of the possibility of annealing taking place at these temperatures Antonowicz[22] showed that heat treatment at 1500°C of neutron irradiated graphite caused all damage to the structure to be repaired. Polley[23] found graphitisation to start at 1500°K while Mizushima [24,25] studying the crystalline growth found two distinct mechanisms operated. The first, associated with self diffusion began to occur at 1400°C.

3. The latest theory is due to Ong[26] which differs from those mentioned in that it entails only one type of reaction site. The kinetics were examined from the standpoint of two primary reactions to produce CO and CO_2 and a secondary reaction to produce CO from CO_2. To fit Duval's results it was found necessary to assume that the rate controlling step was the secondary reaction and this gave a predicted maximum at 1100°K compared with an experimental value of 1300°K. It is not surprising that this theory does give a certain fit to the results considering the large number of rate constants involved, but even so the fit is not as good as predicted by the Nagle theory. As reviewed earlier it is difficult to see how the CO can be produced by a secondary reaction.

2.5. Nature of Active Sites.

In addition to the annealing theory already mentioned various other ideas on the nature of the ative sites have been proposed. These are dealt with in this section together with related topics.

Strickland-Constable, as stated, put forward the view that O_2 reacted with different sites to other oxidising gases. A similar view is fowarded by Long et al [27] who suggested that H_2O and CO_2 react predominantly with different parts of the surface since reaction of steam is retarded by H_2O while that of CO_2, only, by CO and H_2.

2.5.1. Variation of area with reaction.

Hennig[28] working on single crystals found no relationship between the B.E.T. area and rate of oxygen attack below 1000°C, a result supported by Deitz[29] although he found a slight decrease could follow extensive oxidation. Similarly Duval[3] and Boulangier[12] found the B.E.T. area constant for reaction at various temperatures in different gases.

If as suggested by Duval the hysteresis effect is due to variation in the number of active sites, it is necessary to assume that the total number of these sites is small compared with the total B.E.T. area so the change is not detectable. Evidence to support this has been given by Laine et al[30] for oxidation between 300-875°C. By outgassing the complex formed at 950°C the total active surface area was estimated to be only 2.3% of the B.E.T. surface area.

2.5.2. Hydrogen impurity idea.

Eyring[20] suggested that one of the sites upon which high temperature reaction occurs was associated with hydrogen from only partially graphitised hydrocarbon material, which activates the low temperature reaction. Hennig[31] similarly suggested that the increase in reactivity at the same temperature where the Hall coefficient goes through a maximum can be traced to the removal of H_2.

Various authors[31,32,33] showed that H_2 and H_2O to be temporarily inhibitors between 430° and 700°C, but the effect has been suggested as due to reaction of the gases with catalytic impurities. Hennig[28] on the other hand found the H_2O catalysed the reaction on single crystals, the explanation here according to Duval[34] is that the water reacts with a different kind of impurity.

It is difficult to see how hydrogen can remain in graphitised filaments such as Meyer's[7], which were heated between 2500 and 3000°C, particularly as shown by Diefendorf[35] on degassing graphite that the H_2 content went through a peak below 1400°C; the outgassing being a function of time as well as temperature.

2.5.3. Impurity idea.

The idea of catalyst impurities[3,36] has been used to explain the maximum and hysteresis; the concentration of the catalyst being governed by diffusion from the centre of carbon and the rate of evaporation, the two processes having different thermal coefficents. The effect of oxygen pressure on the noticed shift in the maximum with pressure is explicable on the basis that the mean free path of evaporating atoms would be inversely proportional to the total gas pressure. At any temperature the surface concentration of impurity would be higher at higher pressures.

Heauchamp et al[37] suggested that impurities of a few ppm. accounted for the diminishing of the activation energy and CO/CO_2 ratio with burn off at 637°C. The reaction was assumed to occur on impurities and pure surface and as the ash builds up the reaction is subsequently catalysed more by impurity build up.

Heddon[38] explained the reversible and inhibition of the oxidation with CO_2 at low temperatures by halogen compounds by blocking of reaction sites, and elimination of impurities by production of volatile halides. A similar explanation was used by Palmer[39] to explain the effect of C Cl_2F_2 at 570°C with graphites containing V and Ti as impurities. In this the rate initially increased, thought due to reaction of CO_2 with impurities to form catalytic halides which later evaporated off giving normal results.

What the impurity idea does not explain as discussed by Duval[3] is how workers find rates of the same order using very different filaments, and how filaments find their reserve of impurities after long treatment at high temperatures. In this context Nagle[36] found polycrystalline graphite which contained about 10^3 times as much impurity as pyrolytic carbon followed the same general oxidation behaviour.

2.5.4. Pitting and defects.

Meyer[7] found that graphite was attacked at basal

planes such that hexagonal pits were formed below 1500°K, while above 1800°K reaction appeared to be by edge attack only. In a study on the air oxidation of pyrolytic carbons between 614 and 1580°C using cleaved discs Horton[96] found the edges oxidised about 2.5 times faster than basal planes, the rates appearing to increase with temperature. Blackman[40] found similar pitting at 1660°C but the oxidation on the basal plane appeared irregular and was thought to make very little contribution to the total burn off. Although the original sites of pits were thought to be explainable by impurities, the lateral extension of the pits could not be readily explained by catalytic oxidation alone. Lewis[225] found that auto radiographs showed that widely spaced pits on vitreous carbons did tend to coincide with impurity atoms.

In the presence of a suitable catalyst Hennig[42,43] found hexagonal pits were formed. At 650°C the pits were shallow getting progressively deeper with increasing temperature. At 1100°C no new pits were formed and those in existence ceased to deepen.

Hennig found that these pits were only produced if lattice defects, as well, were present. If crystals were heated to 2300°C pits were formed, but not if the crystals were quenched from 2700°C. Hennig[44] therefore proposed that at 2300°C the concentration of vacancy defects, which caused pitting, was large enough to be detected by catalytic

oxidation and yet their mobility was low so that they can anneal out only with difficulty. Above 2700°C some other defect, possibly interstitial, was supposed present in large enough concentrations to act as sinks for vacancies. Williamson[45] however found that the mobile defects at low temperatures were interstitials and that they condense with vacancies into sheets parallel to the basal plane; the vacancies beginning to diffuse about 1200°C.

Additional support to the idea that pitting occurred at defect was given by Fɒllet[46] who found pitting on the surface could be related to irradiation dose and temperature.

2.5.5. Spin centres.

Efforts have been made to relate the spin centres i.e. free radical centres, in carbon to the active sites participating in reaction. Spin centres have been found to be formed by direct chemical attack by Antonowicz[47] between 700 and 1100°C at high pressures. These spin centres were however removed by heating between 1000 and 1400°C[22]. Harker et al[48] on the other hand found that the spin centre concentration decreased with surface oxide formation. But it was not possible to say whether free radical centres are actually lost during reaction or merely converted to centres of a new type in which unpaired electrons are localised on

O atoms. In later work Harker et al[49] showed that not all spin centres were particularly reactive to oxygen probably due to resonance of unpaired electrons over several atoms, while production of CO_2 showed the same correlation as spin centres with heat treatment between 500 and 700°C.

The particular spin centres formed by reaction were shown by Mrozowski[50,51] to be strongly localised. Both he and Antonowicz[52] also considered a large proportion of these localised spin centres to be due to impurities. At high temperatures the evidence[52,53] tends to lead to the conclusion of the occurrence of a continuous change in the character of spin centres from localised character to a conduction metallic type solid.

2.6. Low Temperature Reaction.

Below 800°C the oxidation is characterised by high CO_2 formation and there is considerable evidence that surface oxides play a predominate part in the reaction; the most likely rate controlling step being the breakdown of surface complexes.

Several workers have found that the initial rate of reaction decreased with increasing burn off. Both Deitz et al[29] and Bonnetain et al[19] explained this, and the variation of the CO/CO_2 ratio in terms of surface heterogeneity and variations of the composition of the surface oxide. On the other hand Vastola et al[54] using a O^{18} tracer technique found that the

fraction of the total CO and CO_2 contributed by complex breakdown decreased with increasing temperature showing that reaction can occur independently of complex formation.

The particular relevance to our work is that all the above authors found that the Elovich equation applied to the desorption of the complex, which implies a hetereogeneous or induced hetereogeneous surface. In studying the chemisorption of O_2 on Graphon, Hart et al[55] found the amount adsorbed increased sharply above 250°C after oxidation suggesting at least two types of active sites. The Elovich equation has been found to be applicable as high as 1375°C for the desorption of hydrogen by Redmond[56].

2.7. Catalytic Work.

2.7.1. General.

Although a considerable amount of work has been

carried out on low temperature catalysis of the carbon oxidation reaction there is considerable debate on the mode of action of these catalysts. Various ideas have been put forward largely depending on whether a catalyst acts in a chemical or physical manner. The main ways in which it is thought catalysts act are:-

a). Intermediate Compound Formation[62]. In this case the catalyst accelerates the reaction through the alternate formation and decomposition between the catalyst and the reactants. For this to be valid the rate of formation and decomposition of the intermediate compound must be faster than the rate of the uncatalysed reaction, and that the compound must besufficiently unstable to decompose under reaction conditions.

b). Electronic Theory. In this case the catalyst accelerates the reaction by becoming a donor or acceptor of electrons weakening bonding for certain carbon-carbon bonds. Considerable work has been done with this approach to catalyst with particular reference to semi-conductors[59,64,63].

c). Dislocation or Disruptive Action of Catalyst. In many cases this mode of action is classified with the electronic approach but the action is somewhat different. In the electronic approach it is assumed that actual transfer of electrons occurs and the catalyst can act over a considerable distance. In the disruptive approach the

foreign atoms weakens bonds in its intermediate neighbourhood or decreases the compact state of the molecule.

2.7.2. Electronic approach.

Following work on the catalysts of the CO_2 and steam reaction with carbon at 750°C Long and Sykes[57] put forward the theory that the catalyst altered the bonding on edge carbon atoms upon which oxygen was adsorbed. For adsorbed oxygen the bondings shown in Fig.2.1 were considered.

The evolution of CO could be faciltated if the C-C bond was first weakened as occurs if the distribution becomes like (b) by transfer of electrons to a transition metal ion, or like (c) by formation of a covalent bond with an alkali metal atom. The direction of changes in bond order produced by the removal or addition of electrons is determined by the fact that oxygen is more electro -ve than carbon; a +ve charge will give (b), whereas a -ve charge will be more stable on oxygen as in (d). Calculation of bond strengths showed the variations to be of significant order of magnitude[58].

The ability of the transitional metals to accept rather than denote electrons was postulated to be due to non-stoichiometric p-type[59] oxides on the surface. More easily reduced compounds of non transitional elements should be inhibitors if they transfer electrons completely to the carbon since a distribution of type (d) would be favoured. However

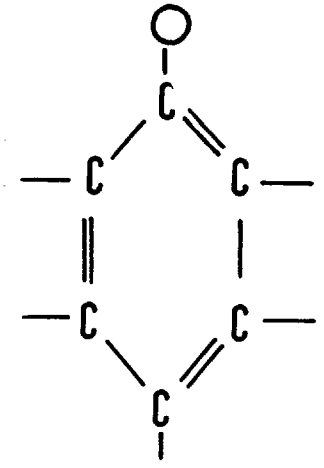

(a)

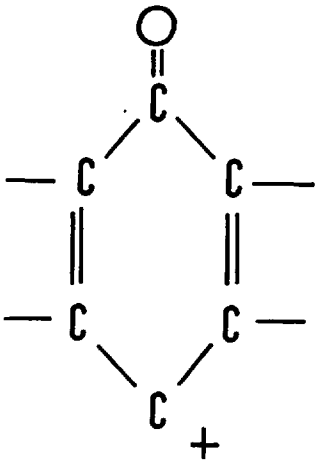

(b)

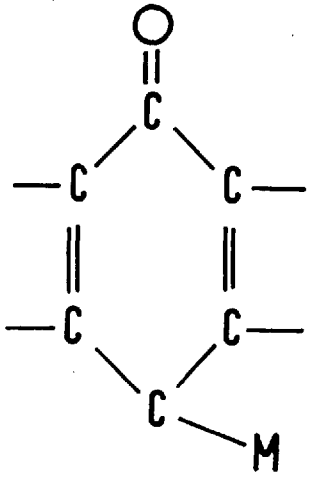

(c)

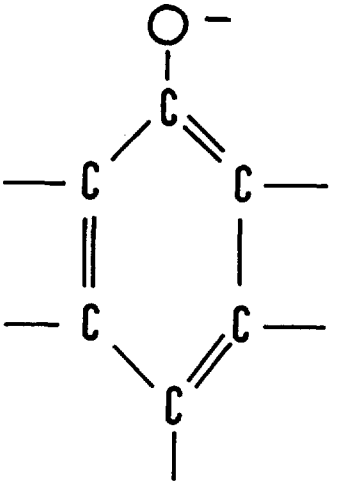

(d)

FIG. 2.1 Long and Sykes (57) distribution of bonds.

they could form a bond type (c) which would account for why catalyst is much more common than inhibition. The mechanism for the catalytic action of alkali metals was thought to be due, by Long and Sykes, to the formation of covalent bonds with the carbon lattice at points of high electron density giving (c).

Long and Sykes found that the general form of reaction mechanism and number of active sites did not change for the catalysed reaction which lends support to their electronic view of catalysis.

Other work which supported the electron view was put forward by Heintz et al[60] who studied the oxidation between 600 and 700°C in the presence of 0.1 mole % of transition and inner transition metals. It was not found possible to correlate the catalytic effect with activation energy.

Their results were analysed in terms of the Long and Sykes model with deficit oxides formed. Minimum activation energies were found for the (n-1) d electron bonds in which 0, 5 and 10 electrons impart unusual stabilities to the divalent state and do not bond actively. Metals which have d^2, d^3, d^7 or d^8 configurations are active π bonding elements because of their strong ability to attain d^5 or d^{10} configurations by denoting electrons, hence giving structure (d). These metals were found to be inhibitors or showed only slight effect.

However the metals whose oxides exert a large vapour pressure at the temperature of reaction were found to be catalysts, the volatility of the oxide appearing of greater importance than π bonding; for example Va, W and Mo. It is interesting to note that Heintz found W, Ni, Ta, Ti, Fe and Nb all inhibited the reaction at 600°C while out of these only Ta inhibited at 700°C. This temperature dependence suggests that the actual composition of the additive on the surface is important.

Finally Rakszawski et al[63] using additives blended with graphite powder found the systematic variation of rates appears to follow the diagonals of the periodic relationship of the elements from the upper left to lower right. A correlation was found between these rates and the average ionisation energy or electron affinity such that the rate increased with increasing ionisation energy to produce maximum positive oxidation state.

2.7.3. Intermediate Compound Approach.

One fact that the electronic theory does not explain satisfactorily is how many non-transitional elements catalyse the oxidation reaction[65]. Amariglio[66] incorporated metal catalyst by impregnation and used the ignition temperature technique so that only the catalysed reaction was taking place. Pb, Mn and Hg were all found to be very good catalysts.

Metals which showed any catalytic effect were able to exist between two degrees of oxidation under reaction conditions, while metals with stable oxides showed no effect. The general variation of catalytic effect and constancy of activation energy with impurity level were thought to be in agreement with localised action of impurities.

Amariglio analysed his results in terms of Kobozev theory of ensembles, a review of which is given by Toplin[67]. Kobozev regarded the activity to be centred in microfissures, which can be considered as grain boundaries, where the catalyst tends to accumulate. Inherent within the theory is that there is an optimum size of the impurity particle for effective catalysis. Thomas[68] also found that there existed an optimum concentration of B_2O_3 for effective catalysis in wet oxygen.

Further support for this idea was given by Hennig[69, 42]. If metals were evaporated, sputtered or deposited from solution they appeared to increase the burning rate only when they aggregated. On the other hand colloids appeared to become less active on aggregation. In both cases catalyst only occurred at the metal carbon interface[70]. Colloidal particles were also shown by Hennig, and later Thomas[65], to move along the surface in channels in the absence of defects, the explanation being in terms of attractive forces at the leading surface of the catalytic particle where reaction occurs.

As discused in section 2.5.3 halogens inhibit oxidation. In this field Mukuibo et al[71] reacted graphites containing 400 ppm Va and no Va with CO_2 containing I_2. The effect of I_2 was negligible on the pure graphite, but on the treated graphite the rate decreased until it approached, asymptotically, the rate for pure graphite. At this stage the graphite still contained 200 ppm of Va. This indicated that only part of the Va was active which was taken to be on the surface since that was easily gasified by I_2. The inner part not being catalytic suggested to Mukuibo that the electronic mechanism was not applicable.

2.7.4. Effect of catalyst composition.

In addition to work already cited several other workers in addition to finding that substances with stable oxides were inefficient catalysts also found that the exact form of the catalyst after various heat treatments and outgassing procedures, altered in activity. This effect can be interpreted by the electronic theory in that a deficit oxide is needed to accept electrons for good activity, or on the intermediate theory in that the oxide must be only quasi stable to allow rapid interchange of its oxygen.

Rakozawski[72] studying the catalysis of the CO_2 reaction at low temperatures found that heat treatments between 1400 and 1635^{o}C did not result in loss of iron but did sharply

reduce the catalysis. The activity could be restored by secondary preheat treatments in H_2 or O_2 prior to reaction. The catalytic efficiency tended to increase with decreasing particle size.

The results were explained on the basis of Fe being active while FeC was non-active. Two counter balancing mechanisms were used to relate the Fe/FeC concentration. Firstly at low temperatures carbon was removed from FeC to make it active. Secondly reaction of CO_2 with iron surface to form an oxide barrier to outward diffusion of carbon and prevent removal of carbon from the iron by reaction with CO_2.

Gallagher et al[73] studied both the oxygen reaction below 550°C and the CO_2 reaction between 700 and 800°C with iron, cobalt and nickel catalysts. They found that different catalysts were effective for the different reactions. For the oxidation reaction Fe_2O_3 and Fe_3O_4 which are n type semiconductors were inefficient while FeO which is of p type was very effective. On the other hand Fe_2O_3 and Fe_3O_4 were very effective for the CO_2 reaction. The authors suggested that at higher temperature the mechanism depended on the liberation of free metal which becomes incorporated into the graphite.

3. APPARATUS AND EXPERIMENTAL PROCEDURE.

3.1. Apparatus.

The reasons for using carbon filaments at low pressures are

1. By coating with pyrolytic carbon a very pure carbon can be used;

2. A filament is easy to heat by high temperatures experimentally;

3. The use of low pressure eliminates the effect of diffusion.

The design of the apparatus was based on that previously used by Strickland-Constable[2,18]. It consisted of three main units of pyrex glassware. A high pressure storage unit connected to the reaction vessel through a needle valve and finally an analysis unit; the whole being connected to a mercury diffusion pump with an oil backing pump.

The high pressure unit shown in Fig.3.1 was used to store the hydrogen methane mixture, oxygen and either N_2O or CO; the latter being used for trial analysis. The drying tube was filled with granular anhydrous calcium sulphate, this being the most efficient drying agent which did not adsorb organic vapours. One other inlet tube by passed the drying tube and hence cut down the volume of the plant. This was used to obtain accurate gas mixtures when required,

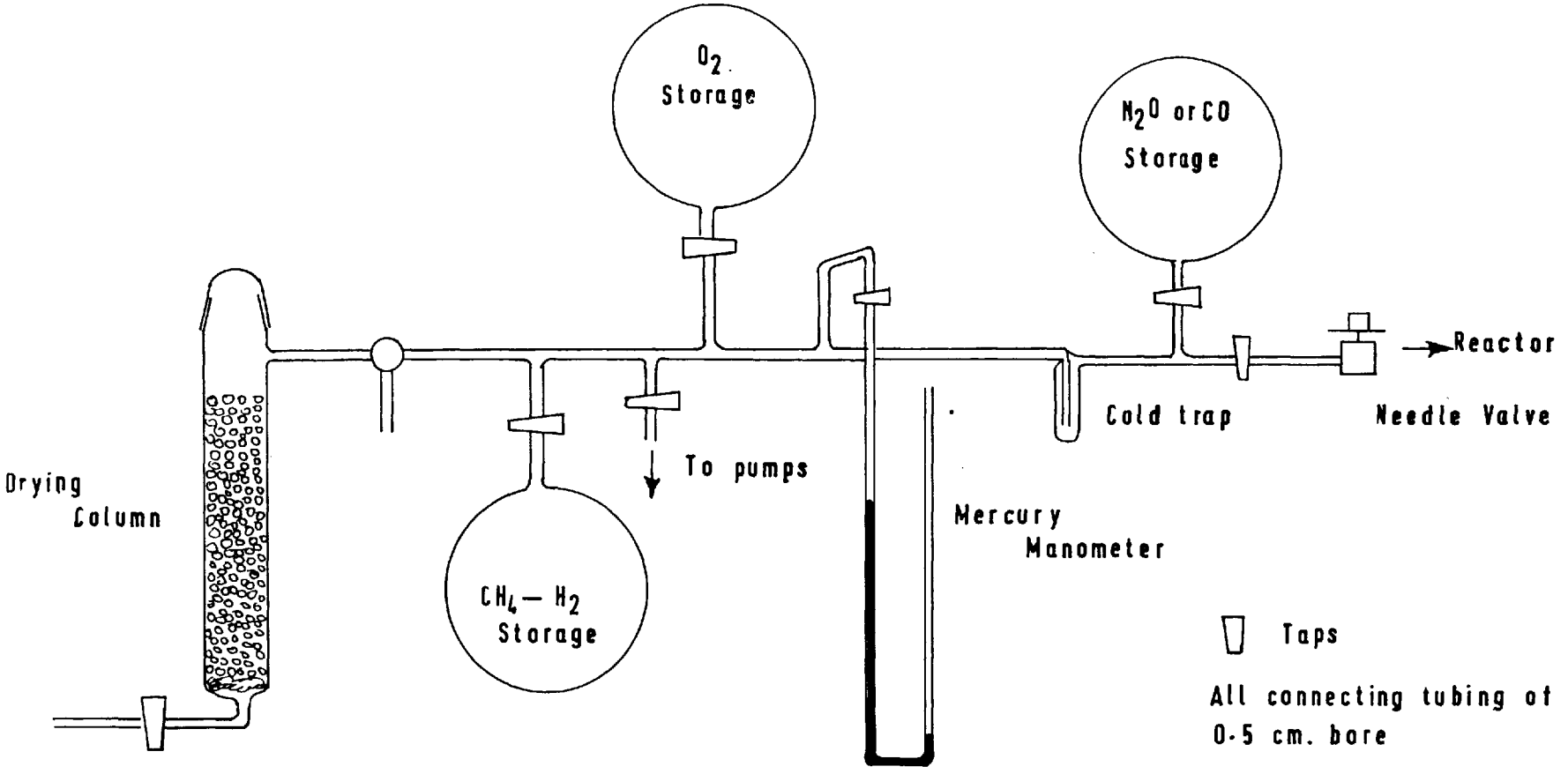

FIG. 3.1 HIGH PRESSURE PLANT.

a mercury manometer being attached to determine the proportions of gas mixtures made up.

A needle valve (Edwards Type D air admittance valve) was used to connect this plant to the reactor vessel. This was to enable small flow rates at low pressures to be controlled. Because of slight leakage through this valve when fully wound down it was found necessary to isolate it with two taps.

The reactor vessel shown in Fig.3.2 was designed so that it could be easily removed to facilitate cleaning. The filament assembly is shown in Figs. 3.2 and 3.3, the design of the holders being based on that used by Strickland-Constable[18]. In the original design stainless steel blocks were used which here were made of spectrographic graphite. This seemed to cause less degassing problems and the filaments did not break so often at the point where they were pinched in the blocks. The filament was pressed tightly between these blocks which were themselves pressed together by a leaf spring, the whole being held in a stainless steel ring by a screw. The rings were free to slide along the glass tubes. A steel spring was used to carry the current to the first block and to maintain a tension on the filament which sagged considerably on heating if this tension was not sufficient. At the other end firm copper wire carried the supply. The D.C. supply used to heat the filament was

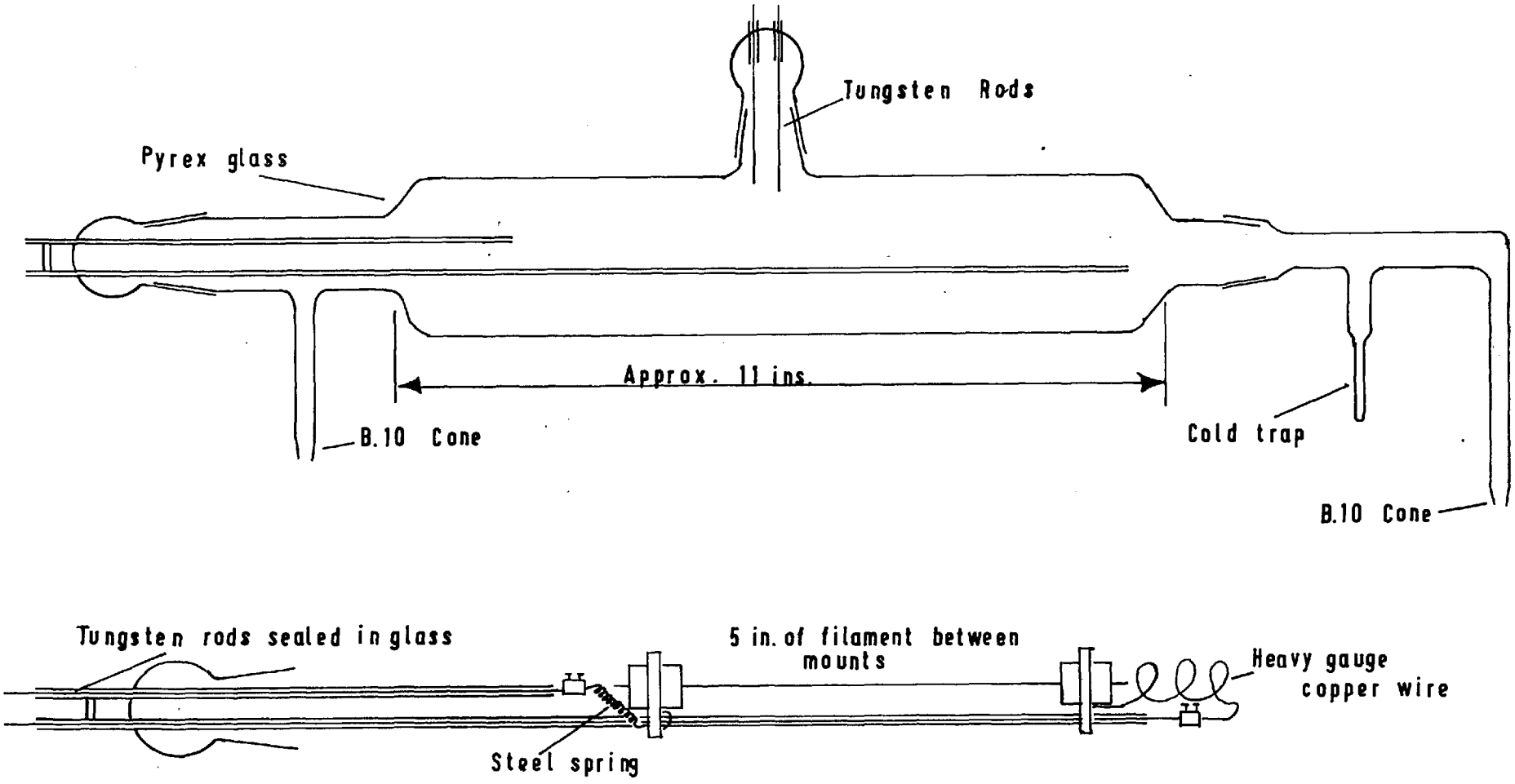

FIG. 3.2 Reactor and filament assembly

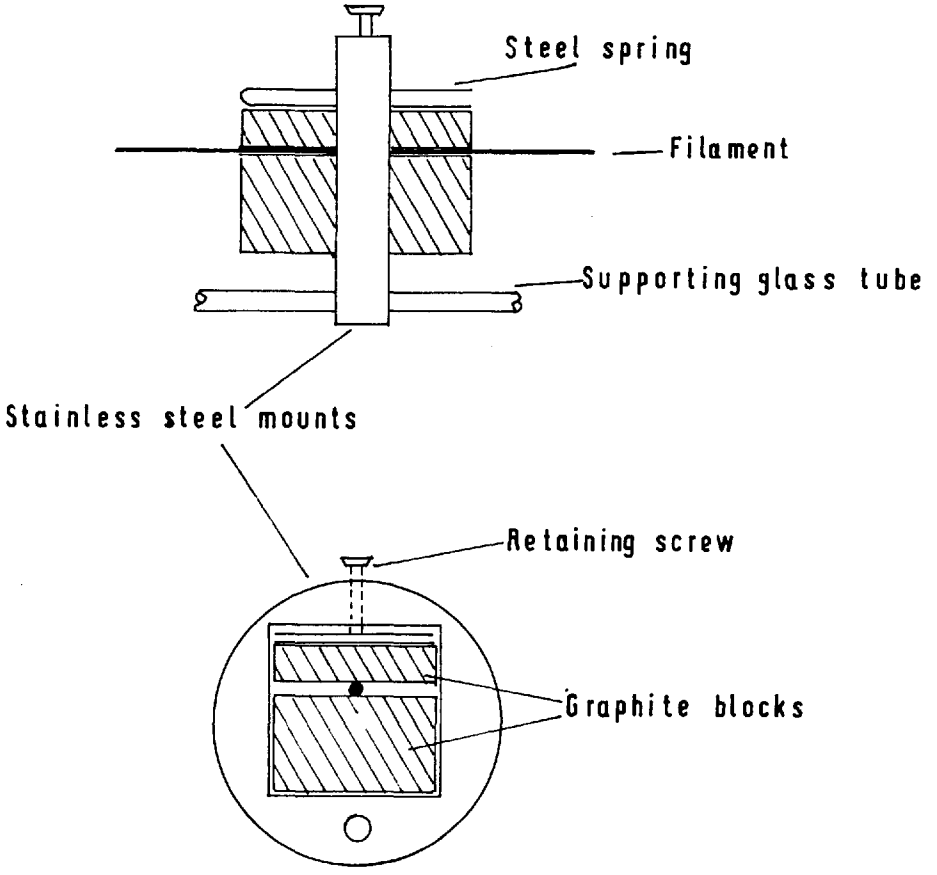

FIG. 3.3 Strickland-Constable type filament mounts.

dropped in voltage by resistors, the negative lead going to the bottom wire to avoid glow discharge[18]. The maximum voltage required was about 100 volts and in all cases exactly 5 inches of filament were heated; the temperature being measured by a Pye disappearing filament pyrometer, provided with a screen to extend its range to 2400°C, which could be read to ± 20°C.

Two other 1 mm diameter crystalline tungsten leads were sealed in a B.19 socket at the top of the filament so that subsidiary filaments could be used for coating the carbon filament with impurities. On the outlet side of the reactor a Pirani gauge head was situated for measuring the initial quantity of gas put into the reactor.

The analysis section in its final form is shown in Fig.3.4 with two cold traps. The first was about 1 inch in diameter with a centre tube of 10 mm bore and was only used in leak tracing and degassing procedures. The actual analysis cold trap was identical to the trap on the reactor vessel, the smaller tube being about 1 inch long and 3 mm. bore. Only about 1/2 inch of this tube was put in liquid nitrogen to avoid volume contraction and cooling effects.

The accurate pressures were measured on a linear scale McLeod gauge[74]. This type of gauge has a single capillary scale; the reading being taken by moving the mercury up to an engraved mark in the main tube. The capillary

All connecting glass of 1cm. bore

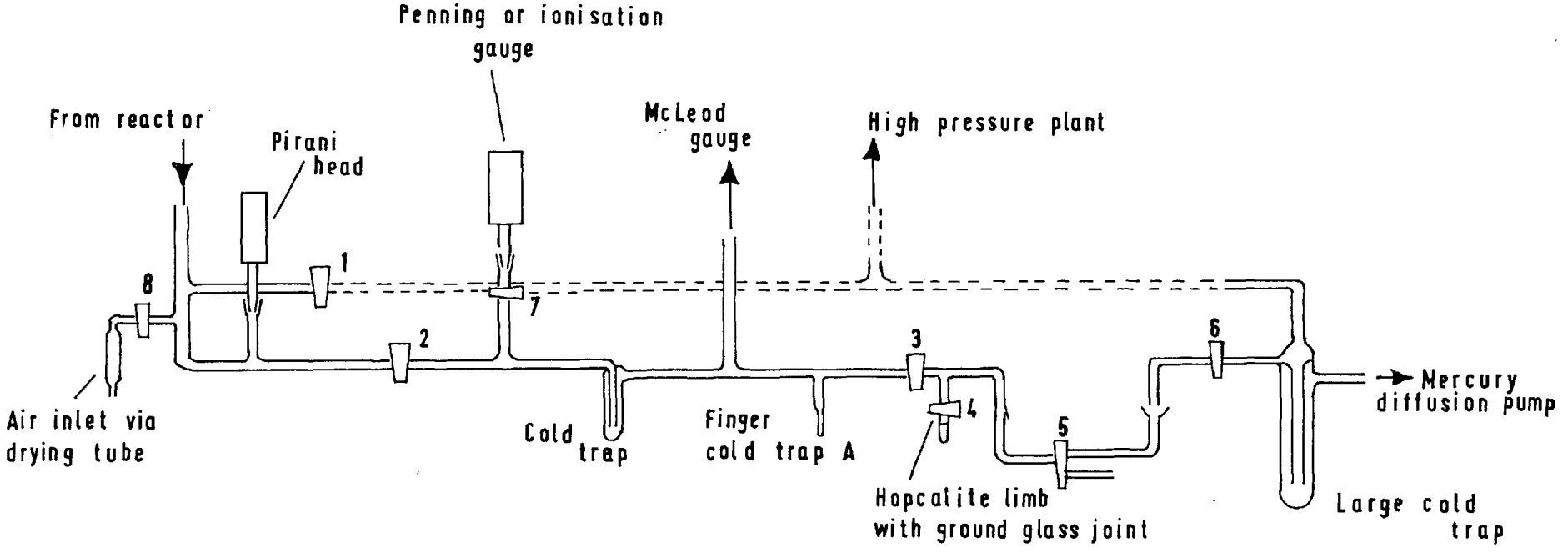

FIG.3.4 Layout of analysis section

marks were calibrated so that this distance was normally 25 cm. A Penning or ionisation gauge could be put next to the McLeod and these were used for continuously measuring the rate of degassing and in leak tracing.

The Hopcalite was contained in a small removable limb isolated by a tap. Next to this a similar tap and limb could be pushed into the B.19 socket for the use of Sofnolite to measure the CO_2 concentration in the absence of oxygen. Alternatively, as shown in Fig.3.4, another connecting line to the vacuum pump could be used allowing the Hocalite to be replaced and degassed independently of the rest of the apparatus.

The connecting pyrex tubing in all the low pressure apparatus was of 10 mm bore. This was though a reasonable compromise between the necessity of large bores to reduce diffusion effects and undesirability of very large bores because of the extra volume introduced. All taps and sockets were greased with Apiezon "L".

The volumes of the apparatus were measured by sharing gases between the various parts of the apparatus measuring the pressure before and after, the absolute volume being found by sharing with a known volume, previously evacuated, attached to where the air admittance tube is shown on the reactor. The mean volume of the reactor and analysis section was found to be 1996 cc.

3.2. Filaments and Gases Used.

The filaments used were supplied by F.J. and J. Planchon, Paris and were 0.3 mm diameter before coating with pyrolytic carbon and in all cases 5 inches of filament were reacted. The mechanism of pyrolytic carbon formation has been discussed by Diefendorf[75] and Meyer[17] and it appears to be a function of the geometry of the apparatus. However, generally above 1800°C and a pressure higher than 15 mm Hg gives a well deposited layer. In our case a mixture of 20 mm Hg of H_2 and 10 mm Hg of CH_4 was used and heating was to 2000°C for 10 minutes, after which the filaments assumed a silvery appearance. In the course of this treatment the pressure rose to about 40 mm Hg and the resistance at 2000°C changed from typical values of 52 ohms to 24 ohms. This compares with a change of only 10% found by Strickland-Constable[18] using the same procedure. Some of the pressure rise was thought due to degassing.

All the gases used were taken from commercial cylinders via the drying tube into the storage flasks; the lines first being evacuated and flushed through twice with the particular gas. For CO and H_2 further drying was carried out by allowing the gases to stand over a liquid nitrogen cold trap. The tap to the storage flask was then closed and the lines and trap degassed. The N_2O and CH_4 were frozen out by a cold trap and re-evaporated, only the top fraction which

came off being stored. The same was done with oxygen, although in this case it did not condense out completely.

3.3. Analysis of Product Gases.

In the earlier stages of the work analysis of CO was carried out by using a platinum filament. This method however gave erratic results. A considerable time was spent in trying to get the right conditions for this catalysis but in vain. Attempts to activate the filament by coating it with platinum black and heating it in a H_2/O_2 mixture as suggested by Langmuir[183] had no effect. Heating the filament at high temperatures appeared to activate it but only temporarily. Neither the use of a P_2O_5 drying tube on the analysis bulb nor standing the reactant gases over liquid air appeared to help. The use of the Pt filament had finally to be abandoned.

The method of analysis for CO finally evolved was to use Hopcalite at room temperature in a small removable limb as suggested by Madley[74]. The exact quantity of Hopcalite used was found to be fairly critical. If too much was used it was difficult to degass sufficiently without adsorption of oxygen following during analysis, and if the quantity was too small its activity fell off very quickly. An optimum quantity for analysis at 50μ was found to be about 0.1 gr., and at 5μ about 0.04 gr.

It is known that Hopcalite oxidises Co by two mechanisms.[62] The first is by oxidation from the MnO_2 which is irreversibly decomposed and the second is normal oxidation by molecular oxygen. In our case the first mechanism alone seems to apply since no molecular oxygen was used up. During analysis part of the CO_2 appeared to be adsorbed by the Hopcalite which part froze out in the cold trap. After about 25 analyses the Hopcalite required changing since it started to 'adsorb' oxygen slowly and the rate of conversion of CO became much slower.

The degassing of new Hopcalite took about 8 hours without heating. For the analysis a cold trap was already in position in the McLeod section and a pressure reading had been taken. The reactants were then allowed to meet the Hopcalite by opening the tap on the limb. A further pressure reading was taken after 2 minutes, the drop in pressure giving the quantity of CO which had reacted to CO_2 and condensed out. Check readings of the pressure were periodically carried out after a further 2 minutes, i.e. a total time of 4 minutes, and these indicated if the Hopcalite had become inactive.

The CO_2 was analysed by simply condensing out in a liquid nitrogen cold trap and measuring the pressure before and after applying the trap. The difference in pressure giving the CO_2 in the reactants. Again a contact time of 2 minutes was found to be sufficient. By merely having

oxygen in the vessel and applying a cold trap a pressure reading correction of 0.8μ, for between 40 and 60μ total pressure was found necessary.

Trial analysis was periodically carried out by making up a gas mixture at about 50μ. A typical analysis is given below, [Run T_{200}].

Mixture	Analysis	
14.0% CO	14.1% CO	
86 % O_2	85.9% O_2	By difference.

For nitrous oxide runs with small burn offs the analysis consisted of merely freezing out the N_2O after reaction, the remaining gases being taken as equal proportions of N_2 and CO as was found by Strickland-Constable[11].

3.4. Experimental Procedure.

Before putting in a new filament the reactor was cleaned out with hot chromic-sulphuric acid and rinsed out with distilled water. The reactor was then degassed until the pressure rise over one hour was not detectable on the Pirani gauge, i.e. less than 1 μ. This normally took about 2 days, the filament being heated at 1500°C in 10 minute periods towards the end of the procedure. The filaments were then coated with pyrolytic carbon; the reactor being evacuated immediately after and allowed to cool. On introduction of O_2, but not N_2O, a certain amount was absorbed

probably by the filament blocks.

In outline the procedure during runs was as follows; a full run with the method of calculating the results is given in Appendix 1.

1. After degassing taps 1 and 4 shut. Taps 5,6,7 and 8 were normally already shut. Taps 2 and 3 being open.

2. O_2 introduced via the needle valve until 50μ indicated on the Pirani.

3. After 5 minutes to allow for any adsorption and to allow the McLeod to reach equilibrium the pressure was read by the McLeod. This was taken as the initial pressure.

4. The filament was heated for the required time, the temperature being measured by the pyrometer.

5. After 5 minutes to allow for cooling of the gases and the filament tap 2 was shut. This allowed the analysis to be carried out on a small sample of gas contained between taps 2 and 5. At the same time tap 1 was opened to allow the reactor to be degassed while analysing the gases. The pressure was read on the McLeod after closing tap 2 and this was taken to be the total pressure after reaction.

6. Liquid nitrogen was then applied to cold trap A, to freeze out the CO_2. After 3 minutes the pressure was again read on the McLeod, and the drop in pressure gave the amount of CO_2.

7. With the cold trap still in position the gases, now

CO and O_2, were contacted with the Hopcalite by opening tap 4. The pressure was read on the McLeod after 2 minutes. The pressure gave the amount of O_2 unreacted, and the drop in pressure (after 6) gave the amount of CO.

8. The cold trap was removed and tap 2 opened to degas the whole of the analysis section and reactor.

Degassing of the reactor normally took 10 minutes. If the degassing was carried out for too long adsorption of the oxygen initially introduced took place. Often on a new day longer periods of degassing were required before starting runs; the oxygen balances after runs giving a good indication of whether the degassing was too short or too long.

Periodically, readings were repeated after 2 minutes to make sure steady values had been attained, and to check the Hopcalite.

4. EXPERIMENTAL RESULTS FOR OXIDATION OF UNTREATED FILAMENTS IN OXYGEN AND NITROUS OXIDE WITH PRELIMINARY DISCUSSION.

4.1. Introduction.

As already stated in Section 2, Duval found the hysteresis for oxygen to be in the opposite sense to that found earlier by Strickland-Constable. These differences could be due to one of the following factors.

1. Differences in pressures used by different workers;
2. Differences in the filaments used;
3. Differences in the quantity burnt off during each run, this being related to the pressure;
4. The use of static or flow systems.

While it was not possible to examine the differences between flow and static systems using the present apparatus, an examination was made of the other factors.

It was also decided to see if the earlier results for oxidation of nitrous oxide were repeatable and if reacting a filament in nitrous oxide affects its subsequent reaction in oxygen and vice versa. This is of particular interest since one of the possible explanations for the differences in hysteresis observed by Strickland-Constable for N_2O and O_2 is that the gases react at different sites on the graphite.

4.2. Rate-Temperature Hysteresis Curves for Reaction in Oxygen.

4.2.1. Rate temperature curves at 50μ pressure.

A series of rate-temperature curves were determined at 50μ pressure on pyrolytic carbon filaments in the reactor which had previously been cleaned out with hot chromic acid and distilled water. Nt preoxidation of the filament was carried out before the runs which consisted of first determining the rate of reaction at increasing temperatures and then at decreasing temperatures. The whole series of runs were then repeated on the same filament to see if reaction had altered its behaviour.

Maximum and change in Hysteresis (*). These results are plotted on Graph 4.1 and shown more fully in Table A.4.1. The hysteresis changes sense between 1390° and 1450°C such that above the crossover point it is in the low sense as found by Duval. Below this point the hysteresis is in the high sense which confirms the earlier results of Strickland-Constable whose results at 20μ also showed a crossover in the hysteresis sense at 1500°C. The maximum in the 'down' curve lies at a higher temperature than the maximum in the up curve which also confirms previous workers results.

The second series of curves, dotted lines on Graph 4.1, show a decrease in the hysteresis effect. This could be due to the filament becoming inherently less susceptible

(*) The results given here in 4.2 are rate temperature curves; the more detailed hysteresis results are shown in section 4.5;4.6 and appendix 6 1

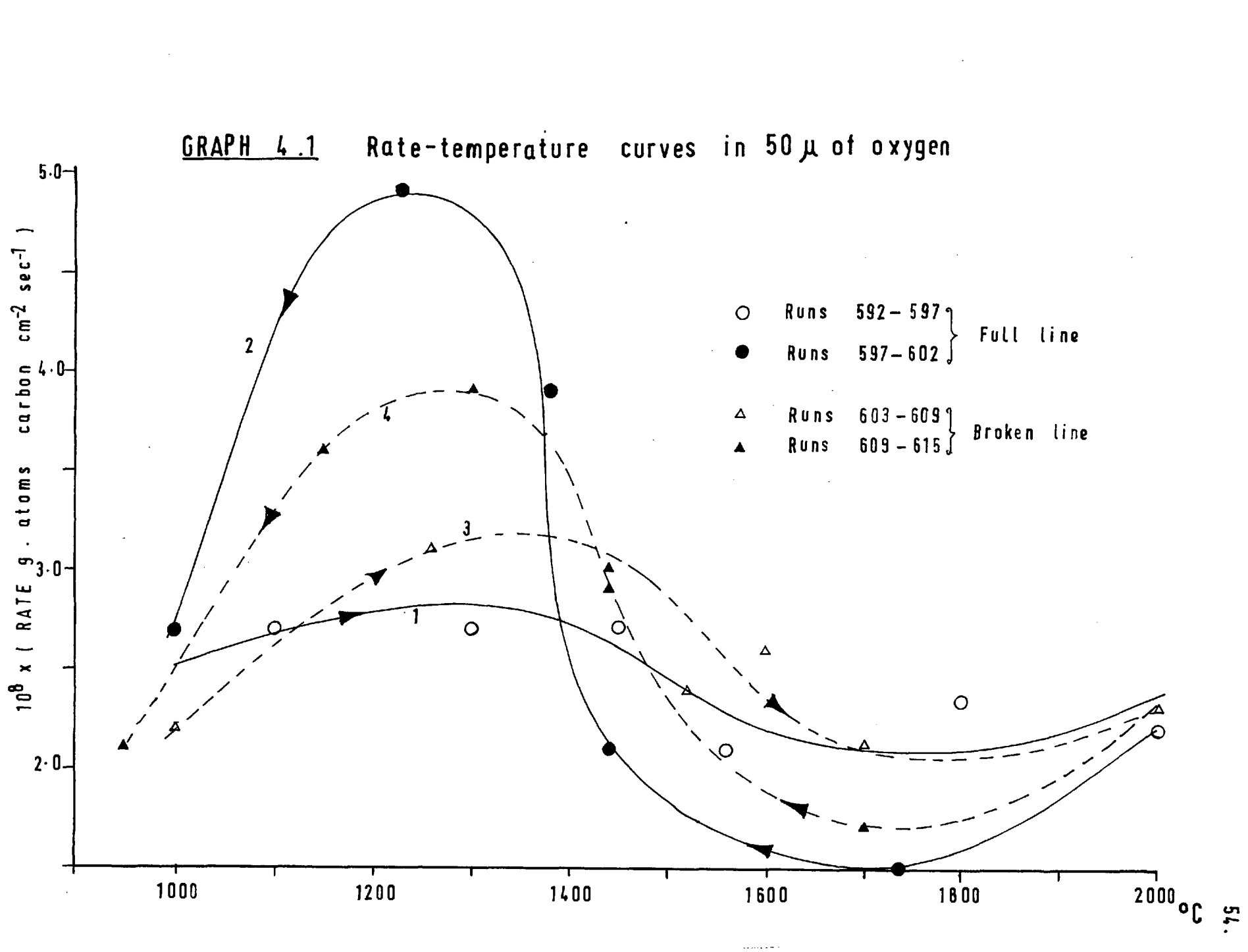
GRAPH 4.1 Rate-temperature curves in 50 μ of oxygen
5·0
4·0
3·0
2·0
10⁸ x (RATE g. atoms carbon cm⁻² sec⁻¹)
1000
1200
1400
1600
1800
2000
°C
Runs 592 – 597
Runs 597 – 602
Full line
Runs 603 – 609
Runs 609 – 615
Broken line
1
2
3
4

to hysteresis with increased burn off, or it may be due to the experimental conditions in the two series being slightly different; the hysteresis being dependent on the exact amount and temperature of reaction at the proceeding point.

In order to examine the reproducibility of these curves a further series of rate-temperature curves are plotted on Graph 4.1 for two freshly coated filaments. Considering that the hysteresis will vary because of the factors stated above, the agreement between the results is very good.

All the results at 50μ show that the rate increases very slightly again above 1700°C, unlike the earlier results of Duval and Strickland-Constable. This is further shown on Graph 4.2, where the hysteresis curves were started at 1440°C to see if starting at a higher temperature made any difference to the rate-temperature curves. The only noticeable difference between these results and the earlier series is that the temperature at which the hysteresis changes sense is higher. This could be due to the greater burn off at high temperatures in this series because of the greater number of runs carried out in the region 1400-2000°C.

Oxygen Balances.

The oxygen balance except for isolated cases was found to be very nearly 100% while the product was predominantly carbon monoxide. The relative amount of carbon dioxide increased with increasing temperature as shown on Graph 4.3.

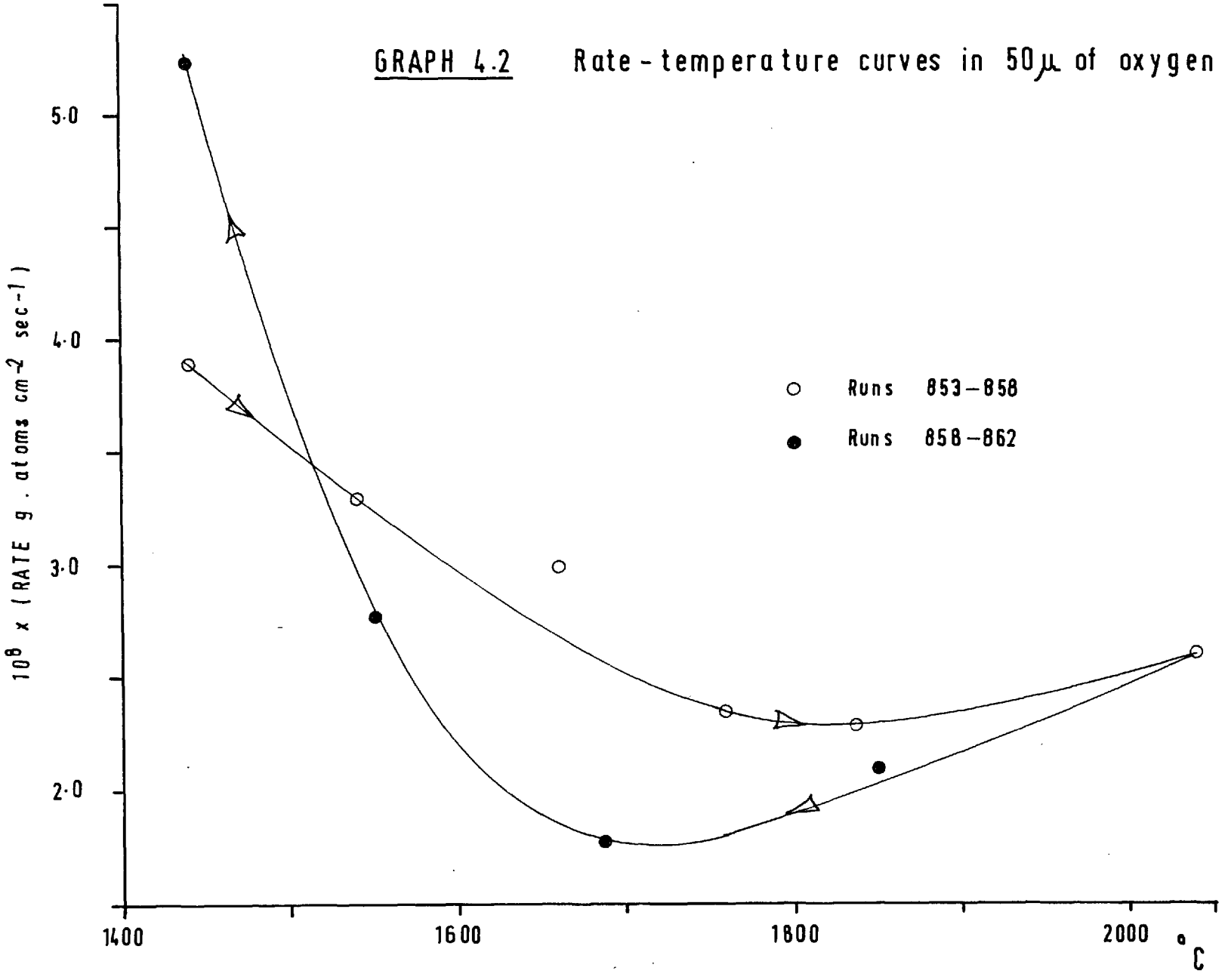
GRAPH 4.2 Rate - temperature curves in 50μ of oxygen
5·0
4·0
3·0
2·0
10^8 x (RATE g . atoms cm^{-2} sec^{-1})
Runs 853–858
Runs 858–862
1400
1600
1800
2000
°C

GRAPH 4.3 Variation of CO_2/CO ratio with temperature

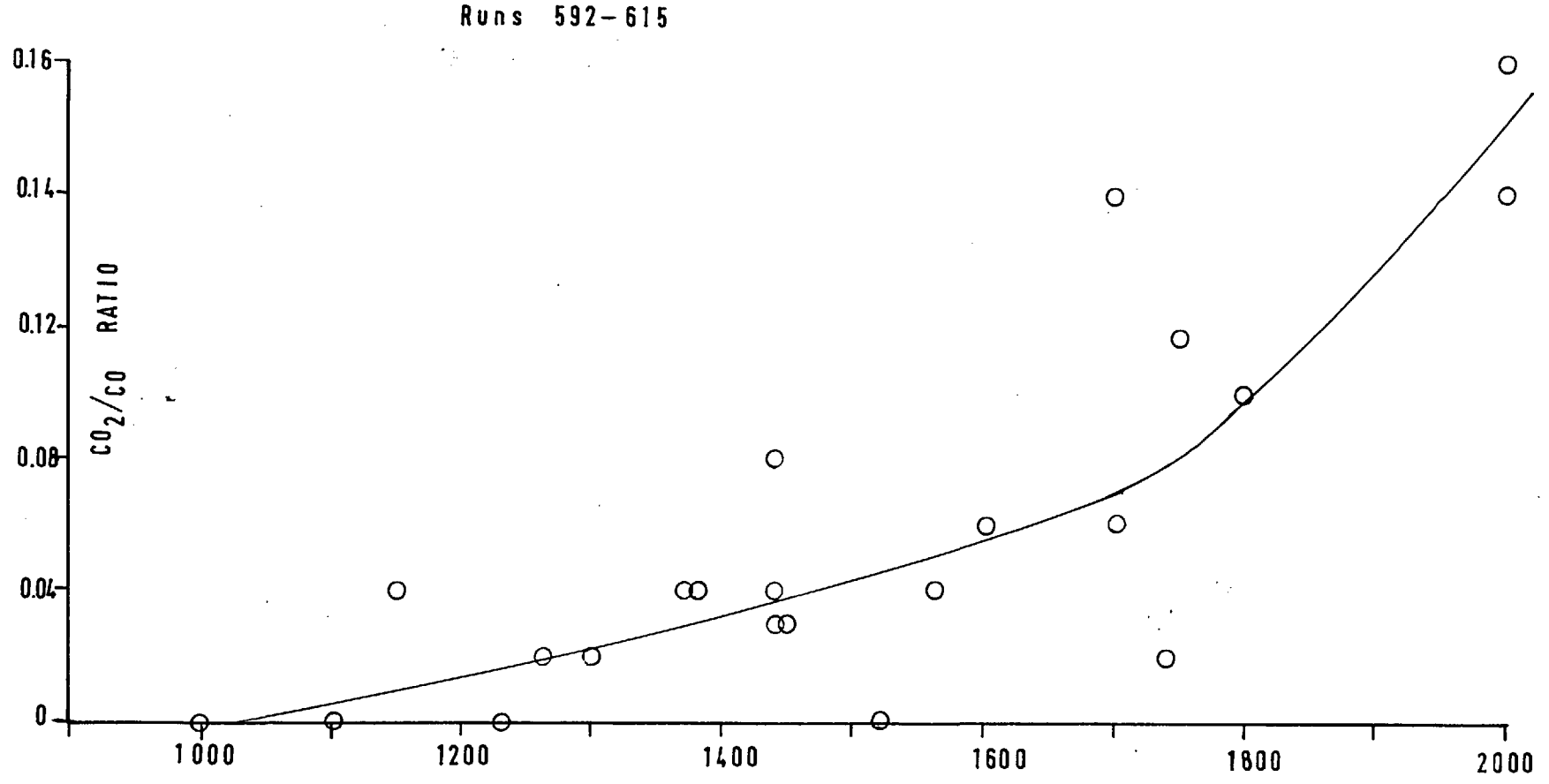

There is a lot of scatter on these points because of the small quantities of CO_2 measured which are obtained by the differences between two large readings. The amount of CO_2 is in good agreement with the results of Strickland-Constable who found a CO_2/CO ratio of about 0.13 at 1900°C and of 0.02 below 1600°C. The fact that the CO_2/CO ratio starts to increase with temperature after 1550°C while the total rate of reaction is fairly constant is indicative of another reaction mechanism starting to predominate at high temperatures

4.2.2. Effect of pressure on Rate-temperature curves.

150μ runs. Rate temperature curves were determined at two other pressures, 5μ and 150μ. The earlier results at 150μ plotted on Graph 4.4 were obtained using the less accurate method for CO analysis, namely a platinum filament, but the increase in pressure was in good agreement with the amount of CO found by analysis. The hysteresis at 150μ appears to be in the same sense over the whole temperature range, the whole hysteresis being in the high sense. This could be due to the higher burn off or pressure used, but it is also possible that it is because the filament was only taken up to 1800°C while those showing crossover in the hysteresis were reacted up to 2000°C.

5μ runs. In order to see if at lower pressures the hysteresis changed sense at a lower temperature and thereby tended towards Duval's results, a series of runs were also carried out at 5μ.

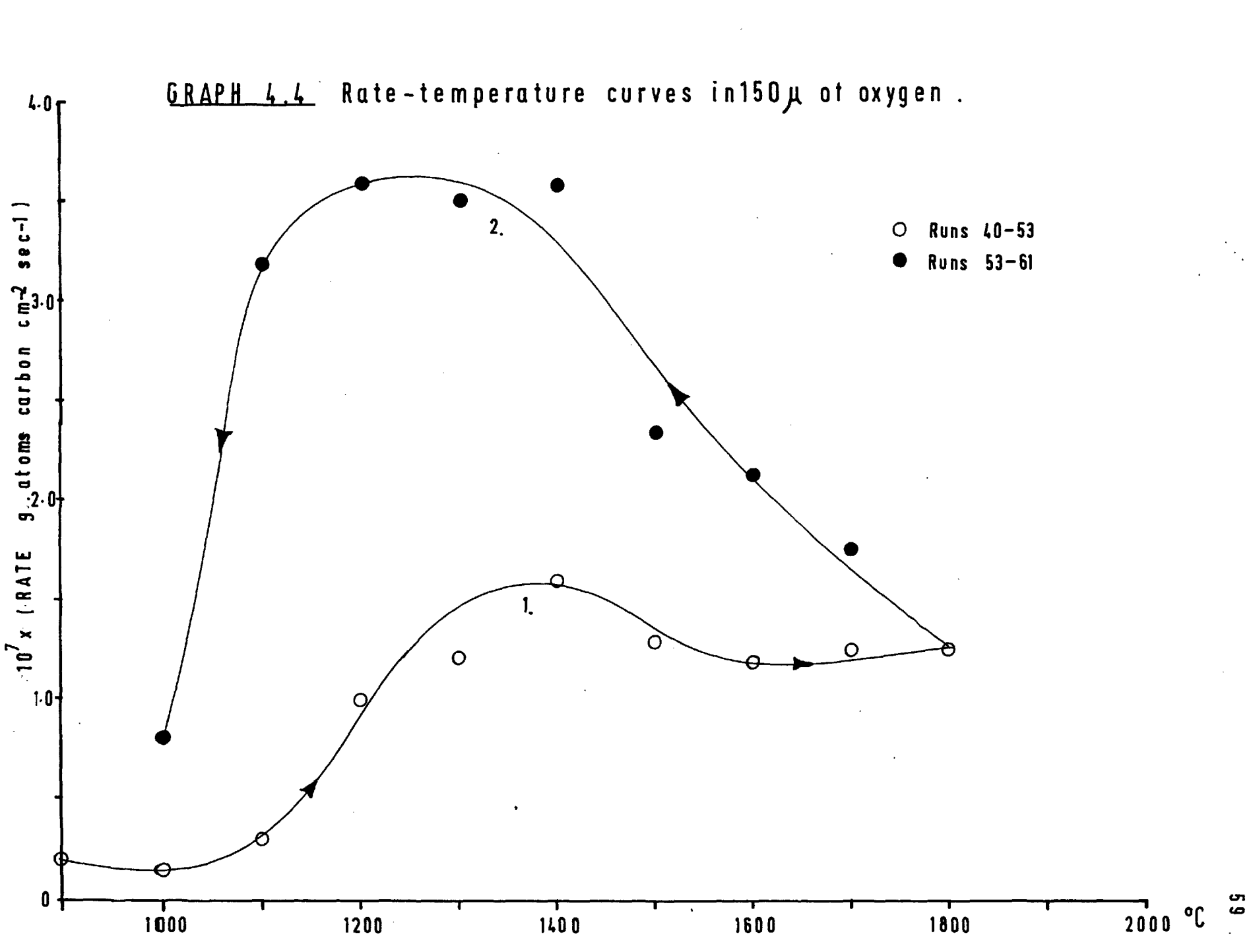
GRAPH 4.4 Rate-temperature curves in 150μ of oxygen .
4·0
3·0
2·0
1·0
0
10^7 x (RATE g atoms carbon cm^{-2} sec^{-1})
1000
1200
1400
1600
1800
2000 °C
Runs 40-53
Runs 53-61
1.
2.

GRAPH 4.5 Rate-temperature curves in oxygen at 5 μ

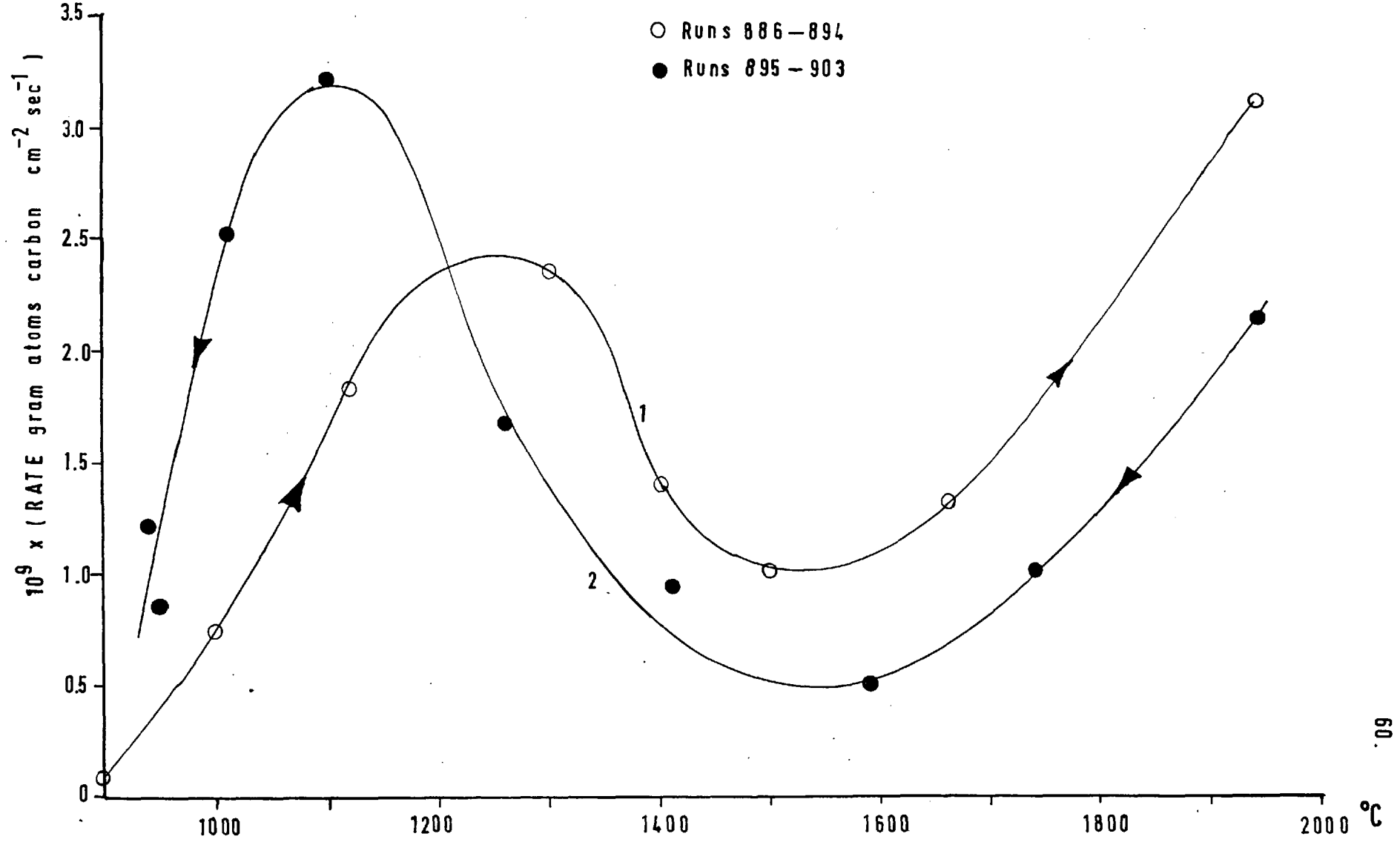

The results of these runs are plotted on Graph 4.5 and given in Table A.4.5.

The particular filament used had previously been reacted in oxygen at 50μ, Runs 864-884 and so to remove any possibility of pressure hysteresis effects the filament was first reacted at 850°C for a total of 30 mins. while 5μ pressure of oxygen was flowing through the reactor. This was followed by further reaction at 1000°C for 10 minutes and at 850°C for 22 minutes, the filament remaining matt black throughout this treatment.

The rate-temperature curves obtained differ from the results at 50μ in that the rate increases with a strong positive temperature coefficient above 1550°C. This effect is similar to that found by Meyer, whose results were explained by Duval[2] and Strickland-Constable[3] in terms of a enhanced reaction due to glow discharge and by the catalysis of CO on Meyer's platinum lead wires. In this work, although no platinum wires were present in the reactor a glow discharge was visible during Run 894 at 1940°C, although the polarity of the leads were the same as Strickland-Constable found necessary to remove the glow discharge i.e. negative to the bottom. In our case the filaments were twice as long as used by the former worker. For the remaining runs, which were the whole of the down curve a cold trap cooled with liquid nitrogen was operating while reaction was taking place. Duval found

that such a cold trap removed the enhanced reaction but in the present work although the visible glow discharge was removed, the results still showed characteristics of the enhanced reaction. This is particularly evident from the high CO_2/CO ratios found at these temperatures, the ratio raching 1.1 at 1740°C. For the rest of this work the results of the enhanced reaction are ignored.

The results at 5μ do show that the hysteresis does change sense at a lower temperature 1200°C than for the 50u pressure results where the change was about 1450°C. This indicates that the differences between Duval's hysteresis results at 0.7μ and ours at 50μ are related to the pressures used.

Order of Reaction. The order of reaction over the pressure range 0.65μ to 150μ can be obtained by plotting log rate against log pressure, the slopes of the lines giving the order with respect to the oxygen concentration. This is shown on Graph 4.6, the points for 0.65μ and 20μ being obtained from the results of Duval and Strickland-Constable respectively. Above 1000°C the reaction is first order below 5μ changing to 1.5 order over 20μ. As the temperature increases the same change in order .s closely followed while at 1000°C the order appears to be nearer one over the whole pressure range. Above 1600°C no rate values are available at 0.65μ and the results at 5μ are of the zero order enhanced reaction, but

GRAPH 4.6 Log_{10} rate against Log_{10} pressure

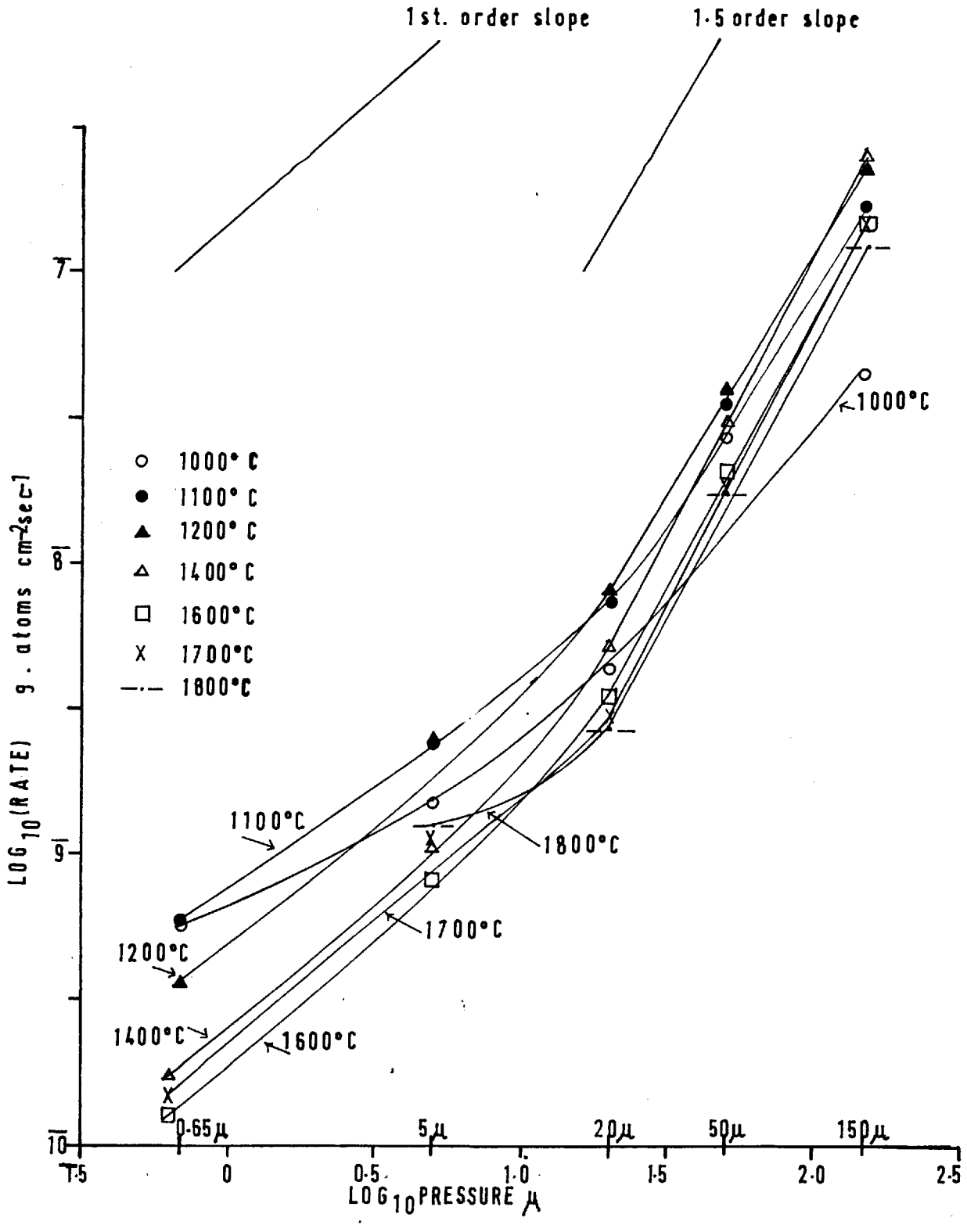

the results at 1800°C for pressures above 20μ still show a 1.5 order reaction. The relevance of these orders is discussed in Section 7.

4.2.3. Effect of burn off on Rate-Temperature curves.

The results at 5μ pressure indicated that the hysteresis changed sense at a lower temperature to the results at 50μ. This shift could have been due to the fact that at 5μ the burn off was much lower, R being about 2 $x10^{-9}$ as against 3 $x10^{-8}$ gr atom carbon/sec, cm^2 at 50μ pressure. In order to test this hypothesis a series of rate-temperature runs were carried out at 50μ as before, but keeping the reaction time down to 5 seconds as against 30 seconds for the earlier results.

A freshly coated pyrolytic filament was first burnt for a total of 4 minutes at 2000°C and then Runs 1077-1098 carried out. Due to the small amounts of products formed it was not possible to analyse for the carbon dioxide. During all these runs a liquid nitrogen cold trap was on the reactor during reaction. After the decreasing temperature runs, the filament was twice burnt for 2 minutes at 930°C in 50μ of oxygen. The results of these runs are given in Table A.4.7 and plotted on Graph 4.7.

From this graph it can be seen that the hysteresis changes sense at 1480°C which is the same temperature range

GRAPH 4.7 Low burnoff rate-temperature curves at 50 μ in oxygen

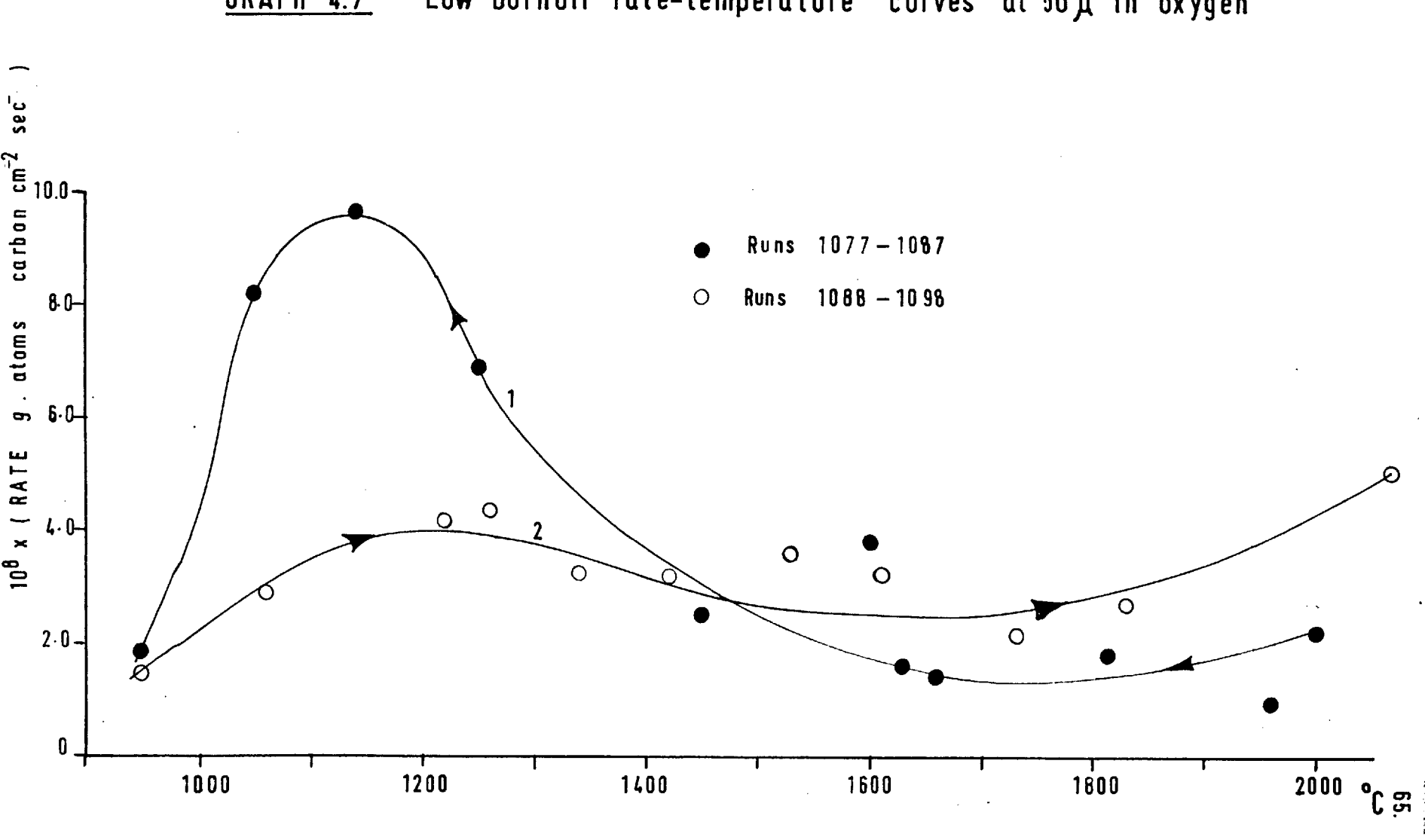

as obtained with 30 seconds burn off. The rates tend to be about 1.5 times higher than those obtained at 50μ but this could be due in a large part to the experimental error being greater because of the smaller amounts of products. It is also possible that the filament does not recover so quickly, because of small burn offs, from its high temperature reactivity.

Apart from the slightly increased rates, the curves at 5 seconds and 30 seconds are in close agreement and therefore the shift of the crossover point cannot be explained by the smaller burn offs at 5μ. The amount burnt off at 5μ was about 1 $x10^{-7}$ gr atoms/cm^2. while at 50μ for 30 and 5 secs. it was respectively about 1 $x10^{-6}$ and 2 $x10^{-7}$ gr atoms /cm^2. for each run.

It follows, a priori, that the lowering of the temperature of the hysteresis crossover point is a true function of the pressure.

4.2.4. - Carbon tetrachloride prepared filament runs.

For the majority of his runs Duval used non-graphitised filaments prepared by cracking carbon tetrachloride. In order to see if the difference in the filament used could explain the differences in the hysteresis results observed here and in Duval's work, a filament was prepared by the same method which is that of Nishiyana[76].

The basic carbon filament was heated in three separate batches of CCl_4 vapour at 1500°C under a pressure of 30 mm Hg for 10 minutes. The CCl_4 was of general reagent quality and was distilled in the apparatus using liquid nitrogen. During the heating of the filament in CCl_4 a thick white mist formed and white and brown solids were deposited on the reactor walls. The white mist was almost certainly chlorine liberated by the reaction. The filament so coated was silvery in appearance but slightly thicker than the methane prepared filaments.

After cleaning out the reactor with chromic acid and distilled water the filament blocks and associated supports were filed clean. The filament was then degassed by prolonged heating at 1500°C under vacuum before Runs 1049-1076 were carried out. The results of these runs are given in Table A.4.8 and plotted on Graph 4.8.

In the first series of runs at increasing temperature, 1049-1059, the CO_2/CO ratio was a factor of about 3 higher than for the decreasing temperature runs and for the methane treated filament. This may be due to some local contamination on the support blocks as noticed by Duval which evaporates off at higher temperatures. The rate of reaction is generally within 20% of the results obtained on methane prepared filaments. There appears to be very little hysteresis below 1300°C but what is present is in the opposite

GRAPH 4.8 Rate-temperature curves for CCl_4 pyrolytic carbon filament in 50μ of oxygen

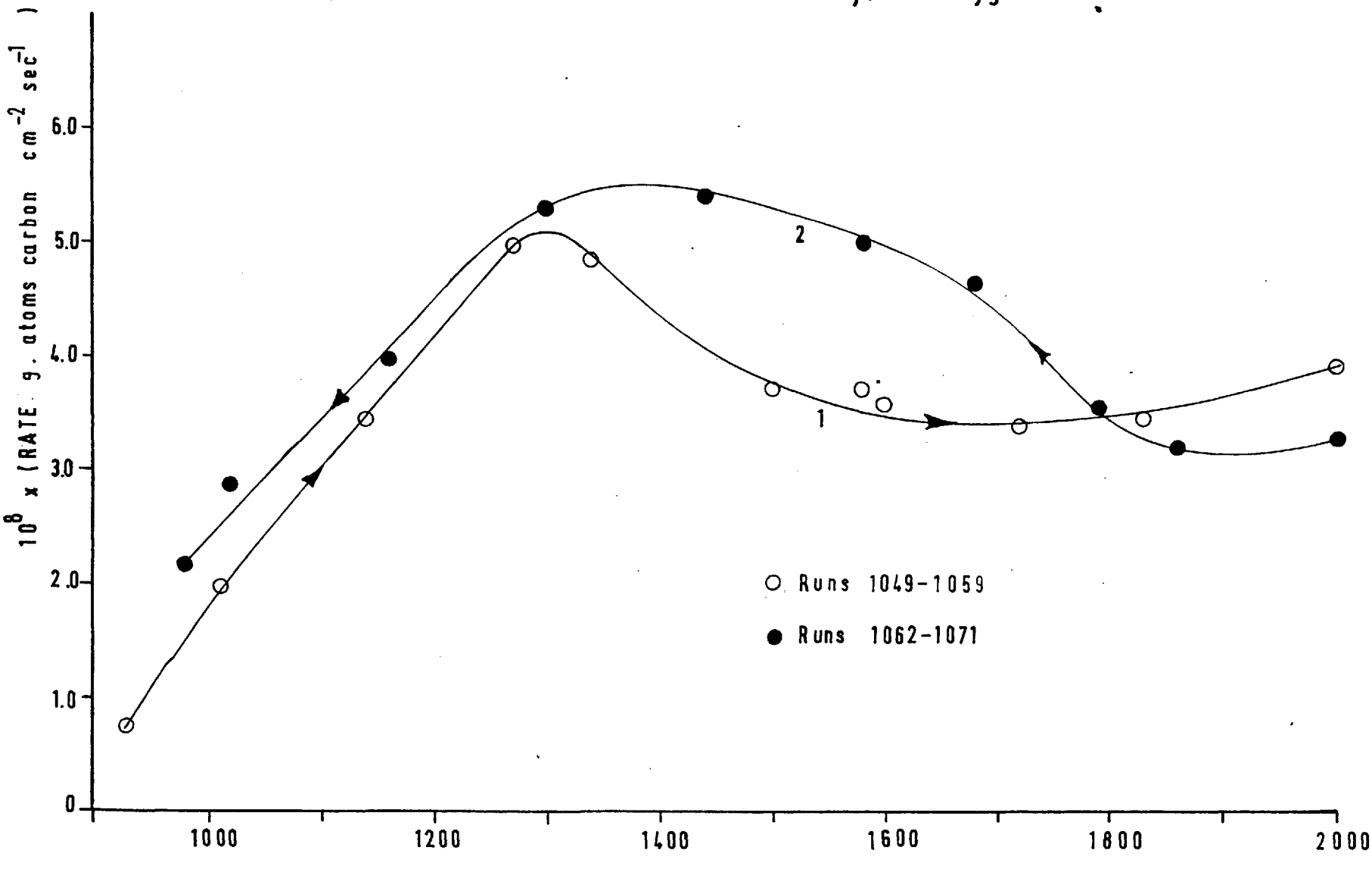

sense to that found by Duval, this effect continuing up to 1800°C after which the hysteresis changes sense.

The hysteresis therefore changes sense at a higher temperature on this non-graphitised CCl_4 prepared filament than for the methane filaments and it seems very unlikely that the differences between our results and Duval's can be explained on the basis of different types of filaments used.

4.3. Reaction in Nitrous Oxide at 50μ Pressure.

4.3.1. Filaments reacted only in N_2O.

In earlier work Strickland-Constable found hysteresis effects for the reaction of filaments in N_2O at 100μ to be in the same sense as Duval's oxygen results, that is low sense hysteresis. The former also found that the rate of reaction of a freshly coated filament was very small and he therefore activated his filaments by heating them for prolonged periods at 2000°C in 1 to 2 mm Hg pressure of N_2O. Whenever this was attempted during the present work the filaments rapidly formed hot spots and fused. The reaction was therefore studied by condensing out the N_2O after reaction and assuming the residual gases to be equal parts of N_2 and CO as found by Strickland-Constable.

The most activated filament used was heated three times for 1 minute in N_2O at 1.5 mm Hg pressure at 2000°C, followed by 2 minutes in 50u of N_2O. After an initial run

at 1810°C a series of runs 960-970 were carried out at 2010°C, the results are given in Table 4.1. The first results, Runs 961-965 show a gradual increase in rate with burn off. After run 965 the filament was again heated for 1 minute in 1.5 mm Hg of N_2O to see if this caused further activation, but the results of the next two runs 966 and 967 show no significant difference in rate. After run 967 the filament was heated for 2 periods of 1 minute each at 2060°C in vacuum to see if this caused degassing or altered the rate. A negligible quantity of gas was desorbed but the results of runs 968-971 showed that this heating in vacuum appears to have activated the filament initially, the same value of R = 1.03 as previously found was attained after a burn off of about 4 $x10^{-7}$ gr atoms of carbon/cm^2.

Rate-temperature curves were then determined on the same filament, the results are shown in Table A.4.1 and plotted on Graph 4.9. The rate goes through a maximum at about 1300°C and also increases after 1600°C as found by earlier workers. This increase at higher temperatures can be explained by the dissociation of nitrous oxide.

Unlike the Strickland-Constable results, where large hysteresis effect was observed between 1100 and 1800°C, the hysteresis is very small below 1600°C. This difference may be due to differences in pressure used but is more likely due to the fact that the previous worker used much more activated filaments.

GRAPH 4.9 Rate-temperature curves in N_2O at 50μ

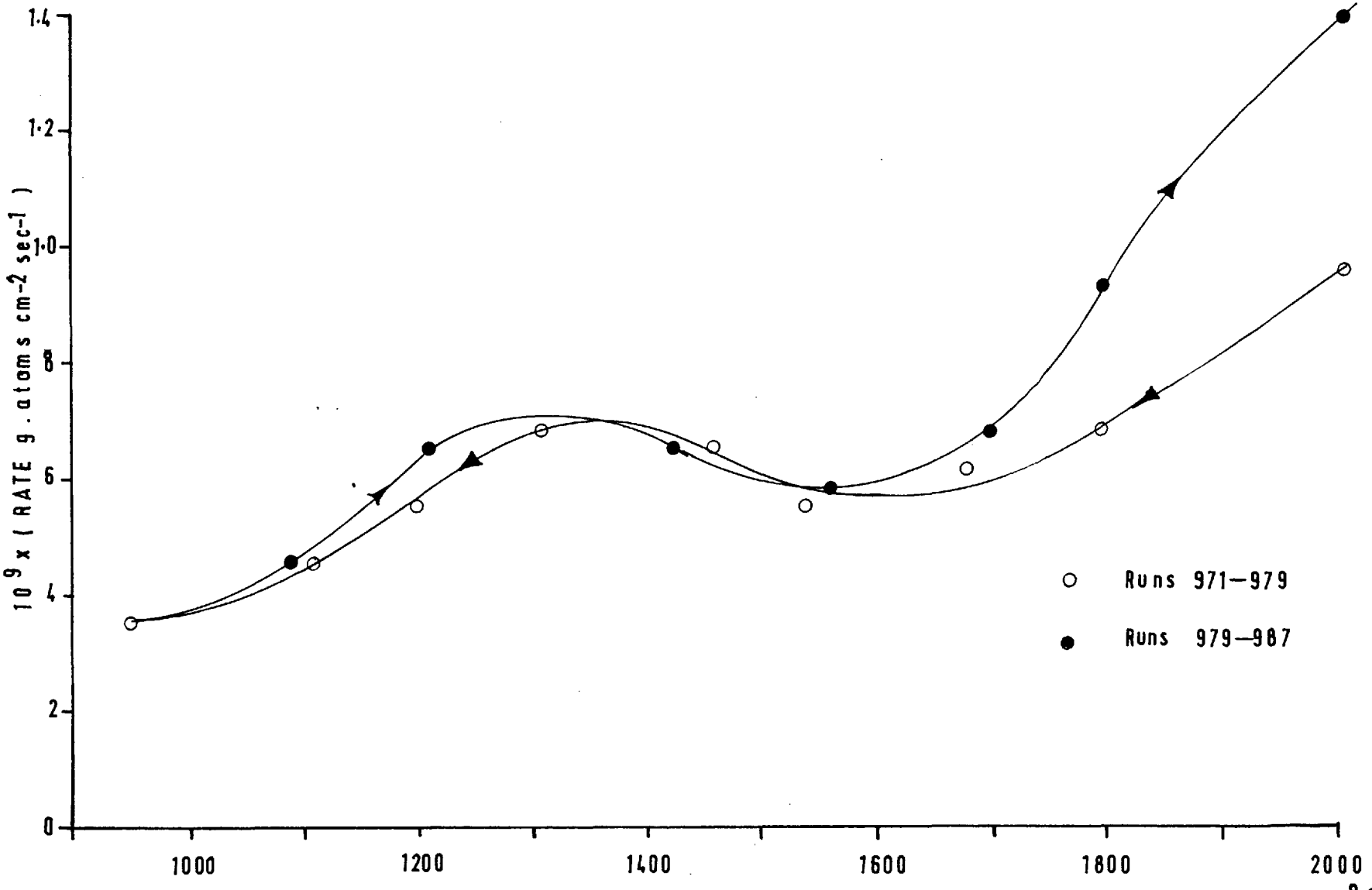

Table 4.1. Reaction in 50μ of N_2O.

Filament No.45.

Run No.	Seconds reaction	Initial pressure μ	Pressure CO + N_2 μ	R x 10^9
960	120	50.6	1.5	0.49
961		50.4	2.7	0.87
962		49.2	2.8	0.91
963		48.0	2.9	0.93
964		50.0	3.1	1.00
965		49.8	3.1	1.03
966		49.2	3.1	1.03
967		47.0	2.6	0.84
968	60	48.4	2.0	1.29
969	60	48.0	2.3	1.45
970	120	47.2	3.6	1.16
971	120	46.2	3.1	1.03

Reaction at 2010°C except Run 960 at 1810°C.

4.3.2. Filament previously reacted in Oxygen.

A series of runs were also carried out using a filament previously reacted in oxygen to see if reaction in oxygen affected the subsequent reaction in N_2O. The filament used, No.43, had previously been reacted in oxygen at 5μ pressure. After degassing by prolonged heating at 1800°C, an initial run at 950°C was followed by ten runs at 1800°C to see if the rate varied with burn off.

These results, Table A.4.14, Runs 905-914, show that the activity of the filament decreases with burn off, but tending towards a steady value. A series of rate-temperature curves were next determined on the same filament, Graph 4.16 (Table A.4.10). For the first two curves several runs were carried out at each temperature to see if the rate varied appreciably with burn off after reaction at the previous temperature. The rates did not vary much and for the purposes of plotting Graph 4.10 the initial rates were plotted so as to give the maximum hysteresis effect.

These curves show that the initial and final rates are the same at 2000°C and 900°C which suggests that the filaments activity is not changing, the oxygen effect having been removed by the earlier reaction at 1800°C. The rates of reaction obtained in the final series become very near to those obtained on a filament reacted only in N_2O.

GRAPH 4.10 Rate-temperature curves for N_2O; filament previously reacted in O_2.

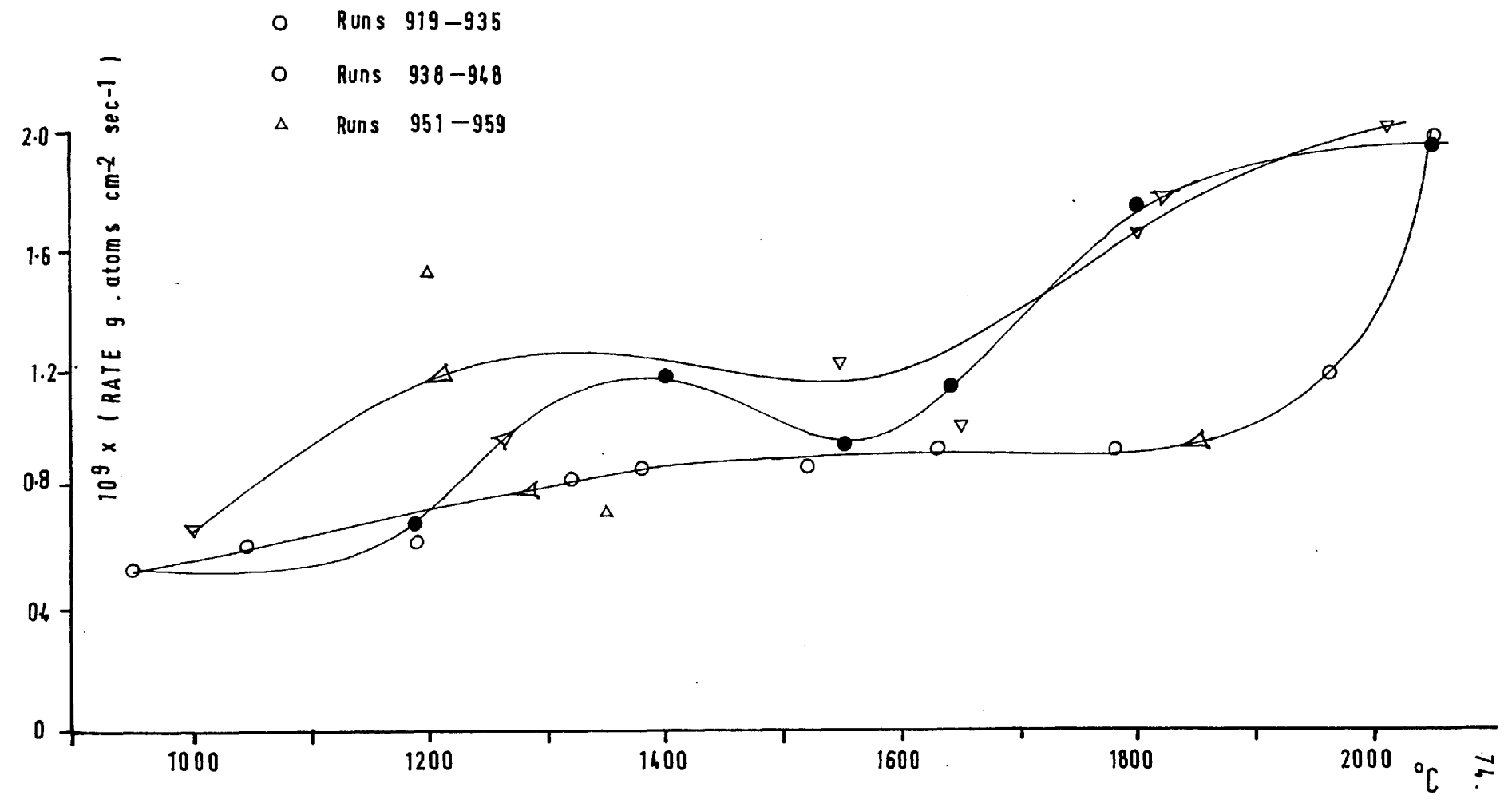

The effect of reaction in oxygen on the subsequent reaction in N_2O is further treated in Section 4.5.4. The results here do show however that it was not possible to permanently activate a filament for N_2O by reacting it previously in oxygen.

4.4. Study of Hysteresis in Oxygen.

In order to further test that the hysteresis as measured on the rate-temperature curves is truly in the opposite sense to Duval's results his method of measuring the hysteresis effect by determing the rate at increasing burn-off until a steady value of rate is attained was used. This method also has the advantage that it enables the steady value of R to be determined at any particular temperature.

4.4.1. Initial Results on different Filaments.

Curve B on Graph 4.11 shows the effect of burning at a high temperature 1350°C after reaction at a lower temperature 960°C for a total of 13 minutes. The rate reaches a steady value after a burn off of about 7 $x10^{-6}$ gr. atoms/cm^2 compared with 3 $x10^{-7}$ gr atoms/cm^2 for Duval's results. The hysteresis is in the opposite direction to the latter's results and in agreement with our rate-temperature results. It might be expected that the constant rate reached would be midway between the up and down curves of the rate-temperature runs, but the results show a rise

GRAPH 4.11 Hysteresis effect as a function of burnoff for reaction in O_2

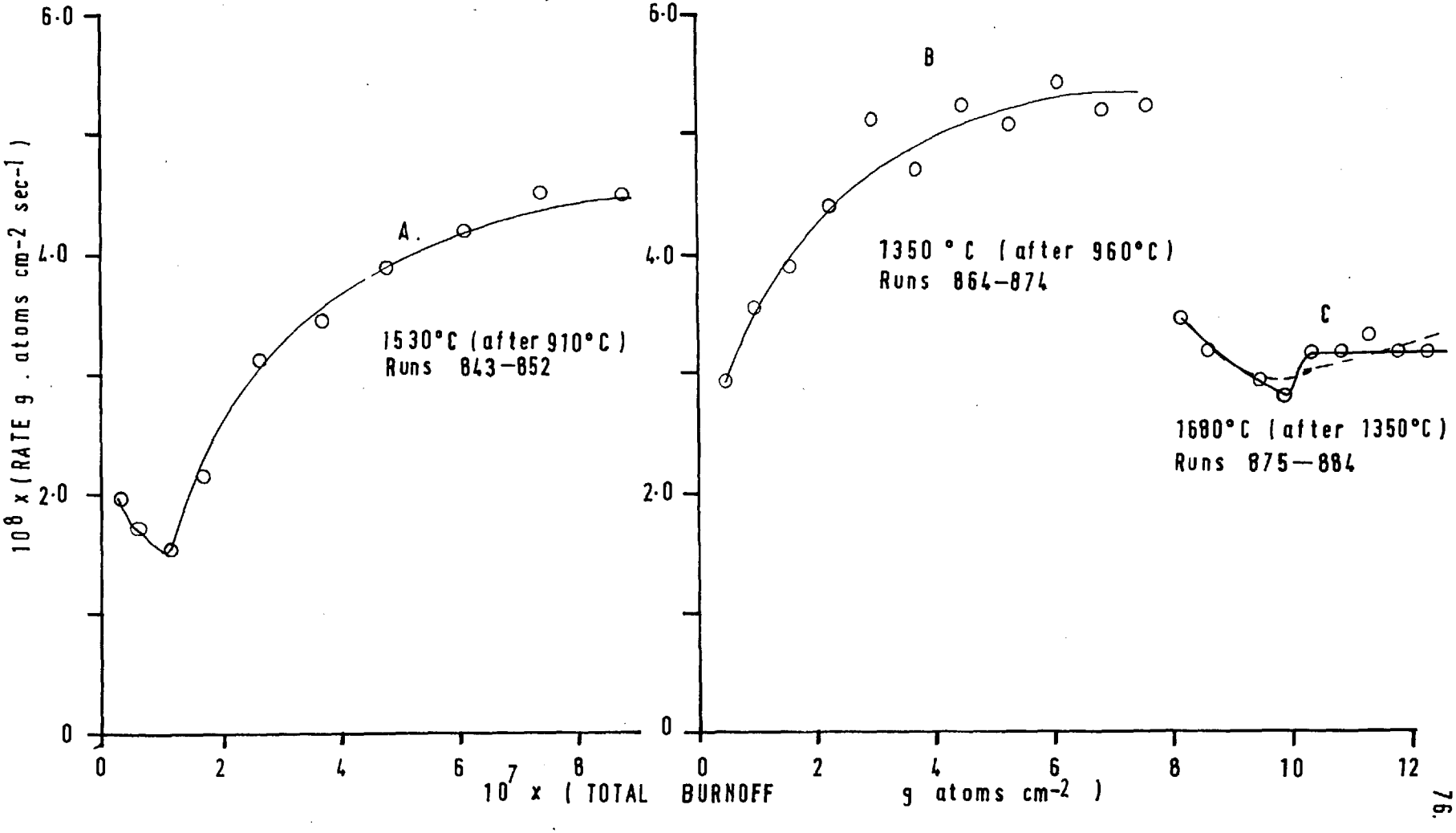

from 3 to nearly 5.4 x10^{-8} gr atoms/cm^2 sec. The constant rate reached is therefore significantly higher than the mean rate value given by Graphs 4.1 and A.4.1.

The same effect is shown on Graph 4.11 where a freshly coated filament was reacted at 1530°C after a total of 17 minutes reaction at 910°C. In this case, however, after an initial decrease the rate goes to a steady value of 4.5 gr atoms/cm^2 sec which is 1.5 times higher than the rate reached in any of the rate-temprature runs at this temperature. Curve C, Graph 4.12, shows a similar effect at 1440°C and in both these cases the constant rate was reached after a burn off of about 5 x10^{-6} gr atoms/cm^2.

Reaction in the opposite direction for example Curve A, Graph 4.10, where reaction was at 1300°C shows the hysteresis in the opposite sense as expected. For these particular results the rate decreased over a burn off of about 2 x10^{-6} gr atoms, which is less than required in the previously mentioned runs to reach a steady value. After this decrease the rate appears to increase slowly, almost linearly with burn off. The same type of result was obtained for reaction at 1380°C (after 1750°C) is shown on Graph 4.13; both results being obtained on the same filament. These results were not expected in so far that they suggested that the filament permanently increased in activity with increasing burn off.

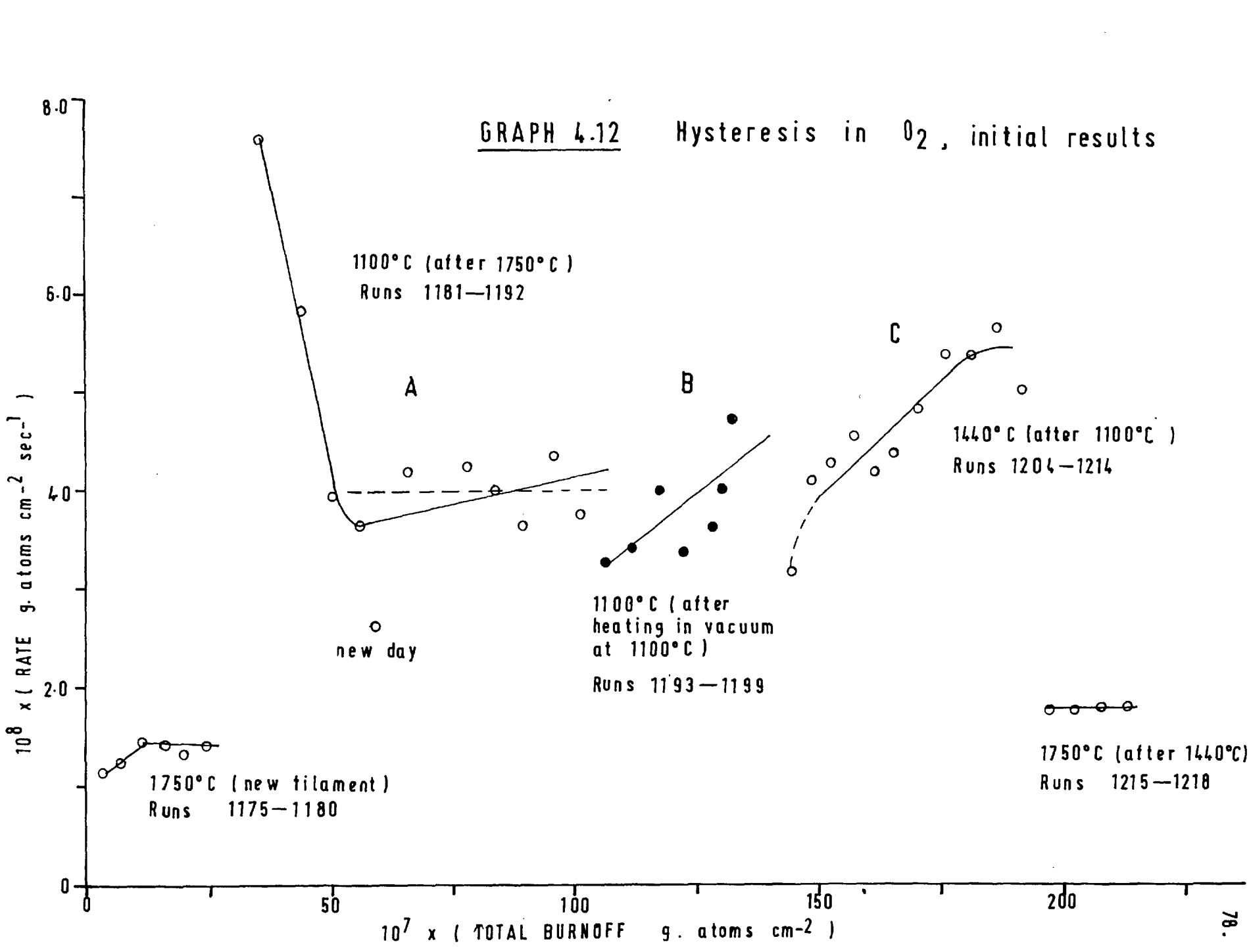
GRAPH 4.12 Hysteresis in O_2, initial results
8·0
6·0
4·0
2·0
0
10^8 x (RATE g. atoms cm^{-2} sec^{-1})
1100°C (after 1750°C)
Runs 1181—1192
A
B
C
new day
1100°C (after heating in vacuum at 1100°C)
Runs 1193—1199
1440°C (after 1100°C)
Runs 1204—1214
1750°C (new filament)
Runs 1175—1180
1750°C (after 1440°C)
Runs 1215—1218
0
50
100
150
200
10^7 x (TOTAL BURNOFF g. atoms cm^{-2})

This last result, and also Curve A, Graph 4.11. for reaction in the opposite temperature direction, showed an increase in rate over the first two runs which covered a burn off of about 5 $x10^{-7}$ gr atoms/cm^2, which is close to the value Duval found necessary to give a constant rate. The relevance, or not, of this factor is further discussed later; this initial abnormality has only been shown in a few of the results (See also 4.5.1 and 4.5.4) and in this particular case is thought due to temporary inhibition caused by the filament standing in vacuum overnight.

On the rate-temperature curves the hysteresis changed sense about 1500°C with a smaller effect above this temperature. Results obtained at 1680°C (after 1350°C) shown on Curve C, Graph 4.11. confirm the rate-temperature curve results; the hysteresis being initially in the low sense and of small magnitude. Again, however, the constant rate attained was higher than that given by the rate-temperature curves.

No hysteresis was detected for reaction at 1750°C (after 1440°C), Graph 4.12, the rate attained being compatible with the rate-temperature curves, while reaction at 1000°C (after 1380°C) showed very little hysteresis (Graph 4.13); but the slight hysteresis shown was compatible with the rate-temperature curves.

GRAPH 4.13 Hysteresis in O_2 ; initial results.

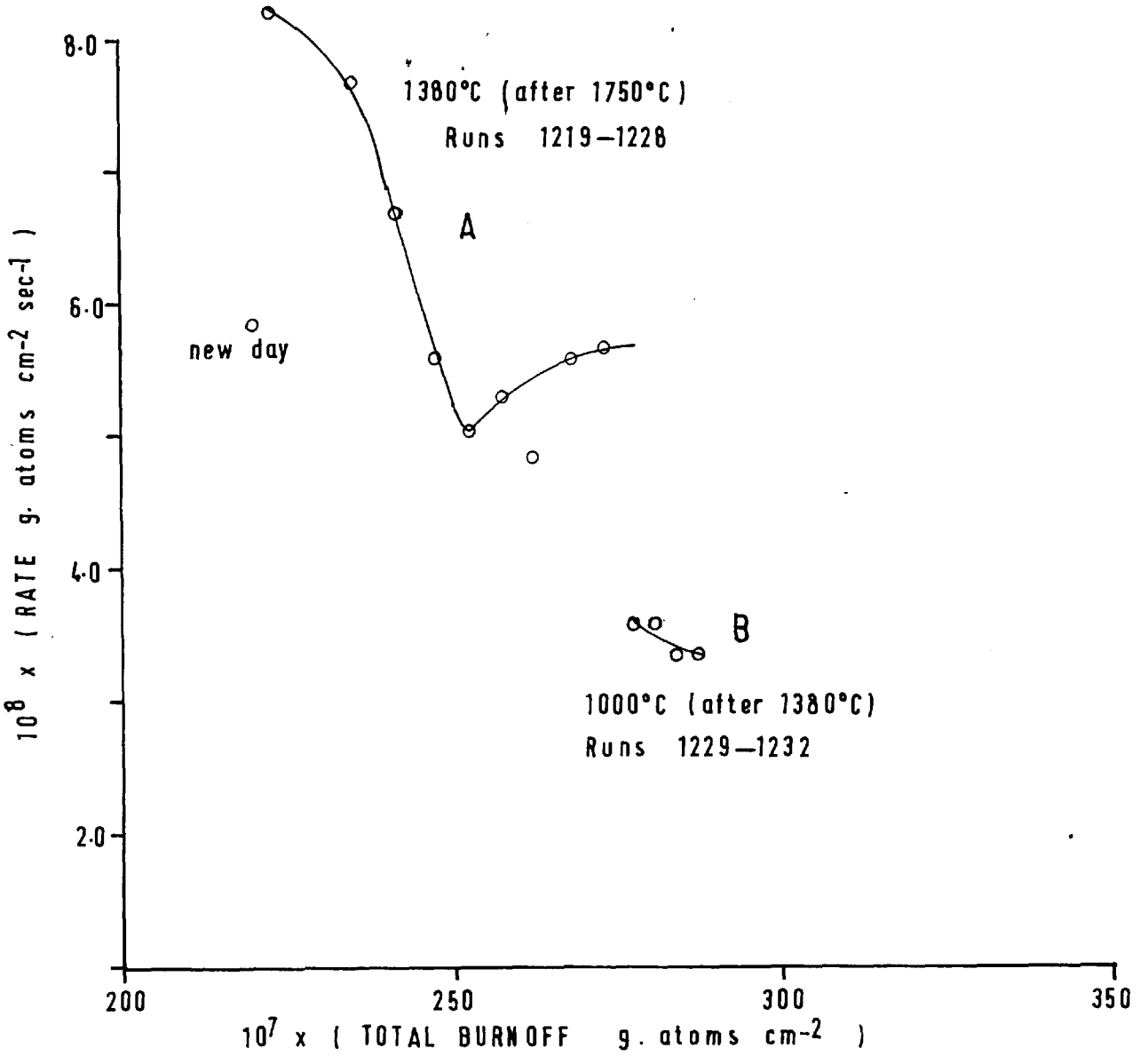

Reaction at 1750°C, on a freshly prepared filament at 2000°C, showed slight hysteresis in the low sense, i.e. the rate was initially low, Graph 4.12 Similarly reaction at 1100°C following heating in vacuum at 1750°C for 5 minutes, Table A.4.12, and following heating in vacuum at 1100°C, Graph 4.12, gave an initial low rate which increased with burn off. Heating in vacuum, therefore, appears to deactivate the filament.

A study of the effect of burn off on the hysteresis was also carried out on the filament prepared from CCl_4. Reaction at 1550°C, after 980°C, shown on Graph 4.14 gave hysteresis in the high sense which is consistent with the rate temperature curves for this filament (See Graph 4.6). Again the constant rate reached was very near the maximum reached on the 'down' curve.

4.4.2. Summary of Initial Hysteresis Results.

1. Generally the hysteresis was in the same sense as given by the rate-temperature curves.

2. A steady state value was not attained after a constant burn off as found by Duval.

3. Heating in vacuum appeared to deactivate the filament.

4. Certain anomalous results were obtained over the initial burn off in certain cases, giving hysteresis in the opposite sense to that expected.

GRAPH 4.14 Hysteresis for a CCl_4 prepared filament in O_2 at 1550°C

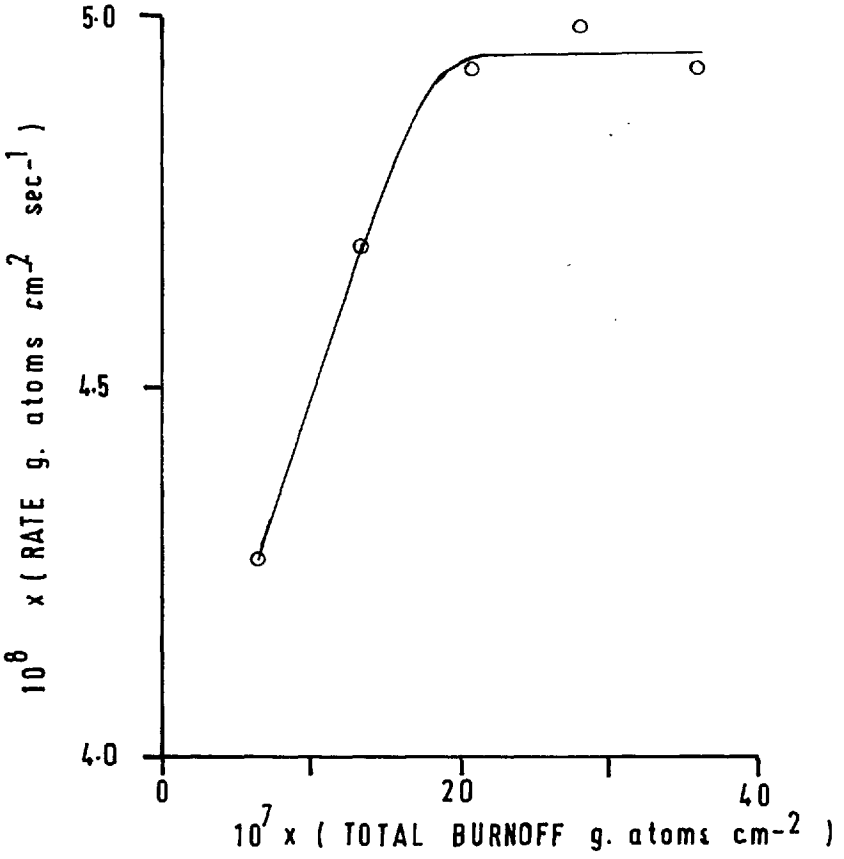

Reaction in O_2 (after 980°C)

Runs 1072—1076

5. The steady rates reached were higher than would be expected from the rate-temperature curves and the filaments showed a tendency for its activity to increase permanently with burn off.

4.4.3. Steady value rate-temperature curve obtained from hysteresis results.

In order to attain a true rate-temperature curve a filament was burnt at various temperatures until steady rates were reached. By using the same filament and burning it at increasing temperatures and then decreasing temperatures it was possible to see if the filament became permanently activated by reaction.

The results of these runs are given in Table A.4.13 and plotted on Graphs 4.15 - 4.17 in the order of first increasing and then decreasing temperature. These hysteresis curves were consistent with previous results, showing very little hysteresis above 1550°C, but any hysteresis which did show above this temperature was consistent with the change of sense shown by earlier rate-temperature curves.

As far as possible the particular curves were determined on the same day but when the filament was left standing overnight an initially low rate was found, as indicated in Graph 4.17. Some of the curves also showed the same anomalies as found earlier; for example for reaction at

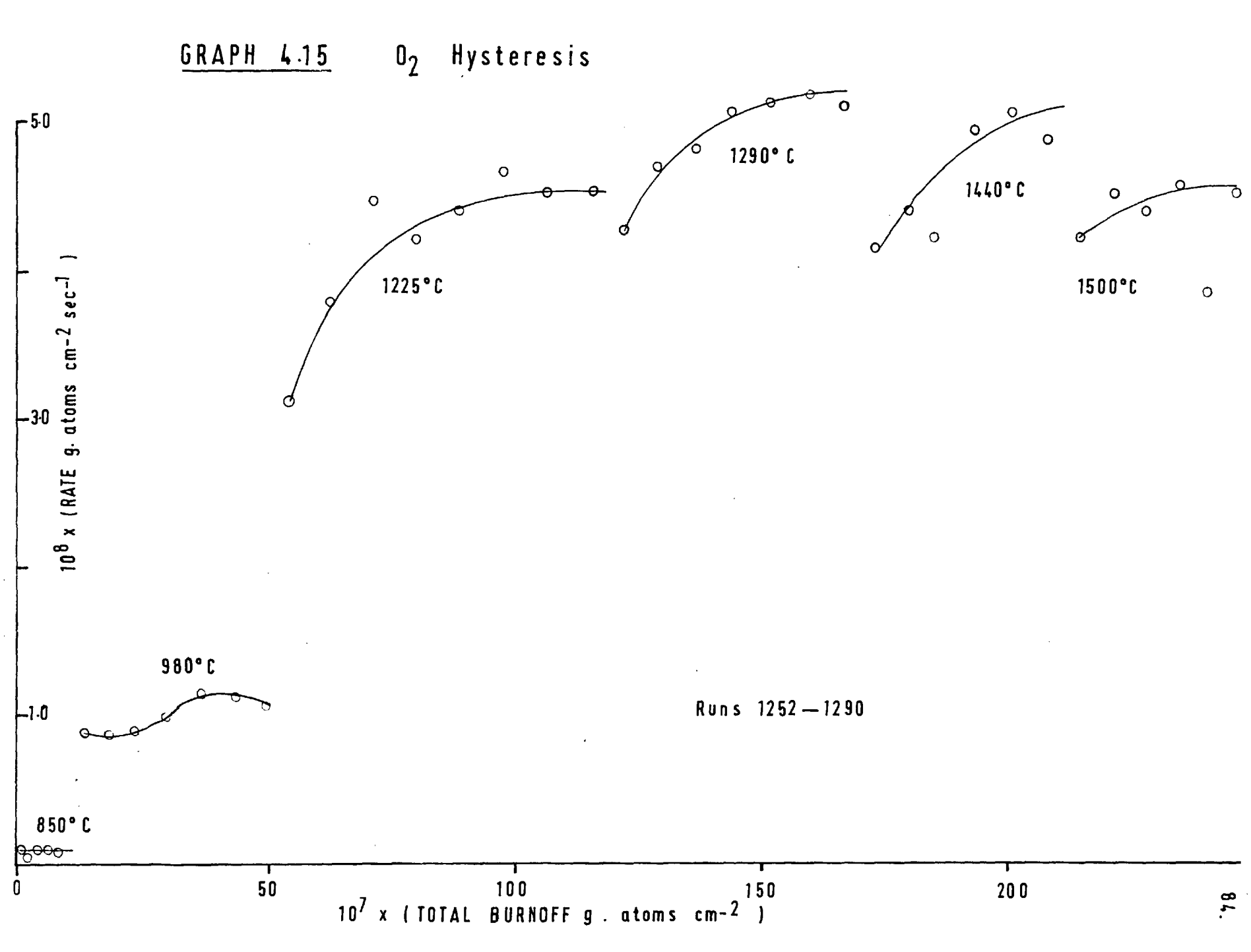
GRAPH 4.15 O_2 Hysteresis
5·0
3·0
1·0
10^8 x (RATE g. atoms cm^{-2} sec^{-1})
1225°C
1290° C
1440° C
1500°C
980° C
850° C
Runs 1252 — 1290
0
50
100
150
200
10^7 x (TOTAL BURNOFF g . atoms cm^{-2})
84.

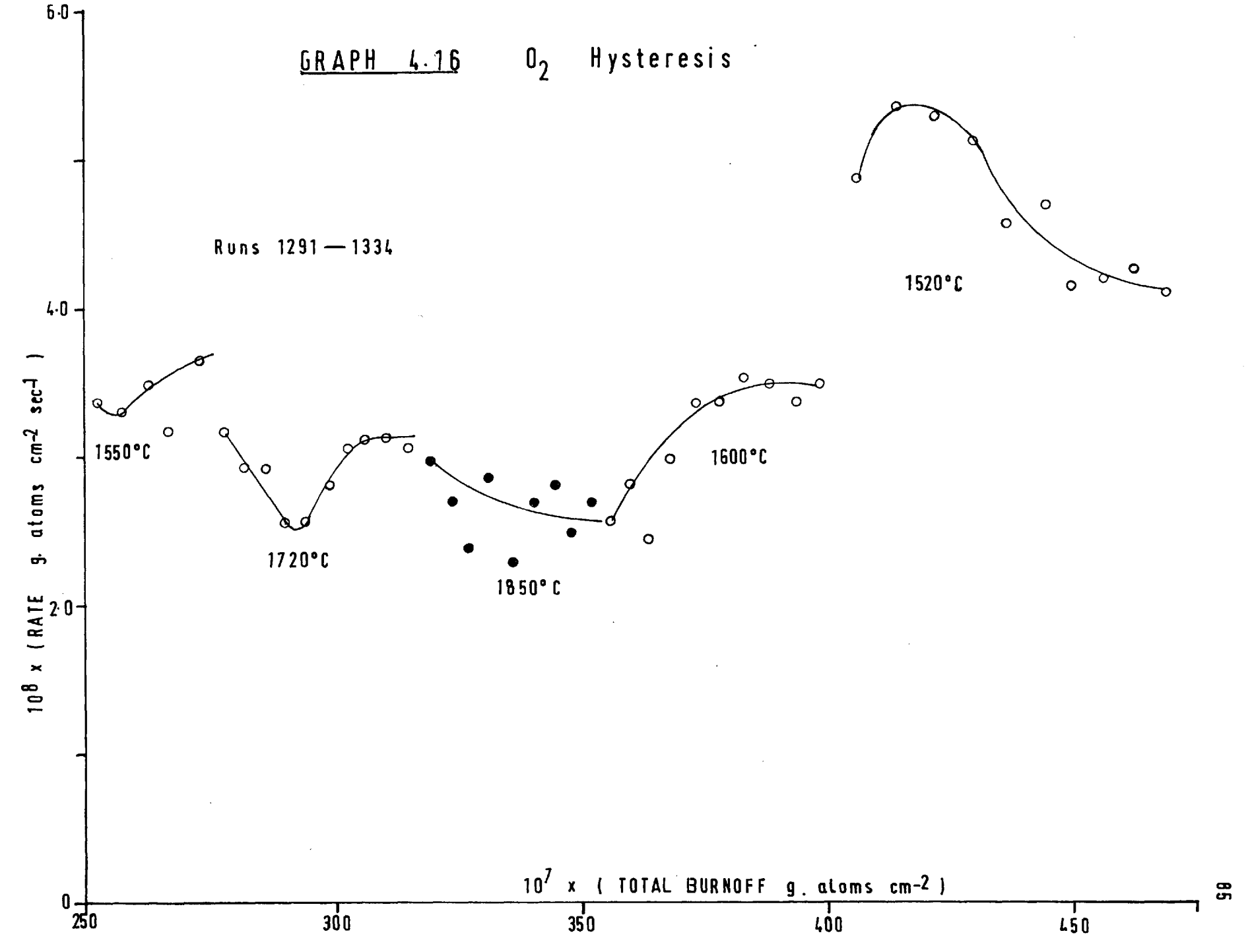
GRAPH 4.16 O_2 Hysteresis
Runs 1291 — 1334
1550°C
1720°C
1850°C
1600°C
1520°C
10^8 x (RATE g. atoms cm^{-2} sec^{-1})
10^7 x (TOTAL BURNOFF g. atoms cm^{-2})
6·0
4·0
2·0
0
250
300
350
400
450

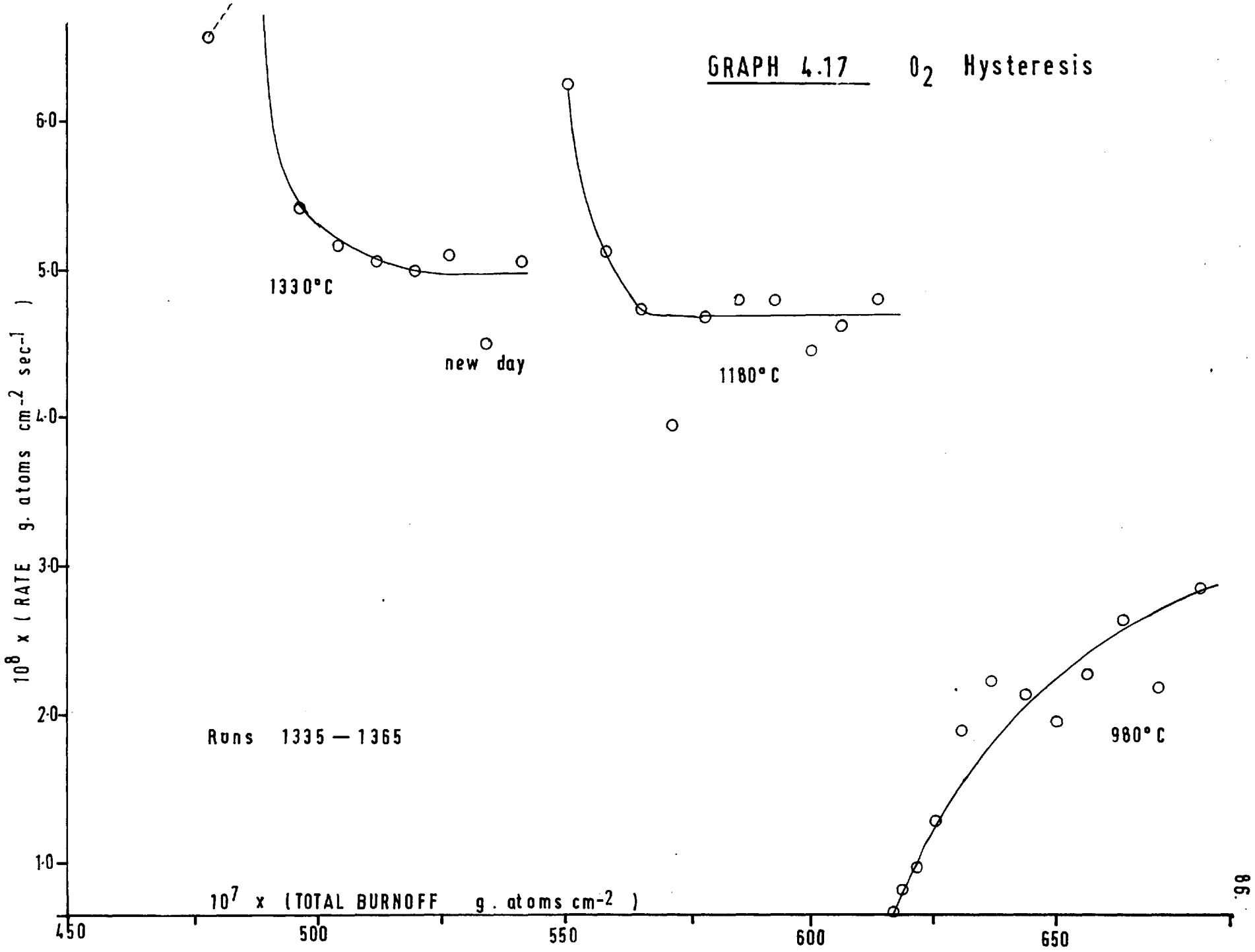
GRAPH 4.17 O_2 Hysteresis
1330°C
new day
1180°C
980°C
Runs 1335 — 1365
10^8 x (RATE g. atoms cm^{-2} sec^{-1})
10^7 x (TOTAL BURNOFF g. atoms cm^{-2})
6·0
5·0
4·0
3·0
2·0
1·0
450
500
550
600
650

GRAPH 4.18. Variation of steady state rate with temperature at 50 μ

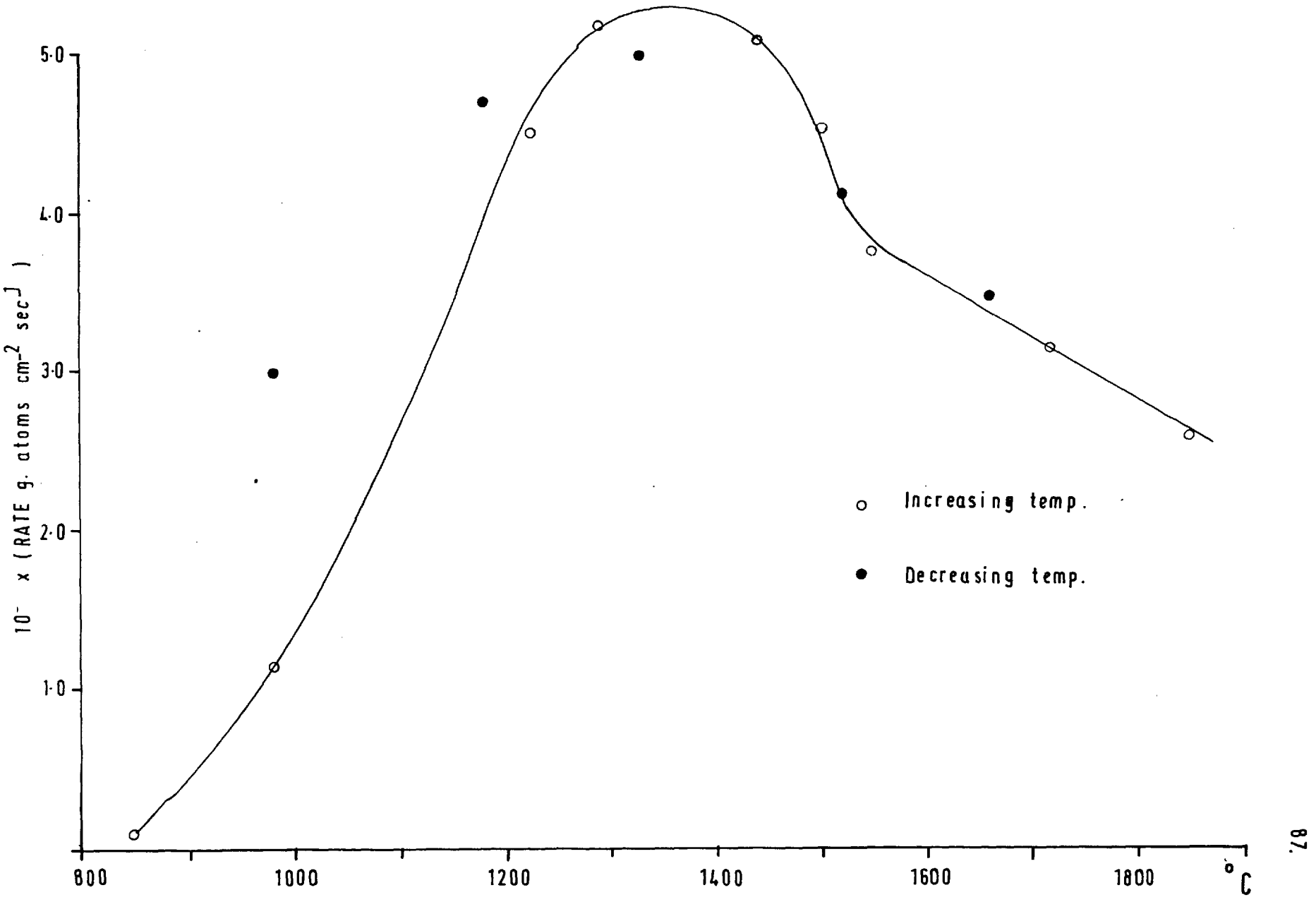

1330°C, Graph 4.17, the initial rate was lower than the general trend of the subsequent rates, although this series was not started on a new day.

From the steady rate values obtained on these hysteresis curves a composite rate-temperature curve was obtained, Graph 4.18.

The down points on this curve indicate that generally the filament was not permanently activated by reaction since the same constant rates were obtained after considerable burn off. However the final runs at 980°C, Graph 4.15, showed no tendency for the rate to stop increasing, and the rates obtained were much higher than those obtained earlier. The burn off on the filament by the time reaction was carried out at 980°C was about 6 $x10^{-5}$ gr atoms/cm^2 and it is possible that by then the pyrolytic carbon had been consumed.

Comparison of Graph 4.18 with the 'up' and 'down' rate-temperature curves, Graph 4.1, indicates that the highest rates obtained on the latter curves were near the steady rate values. That is the true rate does not lie between the 'up' and 'down' curves. This conclusion is in keeping with the hysteresis results described in 4.4.1.

4.5. Effect of Burn off on Hysteresis for Filament Reacted in both N_2O and O_2.

A series of runs on the same filament were carried out to see if treatment affected the rate in oxygen and conversely. The filament used was freshly coated and degassed at 1500°C. The series of runs were carried out in the following order:

1.	Reaction in O_2 at 970°C	2.	Reaction in O_2 at 1300°C
3.	" " O_2 " 960°C	4.	" " N_2O " 1300°C
5.	" " N_2O " 1300°C	6.	" " O_2 " 1300°C
7.	" " N_2O " 970°C	8.	" " N_2O " 1300°C
9.	" " O_2 " 1300°C	10.	" " N_2O " 1300°C

The results of these runs are given in Table A.4.17 and plotted on Graphs 4.19 - 4.22.

4.5.1. Oxygen-Oxygen results. Graph 4.19.

The curve given by reaction at 1300°C after reaction at 970°C follows the same form as the earlier results, although of smaller magnitude, Section 4.4, and again the value of R finally obtained is much higher than the mid value for the rate-temperature curves. Reaction at 970°C and 960°C after heating in vacuum at 1500°C and in oxygen at 1300°C respectively generally showed negligible hysteresis effect, except for the first point. This first point could be due to experimental errors but if the dotted portion of the curve is considered the hysteresis appears to be effective over a total burn off of about 7 $x10^{-7}$ gr atoms/cm^2 sec, which is again of

the same order of magnitude as found by Duval. This hysteresis in the low sense which is again as found by Duval. Curve A gives initially a higher rate after heating in vacuum which is the high sense. This is in keeping with the rate-temperature curves but may be due to some other factor; it being possible that both reaction and heating in vacuum activate the surface at 1500°C, but by different mechanism. This is also the reverse of the results given in section 4.4.1 where heating in vacuum at 1100°C appeared to deactivate the filament for reaction at 1100°C.

4.5.2. Nitrous oxide-Nitrous oxide results.

Reacting a filament in N_2O at 1300°C after reaction at 970°C in N_2O shows hysteresis in the low sense, Graph 4.22 Curve B. The constant rate achieved is about 9.0×10^{-9} gr atoms/cm^2 sec. which is very close to the rate found on the rate-temperature curves for the filament previously burnt in oxygen, Graph 4.10. This rate is reached after a burn off of approximately 7×10^{-7} gr atoms/cm^2 and the hysteresis is consistent with the earlier rate-temperature curves of Strickland-Constable. This author also reported that a filament activity increased with burn off for reaction in N_2O and although this was not found in our earlier results it can possibly be seen in Curve B, Graph 4.21, where reaction was at 970°C after reaction at 1300°C. This particular

GRAPH 4·19 Variation of rate with burnoff in O_2 after reaction in N_2O and O_2.

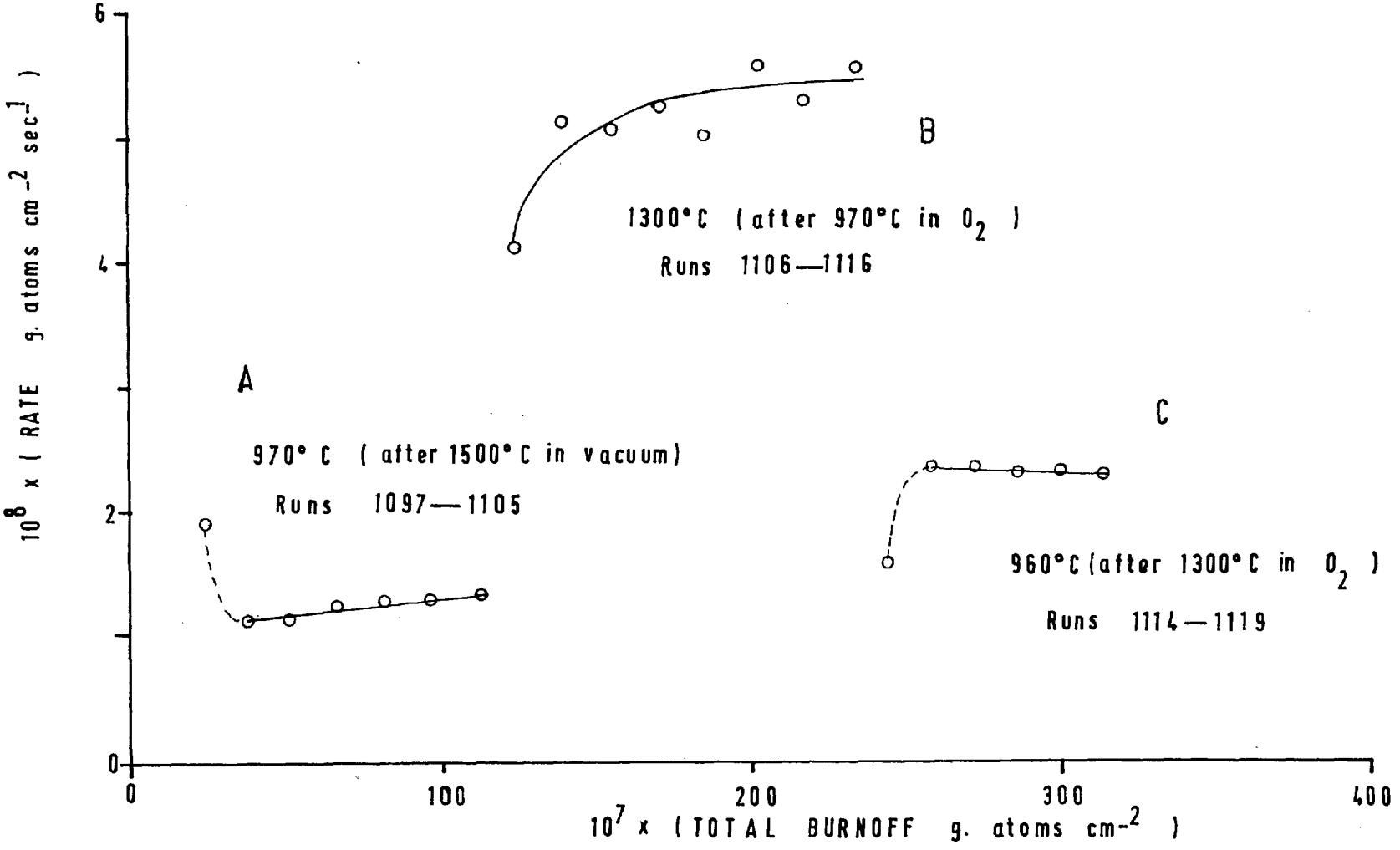

GRAPH 4.20 Variation of rate in O_2 with burnoff, after reaction in N_2O and O_2

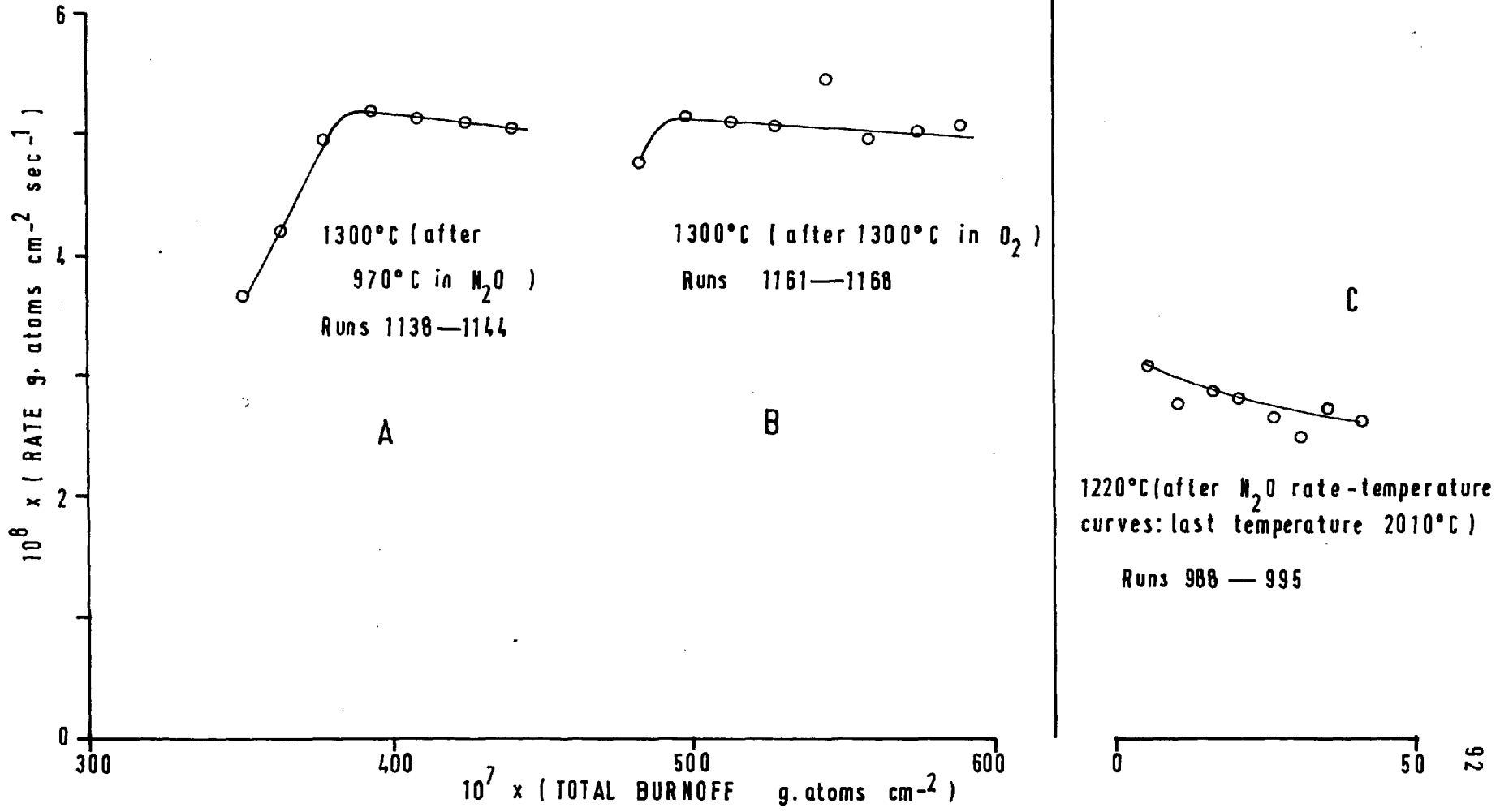

GRAPH 4.21 Variation of rate with burnoff in N_2O, after reaction in N_2O and O_2

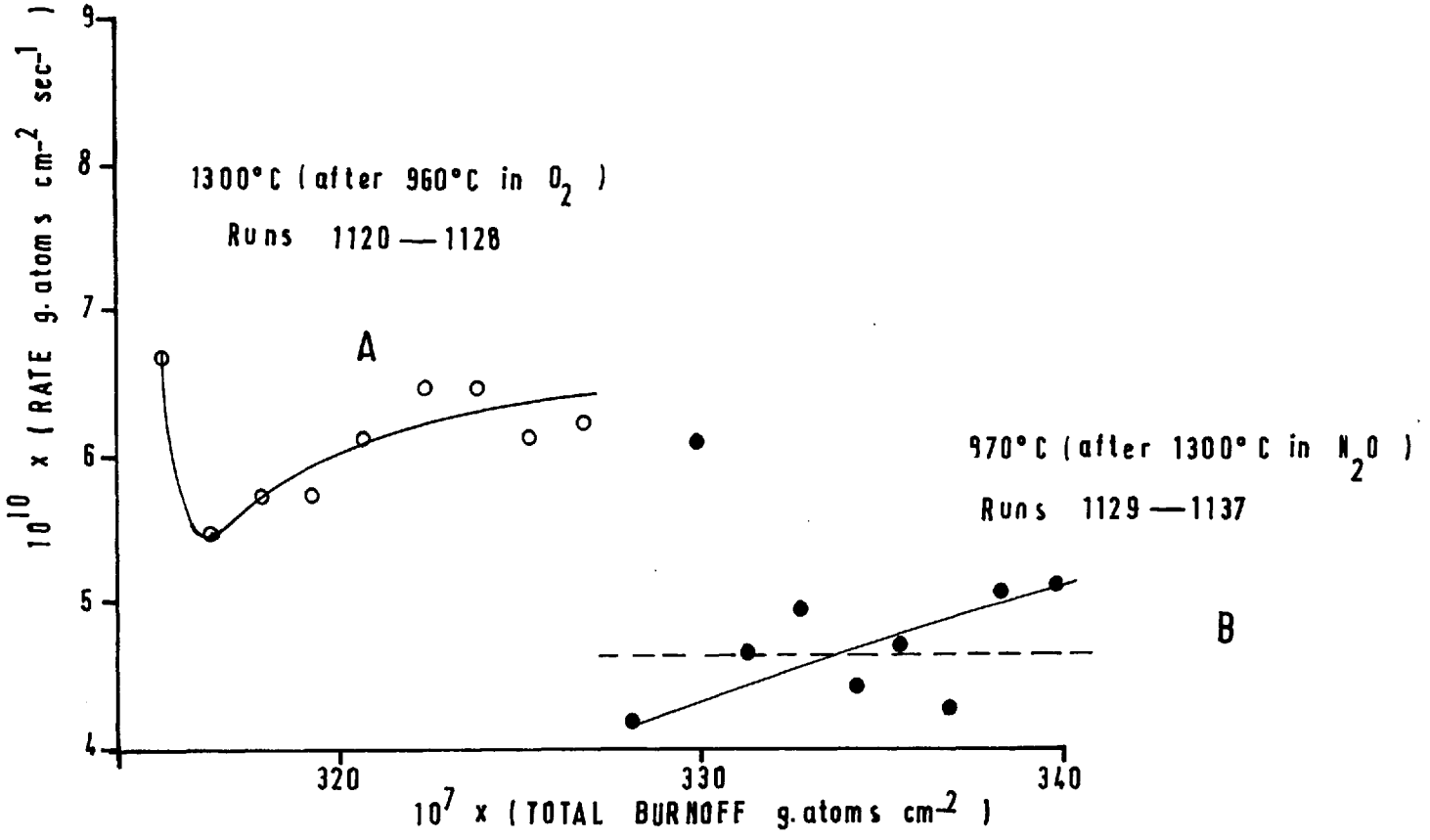

GRAPH 4.22 Variation of rate with burnoff in N_2O, after reaction in N_2O and O_2.

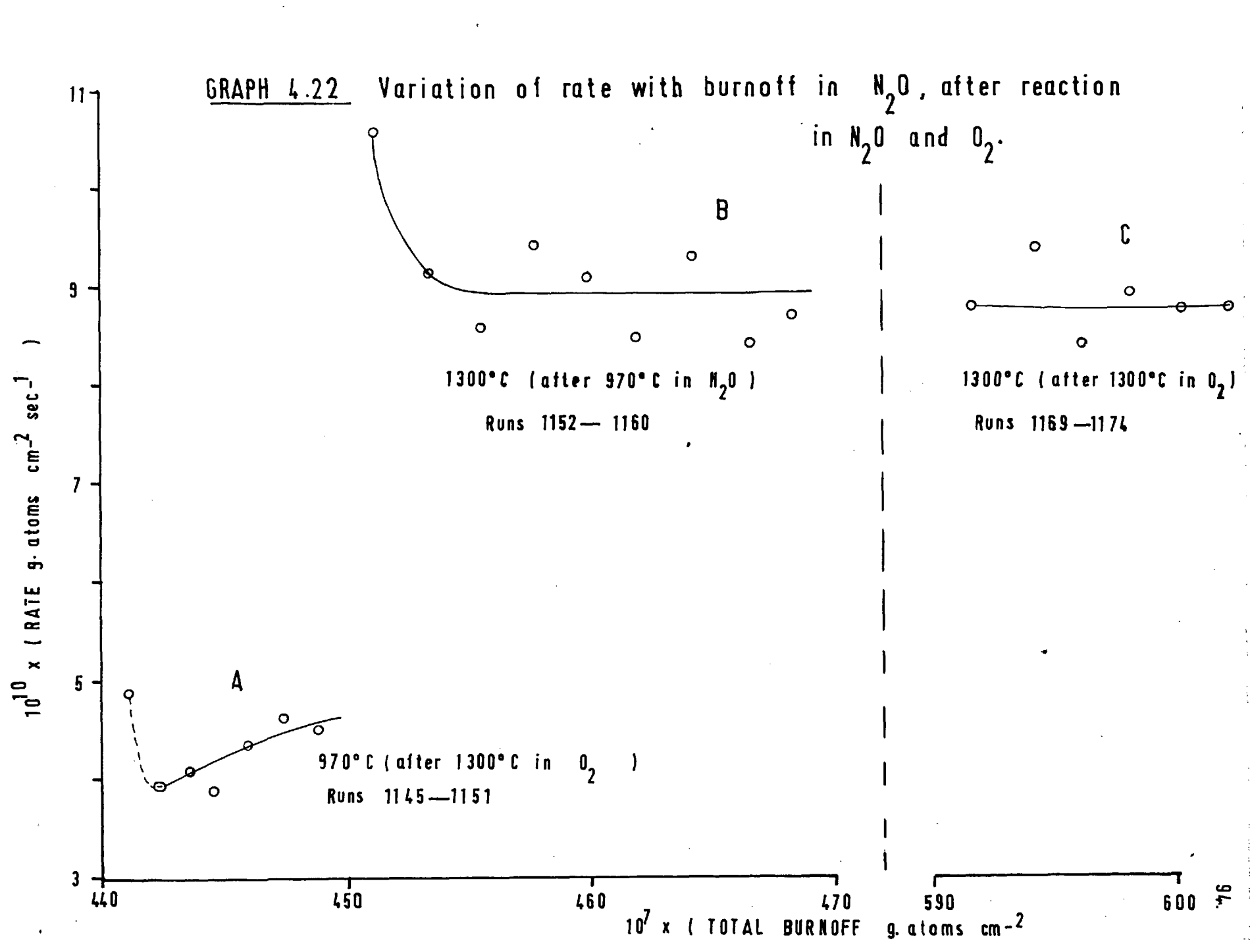

result is in no way conclusive due to the large scatter of the points.

A further example of where increased burn off did not increase the activity of the filament is given in Runs 1004-1009, where reaction was at 1960°C on a freshly coated filament last degassed at 2000°C in vacuum. The rate showed no increase with burn off remaining constant about 0.6 $x10^{-9}$ gr atoms/sec cm^2, Table A.4.14.

4.5.3. Reaction in O_2 after burning filament in N_2O.

Reaction in oxygen at 1300°C after reaction in N_2O at 970°C, Curve A, Graph 4.20, shows that the sense of the hysteresis is not affected, it being in the same sense as if the reaction were in oxygen, although the curve is much sharper. Reaction at 1300°C after reaction in N_2O at 1300°C shows very little effect, Curve B, Graph 4.20, except for the first 7 $x10^{-7}$ gr atoms/cm^2 burn off where the filament seems to have been deactivated by the treatment in N_2O. This could also be due to oxygen adsorption. A filament burnt at 1220°C after the N_2O rate-temperature curves at which the last temperature was 2010°C showed slight hysteresis in the low sense, Curve C, Graph 4.20. This result can be compared with the results given in Section 4.4 where it was shown that reaction at 1100°C after 1750°C in reaction gave a high sense hysteresis while heating in vacuum at 1750°C gave a low sense hysteresis.

4.5.4. Reaction in N_2O after burning in O_2.

At 1300°C the filament does not seem to be affected by previous burning in O_2 for subsequent reaction in N_2O; Curve C, Graph 4.22. The curves A on Graph 4.21 and Graph 4.22 for reaction in N_2O at 1300°C and 970°C after reaction in O_2 at 960°C and 1300°C are of very similar shapes. They both suggest that initially the filament is more reactive. It is also quite likely that the initial runs are due to desorption of O_2 from the filament and blocks.

In support of this hypothesis it is known that oxygen is adsorbed while nitrous oxide is not. When reaction is in oxygen only, by suitable degassing and short reaction times the rates of desorption and adsorption are equal. For following reaction in nitrous oxide the desorption still takes place. Conversely for reaction in oxygen following reaction in nitrous oxide the filament would be in a greater state of desorption and so adsorption would take place. It would also seem possible that this could explain the result on Graph 4.13 where reaction in oxygen at 1380°C following reaction in oxygen at 1750°C gave an initially low rate.

However this result and the result for oxygen following reaction in N_2O given on Graph 4.20 does not seem explicable on this hypothesis because in both cases the oxygen balances where 100% showing no net adsorption. The quantity adsorbed would need to be equivalent to 2.4 and 1.4μ CO which

GRAPH 4.23 Effect of burnoff on rate in N_2O at 1800°C

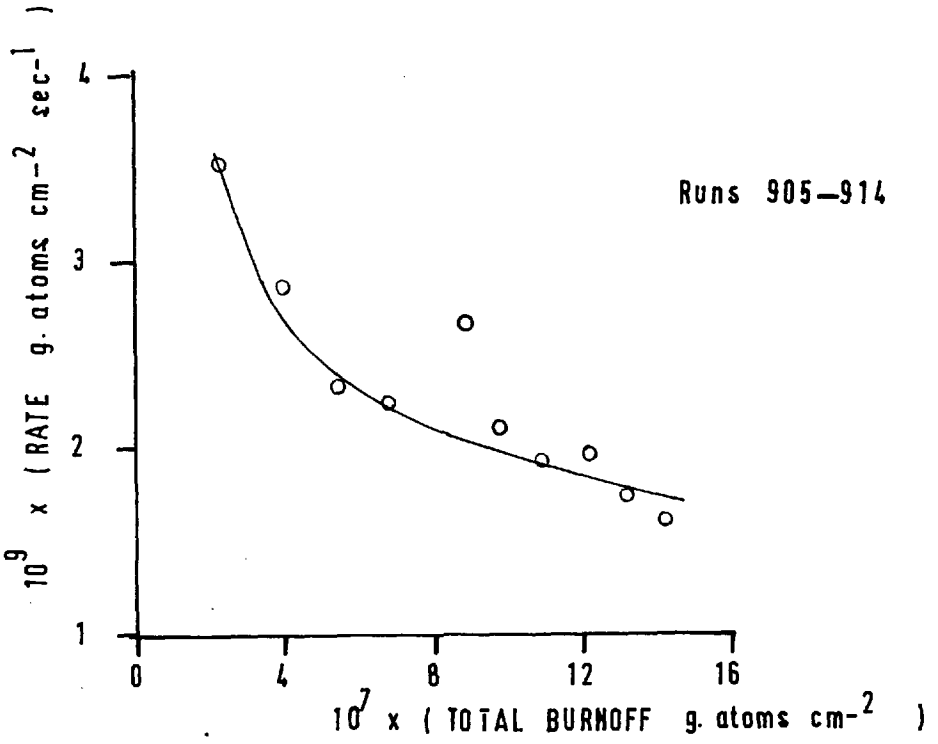

Filament previously reacted in O_2 , and N_2O at 950°C for 2 mins.

would give a significant lowering of the oxygen balances.

In the case of nitrous oxide the reaction times are far longer and the quantity desorbed would only need to be of the order of 0.2μ CO and in this case the explanation appears feasible.

If these initial points are ignored the filament appears to become active with burn off the rate tending to an asymptote and therefore reaction in oxygen appears to deactivate the filament for subsequent reaction in nitrous oxide.

The decrease in activity for reaction in N_2O at 1800°C is shown on Graph 4.23 for a filament previously reacted in oxygen. This case was dealt with in Section 4.3 and it is important to realise that the previous reaction in oxygen was at 5μ, and also the filament was degassed for 27 minutes at 1800°C before reaction in N_2O. In the light of the other results given here it is suggested that this initial activation is not due to the fact that the previous reaction was in oxygen, but rather due to the fact that the previous reaction was at a much lower pressure. It is in fact a pressure hysteresis effect as found by Duval.

4.6. Verification of true hysteresis effect.

In the previously mentioned results there is a certain amount of doubt as to whether the hysteresis is a true hysteresis effect or to whether the effect was largely

due to basic increased reactivity of the filament. The results shown on Graph 19 suggest that the activity of the filament at low temperatures had increased with burn off.

In order to verify the hysteresis effect a freshly coated filament was reacted at 950°C and 1270°C alternatively after steady rate values had been reached. The results are plotted on Graphs 4.24 and 4.25; the numerical values being given in Table A.4.18.

Examination of these curves shows that the reactivity does not increase with burn off. This is particularly evident for the curves at 950°C, curves 1,3 and 5, and the hysteresis is in the same sense as generally shown by the other results. The slight variations in the steady rate achieved could be due to slight differences in the filament temperature it being impossible to estimate the temperature closer than 10°C. Also for curve 6 when the rate was slightly lower, a considerable burn off had already taken place and this lowering may therefore be due to a reduction in the diameter of the filament.

For a new filament Curve 1, Graph 4.24, shows a considerable time of reaction is necessary to achieve a steady rate at 950°C. It is therefore thought that the apparently erroneous results on Graph 19 were due to the fact that initially the reaction at 970°C (Curve A) was not continued sufficiently long for a true steady value to be obtained.

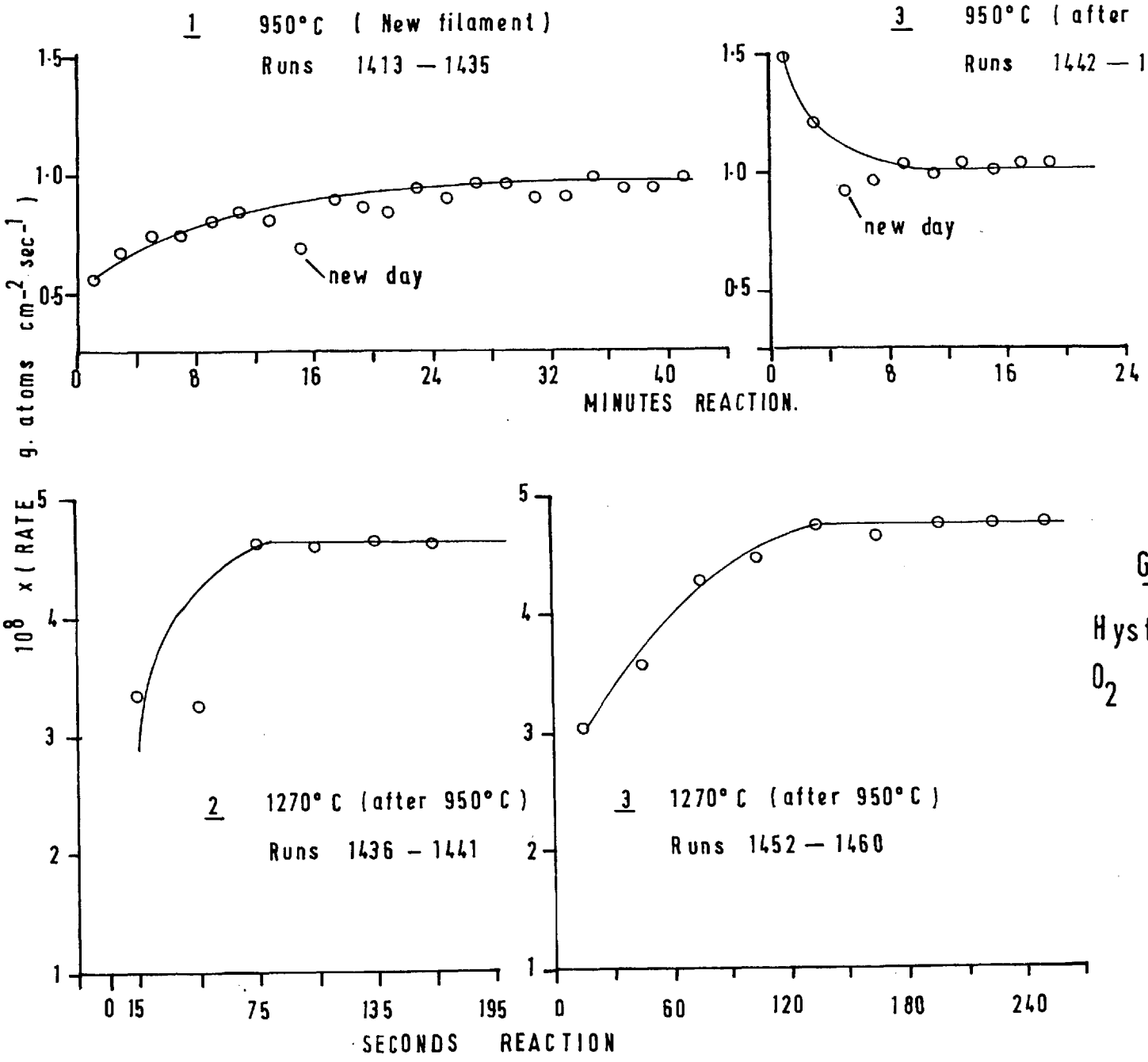

GRAPH 4.24

Hysterisis in O_2 at 50μ

GRAPH 4.25 Hysterisis in O_2 at 50μ

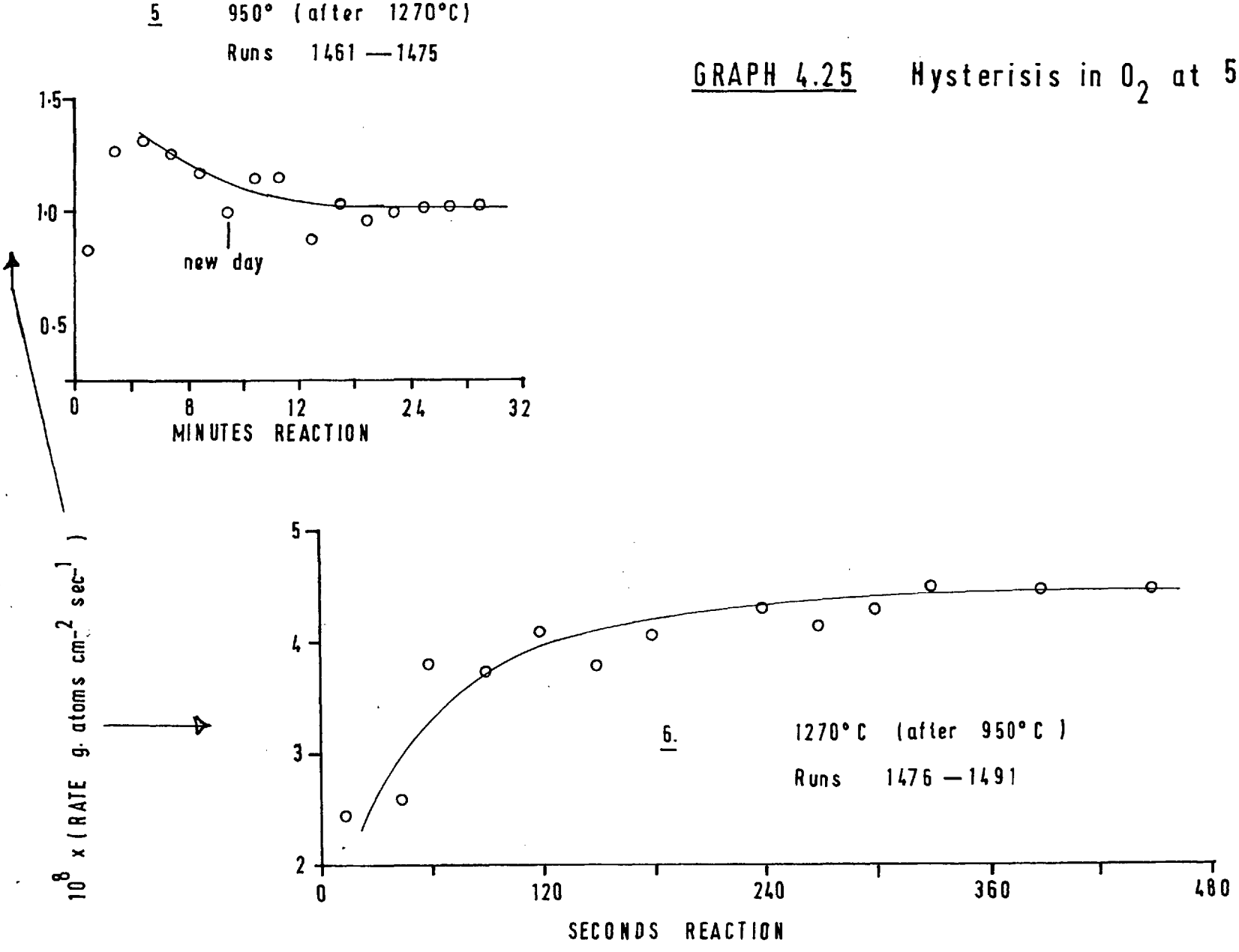

Examination of curves 2,4 and 6 show that the amount of reaction, both in time and burn off, necessary to reach the steady state increases with increasing burn off. There is also evidence of this in comparing Curves 3 and 5. Earlier results on different filaments, Section 4.4, and 4.5, also showed variations in the amount of reaction necessary to reach the steady state.

Also shown on the graphs are certain values obtained after the filament had been standing overnight under vacuum. As before the rates then found were lower than the general trend. The oxygen balances after run 1469 were slightly high. This is thought to be associated with the fact that the Hopcalite was changed before Run 1469, although a trial analysis was very satisfactory.

In all cases the filament burnt black, via a bronze stage, at 1270°C, and silvery at the lower temperatures. The amount of burn off required to turn a silvery filament bronze and vice versa was found to be fairly constant at about 2×10^{-6} gr atoms of carbon/cm^2. The burn off to turn a matt black filament silvery was also found to be fairly constant at about 4×10^{-6} gr atoms of carbon/cm^2. The letters S, B, and M in Table A.18 show whether the filament was respectively silvery, bronze or matt black.

4.7. Appearance of Filaments.

4.7.1. Colour of filament.

During reaction in N_2O only, the filament maintained its silvery appearance, while at certain reaction temperatures in oxygen the filament became matt black. This blackening of the filament occurred around the point of maximum rate, and the filaments returned to a silvery appearance at both very low and high temperatures. This phenomenon was noticed during the rate-temperature curves for both methane and CCl_4 prepared filaments. For the 50μ runs the exact temperatures at which the filament was black or silvery were not well defined depending so much on the past history of the filament. For the 5μ runs the filament was initially black and remained black after 30 minutes reaction at 850°C in 5u of oxygen and throughout the rate temperature runs. For the low burn off runs the initially silvery appearance became greyish after reaction at 1050°C, recovering its silvery appearance at the end of the series of runs.

The way the filament became black at intermediate temperatures and silvery at low temperatures was shown after run 862 when the reaction was in oxygen at 1440°C, the filament being black. After reacting at 930°C for 8 mins. the filament reverted to its silvery colour. The reverse was shown during runs 863-874 at 1350°C when the initially

silvery filament remained silvery for the first 45 seconds reaction but after a further 30 seconds the filament became quite black. The temperature above which the filament goes black must be near 1100°C because during runs 1181-1199 at 1100°C the filament only became slightly tarnished. Reaction at 1750°C, Runs 1175-1180, did not cause the filament to become blackened.

There appeared to be very little direct relationship between the blackening of the filament and its reactivity. For although during reaction at 1330°C after 1520°C and at 1180°C after 1330°C, Graph 4.17, there was a considerable decrease in rate the filament remained black. On the other hand for the reaction at 980°C, Graph 4.17, while the rate was steadily increasing, the filament was becoming progressively more silvery.

Between the dead black and silvery states the filament appeared to go through a bronze state. This is probably due to very slight roughness on a microscopic scale causing optical interference and hence the bronze colour.

Heating a black filament in vacuum at 1800°C for 5 minutes caused no visible change but on raising the temperature to 2000°C the filament became silvery at the ends after 5 minutes and silvery over the whole length after a further 5 minutes. At this temperature the actual vaporisation of carbon becomes significant.

The N_2O results on oxygen treated filaments were such that the filament remained in its initial state either black or silvery. During runs 988-994 the total burn off required to turn a filament black in oxygen was 877 $x10^{-8}$ gr atoms carbon/cm^2. Burning the filament subsequently in N_2O for a total of 345 minutes to give a total burn off of 6.6 $x10^{-5}$ gr atoms/cm^2 caused no visible change in the filament.

Both Duval and Strickland-Constable found blackening of the filament at certain temperatures in oxygen. Duval reported that his filaments burnt black and matt at low temperatures while at high temperatures that they became greyer and more brilliant. Strickland-Constable on the other hand reported that his filaments burnt black at high temperatures but recovered their silvery appearance at low temperatures. In our case the filaments burnt black at high burn off at intermediate temperatures and recovered at low burn offs. Nitrous oxide did not burn a filament black, but neither did it burn a black filament silvery. For the filament to be turned silvery st high temperatures in oxygen considerably longer heating was required if heating in vacuum than if reacting in O_2. It seems likely that the effect in vacuum is due to the slow vaporisation of the carbon at these high temperatures.

4.7.2. Microphotographs of filaments.

A freshly coated filament shows the cone structure typical of pyrolytic carbon, Photo.1. The filament formed from CCl_4 was characterised by more closely packed cones with less size fluctuation, Photo.2.

After reaction the cones were still clearly visible but no hexagonal pits could be detected as reported by some workers[255], even at 900°C. Filaments burnt in oxygen at 1200°C and 2000°C are similar in appearance although the filament at 2000°C does appear smoother with less visible cones as can be seen by comparing Photos 3 and 4.

Filaments reacted in N_2O were often characterised by several deep craters on their surface, small cones again being visible at the bottom of the biggest craters. A typical shallow crater is shown in Photo.5 and it can be seen how smooth the filament is around the crater. The filament burnt in O_2 and then N_2O showed no such craters; a typical part of the surface being shown in Photo.6 which is very similar to the oxygen only reacted filaments. It is thought that the craters are initially formed when trying to activate the filament at 2000°C in 1.5 mm.Hg of N_2O. During these attempted activations many fused and hot spots formed - both facts could be associated with craters. On the filaments actually used only about 6-8 large craters were

visible with no smaller craters visible even at the highest magnification.

4.7.3. Spectrographic analysis of filaments.

Certain filaments were analysed by a spark spectroscope. The results for uncoated, coated and unreacted filaments are shown in Table 4.2. Several substances were present but the main impurity was iron.

The higher boron concentration found on filament 25 could be due to the reactor not being clean after the boron runs. All the other substances were found in very nearly equal quantities and were present in the original cellulose decomposed filaments.

This type of analysis, as such, however,gives no indication as to whether these impurities are present in the pyrolytic carbon by diffusion from the interior.

Table 4.2. Spectrographic analysis of untreated filaments.

Filament 1. Coated with pyrolytic carbon, but not reacted.

Filament 25. Coated with pyrolytic carbon, and then reacted in oxygen. Runs 557-567.

Substance	Detection Limit (ppm)	Filament 1	Filament 25	Uncoated filament
Copper	5	-	-	-
Platinum	50	-	-	-
Boron	10	v.slight trace	*	very slight trace
Tungsten	500	-	-	-
Tin	50	-	-	-
Zinc	20	-	-	-
Iron	10	*	*	* 20-30 ppm
Silicon	20	*	*	*
Magnesium	5	*	*	*
Aluminium	5	*	*	*
Calcium	20	*	-	-
Manganese	10	very slight trace	*	very slight trace
Phosphorus	100	*	*	*

* The substance was definitely found, although only as traces. The boron detected for the uncoated filament could have come from the electrodes since in this case they were not boron free.

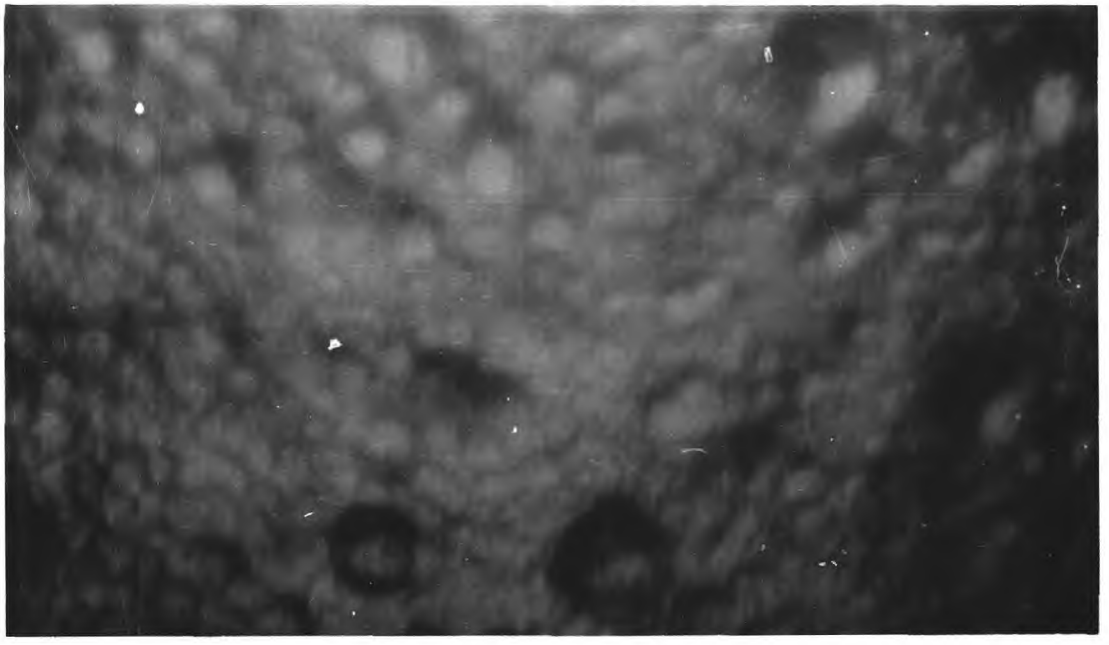

Photo 1. Coated filament but unreacted. x1900

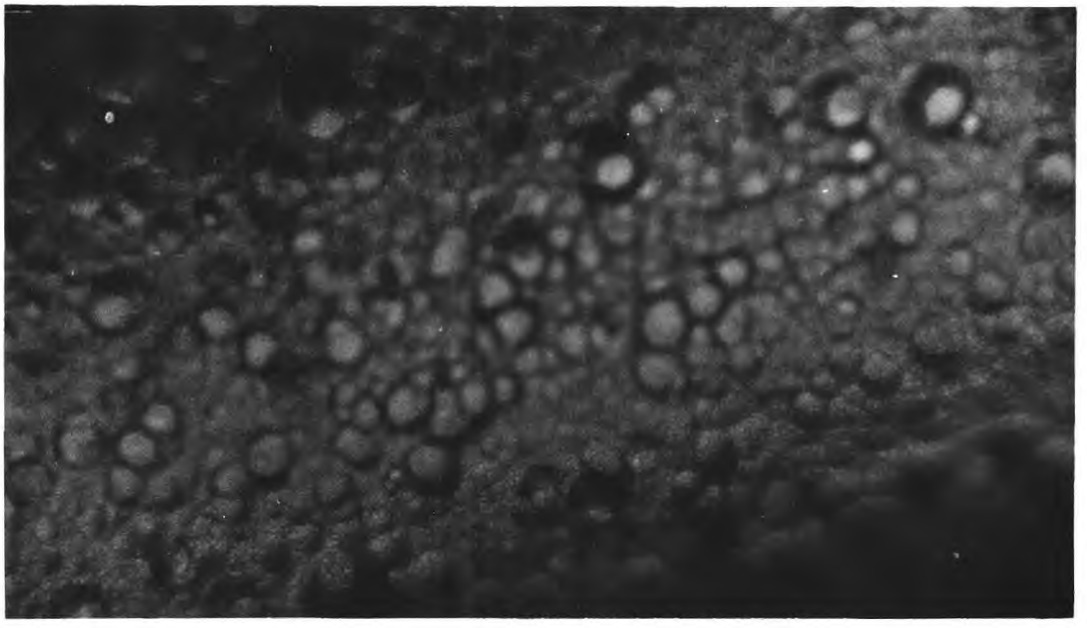

Photo 2. CCl_4 prepared filament, last reacted at 1550°C.
Filament No. 48 x1900

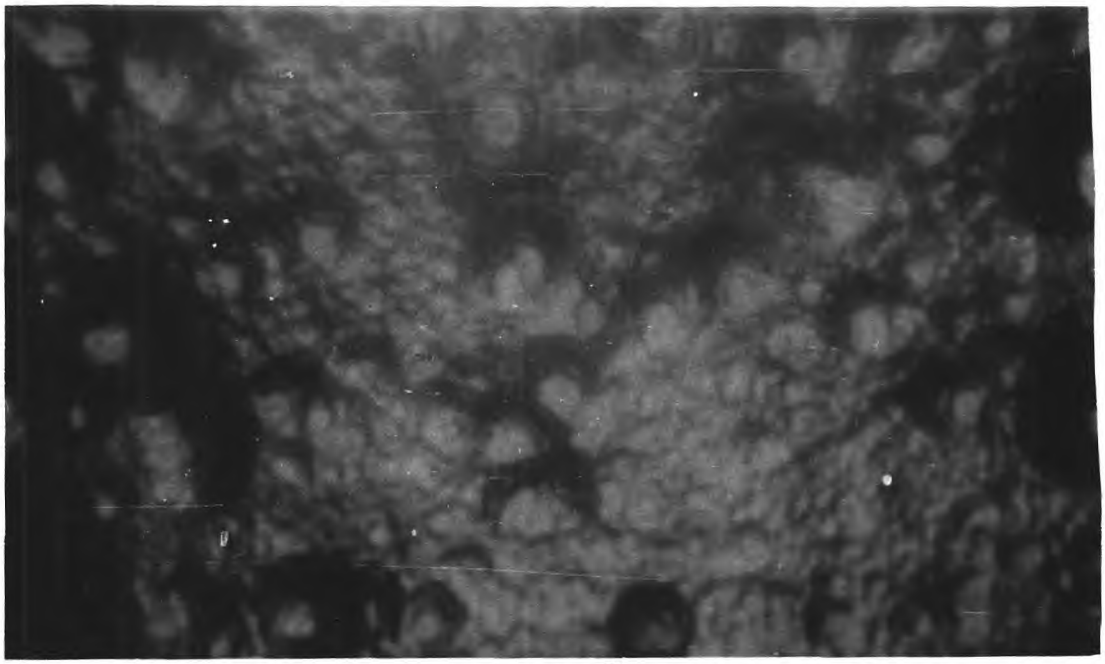

Photo 3. Reacted in O_2 at 1270°C; filament black.
Filament No. 49. x1900

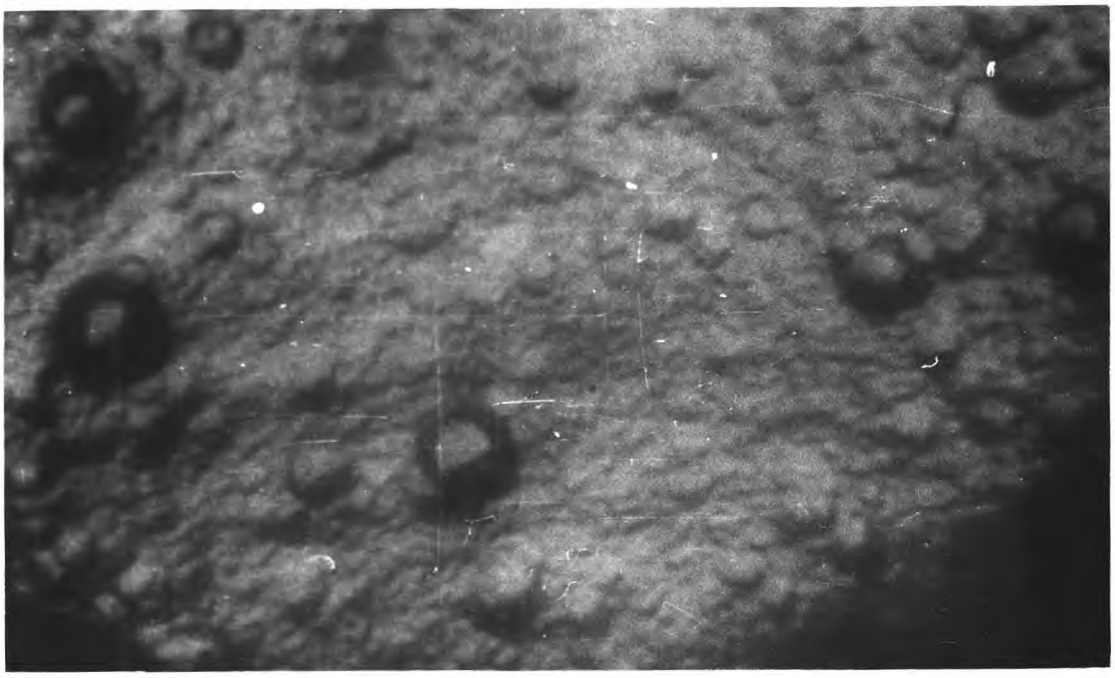

Photo 4. Reacted in O_2 at 2000°C; filament silvery.
Filament No. 50 x1900

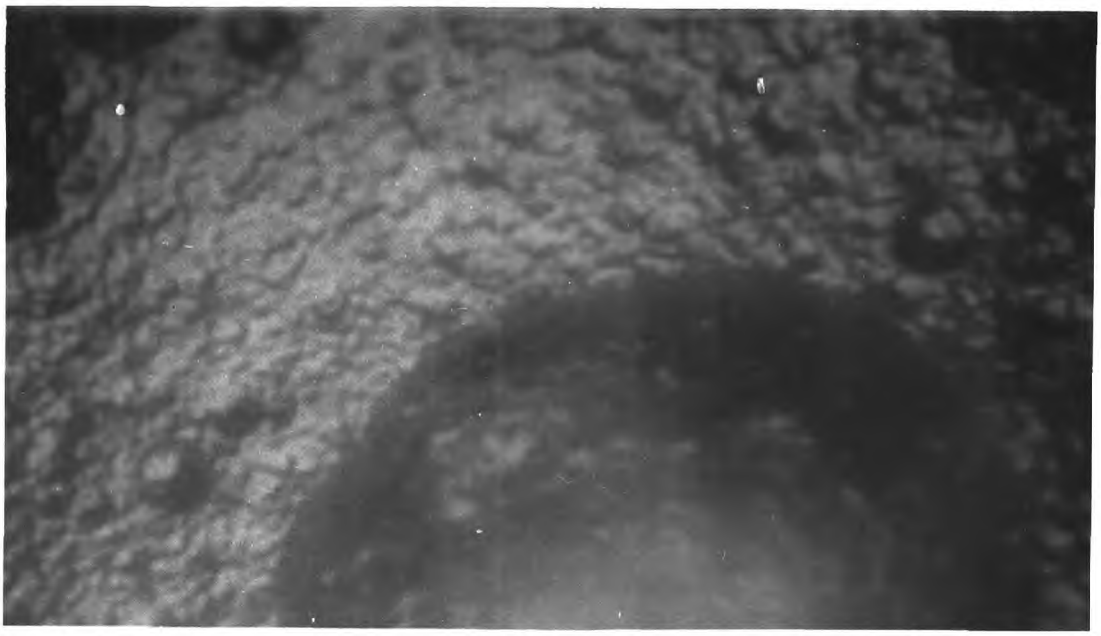

Photo 5. Reacted in N_2O, showing crater. Filament No. 45.
x1900

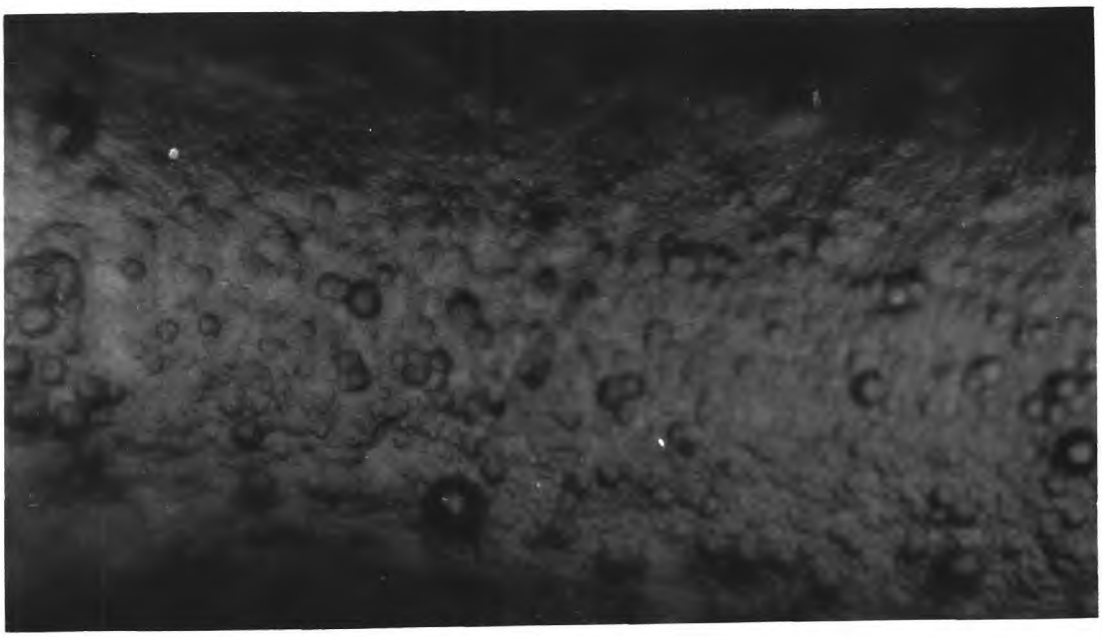

Photo 6. Reacted in O_2 and then N_2O; filament silvery.
Filament No. 43 x800

4.8. Summary of Experimental Results for Untreated Filaments.

4.8.1. Rate-temperature curves in oxygen.

a). At 50μ a second series of runs on the same filament reduced the hysteresis effect and brought the curves closer together. Graph 4.1.

b). The product was predominantly CO but the CO_2 concentration increased after 1500°C. Graph 4.3.

c). At 50μ the hysteresis changed sense between 1390°C and 1450°C.

d). At 150μ for a filament reacted up to 1800°C the hysteresis was all in the high sense. Graph 4.4.

e). At 5μ the hysteresis changed sense at 1200°C while above 1500°C the enhanced zero order was evident.

f). Low burn off curves at 50μ were in good agreement with the earlier results.

g). A carbon tetrachloride filament showed a hysteresis crossover at 1800°C, the rates of reaction being comparable with the methane prepared filament.

Selected figures from these results are given in Table 4.3.

4.8.2. A steady value rate-temperature curve showed no increase in rate above 1500°C; the rates of reaction were found to be near the highest rates reached in the 'up' and 'down' rate-temperature curves.

4.8.3. The order of reaction above 1000°C was 1.5 order between 20μ and 150μ. At 1000°C the reaction tended to be first order over the whole pressure range. Using other workers data the reaction between 0.65μ and 5μ was first order. Graph 4.6.

4.8.4. The rate-temperature curves for nitrous oxide showed very little hysteresis below 1500°C and above this temperature the rate increased steadily with temperature. The filaments were far less active towards N_2O than towards O_2. Graphs 4.9 and 4.10.

4.8.5. Hysteresis in oxygen. In general the sense of the hysteresis observed was the same as found by the up and down temperature curves and showed signs of a crossover in sense. At very high temperatures the magnitude of the hysteresis was much smaller.

The burn off required to attain a steady rate value was not constant, and the amount was considerably larger than found by Duval. A CCl_4 prepared filament gave results consistent with the others at 50μ.

Heating in vacuum, and leaving a filament standing in vacuum overnight appeared to temporarily deactivate the filament.

4.8.6. Steady rate curve. A series of hysteresis runs, burning the filament until a constant rate was obtained, gave a rate-temperature curve with the rates of reaction near the

values obtained on the up curve of the earlier rate-temperature curves. The maximum was also shifted to a higher temperature than predicted by the earlier non steady-state curves. The filament did not appear to be permanently activated by reaction until after a considerable burn off.

4.8.7. This last conclusion was verified by the results given in section 4.6, where repeated reaction between 950°C and 1270°C gave constant rates for each temperature. These results also showed a tendency for the time required to reach a steady rate to increase with increasing burn off of the filament.

4.8.8. Hysteresis in N_2O. The hysteresis in N_2O was much smaller than found for oxygen but that which existed was in the low sense which is opposite to the oxygen results but consistent with earlier workers results.

The filament did not appear to become very activated by prolonged reaction in N_2O as has been reported. There was a suggestion in the results that reaction in O_2 tended to deactivate the filament for subsequent reaction in N_2O.

4.8.9. Reaction in N_2O appeared to have a negligible effect on subsequent reaction in O_2.

4.8.10. The filaments went black at high reaction rates in the intermediate temperature range for O_2 and returned to a silvery colour by reaction below 970°C; or reaction, or

heating in vacuum at 2000°C. The burn off required to turn a silvery filament black, and vice versa, was about 4 $x10^{-6}$ gr atoms of carbon per cm^2; about half the burn off turning the filament bronze.

N_2O reacted filaments did not burn black, but remained black if initially black.

A filament reacted at 2000°C appeared only slightly different under the microscope to one reacted at 1200°C, the former being somewhat smoother. A filament prepared from CCl_4 had more prominent cones on the surface than CCl_4 prepared filaments.

Several impurities were analysed in the bulk of the filaments, the main one being Fe which was at 20-30 ppm.

Table 4.3. Results of rate-temperature curves in oxygen.

Pressure	50μ	50μ	50μ	50μ	50μ	50μ	150μ	5μ	50μ
Runs Nos.	592-602	603-615	557-567	568-579	853-862	1077-1098	40-61	886-903	1049-1071
Graph No.	4.1	4.1	A4.1	A.4.1	4.2	4.7	4.4	4.5	4.8
Filament	27	27	25	26	43	51A	4	43	48
Max. rate in up curve	2.7	3.2	3.4	3.2	(3.8)	4.0	16	0.24	5.1
T°C of above	1300	1360	1340	1000	-	1210	1400	1250	1300
Max. rate in down curve	4.7	3.9	6.2	5.2	(5.7)	9.6	36	0.32	5.5
T°C of above	1240	1270	1180	1230	-	1140	1260	1100	1350
T°C of hysteresis curve	1390	1425	1410	1620	1530	1470	None	1210	1800
Rate at cross over	2.6	3.2	3.3	2.1	3.4	2.8	-	0.24	3.5
	1	1			2	3			4

All rates x 10^{-8} gr atoms carbon cm^{-2} sec^{-1}

Up means increasing temperature.

1. Same filament
2. Reaction only from 1400°C to 2000°C.
3. Low burn off runs.
4. CCl_4 prepared filament.

Steady rate value curve, Graph 4.16, maximum at 1350°C for a rate of 5.3 x10^{-8} gr atoms cm^{-2} sec^{-1}.

5. EXPERIMENTAL RESULTS FOR TREATED FILAMENTS.

5.1. Tin, Zinc and Platinum (Blank runs).

In all cases the particular substances were evaporated onto freshly coated pyrolytic filaments. In the case of the tin, platinum and earlier zinc runs up to Run 331 the CO was analysed by combustion on a platinum filament. Although this method was subsequently found to be less accurate than the use of Hopcalite, for the particular runs tabulated check analysis before and after the series were satisfactory and oxygen balances were fairly close to 100%.

5.1.1. Pieces of tin were supported in a platinum coil and when the latter was heated the tin melted into globules. A carbon filament was treated by heating the tin in vacuum at 1100°C for 5 minutes, twisting the carbon filament assembly every minute to present a different part of the filament to the evaporating source. During this treatment the pressure in the reactor rose by less than 1μ. Runs were then carried out at 1800°C and these are shown in Table 5.1. The rates realised did not differ greatly from those obtained on untreated filaments where R = 2.88. Table A.5.1.

Since at this high temperature it seemed very likely that the tin would have evaporated off, the carbon filament was recoated and the reaction carried out at 1200°C, Runs 239-242. Again the rates were not significantly different

from those obtained on untreated filaments. At 1800°C the CO_2/CO ratio was found to be higher than at 1200°C again consistent with the untreated results. Examination of the filament after reaction showed deep pitting at the two ends near where the filament was held in the supports while the rest of the filament was covered by a copper-coloured layer.

5.1.2. For runs 332-338 the zinc was evaporated from a Pt filament at 800°C in 50μ of oxygen. During this evaporation a considerable greyish blue deposit was formed on the reactor walls. Subsequent reaction at 1200°C showed a tendency for the rate to be slightly lower, Table 5.2, but the lowering cannot be considered outside the experimental error. During an earlier series of runs the zinc was evaporated from a tungsten filament at 800°C in 50μ of oxygen and although it was subsequently found that tungsten catalysed the reaction, the rates were again marginally lower. In this case it would appear that the temperature of the tungsten filament was too low for tungsten oxides to evaporate off and catalyse the reaction.

The filament, after reaction, showed the same sort of coloration noticed for tin treated filaments, typical of very thin layer of metal.

5.1.3. In order to eliminate the possibility that the platinum wire used to support the additives was affecting the

results a number of blank runs were carried out. A platinum wire was heated in 50μ of oxygen at 1050°C for 30 secs. followed by 30 secs. at 1200°C. During this treatment the pressure change was undetectable on the Pirani Gauge. Runs 329-331, Table 5.3 were then carried out at 1200°C and they showed a slight increase in rate, but again this cannot be considered significant.

5.1.4. It is quite probable that these substances had no effect on the rate because they could not exist on the filament under the reaction conditions. Spectrographic analysis of the filaments, Table 5.4, showed that none of the particular substances were detected on the used filaments. Tin and zinc would evaporate almost completely at 1200°C while any oxides could also have been reduced or evaporated off.

Microphotographs of the same filaments showed a bronze type coloration which only covered patches of the surface, such a patch can be seen in Photo.7, for zinc, which also shows a clear line between the bronze and darker regions. The bronze patches appear lighter on the photographs because they reflected more of the particular incident illumination used. A further example of the speckled surface is shown in Photo 8, almost exactly similar photographs being obtained for the other filaments.

The spectrographic analysis discounts the

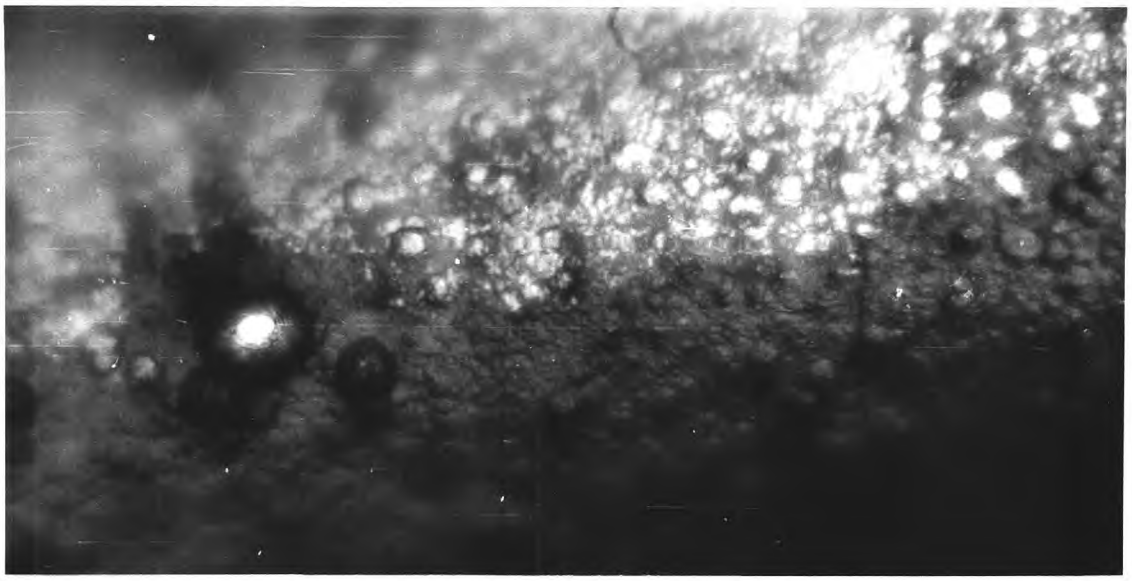

Photo 7. Zinc treated filament. x800

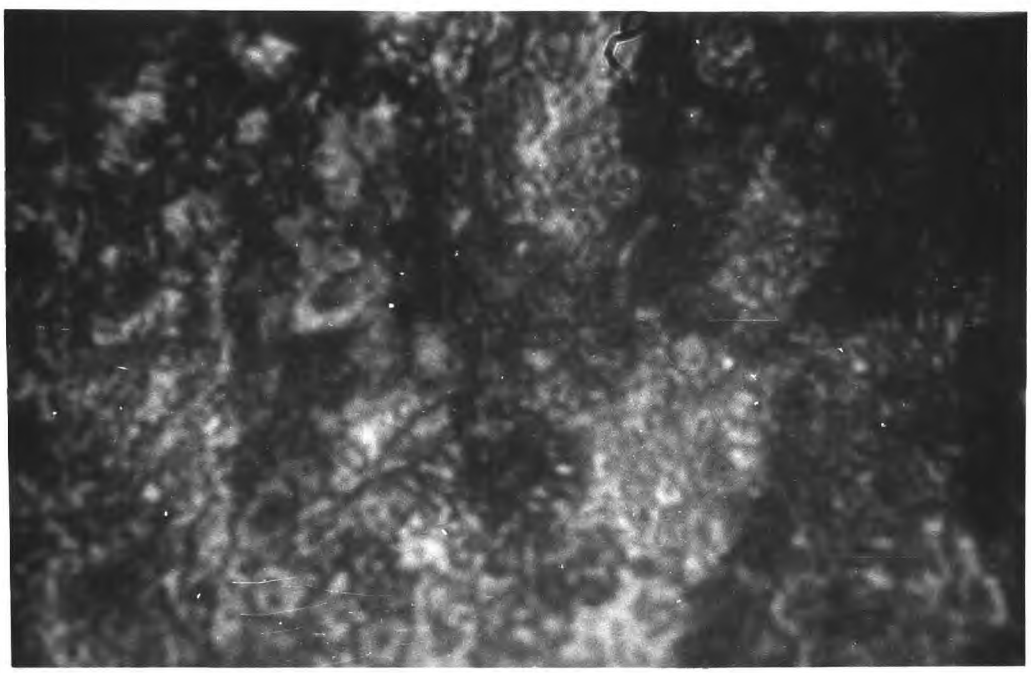

Photo 8. Zinc treated filament. x1900

possibility of these bronze patches being the additive but they could be associated with where the additive has been or has not been. Bronze colouring of the filaments was observed on untreated filaments for the stage between an initially silvery filament and a matt black filament [See section 4.6.1].

Table 5.1 Runs to examine affect of Tin on reaction rate

Filament No.6.

Run No.	T°C	Secs. react.	Initial pressure μ	Pressure CO μ	CO_2/CO ratio	R_8 x10^8	Oxygen balance
235	1800	15	49.6	4.3	0.22	3.22	102
236		30	50.5	9.3	0.18	3.33	100
237		30	51.9	8.9	0.19	3.23	101
238		30	50.7	8.1	0.18	2.91	101
Filament recoated with tin.							
239	1200	30	52.1	15.0	0.08	4.93	104
240		30	53.2	16.0	0.08	5.24	102
241		30	53.4	12.0	0.10	4.01	101
242		30	51.5	11.5	0.07	3.74	101

Table 5.2.

Zinc treated filament. Filament No.15.

Filament reacted at 1200°C.

Run No.	Initial pressure μ	CO pressure μ	CO_2/CO ratio	R $x10^8$	Oxygen balance
332	50.6	8.1	0.44	3.56	98
333	50.7	8.1	0.02	2.55	95
334	47.4	8.4	0.04	2.77	99
Filament retreated					
335	46.6	8.9	0.13	3.07	99
336	47.0	9.6	0.19	3.47	100
Filament retreated					
337	46.4	9.8	0	2.98	99
338	48.8	11.0	0.07	3.35	96

Table 5.3.

Pt treated filament No.15. All reaction at 1200°C.

Run No.	Secs. react.	Initial pressure μ	Pressure CO μ	CO_2/CO ratio	Oxygen balance	R $x10^8$
Untreated filament.						
326	30	47.4	9.8	0.11	100	3.32
327	30	57.4	18.0	0	106	5.47
328	30	48.8	15.4	0.02	104	4.78
Treated with Pt						
329	15	48.7	9.0	0.03	105	5.66
330	15	49.1	9.9	0	102	6.02
331	15	52.7	10.5	0.15	106	7.36

Table 5.4.

Filament No.	Run Nos.	Treatment	Analysis
6	235-242	Tin from Pt filament	Sn N.D. 50ppm DL Pt N.D. 100ppm DL
11	284-293	Zinc from W basket	Zn N.D. Pt N.D. W N.D.
12	294-297		
15	329-358	Pt as oxides from filament	Found 0.06% Fe, and traces of Mg and Si.

Substance	M.Pt.	B.Pt.
Tin	232°C	Vaporises largely at 1200°C.
Tin dioxide	Sublimes above 1800°C.	Reduced by carbon to tin
Zinc	419°C	906°C.
Zinc oxide	Sublimes at 1800°C.	Reduced by carbon
Platinum	1774°C	
Platinum oxides	None stable in oxygen under 1 atm. above 500°C.	

Data from Ref. 94

5.2. Boron treated filaments.

Considerable work was carried out with various boron treated filaments since there have been reports of boron behaving as an inhibitor of the oxidation reaction below 1000°C. Unlike the substances discussed in Section 5.1, boron and its oxide would be expected to remain on the filament under the reaction conditions. Because of the high melting point and low volatility of boron and its trioxide the substances were painted onto the filaments in suspensions.

Attempts were made to evaporate boron trioxide from a Pt filament but no effect was shown on the oxidation at 1200°C. (Table A.5.2). Although more volatile boron compounds could easily be evaporated onto the filaments these were not used because it was thought unlikely that these substances would remain once the filament was heated.

5.2.1. Crystalline boron was first used, it being ground up in a pestle and mortar and an acetone suspension of the resulting powder painted onto the filament No.20. The filament was covered by a light grey colour after the acetone had evaporated off. Subsequent reaction at 1200°C, Runs 469-480, Table A.5.3, showed an initial uptake of oxygen with a slightly lower rate followed by rates of about 5 $x10^{-8}$ gr atoms $/cm^2$ sec. Heating the filament at 2000°C in vacuum for 5 minutes caused no difference in the rate at 1200°C (Runs 481-

485), but after the heating at 2000°C the filament had lost its grey colour and several grey whiskers appeared as if a stain had peeled off. A new filament, No.21, treated in the same way but with more boron showed the same initial uptake of oxygen and as before an initially lower rate then untreated filaments (Runs 486-500, Table A.5.4). These runs were followed by two runs with a cold trap in place on the reactor but this caused no significant difference in rate.

The grey colouration of the filament and the whiskers formed after heating at 2000°C were almost certainly due to the composite from the pestle and mortar. The initial uptake of oxygen could have been associated with this composite or could have been oxidation of the crystalline boron. The initial low rate in Runs 486-500 could also have been due to a shielding effect by the composite. These conclusions were confirmed by treating a filament with crystalline boron smashed to a powder between brass shims and painting a suspension of the powder onto the filament. Reaction at 1200°C followed by heating at 2000°C for 15 minutes in vacuum and then further reaction at 1200°C showed no significant differences over untreated filaments except for an increase in the CO_2/CO ratio for the first set of runs, (Nos. 503-510, Table A.5.5). The oxygen balance tended to be low but this was not nearly as marked as during the composite runs.

The results of Runs 481-502 can therefore be

considered as being due to the composite and that crystalline boron in itself has no effect on the reaction.

5.2.2. Amorphous boron which is much more reactive and was in a much finer powder than crystalline boron was used for another set of runs.

A freshly coated filament, No.28, was painted with a suspension of amorphous boron in acetone and then heated in vacuum at 1200°C with only a slight rise in pressure resulting. The ends of the filament which had not been painted with the suspension were about 100°C higher in temperature. Heating the filament in oxygen to be adsorbed by the filament almost certainly due to the formation of basic oxide which is known to be formed from amorphous boron below 1000°C. Following heating at 2000°C in 150μ of oxygen until the pressure no longer fell runs were carried out at 1250°C and then complete rate-temperature curves over the range 1000-2000°C were determined. These results are given in Table A.5.6 and shown on Graph A.5.1. The results show that after the slightly high oxygen balances at 1250°C, probably due to a certain decomposition of the basic oxide from going to a lower pressure and temperature, the rates and CO_2/CO ratios are very close to those obtained on untreated filaments. The only difference is that the hysteresis changes sense at a lower temperature 1200°C as against about 1450°C for the untreated case. In this case analysis of the filament after reaction,

GRAPH 5.1 Boron treated filament : effect of burnoff on rate at 1200° C

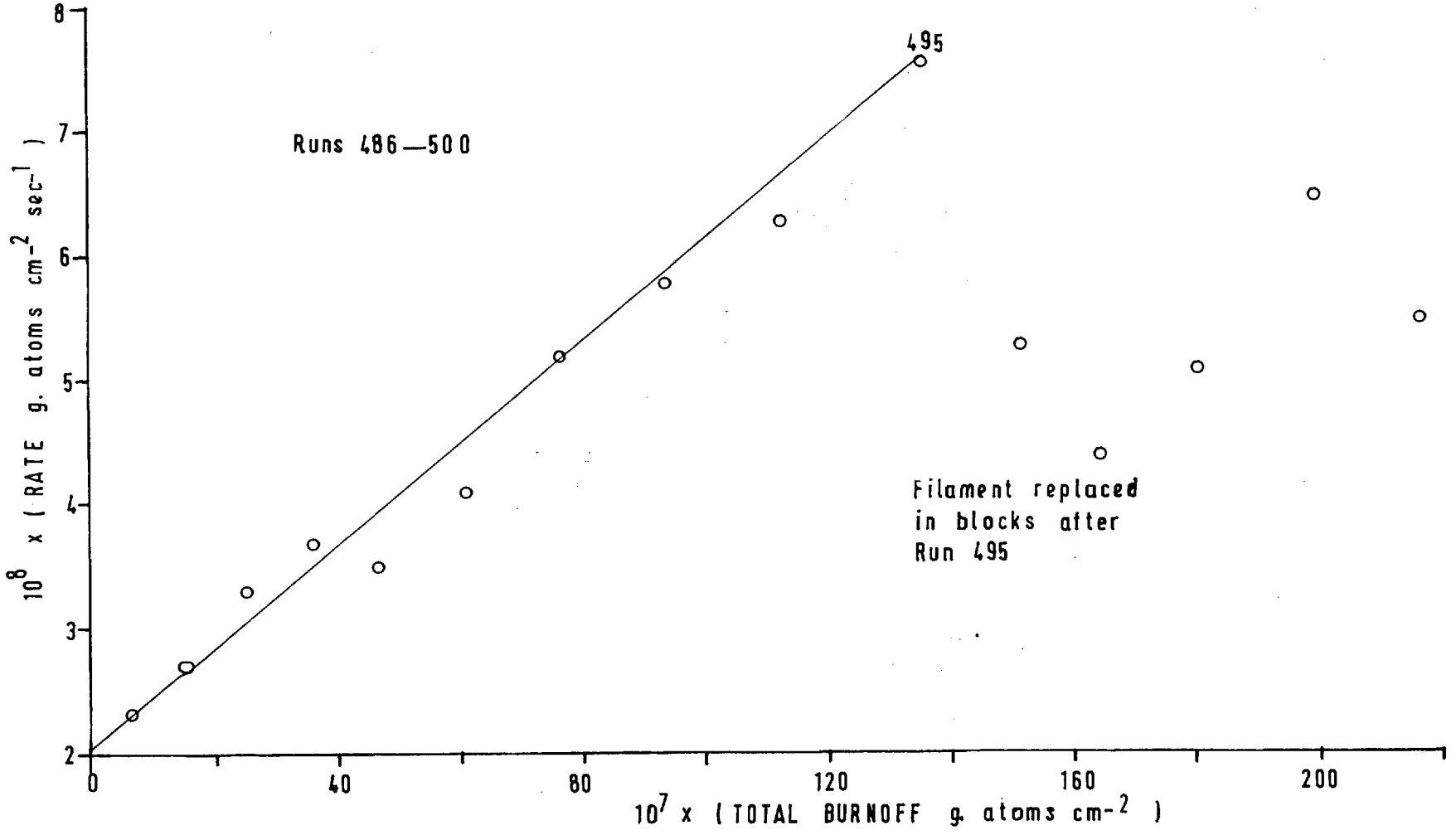

Table 5.8, showed only 0.006% boron left on the surface, suggesting the treatment at 2000°C, initially, had caused volatilisation to take place.

Another filament, No.30A, treated with amorphous boron suspension was heated at 2000°C for 30 minutes in vacuum with the resulting possibility of boron carbide formation. Rate-temperature curves were then determined and the results are given in Table A.5.7 and on Graph 5.2. This treatment did not alter the rate or CO_2/CO ratio but again differences in the oxygen balance were observed. In the first series of runs, Nos. 644-651, the oxygen balance decreased with increasing temperature going to as low as 41% at 2030°C. After 30 seconds heating at 2030°C in oxygen the oxygen balances recovered and were close to 100% for the remaining runs with a slight increase with decreasing temperature. These oxygen balances can be explained by the amorphous boron being oxidised, the rate of oxidation increasing with increasing temperature and after the reactions at 2030°C most of the boron having been oxidised and removed.

In order to see if boron in the bulk of the carbon rather than on the surface affected the rate a new filament, No.29, was painted with a suspension of amorphous boron and then coated with pyrolytic carbon for 10 minutes. At the temperature used, 2000°C, the boron would be expected to have diffused through the carbon to a certain extent. The

GRAPH 5.2 Rate-temperature curves for amorphous boron treated filament heated at 2000°C prior to runs.

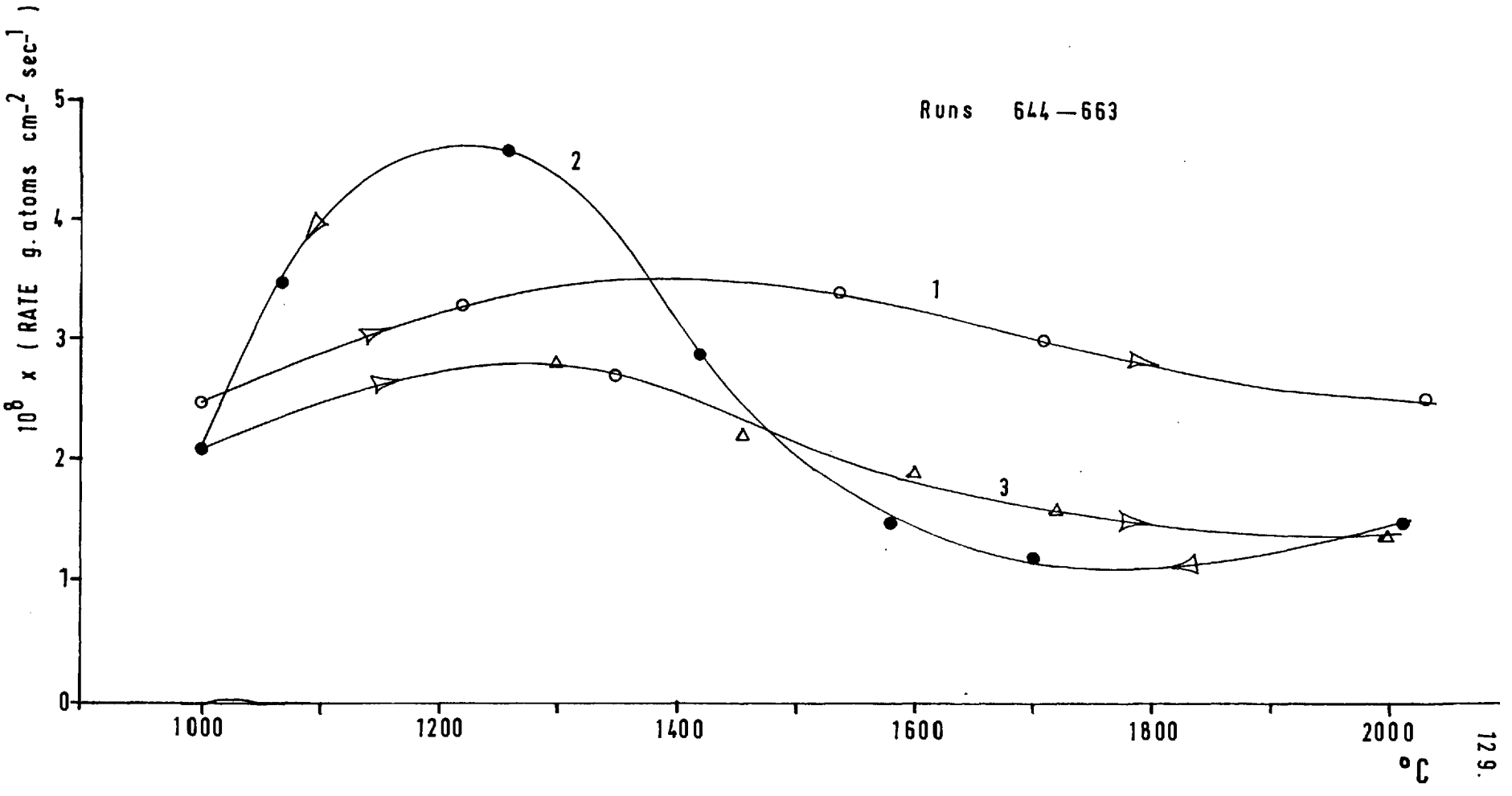

pyrolytic carbon was far less evenly deposited than for normal untreated filaments this being thought due to the actual boron particles giving a less even surface for the carbon to deposit itself on. (See also Section 5.8.). Rate-temperature curves then determined are shown in Graph 5.3 and it can be seen that the rates are very close to untreated filament rates. It is particularly interesting that during these runs the hysteresis did not change sense. The fact that the filament was only taken up to 1800°C is indicative that it is only when the filament is heated above 1800°C does it change so as to cause a decrease in the rate of reaction at lower temperatures.

5.2.3. A thick suspension of boric acid was painted onto a freshly coated filament, No.23. The filament was then heated in vacuum at 1200°C with a resulting evolution of gas associated with white deposits being formed on the reactor walls. This was almost certainly due to decomposition of the acid into water and boric oxide. The heating was continued until no further pressure rise was detectable, after which the filament was covered with several globules of glass like substance, probably B_2O_5. The rate at 1200°C, Runs 512-519, was found to be unaffected by this treatment and runs at various pressures showed the reaction to be very close to first order; the filament also showing pressure hysteresis effects. (Table 5.5). Runs at higher temperatures showed no tendency

GRAPH 5.3 Filament treated with amorphous boron and then coated with pyrolytic carbon.

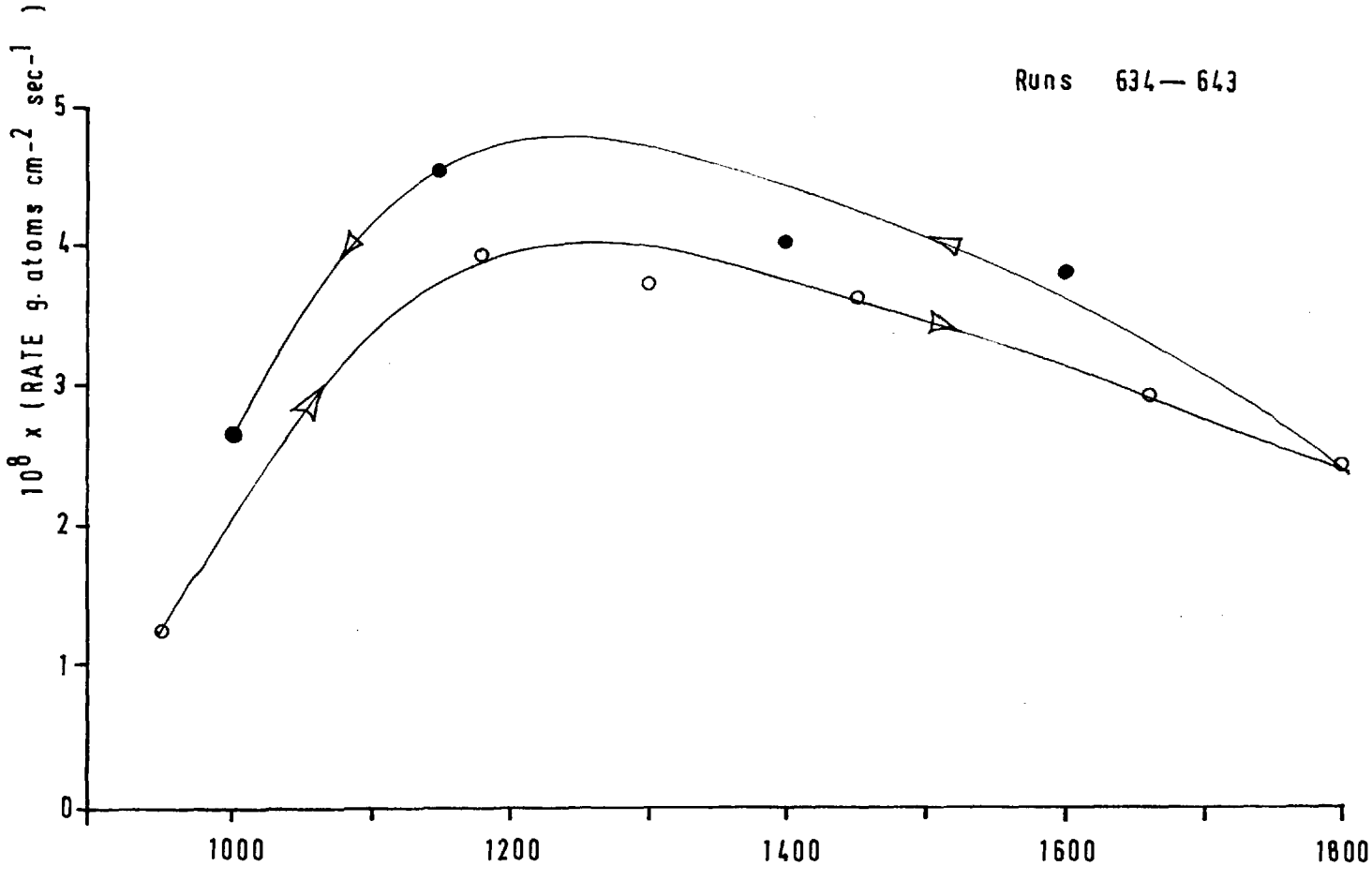

Table 5.5. Filament 23.

Filament painted with a suspension of boric acid in acetone, and then heated at 1200°C for a total of 2 minutes in 50μ of oxygen.

Reaction at 1200°C for 30 seconds.

Run No.	Initial pressure μ	Pressure CO μ	CO_2/CO ratio	Oxygen balance	R_8 x10^8	
512	48.1	9.3	0.49	104	4.2	
513	48.4	10.3	0.23	99	3.9	
514	49.4	10.8	0.22	98	4.0	
Order runs at 1200°C for 30 seconds.					R	k min^{-1}
515	12.4	2.7	0.33	104	1.1	0.40
516	31.0	7.0	0.16	98	1.4	0.37
517	59.9	13.9	0.16	95	4.9	0.37
518	93.5	22.5	0.12	98	7.7	0.36
519	135.0	30.25	0.14	100	10.5	0.34
Runs at 50 μ.						
520	48.8	13.7	0.49	108	6.2	
521	50.1	11.9	0.25	99	4.5	
522	50.2	12.2	0.25	99	4.7	
Filament heated at 1200°C for 1 minute in vacuum.						
523	49.0	11.4	0.16	98	4.0	

for the globules to wet the surface; the rate-temperature curves being similar to those obtained on untreated filaments in shape but with slightly increased rates which may have been due to water still being present in the reactor (Graph A.5.2). In order to see if these higher rates were peculiar to the particular filament used, another filament, after reaction in oxygen, was painted with boric acid suspended in water and degassed at 850°C for 45 minutes. The resulting rate-temperature curves shown on Graph 5.4 show nearly a twofold increase in the rate for the down curve around the maximum; the oxygen balances and CO_2/CO ratio being normal (Table A.5.10). The increase in rates are therefore a characteristic of the treatment.

5.2.4. Since the product of the decomposition of boric acid is boric oxide a series of runs were carried out to see if this affected the rate in the same way as boric acid. Filament 24 was painted with a suspension of boric oxide powder in acetone. After heating for a total of 90 seconds at 1200°C globules of oxide collected at various points on the filament as for the acid treated filaments. Initial runs at 1200°C, Table 5.6, showed a lower rate than for untreated filaments but after 30 mins. heating at 1200°C in vacuum the rate increased to that obtained on untreated filaments. Reaction following heating at 2000°C in vacuum

GRAPH 5.4 Rate-temperature curves for boric acid treated filament

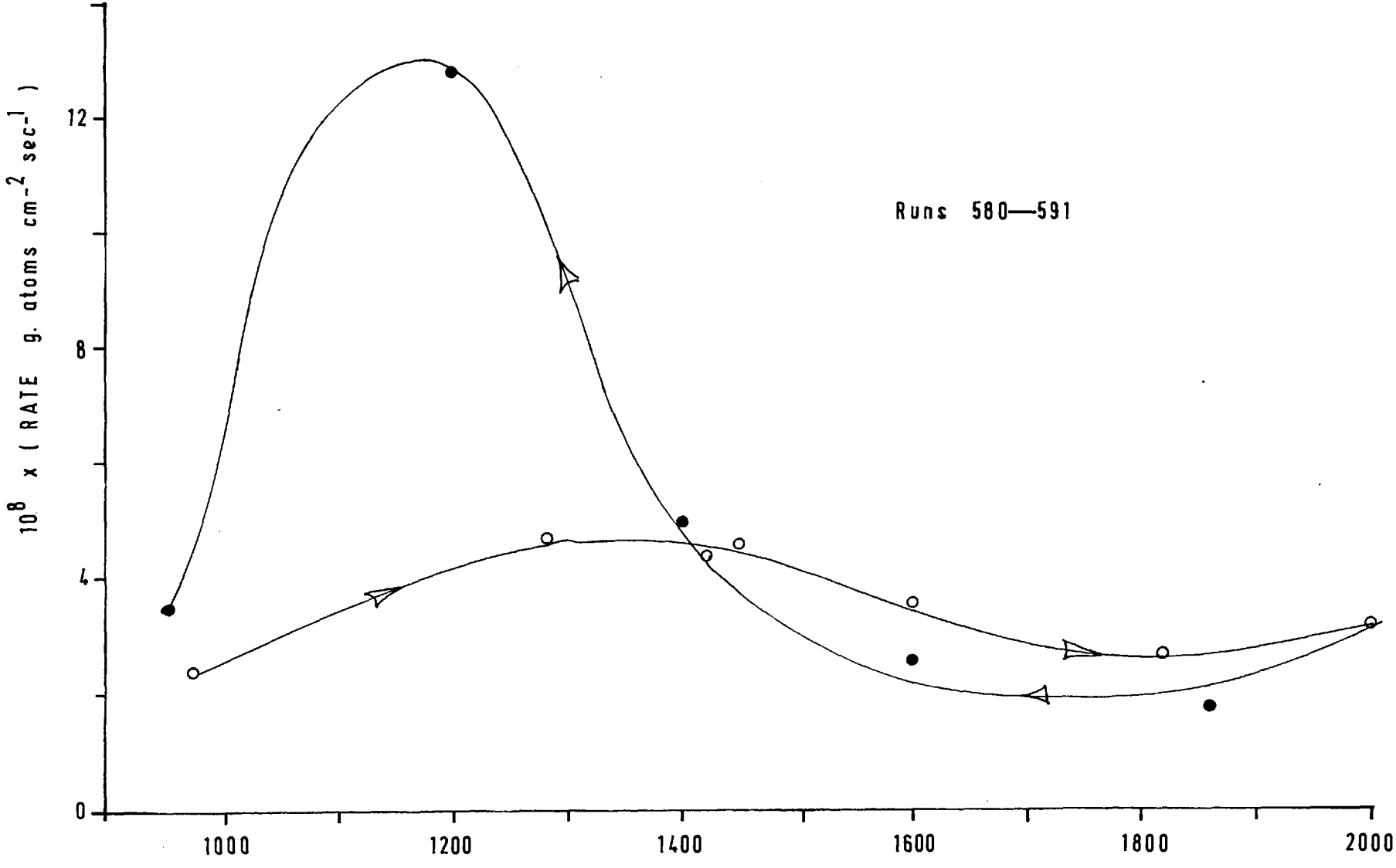

Table 5.6. Filament 24.

Filament painted with boric oxide in acetone and heated for 90 seconds at 1200°C in vacuum.

Run No	Initial pressure	CO formed μ	CO_2/CO ratio	Oxygen balance	R x10^9
539	48.7	7.1	0.20	99	25.9
540	49.7	4.6	0.64	98	29.5
541	49.6	7.5	0.35	99	30.7
Filament heated for 30 minutes at 1200°C in vacuum					
542	50.7	12.6	0.09	97	41.7
543	50.3	12.8	0.12	98	43.8
Filament heated for 15 minutes at 2000°C in vacuum					
544	50.8	16.2	0.01	97	50.2
545	52.2	16.6	0.02	99	51.4
546	49.6	14.1	0.07	99	45.9

All reaction at 1200°C for 30 seconds.

Table 5.7. Analysis of Boron treated filaments.

Filament	Run No.	Treatment	Boron
20	465-485	Crystalline boron	0.05%
21	486-502	Crystalline boron	0.001%
22	503-510	Crystalline boron	0.5%
23	511-531	Boric acid	50 ppm
24	532-556	Boric oxide	50 ppm
26	570-580	Boric acid	50 ppm
28	616-633	Amorphous boron suspension in water	0.006%
30A	644-663	Amorphous boron in acetone	0.004%

For 30A strong traces of Si and Mg were detected, together with traces of Fe, Mn and other impurities.

caused a slight initial increase in rate while rate-temperature curves over the range 1000°-2000°C also showed a slight increase in rates, particularly on the up curve at high temperatures. Graph 5.5.

It would appear that the greatly increased rate at the maximum for the boric acid treated filament is not due to the boric oxide; leaving the possibility that residual water is responsible.

5.2.5. Spectrographic analysis of the earlier filaments showed varying amounts of boron left on the filaments after reaction. The amounts found for the crystalline boron filaments were far higher but need not have been associated with good coverage since the particles in this case were fairly large.

Microphotographs of the filaments showed that for the crystalline boron treated filaments the surface was pitted, Photo 9, while for the boric oxide and amorphous treated filaments the surface was quite smooth and normal, Photo 10 showing a typical part of the surface. Filament 26 treated with boric acid had a streaky surface with globules, of presumably oxide, visible on the surface, Photo 11. The filament treated with amorphous boron and then coated with pyrolytic carbon was far less well deposited and large clusters of cones coming out of the surface can be seen in Photo 12.

GRAPH 5.5 Effect of Boric oxide on rate-temperature curves.

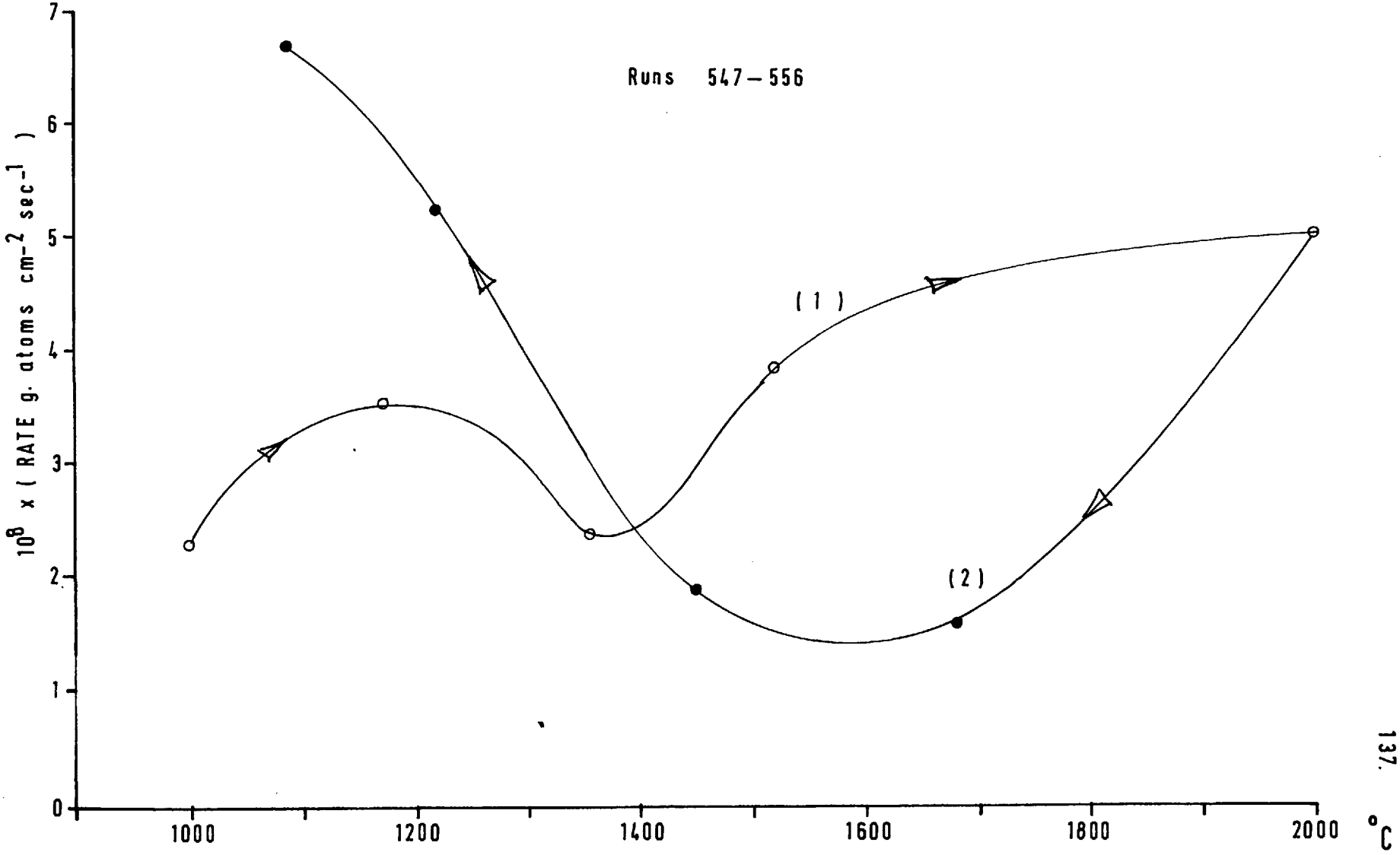

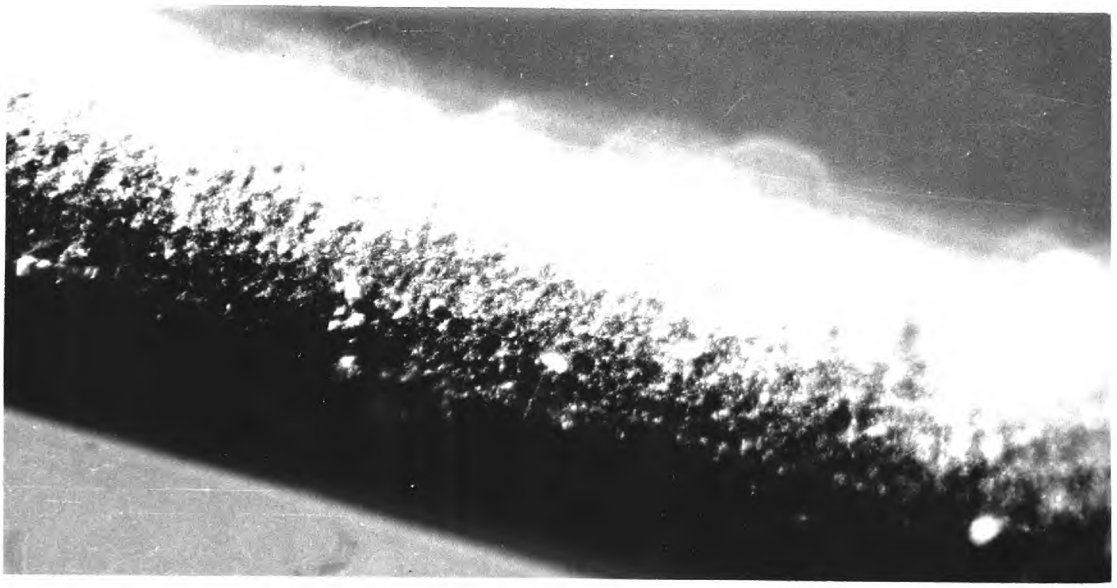

Photo 9. Boron treated filament No. 21 x200

Photo 10. Boron treated filament No.30A. x800

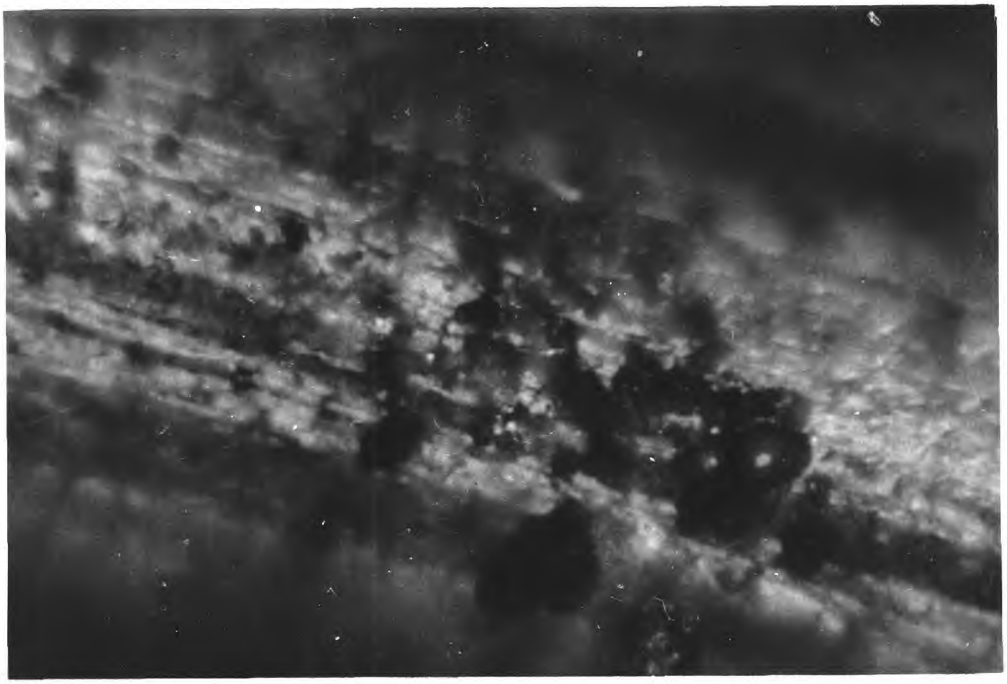

Photo 11. Boric acid treated filament No. 26. x800

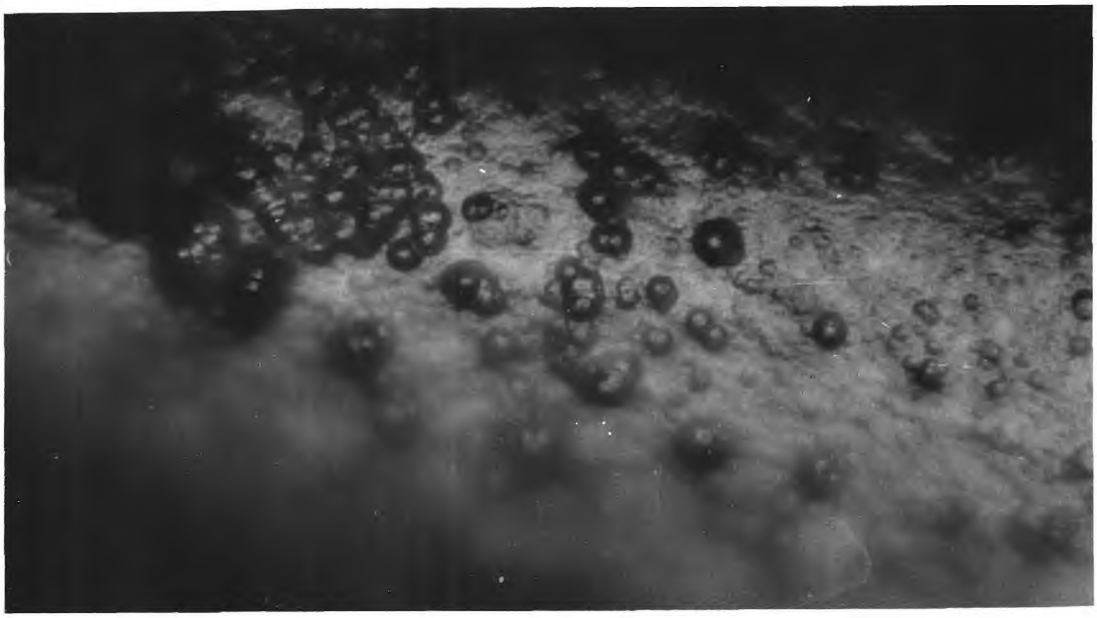

Photo 12. Amorphous boron treated filament No.29, then coated with pyrolytic carbon. x800

5.2.6. Thermodynamic calculations, Appendix 3, show that while boric oxide will not decompose into free boron by itself, it can be reduced by carbon above 1200°K to give the carbide and CO, while above about 1500°K CO_2 can be produced. It is not thermodynamically feasible for reduction to occur by CO, but the free metal can also be produced by reduction by C. In this latter case it would be expected that any free metal was converted to the carbide at high temperatures.

The thermodynamics therefore favour carbide formation at high temperatures and oxide formation at low temperatures. Our results are explainable on this basis although some oxide is still present at the highest temperatures used.

5.3. Silicon treated filaments.

A pyrolytic filament, No.37, was painted with a suspension of pure silicon powder in acetone. Reaction then carried out at 1060°C showed an initial rate lower than for untreated filaments, the rate increasing with burn off to reach a value equal to that for untreated filaments. Reaction at 1600°C showed a net uptake of oxygen probably due to the formation of silica with a rate initially about 3 times higher than the untreated filament case. This was followed by reaction at 1720°C and the rate-temperature curves were determined over the range 950-2000°C, these results showing no abnormal behaviour. The results for silicon are given in Table A.5.12 and on Graph A.5.3.

The initially low rates observed at 1060°C and for certain boron treated filaments cannot be considered as significant. They are quite possibly due to using a previously untreated filament whose last treatment was at 2000°C, a temperature from which the filament would be initially less reactive for subsequent reaction at lower temperatures,(Section 4.)

The results of painting a filament with a silica suspension in water followed by reaction at various temperatures after heating at 2000°C are given in Table 5.8. Also given are the results of runs carried out on a sodium silicate treated filament.

None of these results are significantly different from those obtained on untreated filaments. The initial high oxygen balance in Run 791 was probably due to reduction of the silica, Table A.3.3. While first degassing the sodium silicate treated filament a considerable amount of gas was evolved, the gel going translucent after treatment. This again would be decomposition with water evolved, and the sodium would not be expected to have remained on the filament.

Microphotographs showed that the silicon appeared to have melted on the surface as shown in Photo 13. The surface was otherwise similar to untreated filaments. Bronze patches were also noticeable on the silica treated filaments

Table 5.8. Filament 38 painted with a suspension of silica in water and then heated at 2000°C for 5 mins. in vacuum.

Run No.	T°C	Secs. react.	Initial pressure μ	Pressure CO μ	CO_2/CO ratio	Oxygen balance	R x10^8
791	1200	30	50.3	10.1	0.09	110	3.35
792	1200	30	50.4	15.2	0.04	97	4.80
793	1700	30	50.8	6.4	0.07	98	2.13
794	1700	30	49.4	5.8	0.10	97	1.95
Filament painted with silicon suspension and heated for 1 min. at 2000°C in vacuum							
789	1370	30	51.5	15.6	0.02	97	4.83
790	1370	30	50.2	18.5	0.05	98	5.90
Filament painted with sodium silicate gel and then heated for 1 min. at 1500°C for 3 mins., 1800°C for 1 min. and 2000°C for 5 mins in vacuum.							
795	1250	30	49.7	10.4	0.17	98	3.71
796	1250	30	50.4	14.0	0.09	98	4.62

Analysis of Silicon Filaments.

Filament No.	Run No.	Treatment	Analysis	
36	770-778	Si powder in water	0.2 % Si	
37	789-790	Si powder in water	0.2% Si	Also traces of B, Fe and Mg.
38	791-794	Silica suspension in water	0.2% Si	
40	795-796	Sodium silicate solution	0.2% Si	

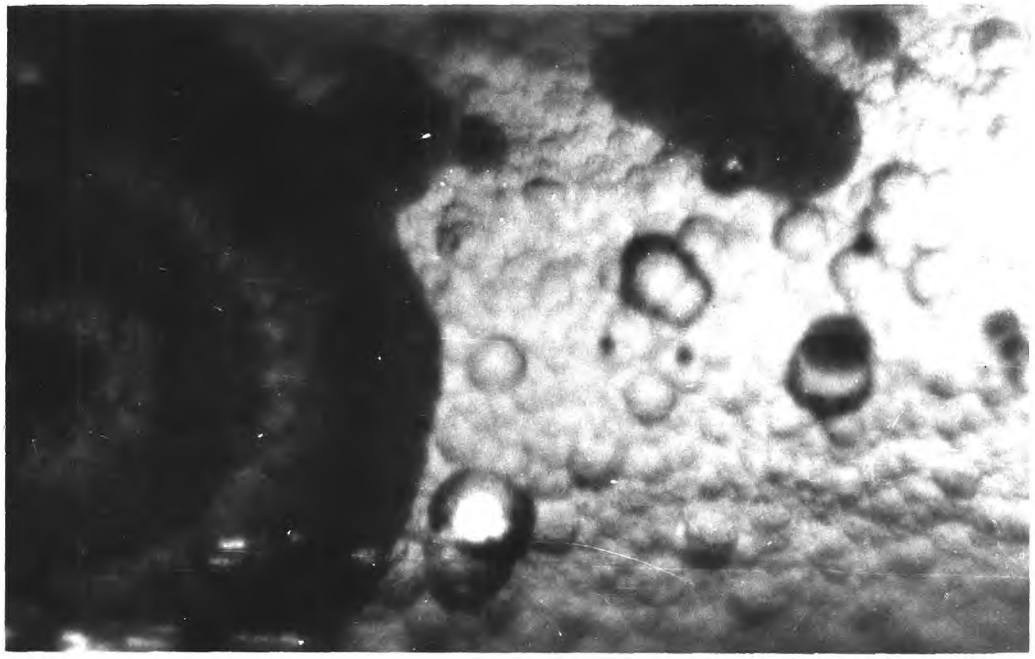

Photo 13. Silicon treated filament No.37. x800

Photo 14. Sodium silicate treated filament No.40. x200

while on the sodium silicate filament deep pitting was noticeable as can be seen at the bottom of Photo 14.

Analysis of these filaments showed a considerable amount of silicon remained on the surface as suggested by the photographs (Table 5.8). Thermodynamic considerations show that it is feasible for carbide formation as low as 1200°K. Appendix 3.

In the case of the silicon treated filament at 2000°C it is thought to form the carbide. A part of this is however oxidised at 1600°C removing some of the carbon. This account both for the high rate and net uptake of oxygen found. After this is a more or less stable state is assumed to exist between the carbide at the carbon-silicon interface, and the silica further out from the surface. Similarly silica is reduced initially, but the increased oxygen balances are not thought sufficient to account for complete reduction.

5.4. Iron treated filaments.

For these runs the iron was evaporated onto the filament by heating a 35 S.W.G. iron wire in the reactor. For the first series of runs, Nos. 413-430, filament No.17 was treated by this method, the iron wire being at 1300°C for 2 mins. in vacuum after which considerable black deposits were present on the reactor walls. Runs carried out at 1200°C shown in Table 5.9 show a rate of about 2.8 $x10^{-7}$ gr atoms/cm^2 sec which is 8 to 10 times higher than for untreated filaments. The rate showed no tendency to fall off with increasing burn off. The oxygen balance was slightly low, 93-97%, while the CO_2/CO ratio was considerably higher and fell with increasing burn off.

The same filament was then heated at 1800°C in vacuum for 15 mins. Subsequent reaction at 1200°C, Table 5.10, showed that the rate had decreased considerably, to about 7 $x10^{-8}$ gr atoms/cm^2 sec, while it appeared to increase with increasing burn off, and again the CO_2/CO ratio was high. When the iron filament was inadvertently heated at 1300°C for 5 seconds the rate was increased.

The heating at 1800°C is thought to have caused the decrease by re-evaporating the iron off the carbon surface.

Order runs were carried out at various pressures, Table 5.11, showed a first order reaction over the pressure

Table 5.9. Iron treated Filament 17.

Reaction at 1200°C.

Run No.	Secs. react.	Initial pressure μ	Pressure CO μ	CO_2/CO ratio	Oxygen balance	R x10^8
Untreated filament.						
413	30	50.4	9.9	0.01	99	3.33
414	60	49.0	17.8	0.02	98	2.6
415	30	49.5	10.1	0.05	99	3.2
Treated filament.						
417	10	48.7	14.5	0.46	96	19.3
418	10	48.0	16.1	0.37	94	20.1
419	5	50.2	11.8	0.32	97	28.5
420	5	47.3	10.9	0.29	96	25.7
421	5	48.8	12.3	0.29	96	28.9
422	5	48.8	12.7	0.28	96	29.6
423	5	48.0	13.1	0.12	93	26.9
424	5	48.7	12.3	0.25	96	28.1
425	No analysis. Filament burnt 3 times in 50μ oxygen for 5 seconds.					
426	5	49.3	13.3	0.22	97	29.6
427	As 425.					
428	5	48.9	12.6	0.17	100	27.0
429	As 425					
430	5	47.3	12.5	0.18	97	27.0

Table 5.10. Iron treated. Filament heated at 1800°C in vacuum for 15 mins.

Filament 17.

Run No.	Initial pressure μ	Pressure CO μ	CO_2/CO ratio	Oxygen balance	R x 10^8
431	49.0	2.2	0.50	97	5.87
432	50.7	5.7	0.26	97	6.60
433	49.0	7.8	0.06	98	7.60
434	Fe filament on for 5 seconds.				
435	50.8	10.3	0.10	96	10.3
436	50.6	9.4	0.10	93	9.40

All reaction at 1200°C for 5 seconds.

Table 5.11. Iron treated. Order runs at 1200°C.

Reaction for 5 seconds.

Filament No.17.

Run No.	Initial pressure μ	Pressure CO μ	CO_2/CO ratio	Oxygen balance	R x 10^8	k min^{-1}
437	51.2	16.5	0.10	100	16.5	2.4
438	50.0	10.2	0.05	103	9.74	1.7
439	50.8	10.1	0.05	102	9.67	1.7
440	13.9	2.2	0	113	4.03	1.0
441	30.2	4.45	0	101	8.14	1.1
442	59.9	9.4	0.11	98	19.0	1.4
443	98.7	15.75	0.08	98	31.2	1.4
444	118.0	20.0	0.04	97	38.0	1.3
445	155.0	22.25	0.02	101	41.5	1.1
446	215.7	25.5	0.14	99	51.4	1.1
447	162.2	19.75	0.09	100	39.3	1.1
448	115.2	15.5	0.01	92	28.5	1.0
449	62.8	8.7	0.10	105	17.5	0.84
450	28.25	4.2	0	112	7.7	1.1
451	52.2	6.5	0.06	113	12.6	1.1
Filament retreated with iron						
452	50.1	12.5	0.13	97	25.7	
453	49.7	11.5	0.12	105	23.5	

range 14-216 μ. These were carried out on the same filament used previously after further treatment by heating the iron filament at 1300°C for 2½ minutes in vacuum. In contrast with the earlier runs the CO_2/CO ratio is low and the rates also tend to be lower. This cannot be due to depletion during the runs since earlier runs at 1200°C have shown that this does not occur. But by retreating the filament with iron in the same way as previously and carrying out further reaction at 1200°C, Runs 452-453, it can be seen that the rate had increased. It appears that the rate is therefore dependent on the exact iron treatment, that is it is dependent on the amount of iron on the surface.

In order to see if iron oxides also affect the rate in the same way a freshly coated filament, No.18, previously reacted in oxygen at 1200°C for a total of 2 mins in 50μ of oxygen, was treated by heating the iron wire in oxygen as described below:-

1. Fe wire at 1000°C for 45 seconds in 50μ of oxygen. Pressure fell to 45μ and then remained constant.

2. Fe wire at 1000°C in 300μ of oxygen. Pressure fell to 125μ after 45 seconds where it remained on further heating.

3. Further heating in 300μ, but with no drop in pressure until the Fe temperature was raised to 1150°C.

After burning the filament twice for 5 seconds in 50μ of oxygen, Runs 454-456, Table 5.12, were carried out,

Table 5.12. Filament No.18. Iron treated.

All reaction at 1200°C.

Run No.	Secs. react.	Initial pressure μ	CO pressure μ	CO_2/CO ratio	Oxygen balance	R x10^8
Iron filament heated in oxygen.						
454	5	50.3	9.8	0.11	98	19.8
455	5	50.0	6.2	0.19	100	13.5
456	5	49.8	5.0	0.12	102	10.2
Filament treated with iron, then coated with pyrolytic carbon Filament No.18						
457	5	51.0	3.7	0	99	6.74
458	15	50.8	8.3	0	97	5.1
459	15	49.8	8.9	0.02	98	5.5
Filament treated with iron while coating with pyrolytic carbon Filament 19.						
461	15	49.2	7.5	0.08	99	4.9
462	15	53.2	9.4	0	100	5.7
463	15	53.2	12.5	0	98	7.6
464	15	54.8	11.6	0.04	99	7.3

Table 5.13.

Filament No.	Run Nos.	Treatment	Analysis.
17	413-453	Fe wire heated in vacuum	Iron shows up on electron X ray microscope on surface but not in craters.
18	457-459	Fe treated then coated with carbon	0.01% or less Fe
19	460-464	Fe evaporated while coating with carbon.	Low% Fe

Iron not detected on filament surface by X ray electron microscope

the results showing that the oxides had increased the rate to between 1 and 2 $x10^{-7}$ gr atoms/cm^2 sec and that the rate fell with increasing burn off. Again the CO_2/CO ratio tended to be high, but the oxygen balance was normal. It would appear from thermodynamics that the oxide would be reduced, Appendix 3.4. It is therefore surprising that the oxygen balances were normal which suggests that the quantity of iron on the surface is very small. This was borne out by the X ray probe study of the surface which found iron to be undetectable.

Filament No.18 was coated with iron evaporated in vacuum at 1200°C for 2 minutes and iron evaporated in oxygen. This filament was then coated with pyrolytic carbon. The resulting rates at 1200°C, Runs 457-459, show no differences from untreated filaments. For another filament, No.19, the pyrolytic carbon was deposited under the normal conditions while the iron filament was at 1200°C. Following an initial burning off for 15 seconds the results of runs at 1200°C are also shown in Table 5.12. The rates are only marginally higher than those obtained on untreated filaments, the CO_2/CO ratio and oxygen balance being normal. These treatments at high temperatures undoubtedly caused most of the iron to volatilise off the filament.

For all the filaments spectrographic analysis,

Table 5.13, showed iron to be present in small quantities on the filament after reaction. An X ray probe microscope was used to examine the surface and showed Fe tended to be scattered on the surface around the craters but not in the craters, Photos. 17-19. The other two filaments on which iron was put in the bulk of the filament, Nos. 18 and 19, showed no detectable iron on the surface without craters. Neither of these filaments showed catalytic reactions and it would appear that only a small quantity of iron had remained on the surface following the heating at 2000°C, less than 0.1% from the analysis. It can be assumed that the quantity left after heating at 1800°C in vacuum, Runs 431-433, was of the same order and this had only a slight catalytic effect. It cannot therefore be said that the small quantity of iron distributed in the bulk of the pyrolytic carbon for filaments 18 and 19 had no effect because it was not on the surface. It is also likely that it had negligible effect because the quantity was too small.

Photographs of the filament surface showed the surface to be covered with craters. This was particularly evident for filament 17, Photo15, on which a considerable amount of reaction had occurred. Unlike the boron case the filament treated with iron and then coated with pyrolytic carbon showed no disruption of the pyrolytic layer. This is probably due to the fact that in the boron case actual

Photo 15. Iron treated filament No. 17. x200

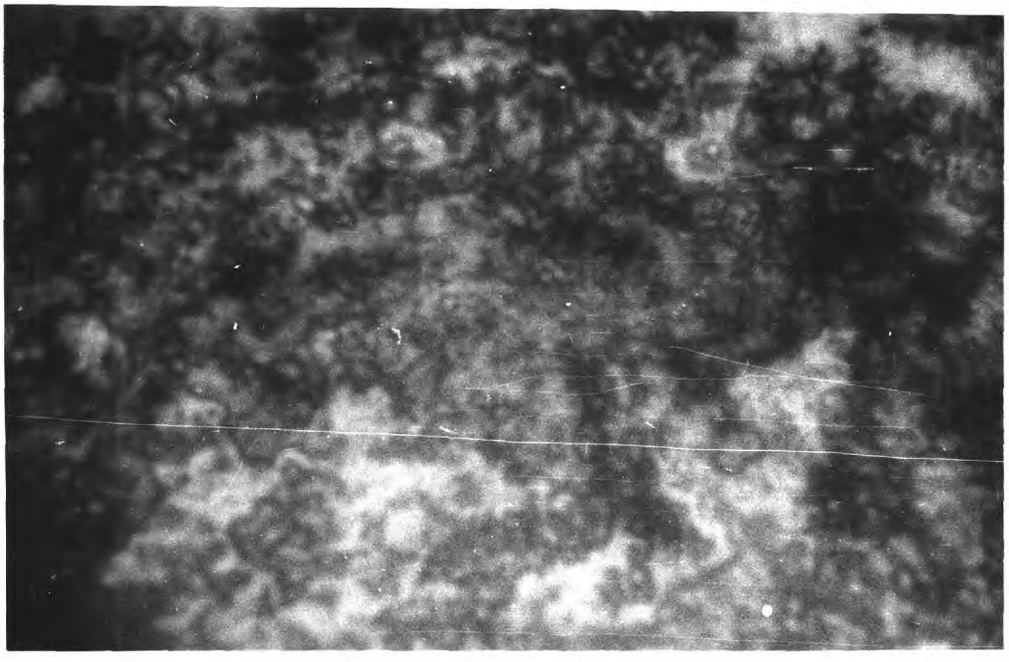

Photo 16. Iron treated filament No.19. x1900

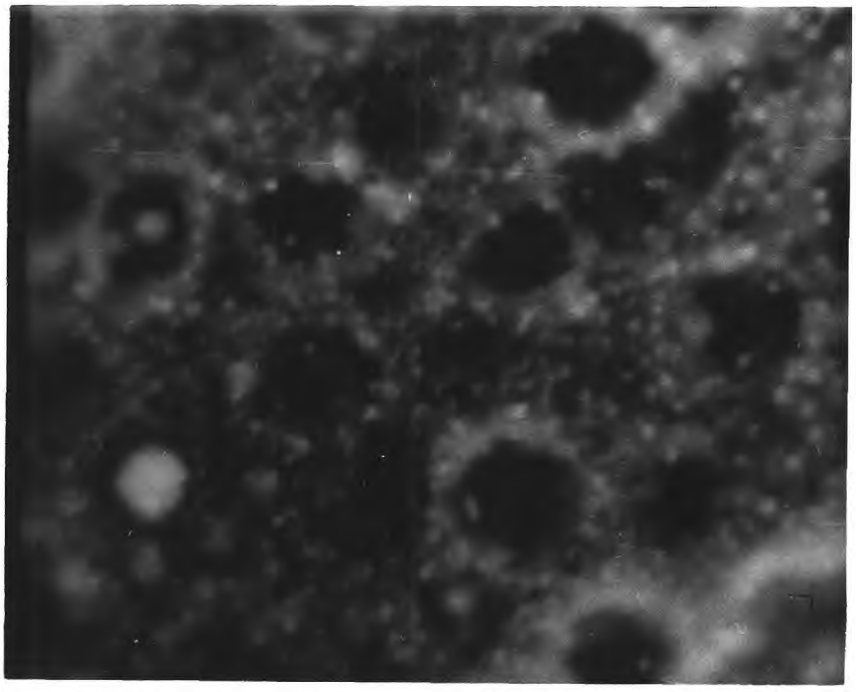

Photo 17. Iron treated. Adsorbed electron picture of the surface. x1200

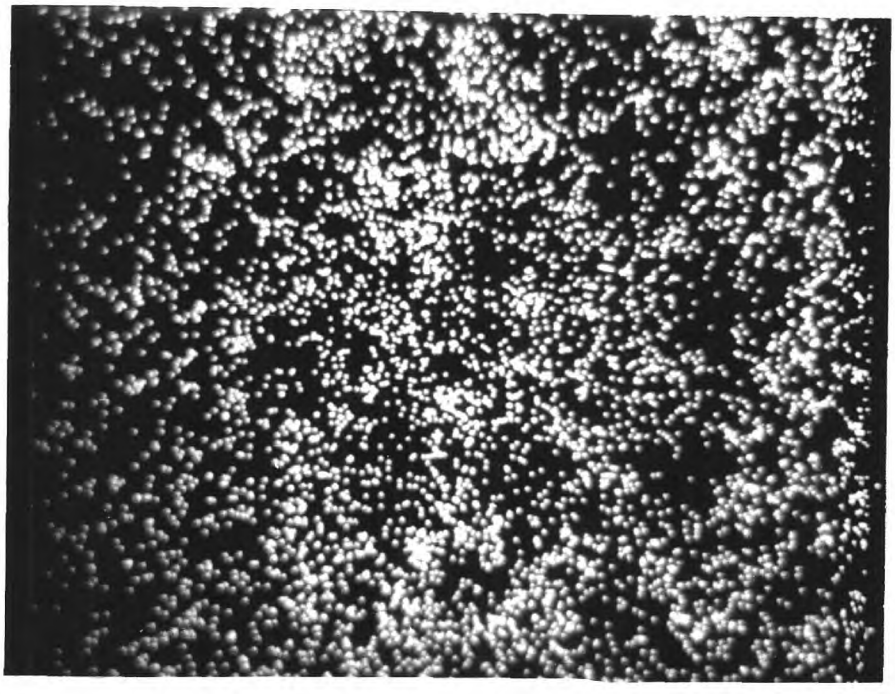

Photo 18. Iron treated. X ray picture of surface showing the distribution of iron. x1200

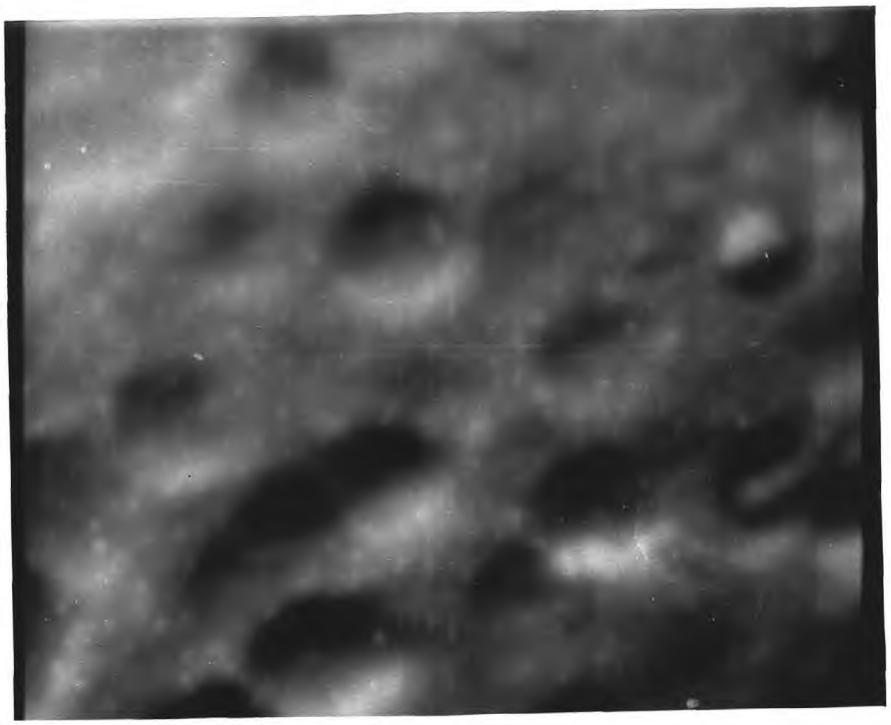

Photo 19. Iron treated. Back scattered electron microscope picture showing the pits. x1200

particles existed on the surface while in the iron case a very thin layer was deposited. Photo 16 shows the surface of the filament to be speckled in the same way as the zinc treated filaments where local blackening of the surface appears to have taken place. For the two filaments on which the iron was deposited and then coated with pyrolytic carbon no pits were visible although for filament 19 the surface was fairly rough.

5.5. Tungsten Treated Filaments.

The method of treatment for these runs was to heat a tungsten wire in the reactor in an atmosphere of oxygen to deposit the volatile oxides onto the filament. Early runs are shown in Table A.5.13 but these runs are less accurate than later runs since the analysis for CO was by the platinum filament method. These results show a nearly tenfold increase in rate while the CO_2/CO ratio is normal, but due to the considerable scatter it is difficult to see and fall off in rate. Runs 308-319 show a tendency for the rate to fall off with burn off at 1200°C.

For the first series of rate-temperature curves determined, shown on Graph 5.6, the tungsten wire was twice heated at 1500°C for 1 minute in 50μ of oxygen. A bluish tinge deposit was formed on the reactor walls during this coating, which could be any of the oxides W_4O_{11}(violet),

GRAPH 5.6 Rate-temperature curves for Tungsten treated filament.

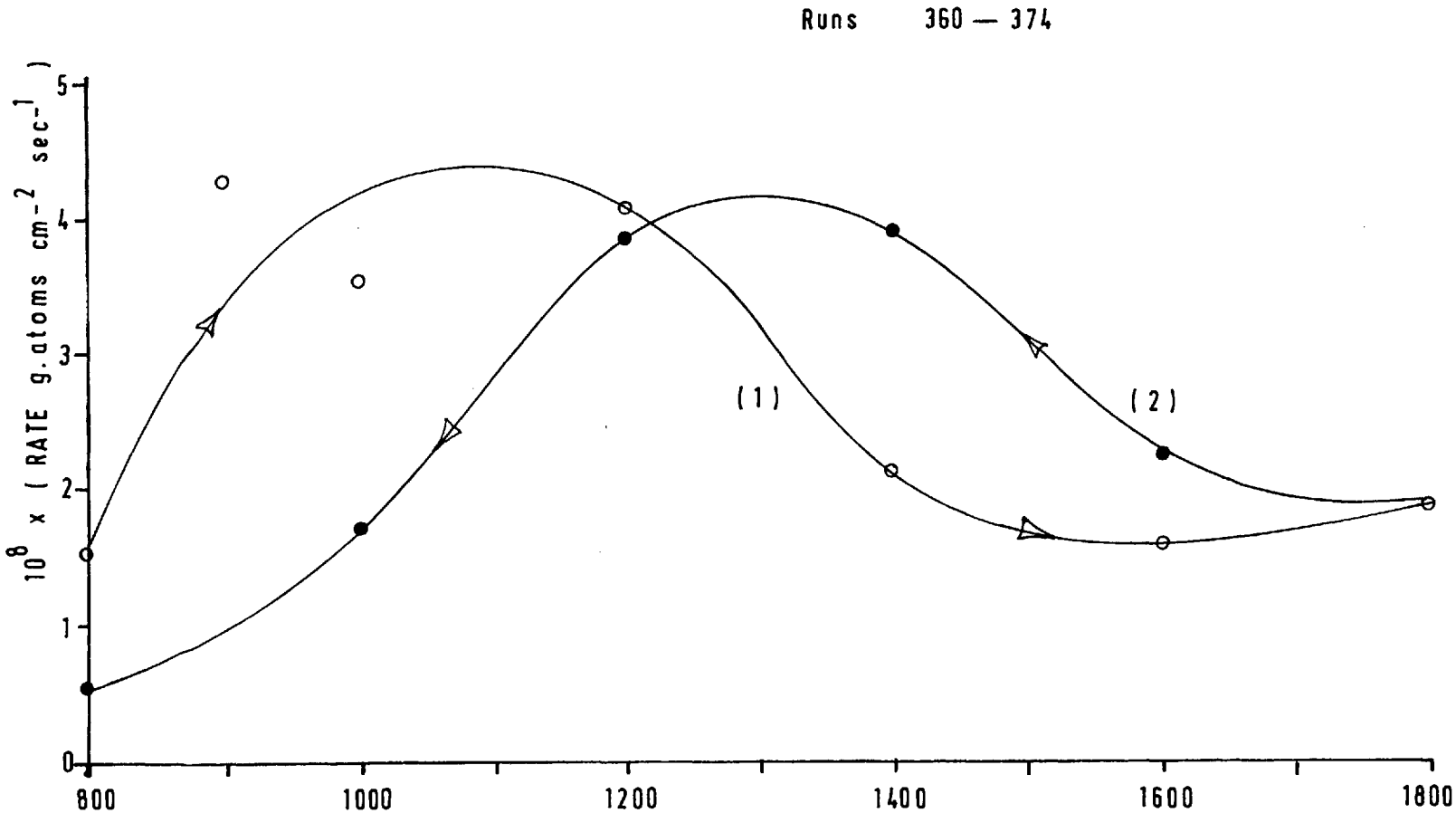

WO_3 or W_4O_{11}[77]. The rates found showed no increase over untreated filaments except on the down curve at high temperatures. The hysteresis is in completely the opposite direction to the untreated filaments and it crosses over as for the latter. The rates on the down curve are in fact lower than for the untreated filaments and these lower rates may be due to the fact that the filament was brought up to temperature in vacuum between runs, which normally took about 30 seconds.

These results show a considerable difference from those obtained by treating the filament between each run by heating the tungsten wire at 1600°C in 50μ of oxygen for 1 minute during which the pressure fell to less than 1μ. These results shown on Graph 5.7 have a hysteresis working in the same direction as untreated filaments but with the rate increased by a factor of about 10 and the maximum shifted to a higher temperature of 1400°C. As for untreated filaments the product was predominantly CO while the oxygen balances were close to 100%.

Heating a treated filament in vacuum at 1200°C caused negligible evolution of gases and this together with the 100% oxygen balances shows that the extra rate cannot be explained by simple decomposition of tungsten oxides.

At the higher temperatures used the tungsten oxides would evaporate off the filament [78]. If tungsten remains

GRAPH 5.7 Tungsten treated filament.

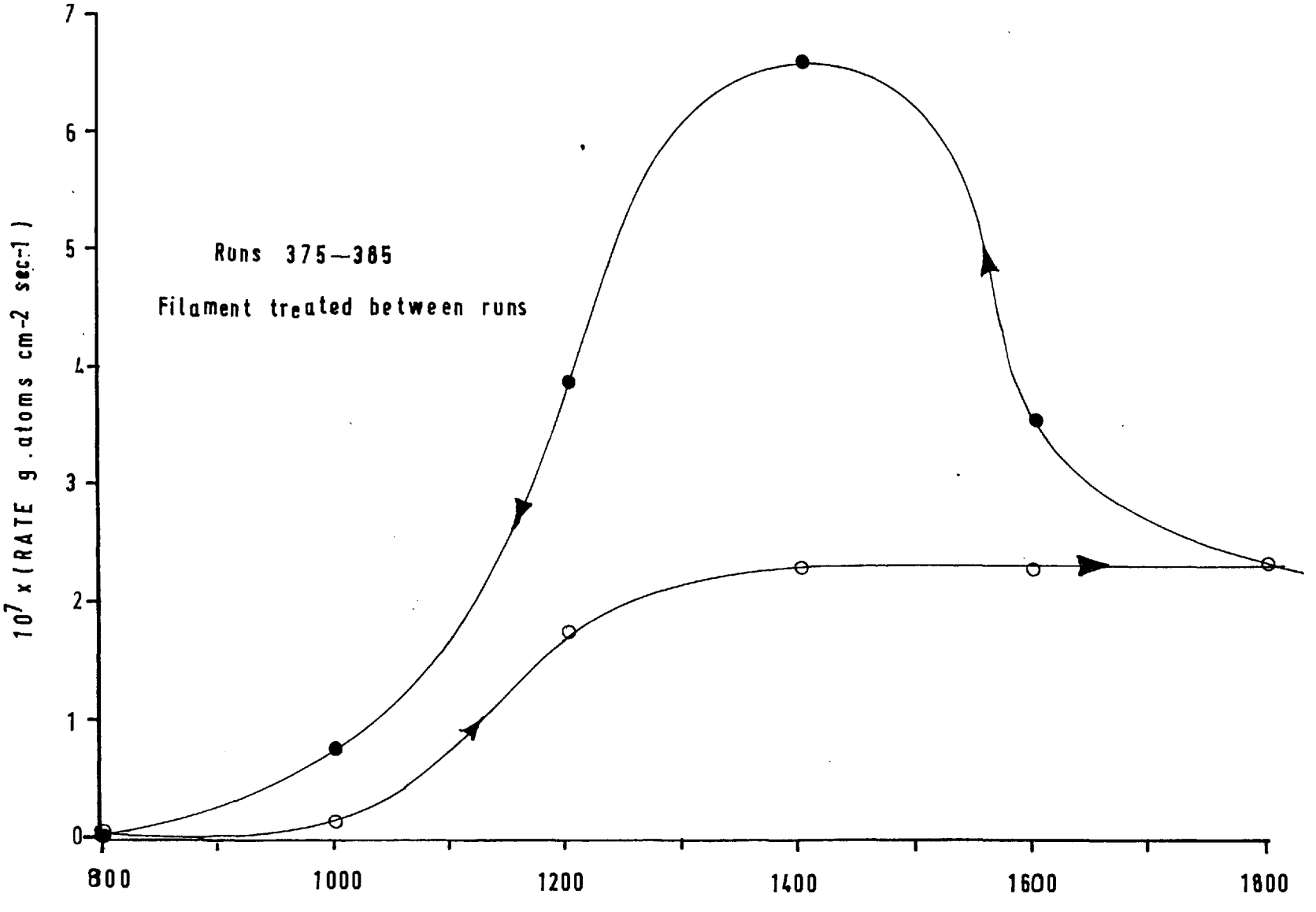

on the filament after high temperature treatment it must be either as metal or carbide. In order to see if there was any depletion or effect on rate after heating at high temperatures a series of runs were carried out at 1200°C with the filament heated at 1800°C between runs, after only an initial coating with tungsten oxides. The results of these runs are given in Table A.5.16 and plotted on Graph 5.8 where it can be seen that after an initial high value the rate decreases for 3 runs until it then increases again reaching asymptotically the rate of 4 $x10^{-7}$ gr atoms/cm^2 sec. The initially high rates could be due to an initially large quantity of tungsten oxides on the surface; a considerable amount evaporating off between the first 3 runs, and the remainder existing on the surface as carbide.

Spectrographic analysis of the filaments showed that no tungsten was detected on the filaments after reaction although Fe was present in larger quantities than for untreated filaments (0.01%). Also in common with the iron treated filaments the surfaces were very pitted. It would appear that there is considerable depletion of the tungsten from the surface and it might be assumed that the extra iron, possibly as an impurity in the tungsten wire, caused the increased reactivity. However order runs at 1200°C., Table 5.14 (and A.5.17.) show that the best fit over the pressure range 14 to 207 μ is given by a 0.6 order compared with a first order

Table 5.14. Rate constants for tungsten order runs.

Run No.	Initial Pressure μ	k 1st order	k 0.6 order
398	14.45	4.2 min^{-1}	0.24
399	25.8	2.4	0.17
400	65.7	2.2	0.23
401	99.5	2.1	0.26
402	136.5	1.6	0.22
403	164.5	1.2	0.19
404	207.25	1.2	0.20
405	120.75	1.1	0.14
406	72.3	1.4	0.15
407	23.65	1.9	0.13

Spectrographic analysis of Tungsten Treated Filaments.

Filament No.	Run Nos.	Treatment	Analysis
14	301-325	W from W filament	W N.D. Fe 0.01% Mg, Si detected.
16	360-412		W N.D. Fe 0.01% Mg, Si detected.

N.B. The detection limit for W was 500ppm.

GRAPH 5.8 Effect of heating in vacuum at 1800°C on the rate for a Tungsten treated filament

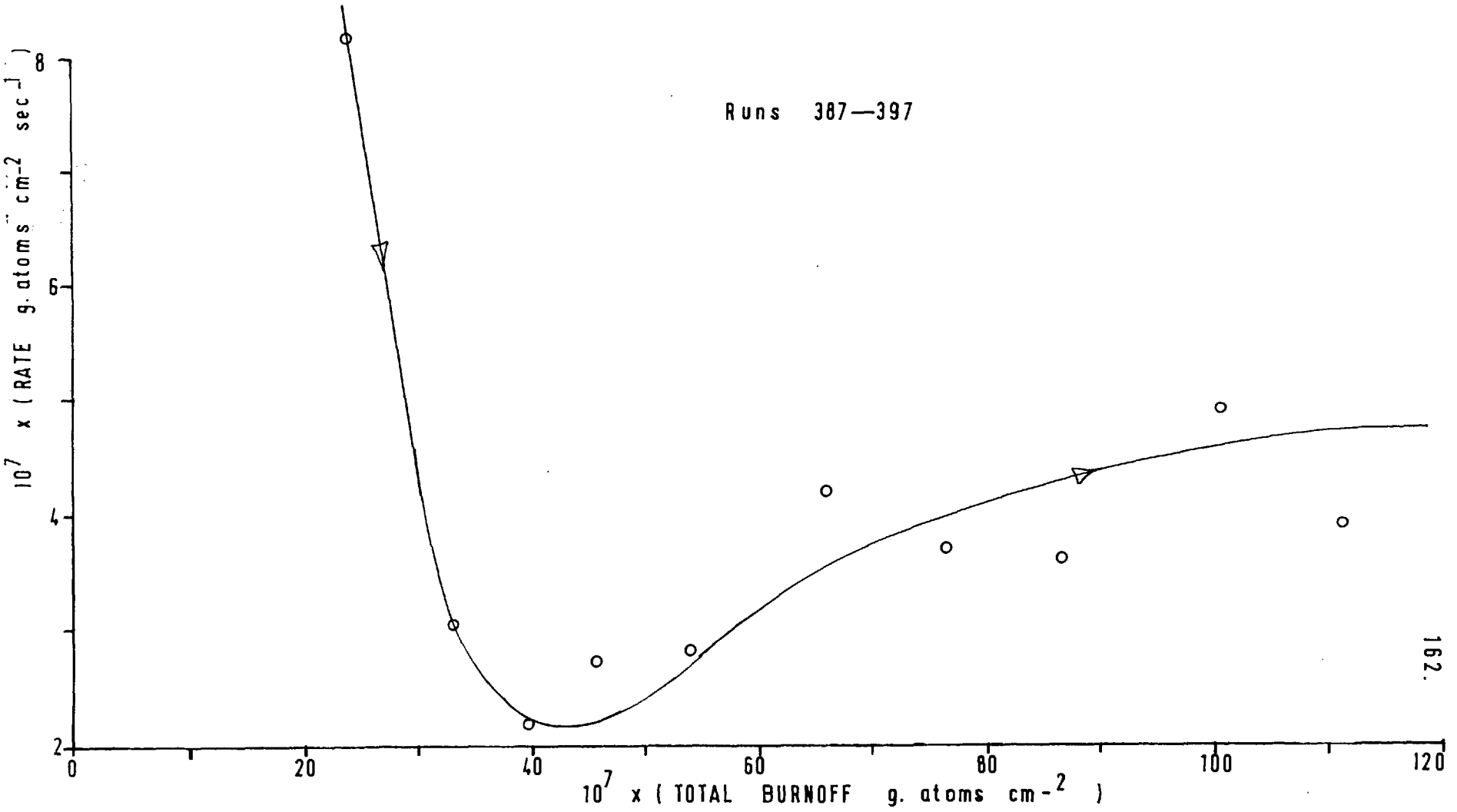

reaction for iron treated filaments. The order runs show a different mechanism is operative although they may be confused by the effect of pressure on the tungsten on the surface. The higher pressure would favour the formation of elementary tungsten or possibly carbide. A full discussion of this question is given in Section 7.

5.6. Molybdenum Treated Filaments.

5.6.1. Mo metal and MoO_3 suspensions.

A freshly coated filament was painted with a suspension of very fine molybdenum powder in acetone and rate-temperature curves were determined. During certain runs it was found that nearly 75% of the oxygen was reacted in 1 second and in order to measure the temperature during runs 734-737 it was necessary to react the filament for 5 seconds in 50μ of oxygen. The results are shown in Table 5.15 and on Graph 5.9, and it can be seen that there is an almost 100 fold increase in rates at high temperatures. The oxygen balances are low, particularly for the initial run 723 where it was 63%, and this suggests that molybdenum oxides are formed (see Section 7).

Examination of runs 730-732 for reaction at 1520°C suggests reduction in the O_2 pressure, or the large quantity of CO produced, is limiting the reaction at high temperatures since almost the same quantity of CO is produced for reaction times of 5, 2, and 1 second. The main difficulties experienced for these very fast reactions were:-

1. Timing 1 second exactly.

2. Knowing the true average temperature since for a considerable percentage of the timed reaction over 1 second the filament was heating up.

GRAPH 5·9 Rate-temperature curves for Molybdenum treated filament

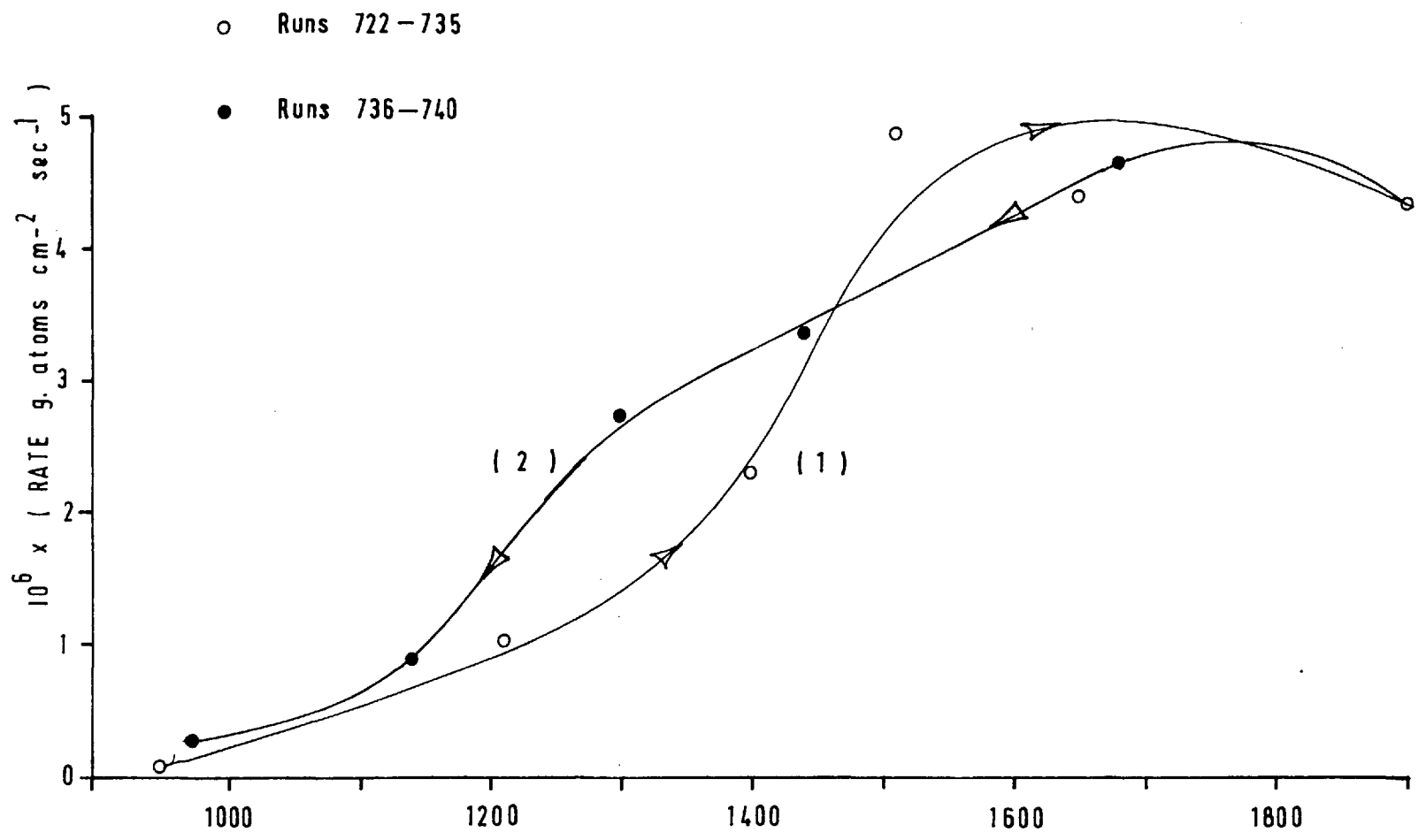

Table 5.15. Molybdenum treated filament.

Filament No.33.

Run 722 Untreated filament.

Run No.	T°C	Secs. react.	Initial pressure μ	Pressure CO μ	CO_2/CO ratio	Oxygen balance	$Rx10^8$
722	1300	60	47.8	13.4	0.03	100	12.6
723	950	30	48.8	28.2	0.04	63	8.4
724	1200	5	50.2	41.4	0.02	82	76.7
725	1210	2	48.4	21.5	0.05	97	103
726	1210		49.0	25.8	0	97	118
727	1210		50.0	28.8	0	97	131
728	1400	5	49.2	66.4	0	94	121
729	1400	2	49.0	50.4	0	89	230
730	1520	5	48.8	69.2	0.01	100	127
731	1520	2	48.6	53.8	0.01	86	248
732	1520	1	48.0	52.8	0.01	88	487
734*	1650	1	49.2	48.2	0	86	440
735*	1900	1	50.0	47.8	0	85	430
736*	1680	1	48.0	51.0	0.01	90	460
737*	1440	1	49.6	36.7	0	92	335
738*	1300	1	47.0	29.8	0	90	272
739	1140	5	47.2	49.2	0	80	90
740	970	5	49.2	16.0	0.01	87	29.2

* For these runs the filament was first burnt in 50 ± 5μ of oxygen for 5 seconds.

3. The possibility that even for 1 second reaction at high rates the reaction was effected by reduction in the oxygen partial pressure.

A new filament, No.34, was also painted with a molybdenum suspension as before and the following series of runs, Table 5.16, carried out.

a) Three runs at 1230°C to see if the rate changed with burn off; Runs 741-743. From these runs it appeared that the rate increases with burn off.

b) Heating the filament at 1230°C in vacuum, Runs 744 A and B showed that mainly CO was desorbed from the filament but the amount desorbed would not alone account for the increase in rate.

c) Further runs at 1230°C, Runs 745-747, showed that heating the filament in vacuum appeared to have increased the rate slightly and again showed that the rate increased with increasing burn off. The increase in rate after heating in vacuum can be considered the same as the increase due to burn off through runs 741-747 and it is not the fact of vacuum that has caused the increase but the oxygen desorbed with carbon as CO, i.e. reaction. After the heating in vacuum the oxygen balances were even lower than before.

d) Heating in vacuum at a higher temperature of 1700°C did not cause any decrease in rate; the rate being about

Table 5.16. Molybdenum treated filament.

Filament No.34.

Run No.	T°C	secs. react.	Initial pressure μ	Pressure CO μ	CO_2/CO ratio	Oxygen balance	$Rx10^8$
741	1230	5	46.8	52.3	0	94	96
742	1230	2	50.8	21.2	0.02	90	98.7
743	1230	2	49.8	26.3	0.01	92	121
744A	1230	15	0	13.2incr.	-	-	-
744B	1230	60	0	4.0incr.	-	-	-
745	1230	2	49.6	28.4	0.02	88	132
746	1230	2	47.8	32	0	89	144
747	1230	2	49.7	37.2	0	92	169
748	1700	5	51.2	-	0	-	-
749	1700	1	51.4	47.0	0.01	84	433
750	1700	300	0	28.6	0.01	-	-
751	1700	1	49.8	52.8	0	96	484

Analysis of Molybdenum treated filaments.

Filament No.	Run Nos.	Treatment	Analysis
33	723-740	Mo powder in acetone	0.67% Mo
34	741-751	Mo powder in acetone	0.67% Mo
35	752-769	MoO_3 suspension in acetone	0.01% Mo
			Also traces Si, Fe, and Mg.

4.5×10^{-6} gr atoms/cm^2 sec, after treatment, where it is possibly diffusion restricted.

Since it was thought possible that some intermediate oxide of molybdenum acted as an intermediate in the reaction a second series of reactions were carried out on a molybdenum trioxide treated filament. Since this is a high oxide state the oxide would reduce the high oxygen balances to the same intermediate state postulated and have the same effect as elementary molybdenum.

A new filament, No.35, was painted with a suspension of MoO_3 powder in acetone and Runs 754-769, Table 5.17, carried out. Reaction at 1100°C showed an increase in rate of about 10 over the untreated filament which is the same order as found for the Mo metal treated filament at 1100°C. The oxygen balances were very near 100% which shows that very little of the oxide has decomposed. Reaction at 1700°C shows no signs of decomposition, the rate falling off with burn off from 17 to 3.8×10^{-7} gr atoms/cm^2 sec. These rates are between 90 and 15 times greater than for untreated filaments but lower than those found for molybdenum metal treated filaments which showed no signs of fall off in rate with burn off. Further reaction at 1100°C showed that the rate had been decreased by reaction at 1700°C but it was still nearly 10 times greater than for untreated filaments. After

Table 5.17. Molybdenum Trioxide.

Filament No.35.

Run No.	T°C	Sec. react.	Initial pressure μ	Pressure CO μ	CO_2/CO ratio	Oxygen balance	$Rx10^8$
754	1100	15	47.0	64.2	0.01	100	39.4
755	1100	5	50.8	27.8	0.02	99	51.7
757	1100	5	51.6	25.4	0.02	98	47.3
758	1100	5	52.0	20.8	0	99	38.0
759	1100	5	48.6	16.6	0.01	99	30.5
760	1100	5	51.6	16.1	0.01	98	29.6
761	1700	15	49.6	5.0	0.06	99	96.4
762	1700	15	49.5	5.9	0.07	98	38.3
763	1700	15	49.6	4.0	0.12	98	27.4
764	1700	30	51.3	7.4	0.03	98	23.1
765	1100	5	52.4	10.4	0.07	98	20.3
766	1100	5	50.0	12.8	0.01	100	23.5
767	1100	5	48.4	13.4	0.02	100	25.0
768	1100	5	50.4	13.0	0.01	100	23.9
Filament heated for 3 mins. in vacuum at 1100°C							
769	1100	5	50.0	9.8	0.02	99	18.3

heating in vacuum for 3 minutes at 1100°C a further decrease in rate was evident, Run 769.

After reaction all the filaments were very pitted, Photo 20, showing the nature of the surface. The second of the metal treated filaments, No.34, had white spots associated with several of the pits, this being further evidence for supposing the metal had been converted to oxide.

The trioxide treated filament was very similar in appearance and for all the filaments the cones were visible on the smooth surface between the pits as shown on Photo 21 where a large crater can also be seen in the bottom right corner.

Analysis of the filaments, Table 5.16, shows a considerable quantity of Mo left on the metal treated filaments as expected from the photographs. However the MoO_3 treated filament had only 0.01% Mo left. This accounts for the lower rates observed for the MoO_3 treated filaments compared with Mo treated filaments. Since normal oxygen balances were found it seems that the MoO_3 evaporated off the surface without decomposing, the remainder being left as metal or carbide. Thermodynamically while the dioxide can be reduced by carbon, Table A.3.6, it is suggested that this only occurs at the botton of the Mo globules where initimate contact exists. On the surface far removed from the carbon, MoO_2 can exist below 2000°K.

Photo 20. Molybdenum metal treated filament No.33. x200

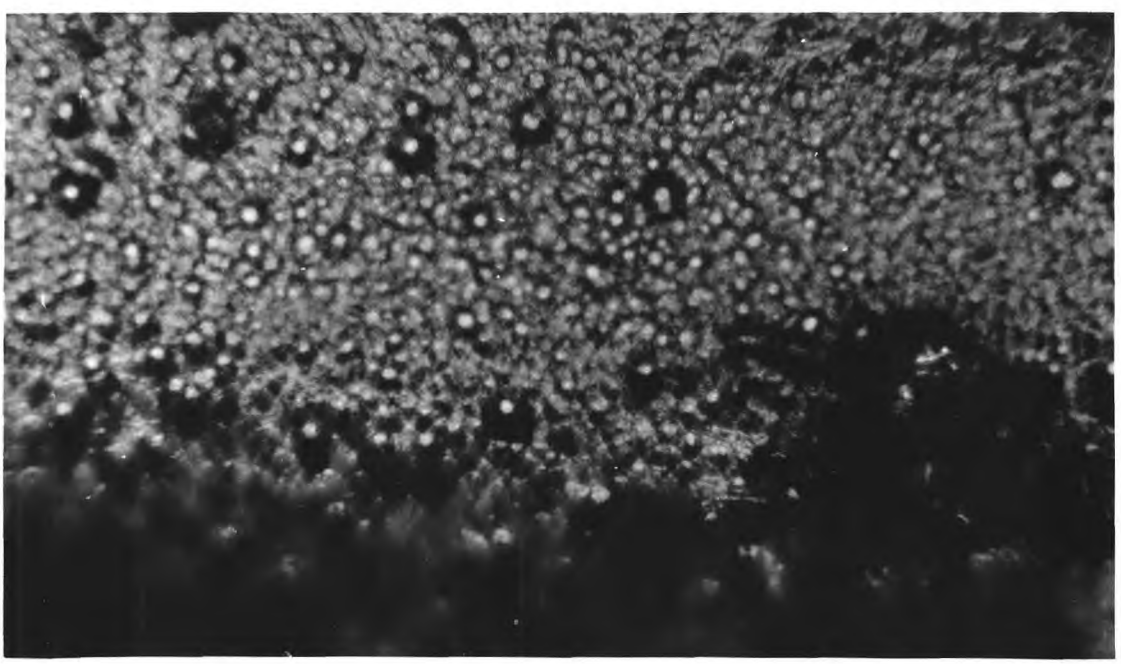

Photo 21. MoO_3 treated filament No. 34. x800

5§6.2. Molybdenum (vacuum deposited) treated filaments.

1. Considering the large catalytic effect noticed for molybdenum in the previous runs, further runs were carried out using smaller quantities of molybdenum. A convenient method of treatment utilized was by heating Mo wire in oxygen whereon the volatile oxides would in part deposit on the filament.

In all cases the treatment was the same; namely heating a molybdenum wire at 1800°C in 50μ of oxygen until the pressure fell to 5μ. During this treatment, which took about 15 seconds, the filament holder was turned through 360° so as to deposit the molybdenum as far as possible on all sides of the filament.

For the initial runs 1499-1504, Table 5.18, the filament was treated twice before the first run. The rate at first showed a strong catalytic effect but this quickly fell off with burn off. Reaction at 2000°C, Runs 1505-1509, showed a lesser catalytic effect, the rate being near normal if the filament was not treated before the actual run. Subsequent reaction at 1510°C, Runs 1510-1511, showed an initially high rate but this may be due to the normal hysteresis effect. Treating the filament before each run, Runs 1512-1514 again showed the catalytic effect, but the rate did not appear to increase due to accumulation of catalyst on the surface.

Table 5.18. Mo Vacuum deposited Runs.

Run No.	T°C	Secs. react.	Initial pressure μ	Pressure CO μ	CO_2/CO ratio	Oxygen balance	$Rx10^8$
*1499	1000	15	50.5	37.0	0.04	101	23.5
1500	1000	10	51.2	7.6	0.21	102	8.40
1501	1000	15	51.0	12.0	0.17	102	8.52
1502	1000	15	51.7	8.9	0.16	101	6.26
1503	1000	15	50.9	6.0	0.07	99	3.89
1504	1000	15	50.0	4.0	0.10	99	2.68
1505	2000	15	49.2	2.5	0.08	99	1.64
1506	2000	30	50.7	3.8	0.53	104	1.76
*1507	2000	15	51.6	3.9	0.	99	2.37
1508	2000	15	49.4	2.2	0.36	99	1.82
*1509	2000	15	49.0	4.2	0.05	100	2.68
1510	1000	15	50.0	10.7	0.04	99	6.75
1511	1000	15	50.5	5.1	0.06		3.28
*1512	1000	15	51.6	13.4	0.09	99	8.88
*1513	1000	15	48.2	15.2	0.04	98	9.61
*1514	1000	15	48.9	13.8	0.01	100	8.52

* treated

These results suggest that while the molybdenum deposited as oxides have a catalytic effect, most of the oxide is driven off during the first moments of reaction. An alternative explanation is that while a considerable amount of the oxide is driven off, the part remaining is reduced to metal and/or carbide which is a less active catalyst.

A series of rate-temperature curves were then determined on the filament, it being treated before each run; this being similar to the tungsten runs, Table A.5.18. These runs, 1515-1534, are plotted on Graph 5.10. A well defined maximum is visible in all the curves but the possibility remains that the maximum may be caused by quicker evaporation of the molybdenum as oxides at higher temperatures.

There also appears to be an hysteresis effect between curves 1 and 2. Curve 3 was determined to see if the reason that curve 2 gave higher rates was due to generally increased reactivity of the filament rather than a fundamental hysteresis effect. The rates obtained for Curve 3 were higher than for curve 1 but there still remains a hysteresis effect between curves 2 and 3. Also the fact that the rates become near one another above 1600^{o}C rather discounts the possibility of the filament increasing irreversibly in reactivity.

A series of curves 4 to 6 were also determined

GRAPH 5.10 Rate-temperature curves for a Molybdenum (from Mo filament) treated filament, at 50 μ

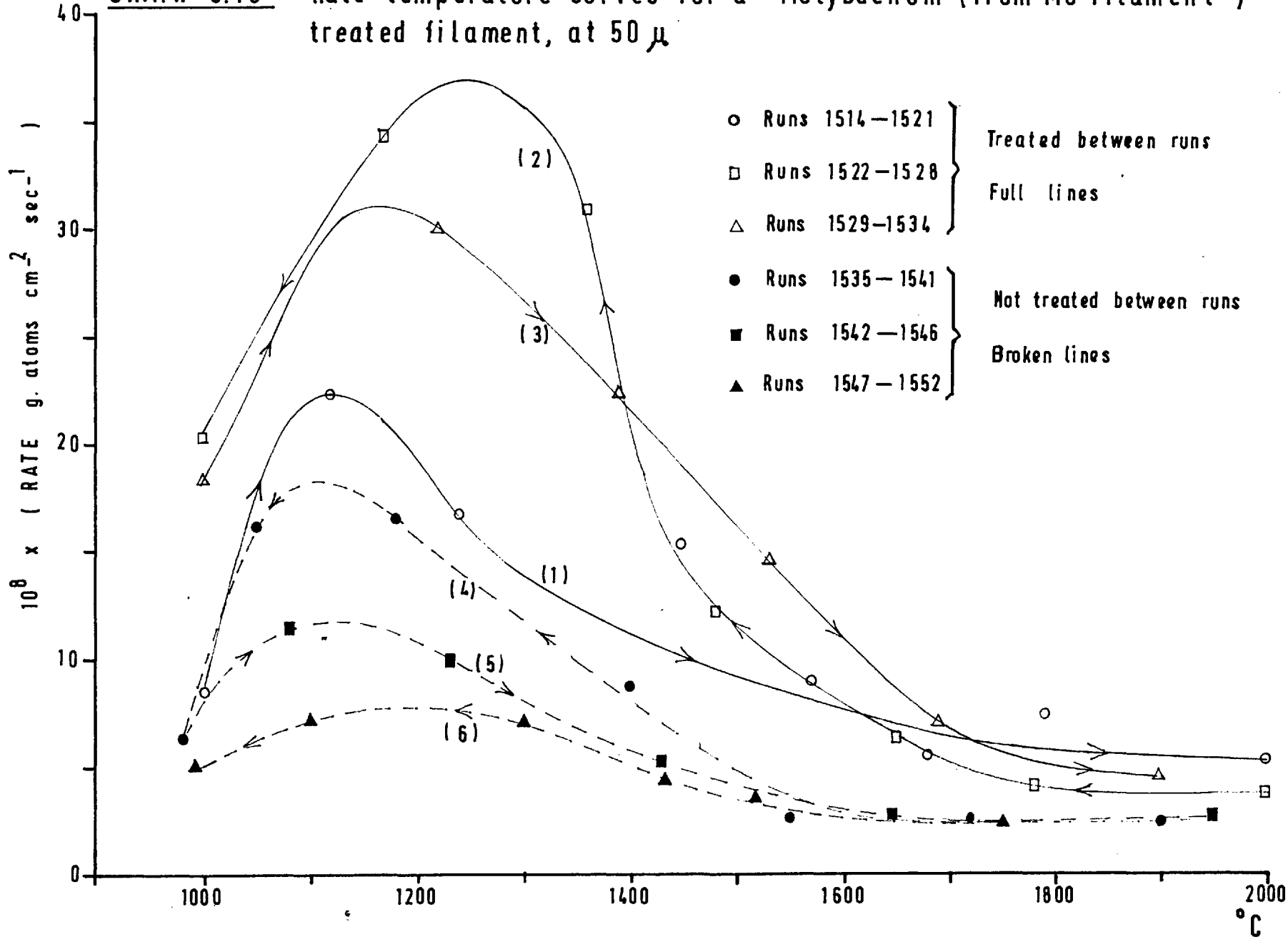

without heating the filament between runs to see if any catalytic activity remained after burn off. For curve 4 there appears to be a certain amount of catalyst still on the filament, the rate being between 3 and 4 times greater than for untreated filaments in the middle temperature range. No fundamental hysteresis can be seen between curves 4-6, rather the activity appears to be decreasing with burn off. The rates obtained for Curve 6 are not very different from those obtained on untreated filaments. For all these curves the rate above 1600°C remains fairly constant and about equal to the untreated filament rates. These last results curves 4-6 strongly suggest that the catalyst is affecting the fundamental mechanism causing a true maximum to appear rather than the maximum due to the impurity being driven off. This is particularly true of curve 4 where the reaction was first at high temperatures.

2. In order to remove the possibility of reduction of the oxides during the course of reaction affecting the reaction and to elucidate the effect of elementary Mo, a second series of runs were carried out. During these runs 1514-1534, Table A.5.18, the filament was treated as before with Mo oxides. The filament was then heated at 1500°C in vacuum to reduce the oxides. During this heat treatment between 1.2 and 1.8μ of gas was given off, but this quantity of gas could be simple desorption.

The first curve 1 should probably be discounted because the reaction times used were too long at intermediate temperatures and depletion of oxygen probably was affecting the results. Curves 2 and 3 show well defined maximum and lie close together. There is no sign of hysteresis and this is as would be expected considering the treatment given to the filament.

Generally the rate was catalysed by a factor of about 20 and the activity of the Mo when reduced seems to be greater than shown in the earlier runs on Graph 5.10. The reaction appeared to occur predominantly over about $1\frac{1}{2}$" of filament where the Mo was deposited; this portion of the filament being in the most direct line with the source of Mo. A visible thinning of the filament was noticeable in this region and the temperature was about 100°C higher than the other parts of the filament.

The product was predominantly CO while the oxygen balances tended to be slightly high. This is thought to be due to the analysis not being so efficient with the large quantities of CO in the product, but the amount of CO found by analysis and predicted from the pressure rise analysis were in good agreement.

Finally a series of curves were carried out without further treatment on the filament, Curves 4 and 5, Graph 5.11.

GRAPH 5.11 Rate-temperature curves for a Molybdenum (from Mo filament) treated filament at 50 μ

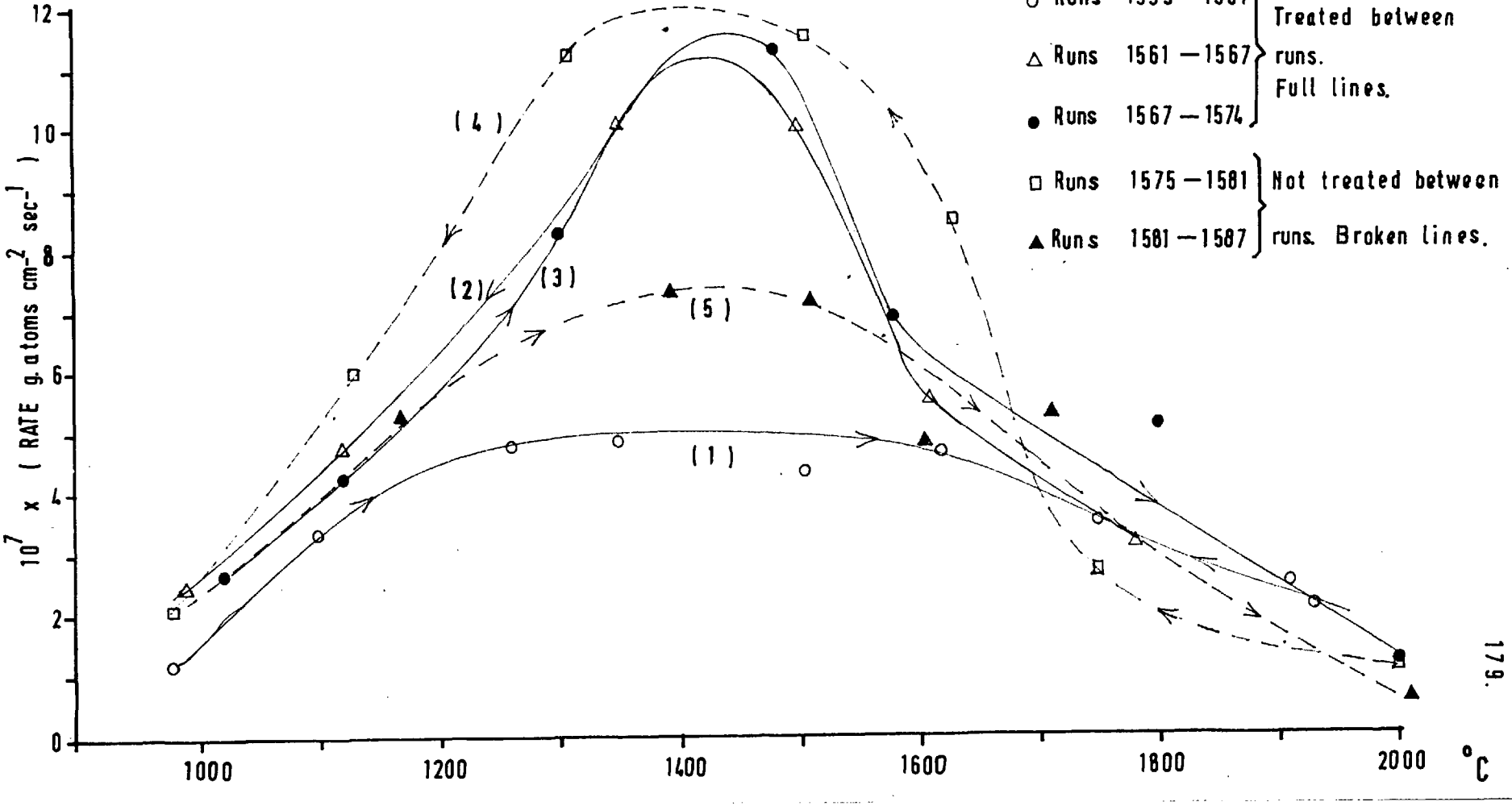

The first of these curves shows that the rate appears to be even greater than for the treated cases. This shows that the Mo must still be on the surface and the slightly higher rates may be due to the fact that the filament was not heated at 1500°C. That is it is a fundamental increase in activity due to reaction at higher temperatures. The final series, Curve 5, shows low rates, and this thought due to depletion of the Mo from the surface, as found in the runs shown on Graph 5.10, Curves 4-6.

Examination of the filaments under a microscope showed a very pitted surface with many small craters and no signs of metal on the surface.

5.7. Zirconium Treated Filaments.

For the first series of runs metallic zirconium particles were used. These were painted onto the filament in acetone and reaction between 950 and 2000°C carried out. These results are shown in Table A.5.19 and on Graph A.5.5 and are not different from untreated filament results. Examination of the filament after reaction showed a few silvery pieces of zirconium lightly attached to the filament, the surface otherwise appearing unblemished.

In order to try and get a better coating of zirconium the filament surface, zirconium was painted onto the filament as before followed by heating of the filament for a total of 30 minutes at 2000°C in vacuum. During this heating carbon deposits formed on the reactor walls possibly due to the advent of a glow discharge and the reactor was therefore recleaned with chromic acid. The filament was covered with patches of a light grey substance showing that the zirconium had melted over the surface. A series of runs, Table 5.19, Curve 1, Fig.5.12, were carried out at increasing temperature, the patches going white after Run 681 at 1620°C. The rate was quite normal up to 1620°C but at 1800°C it was considerably higher than untreated filaments. The oxygen balance was low but increasing up to 1620°C showing a zirconium oxide being formed. The first run at 1800°C

Table 5.19. Zirconium

Filament 30B.

Run No.	T°C	Secs react.	Initial pressure μ	Pressure CO μ	CO_2/CO ratio	Oxygen balance	Rx10^8
678	1100	30	48.8	7.4	0.09	88	2.5
679	1300	30	51.0	9.5	0.12	84	3.2
680	1500	30	51.6	9.7	0.10	91	3.3
681	1120	30	50.5	8.7	0.10	99	2.9
682	1500	30	49.0	34.0	0.01	93	11.3
683	1800	5	51.2	35.2	0.02	86	21.8

suggests that the oxide breaks down at this temperature but the second run at 1800°C again shows a net uptake of oxygen.

Following these runs the filament was heated at 2000°C for 15 seconds during which the pressure rose from 49.5μ of oxygen to 110μ, a pressure rise not possible by oxygen reaction. Further heating of the filament at 2000°C for 5 seconds, this time in vacuum, caused 16.9μ of gases to be released. These runs show how readily at high temperatures the oxide decomposes.

A new coated filament, No.31, was painted with Zr as before and heated at 2000°C for 30 minutes in vacuum. Reaction was then carried out at increasing temperatures followed by decreasing temperatures. The results are shown in Table 5.20 and the rate-temperature curves are plotted on Graph 5.12. The rate is fairly constant over the intermediate temperature range for the up curves but otherwise increases with temperature, no maximum as such being evident. The filament appears to be activated at high temperatures and this is associated with oxygen balances of between 90 and 100% at these temperatures. The initial oxygen balances were very low while some oxide was first formed.

Filament 32 was treated and heated in vacuum as before. In order to see if gases were released from the filament if it was heated in vacuum, the filament was first

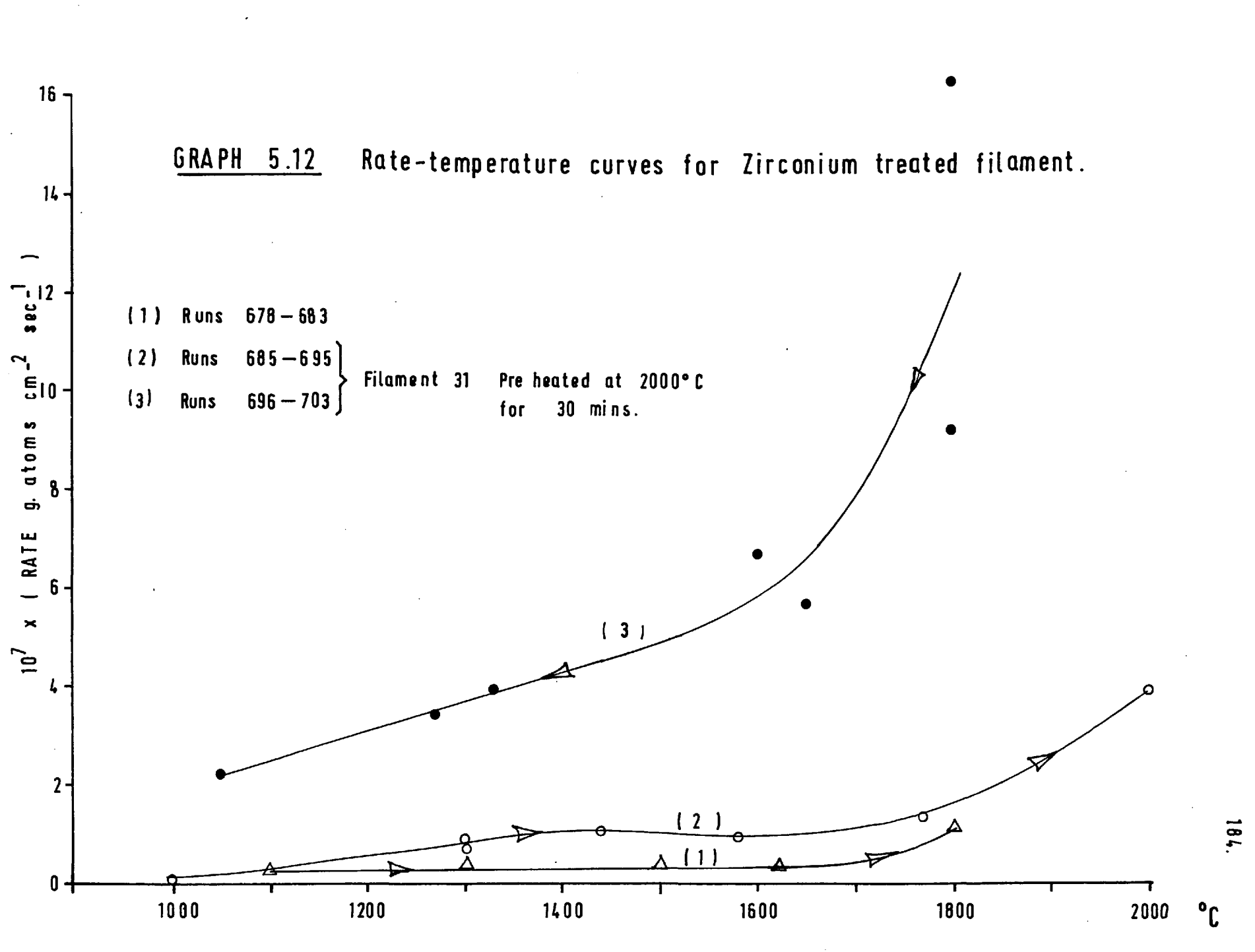
GRAPH 5.12 Rate-temperature curves for Zirconium treated filament.
(1) Runs 678 – 683
(2) Runs 685 – 695
(3) Runs 696 – 703
Filament 31 Pre heated at 2000° C for 30 mins.
10^7 x (RATE g. atoms cm^{-2} sec^{-1})
0
2
4
6
8
10
12
14
16
1000
1200
1400
1600
1800
2000
°C
(1)
(2)
(3)

Table 5.20. Zirconium Runs.

Filament 31, initially heated at 2000°C in vacuum for 30 mins.

Run No.	T°C	Secs. react.	Initial pressure μ	Pressure CO μ	CO_2/CO ratio	Oxygen balance	Rx10^8
685	1000	30	50.6		0	63	0.91
686	1300	30	53.2	19.4	0.06	47	6.3
687	1300	30	51.5	22.0	0.13	52	7.5
688	1300	30	53.7	18.4	0.30	103	7.3
689	1300	30	49.2	26.6	0.05	96	8.5
690	1300	30	50.4	29.0	0.02	113	9.0
691	1300	30	50.4	28.8	0.02	98	8.9
692	1440	30	52.5	32.9	0.03	100	10.2
693	1580	15	51.2	16.0	0	101	9.7
694	1770	15	52.4	22.0	0	100	13.4
695	2000	15	51.5	64.6	0	90	39.3
696	2000	5	52.4		0		-
697	1650	10	50.2	61.4	0	97	56.1
698	1900	5	47.4	50.4	0	101	92.0
699	1900	2	49.4	35.8	0	98	163
700	1600	5	47.8	35.8	0.02	103	66.8
701	1330	5	50.0	21.4	0.01	103	39.6
702	1270	5	49.6	18.3	0.02	100	34.0
703	1050	5	47.0	12.1	0	106	22.1

heated in oxygen at 1350°C for 1 minute. During this time the pressure of oxygen fell from 48.8μ to 22.6μ. Further heating in oxygen caused the pressure to fall from 47.8 to 43.0μ during 25 seconds, after which the pressure started to rise.

The filament was then heated in vacuum at 1800°C, Run 706, for 30 seconds during which the pressure rose to 46.0μ, the products consisting of 92% CO and 1.7% CO_2. Further heating at 1800°C in vacuum gave the following results

Run No.	Secs. Heating	Increase in Pressure μ	%CO_2	%CO
707A	30	20.8	38	81
707B	30	16.8	No analysis.	
707C	60	15.2	Product assumed	
707D	60	5.2	to be predominantly CO	

These results show that the evolution of CO decreases with time of treatment as all the oxide is becoming decomposed.

A series of runs were then carried out at 1800°C to see what effect the heating in vacuum had had on the reaction rates. The results, Table 5.21, show that both the rate and the low oxygen balances increase with time of reaction. The scatter during runs 713-715 was due to the short reaction time of 2 seconds used.

Heating the same filament in an atmosphere of CO

Table 5.21. Zirconium

Filament No.32.

Reaction at 1800°C.

Run No.	Secs. react.	Initial pressure μ	Pressure CO μ	CO_2/CO ratio	Oxygen balance	$Rx10^8$
708	10	51.2	38.6	0.01	72	35.9
709	10	48.8	46.0	0.05	90	44.3
710	5	48.8	38.9	0.02	90	72.5
711	5	47.8	47.8	0	90	87.7
712	5	51.0	52.0	0	91	95.0
713	2	48.6	17.0	0.01	92	78.5
714	2	49.6	24.0	0.04	96	113.6
715	2	48.6	21.6	0	95	98.5

Table 5.22. Zirconium treated filaments

Filament No.32.

Run No.	T°C	Secs. react	Initial pressure μ	Pressure CO μ	CO_2/CO ratio	Oxygen balance	$Rx10^7$
After heating in vacuum at 1800°C							
717	1800	2	47.8	25.6	0.03	88	12.0
718	1800	2	50.7	29.8	0.02	92	14.0
719	1800	2	48.0	30.0	0.02	96	14.0
720	1350	5	49.2	12.9	0.04	95	2.45
721	1350	5	51.2	13.2	0.04	97	2.50

at 1800°C for 10 seconds also caused the pressure to rise, from 45.6 to 64.0μ with a 96% CO product. A further 3 runs at 1800°C, 717-719, Table 5.22, showed the same as runs 713-715, namely increasing oxygen balances with increasing rates with reaction time. Reaction at 1350°C, Runs 720-721, showed that the reaction at 1800°C had activated the filament as seen in the earlier rate-temperature curves.

The filaments after reaction were covered with several large craters in several of which white spots could be seen as shown in Photo 24. These white spots can be associated with the dioxide which would not be reduced far from carbon. The thermodynamics again show that it is possible for both oxide, metal and carbide to exist depending on temperature and how intimate the contact is with the surface.

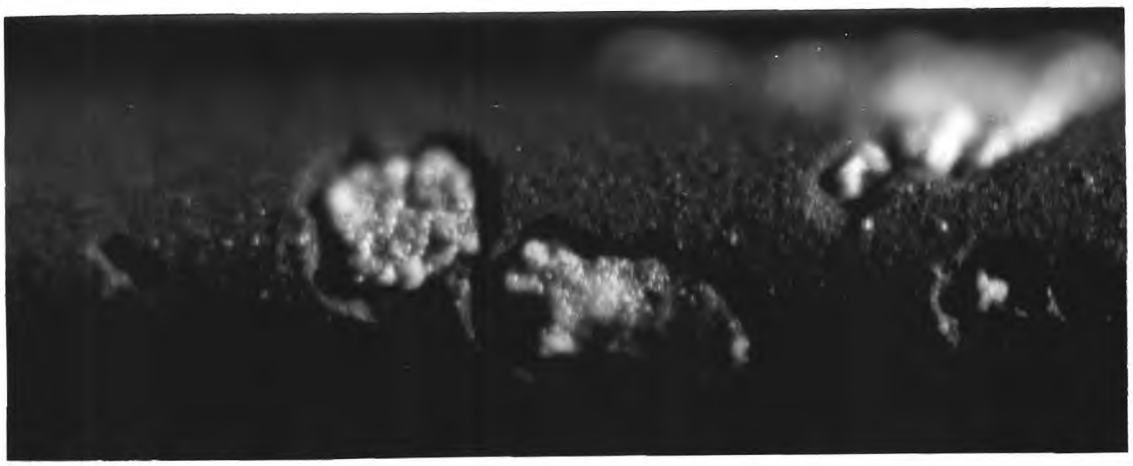

Photo 22. Zirconium treated filament No. 32. x200

5.8. Uranium trioxide treated filaments.

After an initial blank run, 797, a new coated filament was painted with a fine suspension of UO_3 in distilled water after which the filament appeared completely covered by yellow particles. Reaction was then carried out at 1200°C followed by reaction at 1670°C and 1020°C. After the first run at 1200°C, Run 798, the filament was no longer yellow; the full results are given in Table 5.23 and they show that the UO_3 has a strong catalytic effect. After the initially high oxygen balance of 128% due to the decomposition of the trioxide, possibly to the dioxide, the oxygen balances were generally between 94 and 100%, with a large amount of CO_2 in the product. Within the experimental error the rates did not alter with burn off.

Rate-temperature curves at increasing and decreasing temperatures, plotted on Graph 5.13, show a maximum in the rate between 1500°C and 1600°C, comapred with 1200 and 1300°C for the untreated filaments. There appears to be slight hysteresis above 1400°C working in the low sense. The full results are given in Table 5.24 and again show low oxygen balances and high proportions of CO_2.

As shown on Graph 5.14, the CO_2/CO ratio shows a strong relationship with the oxygen balance, the proportion of CO_2 being far lower for low oxygen balances. This

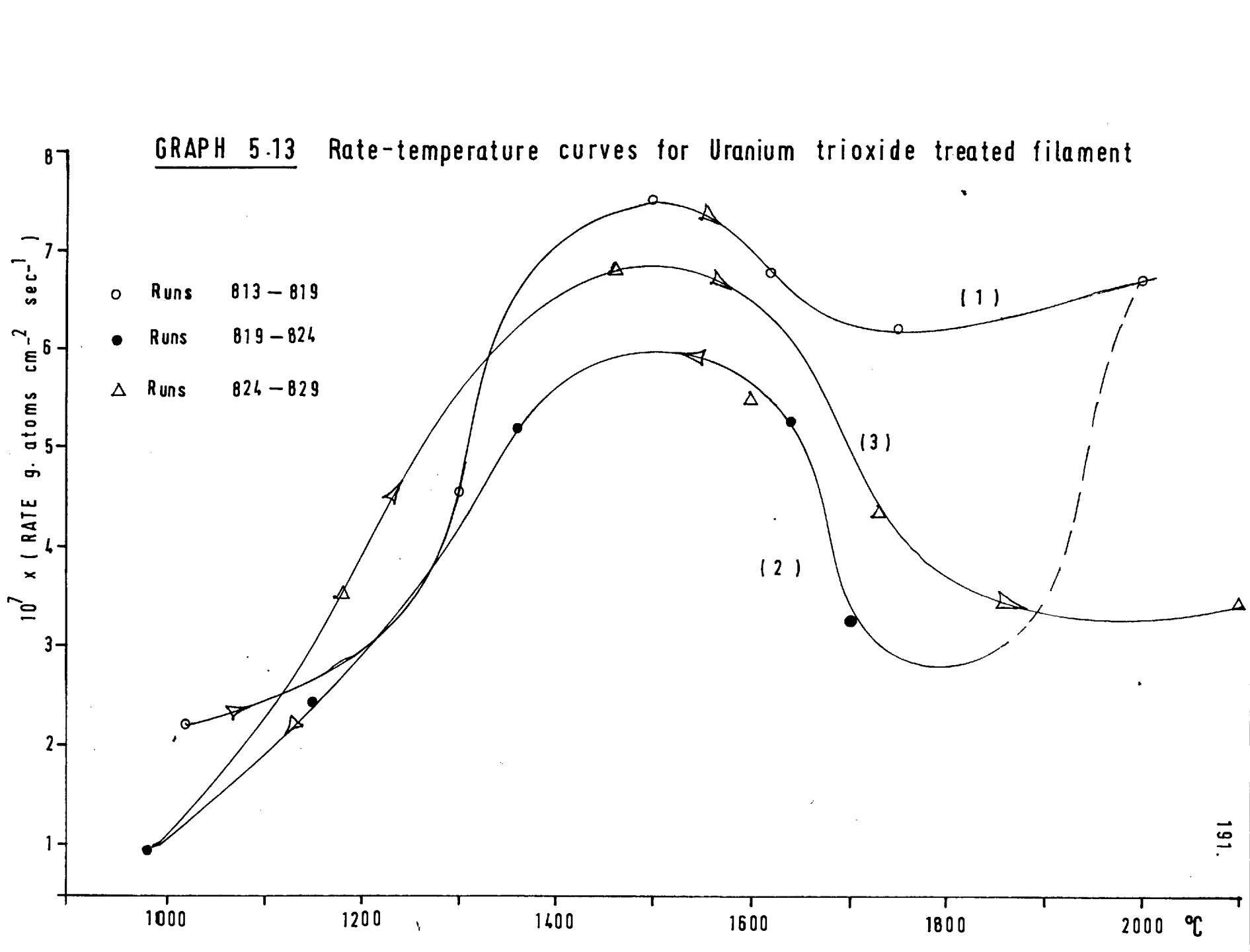
GRAPH 5.13 Rate-temperature curves for Uranium trioxide treated filament
Runs 813 – 819
Runs 819 – 824
Runs 824 – 829
(1)
(2)
(3)
10^7 x (RATE g. atoms cm^{-2} sec^{-1})
8
7
6
5
4
3
2
1
1000
1200
1400
1600
1800
2000 °C
191.

GRAPH 5.14 Variation of CO_2/CO ratio with oxygen balance for a Uranium trioxide treated filament

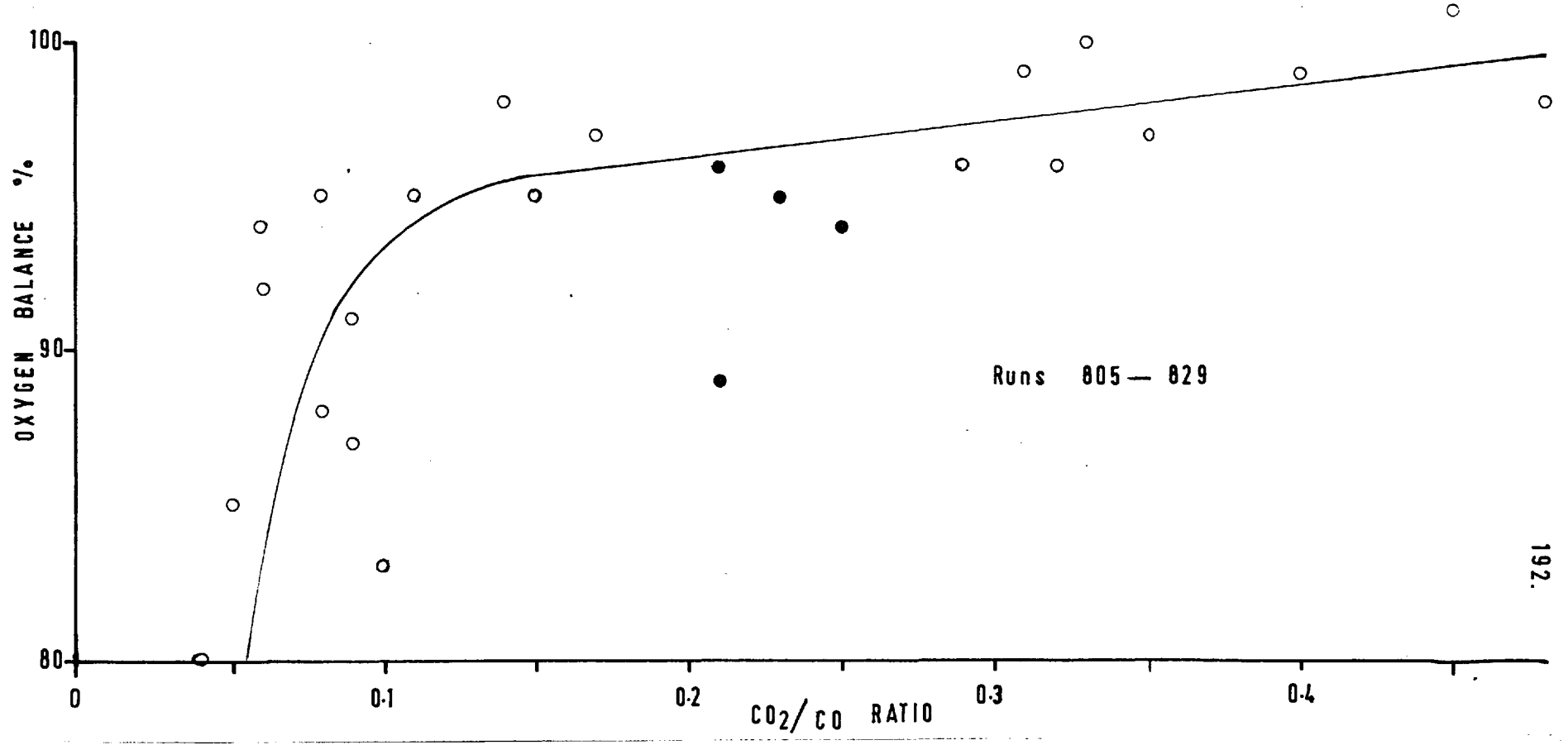

Table 5.23. Uranium trioxide treated filaments.

Filament No.41.

Run 797 untreated filament.

Run No.	T°C	Secs. react	Initial pressure μ	Pressure CO μ	CO_2/CO ratio	Oxygen balance	$Rx10^8$
797	1200	30	51.2	16.3	0.03	98	5.11
798	1200	10	50.8	21.0	0.39	128	26.5
799	1200	30					
800	1200	5	52.0	8.4	0.50	96	23.0
801	1200	10	51.0	17.6	0.39	98	22.3
802	1200	5	50.8	9.8	0.41	97	25.2
803	1670	10	51.5	70.8	0.10	101	70.7
804	1670	2	50.2	22.2	0.21	89	122
805	1670	2	52.0	22.0	0.24	94	125
806	1670	2	50.8	21.6	0.23	95	120.7
807	1670	2	51.8	22.4	0.21	96	124
808	1020	3+2	52.8	5.9	0.64	94	17.7
809	1020	5	53.0	12.1	0.48	98	32.7
810	1020	3+2	51.7	9.4	0.40	99	25.9
811	1020	5	54.2	13.5	0.35	97	33.3
812	1020	5	52.7	9.9	0.32	96	23.9
813	1020	5	52.6	9.2	0.33	100	22.3

Table 5.24. Uranium trioxide treated filament.

Filament No.41.

Run No.	T°C	Secs. react.	Initial pressure μ	Pressure CO μ	CO_2/CO ratio	Oxygen balance	$Rx10^8$
814	1300	5	51.4	17.2	0.45	101	45.7
815	1500	5	52.0	35.7	0.16	97	75.3
816	1500	2	50.2	11.3	0.31	99	67.3
817	1620	5	50.6	32.4	0.15	95	68.0
818	1750	5	52.0	31.6	0.08	88	62.3
819	2000	5	50.3	33.8	0.09	87	67.3
820	1700	5	49.6	16.6	0.10	83	32.9
821	1040	5	50.6	26.5	0.09	91	53.0
822	1360	5	50.7	22.0	0.29	96	52.1
823	1150	5	48.6	11.8	0.14	98	24.5
824	980	15	51.8	14.6	0.04	80	9.27
825	1180	5	51.2	17.4	0.11	95	35.3
826	1460	5	50.0	34.6	0.08	95	68.5
827	1600	5	52.2	28.5	0.06	94	55.0
828	1730	5	51.8	22.4	0.06	92	43.5
829	2100	5	50.0	18.0	0.04	85	34.5

suggests that the CO_2 comes off via an uranium compound, the uranium adsorbing oxygen and releasing it as CO_2, but this simple mechanism cannot account for the full increase in rate. The CO_2/CO ratio also goes through a maximum with temperature at 1300°C, Graph 5.15, the effect decreasing with increasing burn offs. The oxygen balance decreases with temperature, but only after 1300°C, Graph 5.16. These results suggest that at high temperatures some oxide starts to form on the surface taking up oxygen which decomposes about 1300°C for our pressure of 50μ.

Heating a freshly coated uranium trioxide treated filament in vacuum at 2000°C for 30 seconds caused the filament again to become black with a pressure rise of 39.0μ. the product consisting of 64% CO and 9.7% CO_2. Further heating at 2000°C for 30 seconds gave a pressure rise of only 5.5μ.

The filament was then burnt in oxygen for 15 secs. at 2000°C during which the pressure rose from 50μ to 75μ. Subsequent heating in vacuum at 2000°C for 30 seconds gave a pressure rise of only 1.9μ. This was repeated by burning in 50μ of oxygen followed by heating in vacuum at 1800°C with a resulting rise of only 1.3μ. A repeat of this run gave a 2.4μ increase.

These runs show that any oxide on the carbon surface

GRAPH 5.15 Variation of CO_2/CO ratio with temperature for a Uranium trioxide treated filament

GRAPH 5.16 Variation of oxygen balance with temperature for a Uranium trioxide treated filament

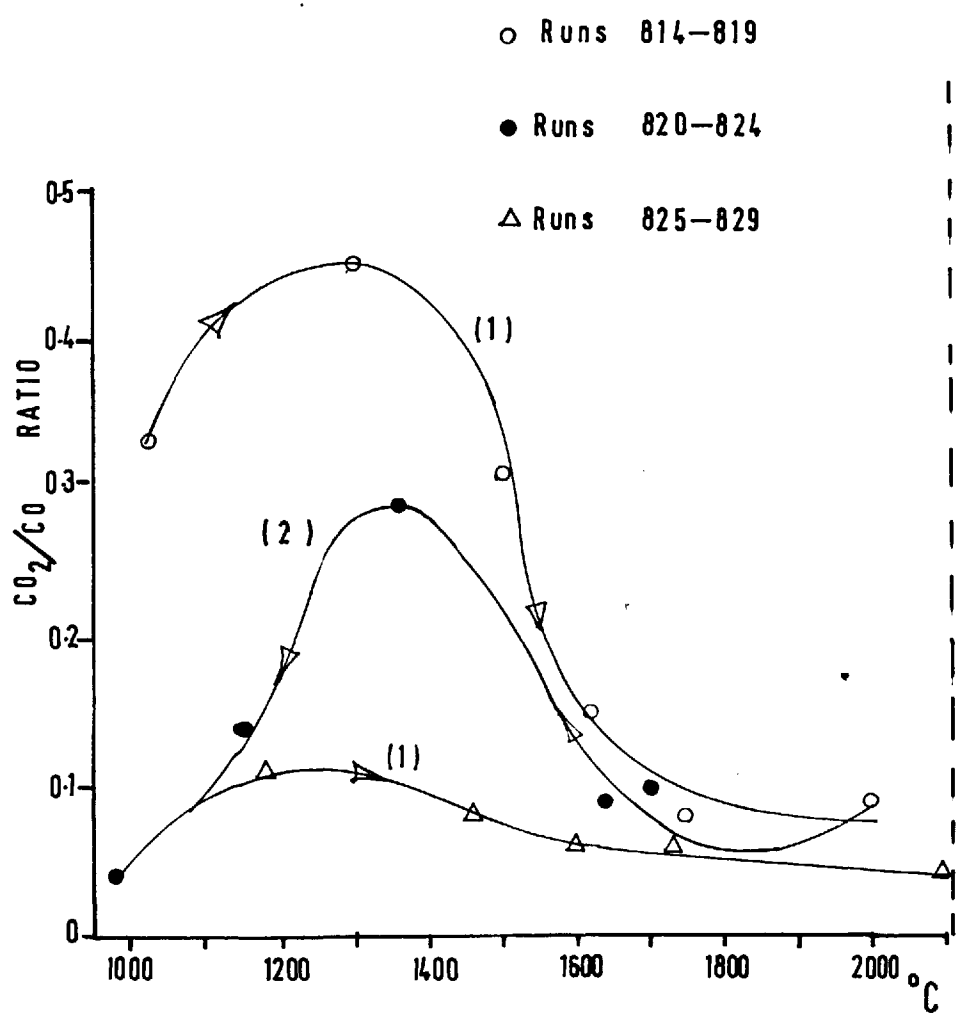

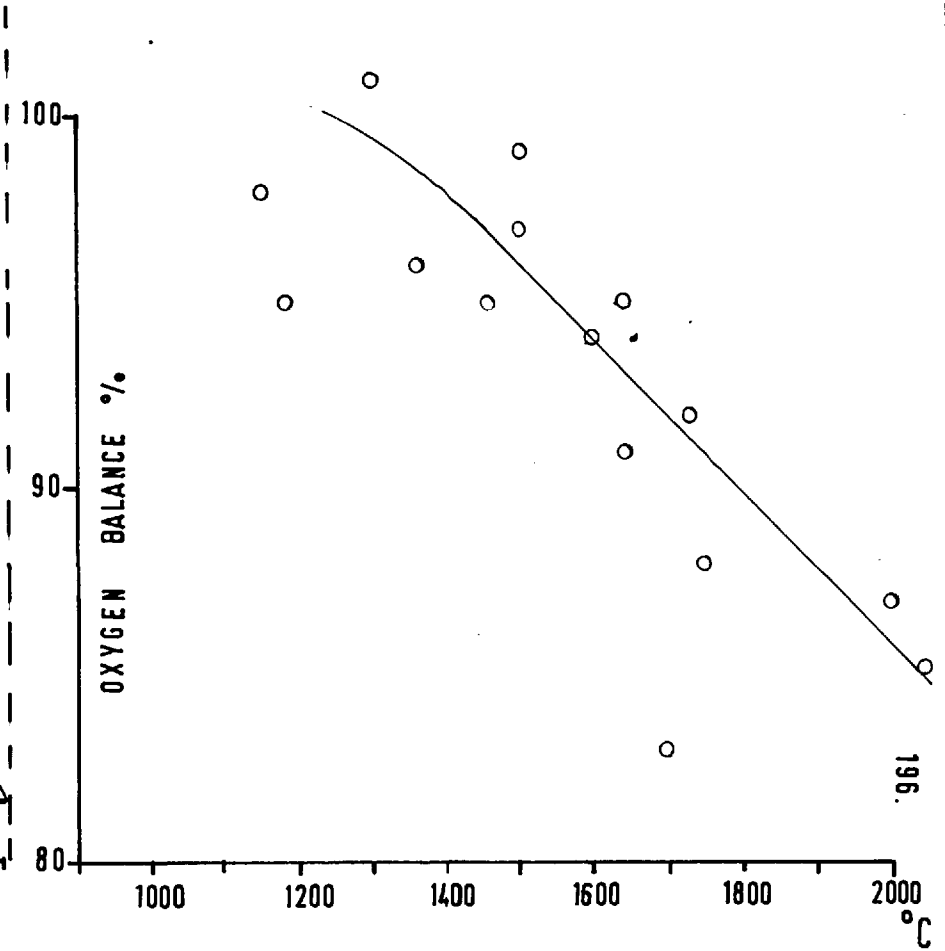

if it exists is not readily decomposed at the reaction temperatures, the very small pressure rises measured could be due to outgassing.

In order to see if uranium in the bulk of the carbon affected the rate a filament, No.42, was coated with UO_3 suspension and heated at 2000°C for 2 minutes after which the yellow colour had disappeared. The filament was then coated with pyrolytic carbon and the runs given in Table 5.25 carried out.

These results show that after the initial runs, where the rate increases with burn off, a rate of about the untreated rate is reached, which is not nearly as large an increase as found for surface treated filaments. The reaction at 1620°C shows that the rate increases with increasing burn off; this could be due to a normal hysteresis effect. The increased rates observed could be due to the fact that the pyrolytic surface was far less well deposited than for untreated filaments. Photo 23 shows the increased clusters of cones produced, the effect being very similar to that observed with boron.

The surface treated filaments were characterised by a considerable amount of pitting on the surface as observed for the other catalysts. Photo 24 shows a particularly badly pitted part of the surface.

Table 5.25. Uranium trioxide treated filament.

Filament first reacted with UO_3 and then coated with pyrolytic carbon.

Filament No.42.

Run No.	T°C	Secs. react	Initial pressure μ	Pressure CO μ	CO_2/CO ratio	Oxygen balance	$Rx10^8$
830	1230	15	48.2	4.2	0	94	2.5
831	1230	30	47.8	12.6	0.11	94	4.3
832	1230	30	50.4	16.0	0.10	95	5.3
833	1230	30	52.1	18.6	0.11	97	6.3
834	1230	20	51.4	13.6	0.07	96	7.0
835	1620	5	49.3	6.0	0	98	10.9
836	1620	5	49.2	6.0	0.03	98	11.3
837	1620	5	49.2	6.6	0.12	99	13.5
838	1210	20	48.8	17.2	0.13	100	8.9
839	1210	10	51.2	11.2	0.10	98	11.3
840	1210	10	50.8	9.6	0.04	97	9.1
841	1210	10	49.2	8.0	0.17	98	8.6

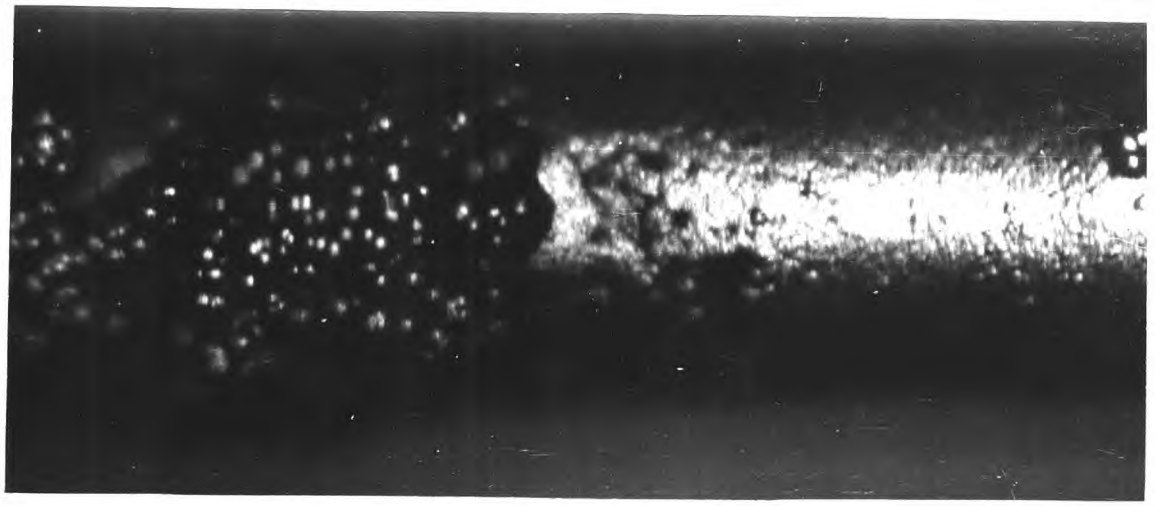

Photo 23. UO_3 treated ~~and treated~~ and then coated with pyrolytic carbon. Filament No.42. x200

Photo 24. UO_3 treated filament No. 41; reacted in O_2.
x200

5.9. Uranium trioxide treated filaments in nitrous oxide.

A series of runs were carried out to see if a catalyst which affected the rate in oxygen also affected the N_2O reaction and to see if any increase in rate caused the hysteresis to change in sense.

The catalyst used was uranium trioxide, the same technique for applying it as was used in the case of the oxygen runs, namely a suspension of powder in acetone was painted onto the filament. Heating the filament at 1900°C in initial vacuum caused a pressure rise of about 200μ in 1 minute, the yellow colour of the filament again disappearing. The filament was further degassed for 10 minutes after which heating it at 1900°C for 1 minute caused a pressure rise of under 5μ.

For these N_2O runs, the N_2O was frozen out after reaction and the CO measured using Hopcalite and the CO_2 using Sofnolite. It was thought necessary to measure the CO_2 in case catalysis altered the mechanism which might be indicated by a greater CO_2 evolution as in the case of oxygen. The N_2 was taken as being equal to the remaining pressure.

The results are given in Table A.5.20 and are discussed below.

1. The CO_2 detected was always less than 1% of the product gases unlike the oxygen case where the $\%CO_2$ was high.

The N_2/CO ratio shows a lot of scatter but is high when the burn off is low, which suggests a systematic error. This could be due to outgassing or to dissociation of the nitrous oxide. Strickland-Constable[18] found that dissociation was negligible for the untreated reaction in so far as it liberated free oxygen in the product gases. But if the filament and blocks outgassed only 1μ of gases during the course of each run the error in Run 1037 would be only 7% in the percentage of CO and N_2 while in Run 1039 the error would be 100%. The nitrogen balances as such were normal and close to 100%.

The oxygen balances tend to be less than 100% as was found for the oxygen runs, but the effect is less marked. Adsorption of CO or O_2 from N_2O would give high N_2/CO ratios and low oxygen balances with normal nitrogen balances.

2. The filament was initially silvery but after Run 1037 black patches appeared which by Run 1042 covered nearly half of the filament, at which state the filament then remained constant for the remaining runs. These patches suggest localised attack on the surface where the UO_3 particles were deposited.

3. A plot of the initial rates at 1800°C against burn off is shown on Graph 5.17. The rates show a definite decrease with burn off which was not observed in the case of

GRAPH 5.17. Initial runs at 1800°C for UO_2 treated filament reacted in N_2O

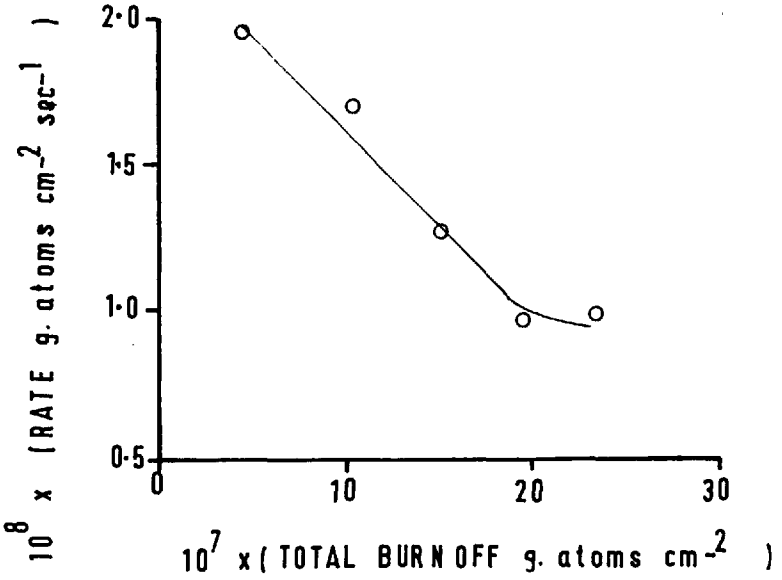

oxygen (Runs 787-806). It is not possible that the high initial rates at 1800°C were due to further decomposition of the UO_3, or other oxides, because if this was the case the oxygen balances would be high and also prior to Run 1029 heating the filament in vacuum caused virtually no degassing.

4. The rate-temperature curves, Graph 5.18, show the catalytic effect of the UO_3 treatment, most probably the metal being active. The rates obtained were about 10 times less than for an untreated filament in oxygen. The curves show a maximum and hysteresis in the normal N_2O sense, i.e. low sense hysteresis.

5. The surface of the filament was pitted as for the oxygen catalysed runs, and as can be seen in Photo 25 white spots can be seen on the surface associated with the craters.

6. The rate of reaction was about 5 times that obtained on untreated filaments, Graph 4.7, compared with an increase of greater than 10 times for the oxygen catalysed reaction. Comparison with the untreated rate in N_2O is to a certain extent arbitrary since this rate depended very much on the particular filament taken.

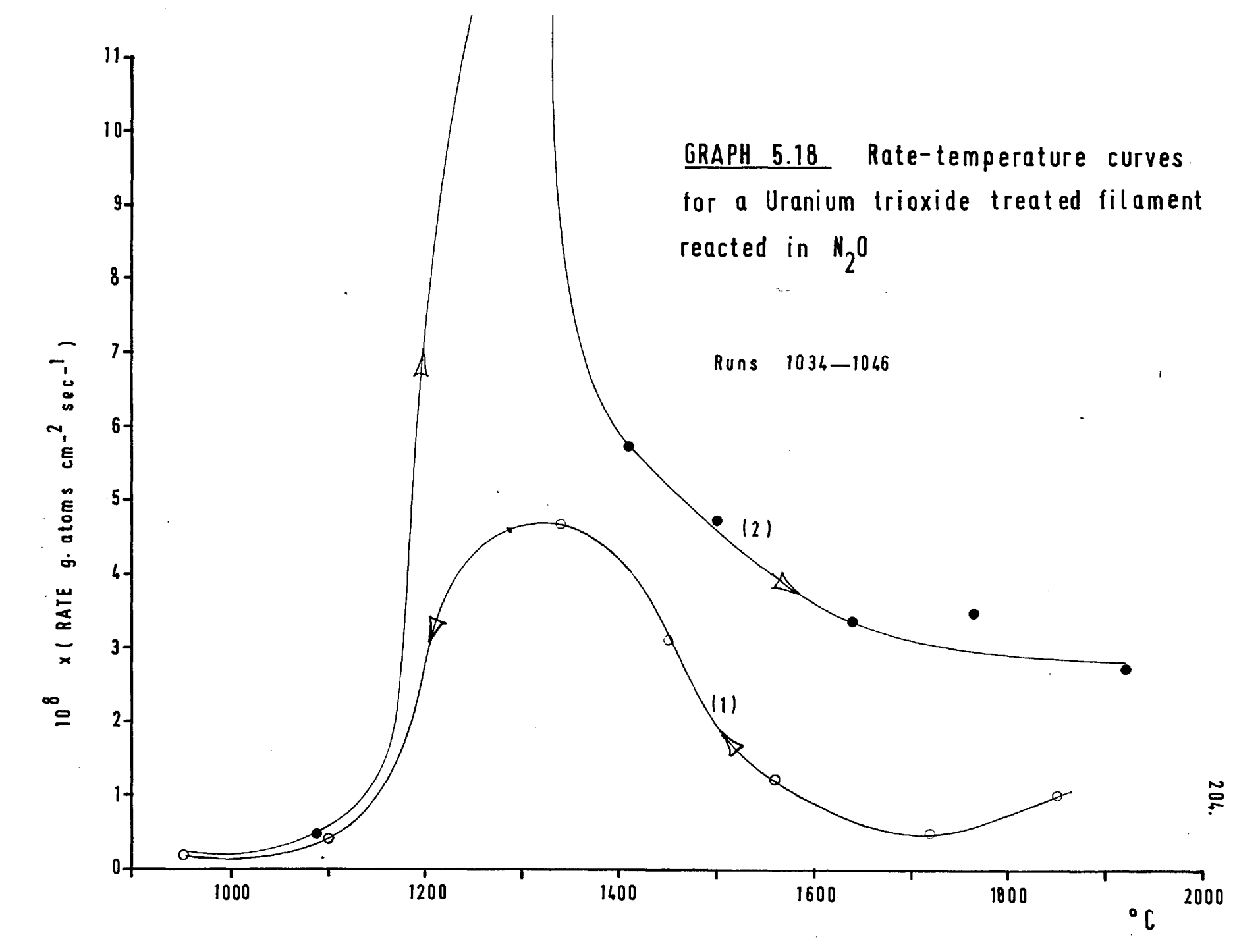
GRAPH 5.18 Rate-temperature curves for a Uranium trioxide treated filament reacted in N_2O
Runs 1034—1046
(2)
(1)
10^8 x (RATE g. atoms cm^{-2} sec^{-1})
°C
0
1
2
3
4
5
6
7
8
9
10
11
1000
1200
1400
1600
1800
2000

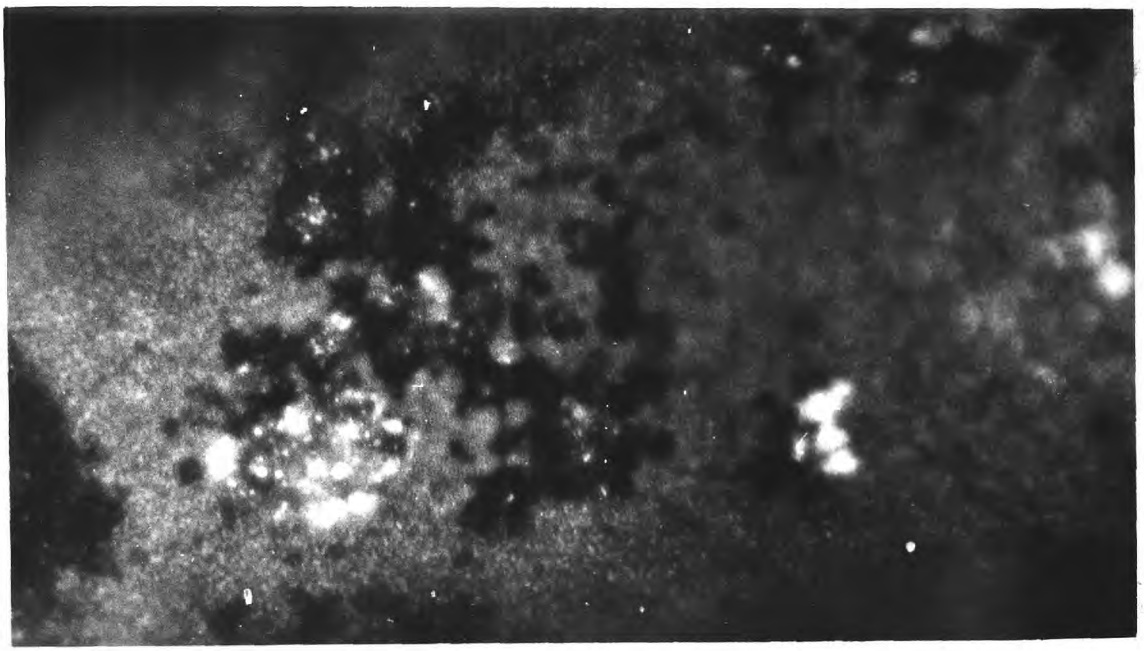

Photo 25. UO_3 treated filament No. 47; reacted in N_2O.
x800

5.10. Platinum Runs.

The method of coating the filament was to paint it several times with chloroplatinic acid solution. It is known that gives PtO_2 which decomposes below 500°C [99]. The filament was gently heated and at a very low voltage about 30μ of gas came off which was taken out completely by the cold trap, suggesting water. Increasing the temperature, still below visible, caused slight further degassing of a non-condensible gas, probably oxygen.

The first runs, given in Table 5.26, for reaction at 1200°C, 1720°C and then 1200°C, show that Pt has a catalytic effect. In the first runs at 1200°C the amount of CO_2 is also greater, probably due to secondary reaction catalysed by the Pt. During these runs the rate increased with increasing burn off.

At 1720°C after an initially high rate, the rates are fairly constant and lower than at 1200°C. On returning to 1200°C the rate while still being higher than at 1720°C showed no marked sign to increase and was about 1/2 the value obtained before.

A freshly coated filament was treated with platinum in the same way and after initial runs at 900°C a series of rate-temperature curves were determined. These initial runs again showed a very high percentage of CO_2, but for the subsequent runs the product was predominantly CO.

GRAPH 5.19 Rate-temperature curves for a Platinum treated filament

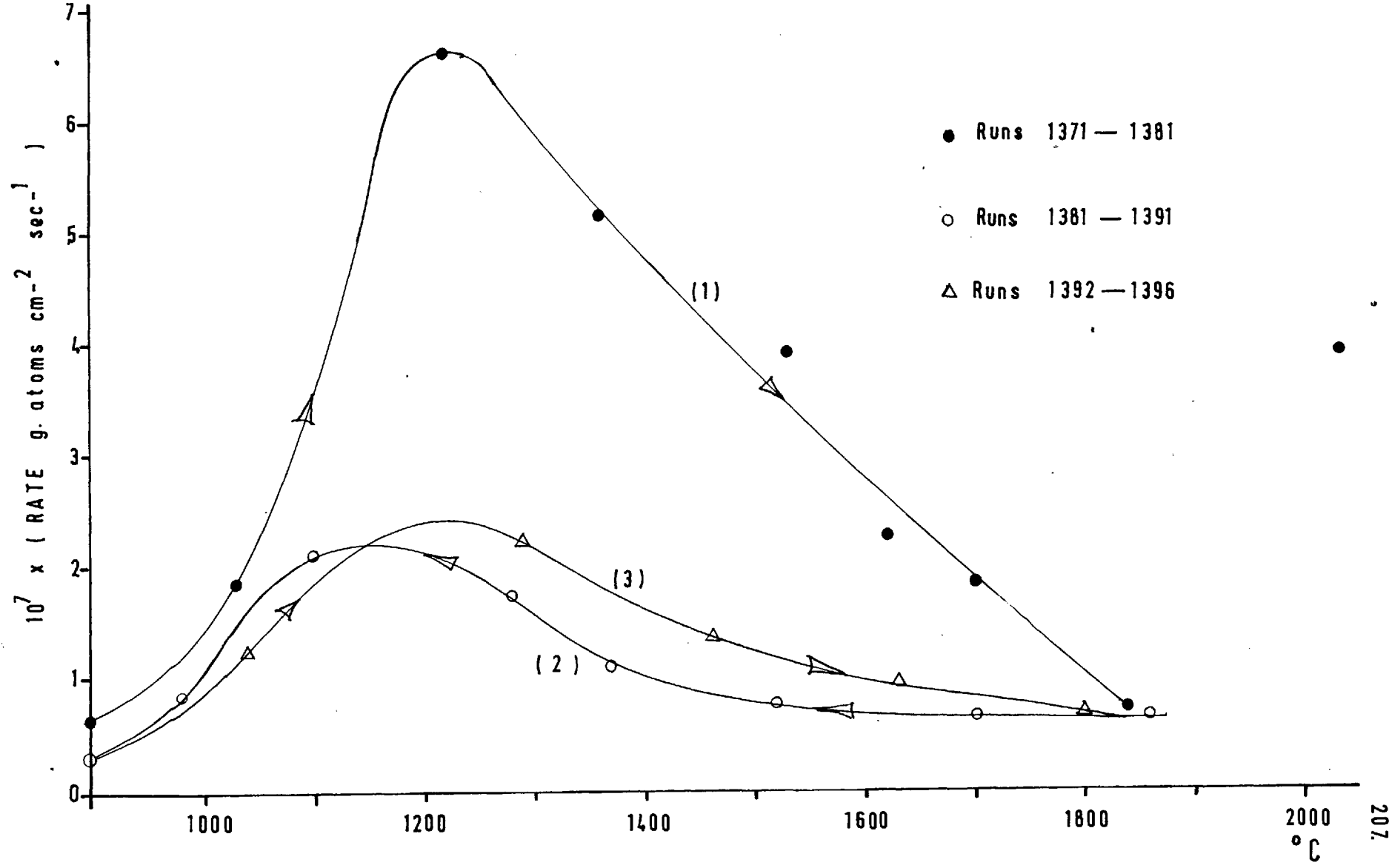

Table 5.26. Platinum treated filaments.

Run No.	T°C	Initial pressure μ	Pressure CO μ	CO_2/CO ratio	R x10^8	Oxygen balance
1233	1200	49.0	40.7	0.17	14.5	101
1234	1200	52.0	14.0	0.33	34.0	98
1235	1200	52.8	17.4	0.31	41.6	100
1236	1200	50.4	19.5	0.31	46.6	98
1237	1200	51.6	21.2	0.35	52.4	99
1238	1200	52.5	22.2	0.39	56.3	99
1239	1200	52.6	23.4	0.36	58.1	99
1240	1720	53.0	10.8	0.09	21.6	96
1241	1720	51.2	5.0	0	9.13	99
1242	1720	49.9	4.0	0.1	8.04	99
1243	1720	52.0	4.5	0.11	9.13	98
1244	1720	52.5	3.8	0	6.94	99
1245	1720	50.2	4.6	0.04	8.77	98
1246	1200	51.8	9.1	0.04	17.3	99
1247	1200	51.6	11.2	0.02	20.8	97
1248	1200	53.2	12.7	0.05	24.3	97
1249	1200	50.0	9.0	0	16.4	99
1250	1200	53.2	10.9	0.01	20.1	99
1251	1200	51.8	12.3	0.10	24.8	97

All runs 5 seconds except 1233(15 secs)

Table 5.27 Analysis of Platinum treated Filaments.

Filament No.	Runs Nos.	Analysis.	
55	1233-1251	0.6% Pt	Also Si, Fe, & Mg
57	1366-1396	0.6% Pt	

The results are plotted on Graph 5.19 and given in Table A.5.21. The first up curve is at much higher rates than the lower curves suggesting that platinum has been driven off, possibly by disruption of the carbon by reaction.

These curves are particularly good examples showing how catalysis while increasing the rate by a factor of about 5 still causes a maximum to be observed. On the more stable curves, 2 and 3, hysteresis is nearly absent.

The analysis of the filaments showed a 0.6% left on the filaments after reaction. The reduction in activity is therefore unlikely to be due to depletion from the surface. The effect might be due to aggregation as reviewed in Section 2.7.3.

5.11. Summary of Main Experimental Results for Treated Filaments.

5.1. Tin, copper and zinc mainly reacted at 1200°C had no effect with a slight lowering of rate for initial zinc runs. Analysis showed no additive left on filament after reaction, but the filament was covered with bronze coloured patches.

5.2. Crystalline boron and amorphous boron had no effect on reaction at 1200°C or on rate-temperature curves, although both substances took up oxygen initially to form the oxide. A filament treated with amorphous boron and then coated with pyrolytic carbon showed normal rates with the carbon less well deposited. Rate-temperature curves on this filament up to 1800°C showed no crossover in the hysteresis.

A boric acid treated filament showed the rate increased at the maximum in the down curve of the rate-temperature curves to about 12 $x10^{-8}$ gr atoms/cm^2 sec, otherwise the rates were near normal. Boric oxide gave a slight increase in rates particularly on the up curve between 1700 and 2000°C, where the rate was near 4.0 $x10^{-8}$ gr atoms/cm^2 sec.

Microphotographs showed surface was normal while analysis showed boron still present in small quantities, about 50 ppm for boric acid and oxide filaments.

5.3. Silicon, silica and sodium silicate gel had no effect Silicon initially took up oxygen and melted on surface as could be seen after reaction.

5.4. Iron catalysed the reaction at 1200°C with a rate of about 2.8 $x10^{-7}$ gr atoms/cm^2, sec, oxygen balances of 93-97%, and a high CO_2/CO ratio which fell with increasing burn off. There was no tendency for the rate at 1200°C to fall with increasing burn off, but heating at 1800°C caused rate at 1200°C to decrease due to depletion. The reaction at 1200°C was first order, over pressure range 14-216μ.

An oxide treated filament showed catalysed rate of between 1 and 2 $x10^{-7}$ at 1000°C with normal oxygen balances and a high CO_2/CO ratio.

The rates depended on the exact quantity of iron on the filament, which was not depleted at 1200°C but was at 1800°C. Treating a filament with iron and then coating with pyrolytic carbon gave normal results.

After reaction the surface of the filaments was very pitted for catalysed runs with about 0.01% of iron left on the filament.

5.5. Tungsten also catalysed reaction but the rate fell with increased burn off at 1200°C, with 0.6 order reaction at this temperature. Rate-temperature curves on a filament only initially treated gave hysteresis in opposite direction to untreated filaments, probably because the 'up' runs were catalysed,

and after high temperature reaction no tungsten was left on the surface. Rate-temperature curves on a filament treated between runs showed increased rates, with a maximum at 1450°C and rate of 7.0×10^{-7}; the hysteresis being all in the high sense.

The product for these reactions was predominantly CO and oxygen balances were close to 100%. The surface of the filaments were again pitted and spectrographic analysis showed no tungsten left after reaction, but an increased amount of iron.

5.6 (1) Molybdenum was the best catalyst found, increasing the rate by a factor of about 100 at high temperatures. Rate temperature curves showed very little hysteresis with a slight maximum between 1600 and 1800°C. The CO_2/CO ratio was normal and oxygen balances close to 100%. Heating a treated filament in vacuum at 1700°C for 5 minutes caused 28.6μ of CO to be desorbed. The metal treated filaments showed no tendency for the rate to fall off with burn off but the MoO_3 treated filaments did. The filaments were very pitted after reaction with white spots of oxide associated with several craters.

(2) Another filament was treated by depositing Mo as oxides from a Mo filament. Two methods were used during the series of runs; first the carbon filament was treated with Mo oxides and then reacted at alternate increasing and decreasing

temperatures. Secondly, after the Mo treatment the filament was heated at 1500°C in vacuum before reacting. In both cases there were maxima in the rate temperature curves, but the actual metal, i.e. after heat treatment at 1500°C, appeared to be a superior catalyst.

If the carbon filament was not treated between runs the rate gradually decreased, but maximum still existed.

5.7. Zirconium melted onto the surface also had a catalytic effect. The oxygen balances were initially low as oxides were formed but after this generally near 100%. The CO_2/CO ratio was also normal. Heating a treated filament at high temperatures activated it; the highest rate obtained being about 1.6×10^{-6} gr atoms/cm^2 sec. No maximum as such was visible in the rate-temperature curves, the rate increasing with temperature while the rates in down curves were much greater than those on the up curves. Heating a treated filament for 30 seconds at 1800°C in vacuum caused as much as 46.0μ of predominantly CO to be desorbed. Again craters were visible on the surface associated with white oxide.

5.8. Uranium trioxide filaments on first heating went black from decomposition of the trioxide. The rate was catalysed with no fall off in rate with burn off at 1020, 1200 and 1670°C The CO_2/CO ratio was high and went through a maximum at 1300°C and increased with increasing oxygen balance, the latter

decreasing with temperature after 1300°C. The rate-temperature curves showed only slight hysteresis in the low sense with a maximum of 7.5 $x10^{-7}$ gr atoms/cm^2 sec at about 1500°C. Treating a filament with uranium trioxide and then coating with pyrolytic carbon caused the carbon to be unevenly deposited and rates to be about 2times higher than for untreated filaments. For this case the rate increased with burn off.

Again craters were visible on the surface but without any visible substance associated with them.

5.9. For the uranium trioxide filament reacted in nitrous oxide, the product was predominantly CO while at 1800°C the rate decreased with burn off. There was a tendency for low oxygen balances with adsorption of O_2 or CO. Rate-temperature curves showed a maximum rate of about 1 $x10^{-8}$ gr atoms/cm^2 sec at 1250°C while the hysteresis was in the normal N_2O low sense. Generally the rates were about 5 times higher than for N_2O untreated filaments, which is about .5 times lower than for untreated oxygen reacted filaments.

The surface was about half covered by black patches which on examination were found to be pits associated with which could be seen white spots of some oxide.

5.10. Filaments treated with platinum from chloroplatinic acid, exhibited true maximums in the rate-temperature curves

between 1150 and 1250°C. There was some suggestion that the activity decreased with burn off but the same rates were found at 950 and 2000°C after reaction at increasing or decreasing temperatures.

SECTION 6. PROPOSED THEORY TO ACCOUNT FOR HYSTERESIS RESULTS.

6.1. Introduction.

In the proposed reaction system reaction is assumed to occur predominantly on sites type A and B. There is further assumed to be very slow reactions which create and remove sites A and B according to the following simplified system

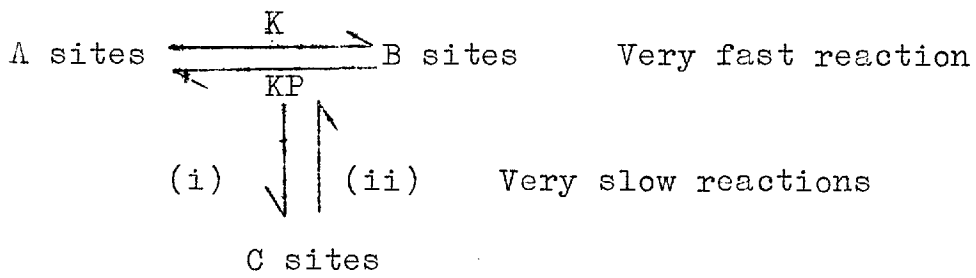

The fast interchange between sites type A and B is taken to be the mechanism proposed by Nagle and Strickland-Constable. The hysteresis observed at very low pressures is assumed to be caused by reactions (i) and (ii) varying the number of sites of type A/B by creating and destroying sites C, which themselves are very unreactive. [Another slow mechanism also operates to create more sites of type A/B as discussed below].

If we take n to be the total number of sites (type A + type B) from the Nagle theory the total number of A sites will be xn, and the total number of B sites will be (x-1)n.

Using the Nagle theory the total rate of reaction, R, is now given by

$$R = \left(\frac{K_A P}{1+K_Z P} \right) xn + K_B P\,(1-x)n$$

$$= \left[\left(\frac{K_A P}{1+K_Z P} \right) x + K_B P\,(1-x) \right] n \qquad (1)$$

Putting the bracketed term = r, that is the rate per site of type A/B :

$$R = r\,n \qquad (2)$$

where r is given by the Nagle theory.

This expression is the same as used by Duval (F = fn) who found the factors f and n to be separable, f being constant with time for a certain temperature and pressure, while the hysteresis was supposed due to variations in n.

6.2.1. Variation of n with temperature (experimental).

Using the expression R = rn a graph of the variation of n with temperature was calculated using the same method as Duval, this being given in Appendix 6.1. The resulting variation of n/n_{1150} is shown on Graph 6.1. The decreasing temperature points, although showing scatter suggest that the basic equation is also true for our results. As discussed in Appendix 6.1 the large amount of scatter in these results is due to the difficulty of estimating the initial rate; any error at a particular temperature being systematically carried over to proceeding points.

The detailed experimental results used here are given in Appendix 6, and section 4.5.

GRAPH 6.1 Variation of steady state site distribution $\frac{n}{n_{850}}$ with temperature (°C) at 50 μ

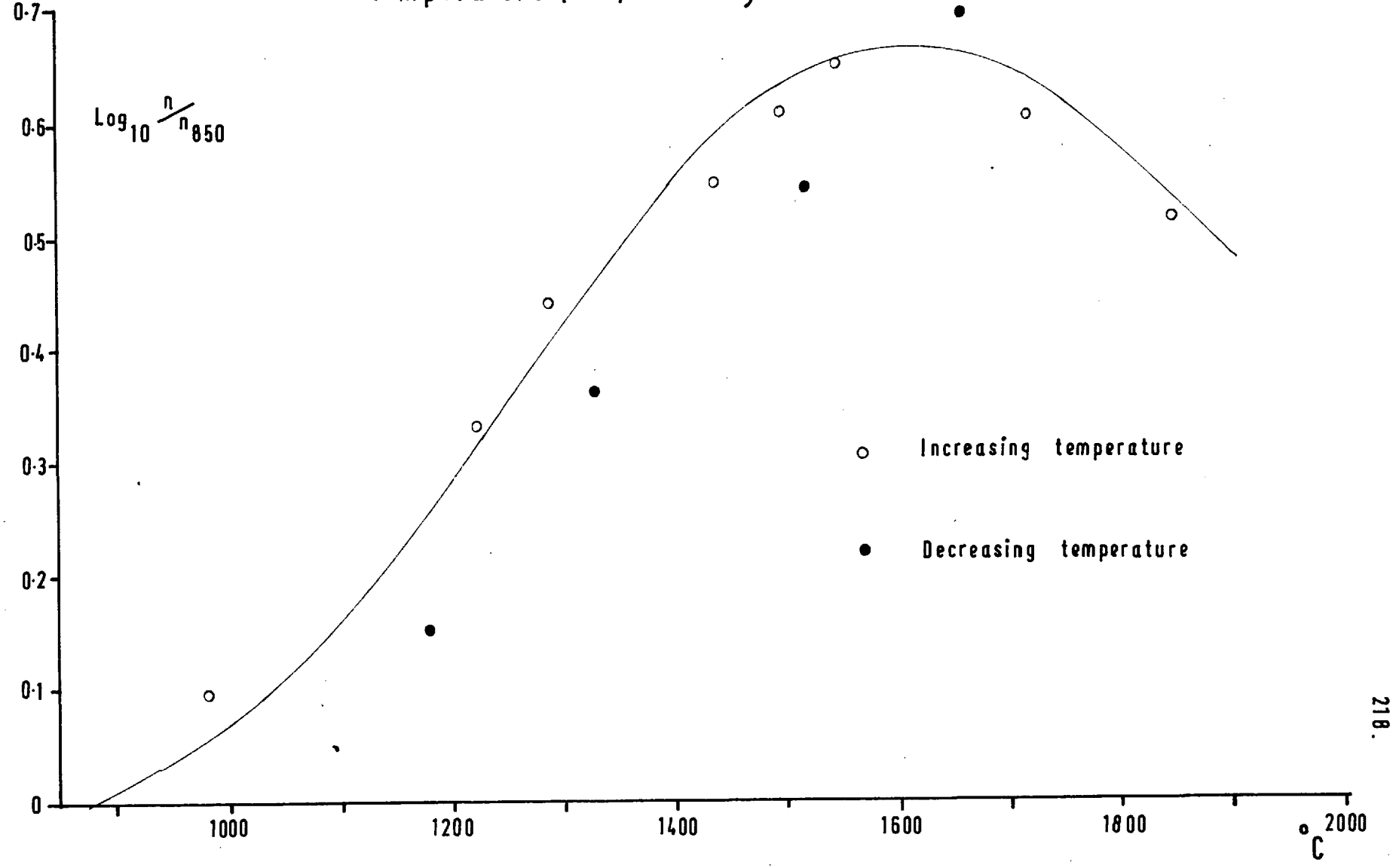

6.2.2. Variation of r with temperature (experimental).

For the purposes of obtaining the actual variation of r with temperature from Graph 6.1 and Duval's results it is necessary to know n_{ref} since $r = R/n$

i.e. $\text{Log}_{10} r = \text{Log}_{10} R + \text{Log}_{10} n_{ref}/n - \text{Log}_{10} n_{ref}$

n_{ref} was taken to be the values obtained later in this section. If in fact n_{ref} differs from the value taken the general shape of the curve of $\text{Log}_{10} r$ against temperature will not change, only its position relative to the rate axis.

The calculation of $\text{Log}_{10} r$ for our results and Duval's results on graphitised filaments, are given in Appendix 6.2 and shown on Graphs 6.2 and 6.3. For Duval's results it was necessary to assume that the site distribution n/n_{1200} is the same for graphitised and non-graphitised filaments.

It is interesting to note that the curve Duval obtained for the variation of r (Fig.17, ref.(3)) for non-graphitised filaments, which gave larger rates, exhibits neither maximum nor minimum.

6.2.3. Comparison of experimental values of R and r with predicted values from Nagle/Strickland-Constable Theory (14).

R is calculated from the theory at 0.76μ and 50μ in Appendix 6 and the values obtained are plotted on Graphs 6.2 and 6.3 together with the actual rates of reaction.

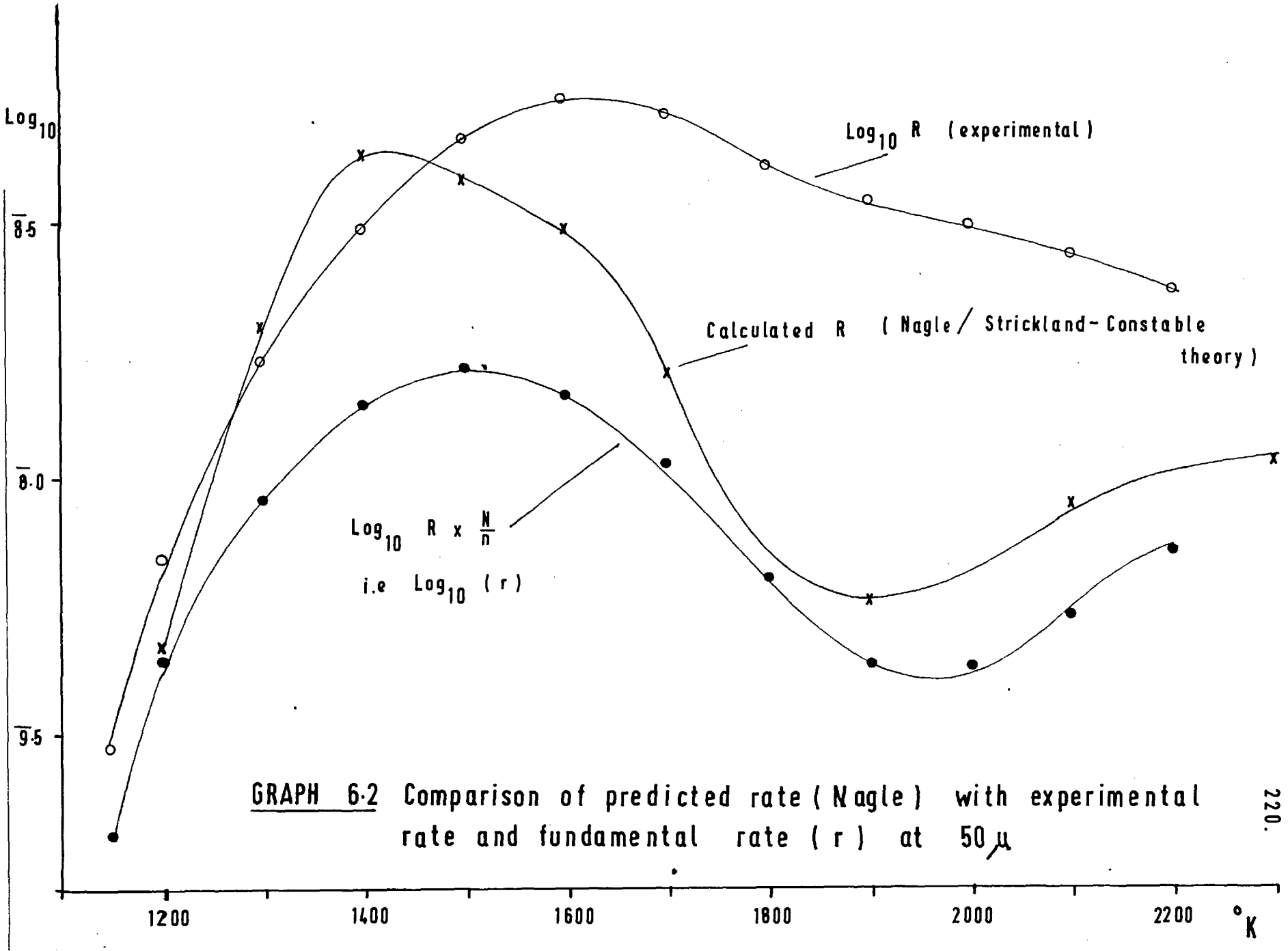

GRAPH 6·2 Comparison of predicted rate (Nagle) with experimental rate and fundamental rate (r) at 50μ

GRAPH 6.3 Comparison of predicted rate (Nagle) with experimental and fundamental rate (r) at 50 μ

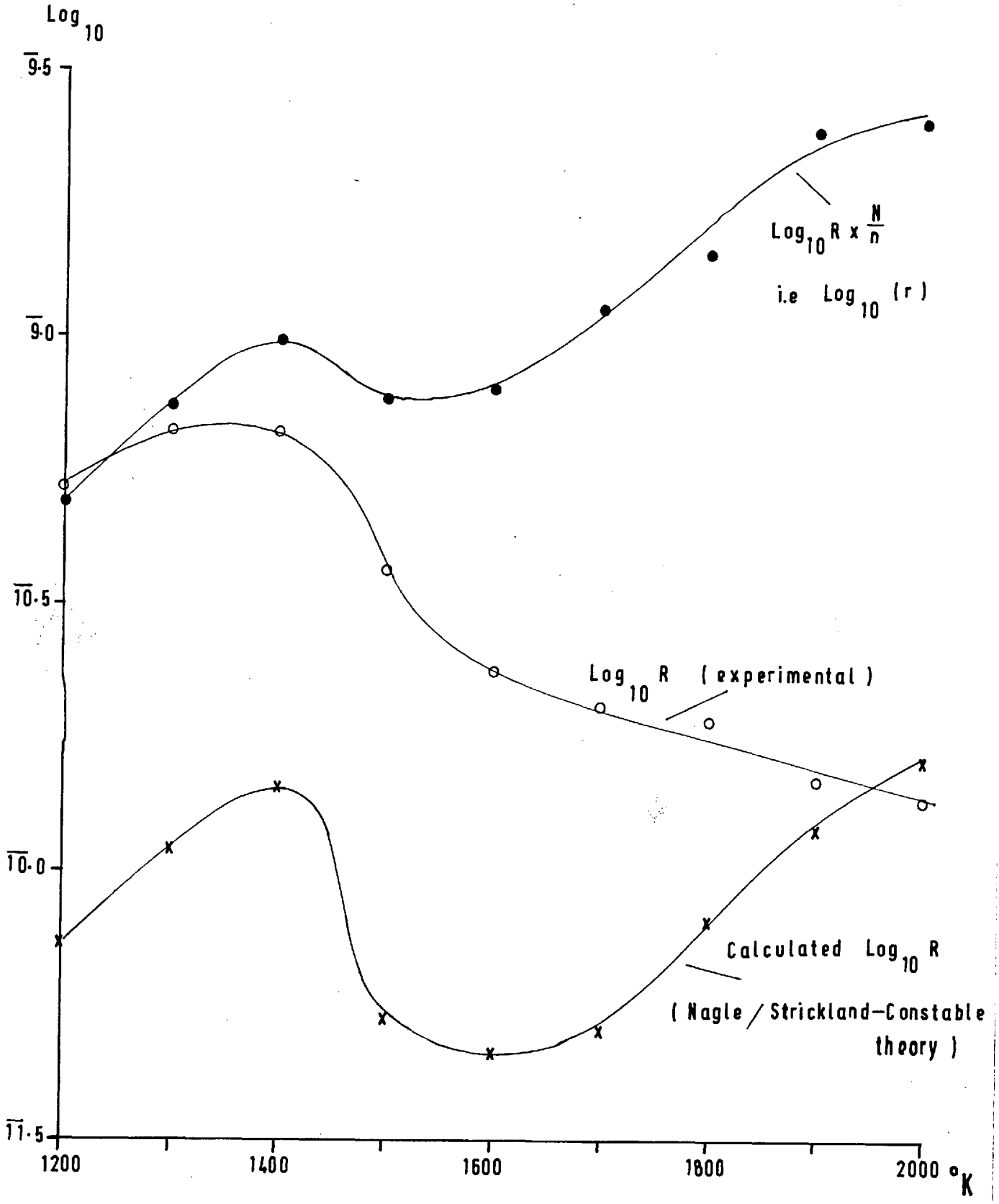

As can be seen from these graphs the shapes of the r curves and the R predicted curve are almost exactly the same, both having maximum and minium. The fit between, in shape, R_{actual} and $R_{predicted}$ is not nearly as good. The displacement of the curves can be associated with the value assigned to n_{ref} and the actual area of the filaments.

The theory used to predict the value of R was evolved with rate constants to fit the earlier work of Nagle and Strickland-Constable and this may also be affecting the displacement noticed on Graphs 6.2 and 6.3. However these results do show that a two site theory of this form predicts the shape of the r curves almost exactly.

The reasonableness of splitting R into r and n is shown in both Duval's and our results. Moreover the variation of r since it exhibits a maximum and minimum necessitates a two site theory, with the variation of x being almost instantaneous at a new temperature or pressure. This last conclusion is inherent in assuming that r is constant with time.

The fact that this is the case is strongly supported by our results at 1440°C (after 1290°C) and at 1500°C (after 1440°C), Graph 4.15.

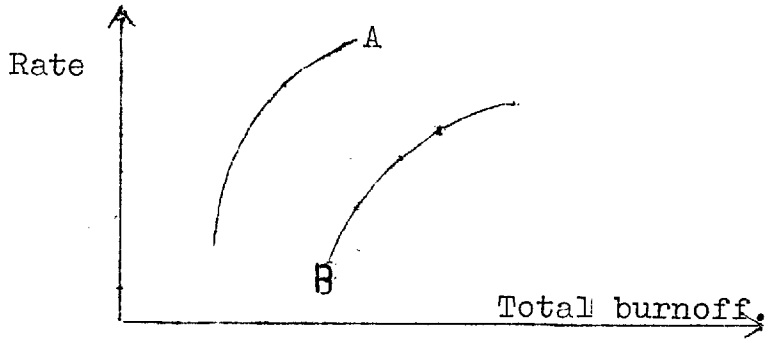

Going from A to B there must be a factor in the rate expression which decreases almost instantaneously. This is taken to be r, which means x is instantaneously adjusted to its new value.

6.3. Proposed Theory to explain variation of n with temperature and pressure.

6.3.1. It is proposed that there are n sites on the surface on which reaction occurs of type A and B. In considering the disappearance or creation of sites (A/B) for the purposes of analysing the hysteresis results it makes no difference whether they are formed of type A or type B, or any combination of A and B. The reason is that the fraction x will instantaneously adjust to its steady state value. The processes involved in $[A+B] \rightleftharpoons C$ being much slower.

The nature of the sites on the surface is open to widely different interpretations. They have been associated

with edge atoms and basal plane atoms. But as discussed by Busso[79] the edge atoms themselves can be of several different types. Also several workers have shown that n must be a small fraction ofthe surface. [See 2.5.1].

6.3.2. The theory tentatively proposed is based on the simultaneous annealing and creation of sites, the relative magnitudes of these factors altering with temperature and pressure.

Process 1. A/B sites are assumed to be annealed out to C sites at a rate proportional to the number of A/B sites n.

$$\text{Rate of annealing of A/B sites} = K_1 n \qquad (3)$$

The rate constant in this case could just as well be a diffusion rate of the form $D = D_o\, e^{-H/kT}$. This is of identical form to the Arrhenius expression, the constants however having a different physical meaning.

Process 2. A certain number of A/B sites are assumed to be created by direct gaseous attack on the surface, the rate being proportional to the non reacting surface (N-n) where N is the maximum number of C sites which can be formed into active A/B sites. This reaction was assumed to have a first order pressure dependence and a rate constant K_2.

$$\text{Rate of creation of A/B sites by 2} = K_2 (N-n)P \qquad (4)$$

This process could occur with or without actual reaction of the O_2 with the surface. If reaction does occur it would only add negligibly to the rate of formation of CO because the process is much slower than the reaction processes on A

and B.

Process 3. The other creation of A/B sites process was assumed to be related to the actual rate of gasification, a small proportion of the reaction on A/B sites causing additional sites to be created. The pressure dependence in this case being the same as that of actual reaction (x) For the purposes of this analysis the rate can be assumed to be related to one rate constant.

Rate of creation of sites A/B by Process 3 = $K_3 P^{x'} n$. (5)
Only a very small number of A/B sites on reaction give more than one site perhaps by uncovering further crystalline defects, or disrupting the surface in other ways.

A further discussion on the nature of the A/B and C sites is given after the analytic sub-sections. The factor N will vary from one type of filament to the next which further accounts forthe displacement observed on Graph 6.3.

The reaction system now becomes diagrammatically

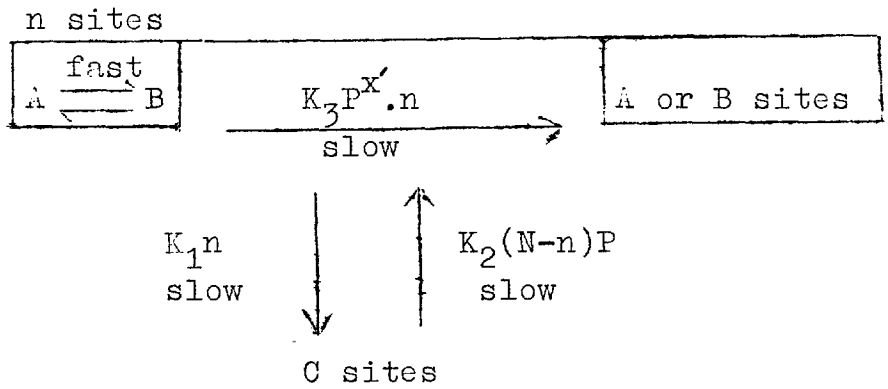

Several other models were tried including making Process 1 dependent on some power of n. Also Process 3 was replaced by another removal process dependent on the gasification reactions. None of these gave equations which showed a change in hysteresis sense. The only other which gave a good fit to the data was obtained by making the rate of Process 3 independent of n. However this is difficult to justify since it is contrary to the assumption that the reaction occurs predominantly on A/B sites.

The change in hysteresis sense with pressure is due to Process 3 being important at 50μ, but unimportant at 0.76 u.

6.3 .3 . Steady Conditions.

This is the case when the rate of reaction R has reached a constant value, and n is constant with time.

$$K_1 n = K_2(N-n)P + K_3 p^{x'} n \qquad (6)$$

$$\therefore \quad n = \frac{K_2 N P}{K_1 + K_2 P - K_3 P^{x'}} \qquad (7)$$

Equation 7 can be put in a more manageable form

$$n = \frac{N}{1 + K_1/K_2 P - K_3/K_2 . P^{(x'-1)}} \qquad (8)$$

$$= \frac{N}{1 + K_5/P - K_4 P\ (x'-1)} \qquad (8)$$

where $K_4 = K_3/K_2$ and $K_5 = K_1/K_2$.

If n is the number of A/B sites at temperature T, and n_{ref} the number at the reference temperature below which no hysteresis appears

$$n_T/n_{ref} = \frac{[1 + K_5/P - K_4P^{(x'-1)}]_{ref}}{[1 + K_5/P - K_4P^{(x'-1)}]_T} \qquad (9)$$

6.3.4. Non-steady conditions.

Consider dn sites formed in time dt at constant temperature and pressure

No. of sites (A/B) created = $[K_2(N-n)P + K_3P^{x'}n]dt$

No. of sites (A/B) annealed to C = K_1ndt

Hence $[K_2(N-n)P + K_3P^{x'}n - K_1n]\,dt = dn \qquad (10)$

Putting $K_3NP = \phi \qquad (11)$

$K_1 + K_2P - K_3P^{x'} = \theta \qquad (12)$

$\frac{dn}{\phi - \theta n} = dt \qquad (13)$

Let n_o be the number of (A/B) sites at t = 0. n_o is a function of the previous temperature and pressure of reaction and is given by equation (7), if steady conditions were attained.

Integrating (13)

$$\theta n = \phi - (\phi - \theta n_o)\, e^{-\theta t} \qquad (14)$$

At time = ∞ , n = constant = n_∞

From (7) $n_\infty = \phi/\theta$

$$\therefore \quad n/n_\infty = 1 - [1 - n_o/n_\infty]\, e^{-\theta t} \qquad (15)$$

For decreasing number of A/B sites with time the original equation is

$$[K_1 n - K_3 P^{x'} n - K_2 P(N-n)]\, dt = -dn$$

This is identical to (10) and the resulting equation (15) covers both cases.

6.3.5. Fit of theory to experimental results.

In Section 4.2.2 the order of reaction was found to vary between first order at 0.76μ and 1.5 order at 50μ. The order was also shown to be greater than 1 over this range by Duval[3]. For the purpose of solving (9) it was put equal to 1.25.

Putting

$$K_5 = A_5\, e^{-E_5/T} \quad \text{where} \quad E_5 = \frac{E_1 - E_2}{R}$$

$$K_4 = A_4\, e^{-E_4/T} \quad \text{where} \quad E_4 = \frac{E_3 - E_2}{R}$$

equation (9) becomes

$$\ln n_T/n_{ref} = \ln \frac{(1 + A_5/P.e^{-E_5/T} - A_4 P^{0.25}\, e^{-E_4/T})_{ref}}{(1 + A_5/P.e^{-E_5/T} - A_4 P^{0.25}\, e^{-E_4/T})_T} \qquad (16)$$

The solution of (16) was carried out by assuming at low temperatures at 50μ the K_5 term was negligible. Hence an initial value of K_4 was obtained by fitting to our data below 1700°K. An initial value of the K_5 term was obtained

Ⓐ, although the qualitative fit in predicting the increase & decrease of number of sires with pressure was still shown.

by assuming the K_4 term to be negligible at 0.76μ. K_4 and K_5 were then recalculated using the complete equation in turn at 50μ and 0.76μ, several trial and error procedures being necessary before a satisfactory fit was obtained. It was also found that neither $x' = 1$, nor $x' = 1.5$ gave a satisfactory fit, Ⓐ

This solution gave the following values

$$K_5 = 9.0 \times 10^{-2} \; e^{\frac{-1.67 \times 10^4}{T}}$$

$$K_4 = 75.4 \; e^{\frac{-0.35 \times 10^4}{T}}$$

6.3.6. Fit to non-steady conditions.

In order to determine all the rate constants equation (15) was fitted to data at 50μ and 0.76μ. As shown In Table A.6 7 the value of θ at 0.76μ for reaction at 1700°K, following 1200°K was found to be 3.0×10^{-2}. In fitting the data at 50μ considerable scatter in values of θ were found but the curve for reaction at 1508°K, after 1153°K, was chosen since this did not show any abnormal behaviour and also gave a value of θ at a temperature 308°K higher than the 0.76μ results. Here θ was found to be 3.48×10^{-2}.

With two values of θ at different conditions it was possible to determine K_1, K_2 and K_3.

From (12) $\theta = K_1 + K_2P - K_3P^{x'}$

$$\therefore \theta = K_2P \left[1 + K_5/P - K_4P^{(x'-1)}\right]$$

Since K_4 and K_5 are known from 6.3.5, K_2 can be determined at 0.76μ and 1700°K. The bracketed term = 5.438 (Table 6.3).

$$\therefore \quad 3.0 \times 10^{-2} = 5.438\ K_2 \times 10^{-6}$$

Similarly at 50u and 1508°K

$$3.48 \times 10^{-2} = 0.346\ K_2 \times 6.6 \times 10^{-5}$$

Solution of these equations gives

$$K_2 = 1.29 \times 10^{8}\ e^{-\frac{1.71 \times 10^{4}}{T}}$$

Since $K_4 = K_3/K_2$ and $K_5 = K_1/K_2$ using the values of K_4 and K_5 obtained in 6.3.5. with K_2

$$K_1 = 1.16 \times 10^{7}\ e^{-\frac{3.38 \times 10^{4}}{T}}$$

$$K_3 = 9.73 \times 10^{9}\ e^{-\frac{2.02 \times 10^{4}}{T}}$$

GRAPH 6.4 Comparison of experimental and theoretical steady state site distribution at 50μ.

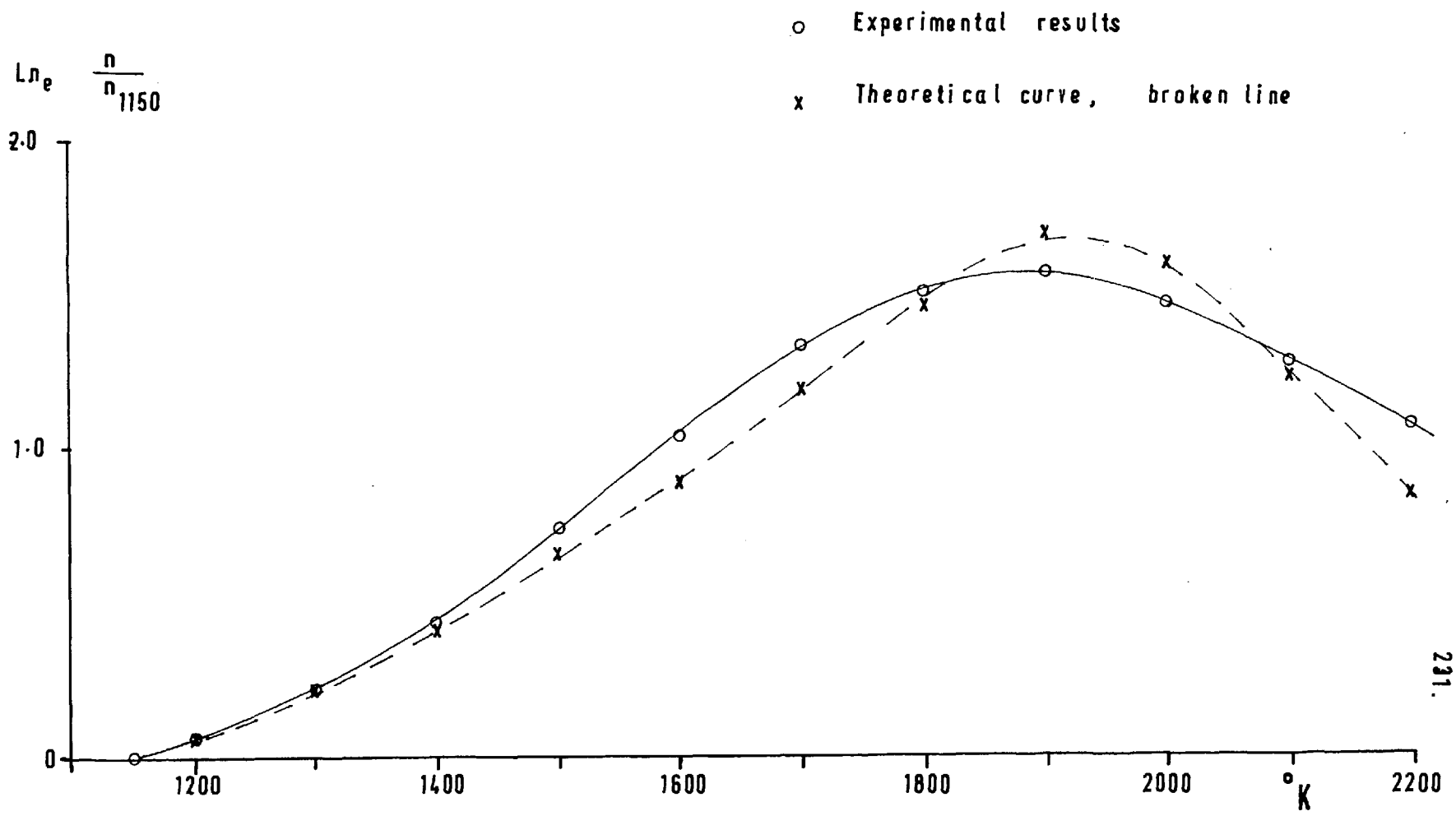

GRAPH 6.5 Comparison of experimental and theoretical steady state site distribution at 0·76 μ

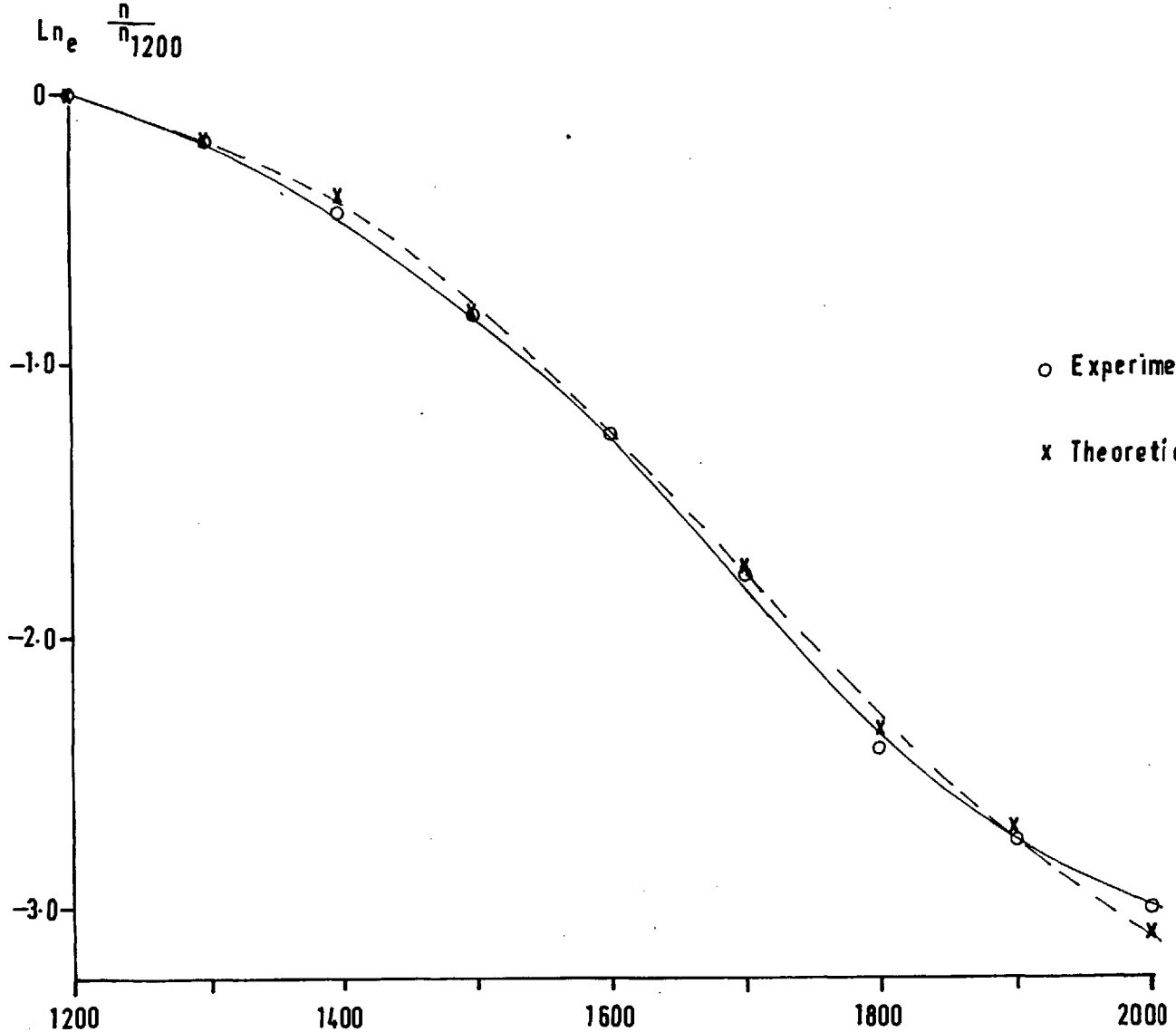

GRAPH 6.6 Comparison of experimental and theoretical variation of number of sites with time at 0·76 μ.

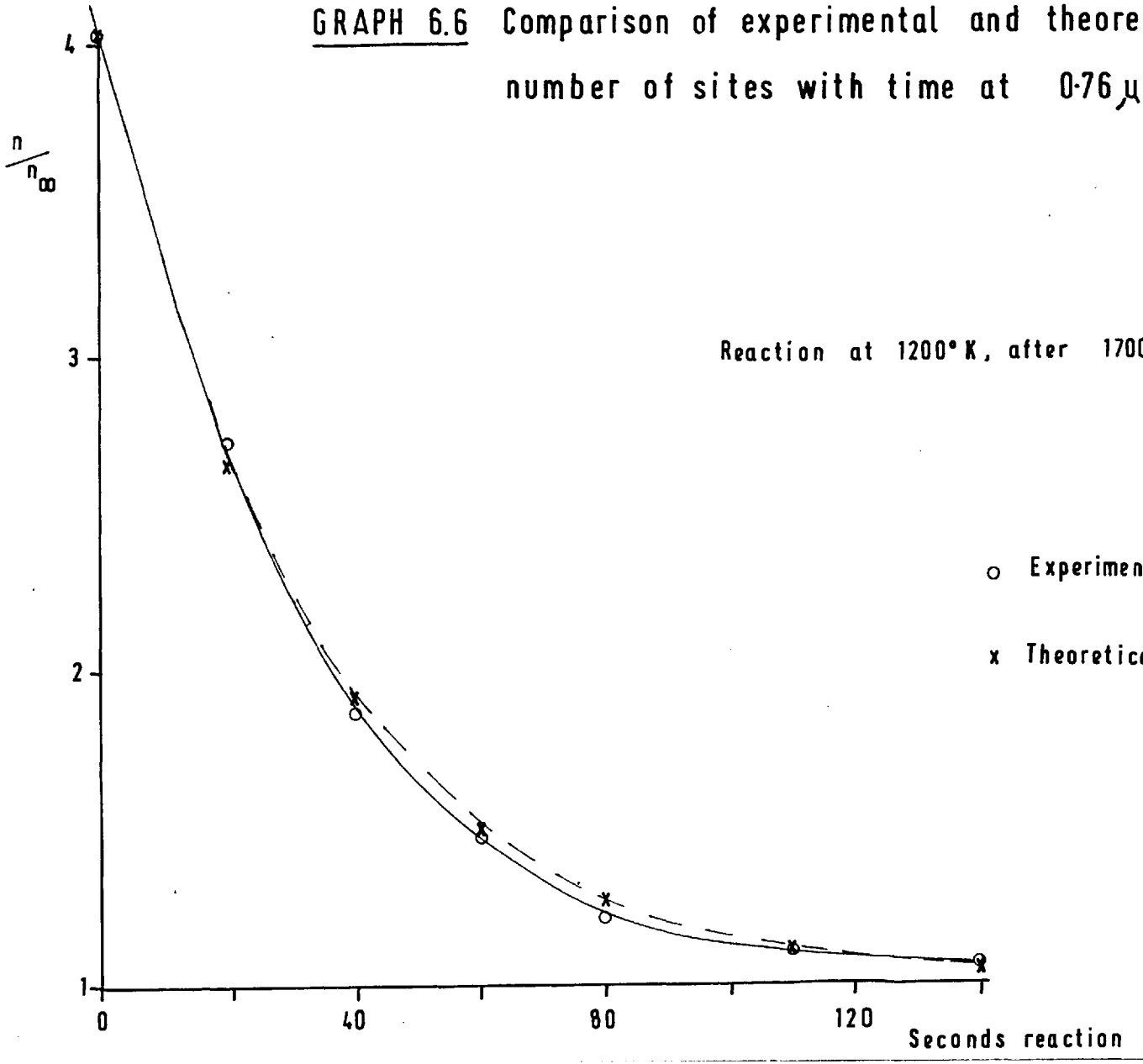

Reaction at 1200° K, after 1700° K at 0·76 μ

o Experimental results, from Duval (3)

x Theoretical curve, broken line.

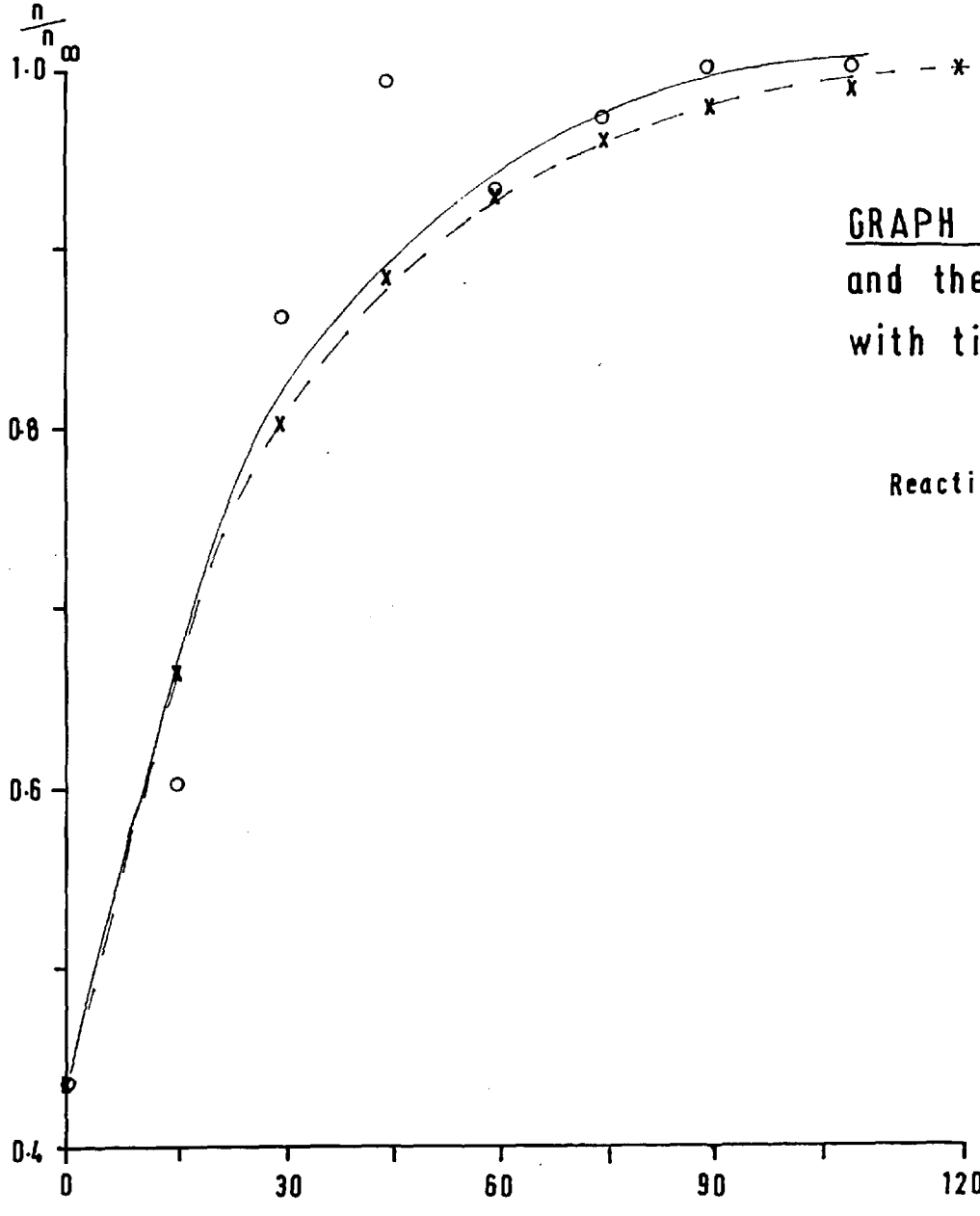

GRAPH 6.7 Comparison of experimental and theoretical variation of number of sites with time at 50μ.

Reaction at 1508°K, after 1153°K

o Experimental points, full line.

x Theoretical curve, broken line

6.4. Discussion of Hysteresis and Proposed Theory.

6.4.1. General.

For steady site concentration the predicted curve at 0.76μ, Graph 6.5, shows a very good fit, while at 50μ, Graph 6.4, although the fit is not so good it satisfactorily predicts the maximum in the number of sites. The experimental curves at 50μ cannot be considered very accurate due to the error in estimating the initial rate as discussed in Appendix 6.1. This same error also affects the unsteady state conditions, but again the predicted curve follows closely the experimental results.

The theory can only be applicable to low burn offs. As the rate of reaction increases with pressure the surface atoms are being removed so rapidly that the hysteresis processes do not have time to operate. Under the conditions in the present work and in Duval's work the reaction removes several monolayers only per second.

The activation energies for the annealing process (1) process (2) and process (3) were found to be 67, 35 and 40 kcals/g. mole. The sites A/B anneal out in two ways. The majority of type A, anneal out to give less active B sites, this being a fast reaction. A few (A or B) also anneal out slowly to give inactive C sites. The difference could be due to differences in neighbouring atoms. This value of 67

k cals is in keeping with the work of Feldman[80] who found a value of 40 kcals/g.mole for combined volume and grain boundary diffusion, and Diener[81] who calculated a value of 90 kcals for volume diffusion in a graphite lattice. It is not possible to completely justify the values of 35 and 40 kcals/g.mole but they are of the right order of magnitude.

In support of the idea of variations in the number of active sites causing hysteresis it is interesting to note that Taylor and Thon[82] have shown that the Elvolich equation is inconsistent with the classical concept of a fixed number of adsorption sites. To explain the adsorption these authors proposed a mechanism based on the creation of active sites by gaseous attack and an annealing out of these sites.

6.4.2. Variation of n with temperature.

The total number of sites A/B can increase through two possible mechanisms. Firstly the total surface area can increase, i.e. the roughness factor, with reaction, while the fraction of (A+B) with the total surface area remains constant. The net effect is that n increases relative to the geometric area. The second possibility is that the true surface area remains constant and n increases because the relative proportion of (A+B) sites increases relative to the true area.

Duval[3] at 0.76μ using the adsorption of ethylene

found insignificant differences in the roughness factor for filaments burnt at 1200°K, 1400°K and 1850°K, the values obtained being 23.4, 23.5, and 27.2. All these values were considerably higher than a new filament heated at 2000°C, which had a roughness factor of only 4.1.

U.K.A.E.A., Harwell kindly attempted to measure the B.E.T. area of filaments reacted at 50μ. Unfortunately due to the very small areas involved this was not feasible. However it is thought that due to the increasing importance of Process 3 at 50μ some variation in the surface area may be expected.

The variation of n could possibly be associated with blackening of the filament. At 0.76μ Duval found the filament burnt black only at low temperatures and it is in this region that n is largest. For our results the blackening occurred between 1000 and 1300°C and it is in this region at 50μ that n goes through a maximum. This cannot be the complete picture because for reaction at 980°C, Graph 4.17 while the rate increased the surface became progressively more silvery.

6.4.3. Nature of active sites.

In the Nagle and Strickland-Constable theory it was tentatively proposed that the sites which constitute n, i.e. A and B sites, can be associated with edge and basal plane

atoms. While this cannot be the case with our theory, it is possible that the A and B sites are different edge atoms and the C sites basal plane atoms. n then increases because the number of edge atoms increases.

It is further possible that the C sites are all edge atoms., A and B sites being specific types of edge atoms. In this case the increase of n can be due to the number of edge atoms increasing, or the number of A and B sites increasing while the number of edge atoms remains constant. Also in this case N would be related to the total number of edge atoms.

The feasibility of there being several different types of edge atoms of different reactivity has been discussed by Busso [79]; an examination of Fig. 6.1. shows several possibilities.

6.4.4. Discussion of the processes involved in the theory.

A. The exact mechanism whereby additional A/B sites are created by Process 3 is open to debate, but two possible ideas are considered.

1. Considering 6.1. it is possible that two or more sites are about equal reactivity towards O_2 attack. However the sites could differ in as much that once the carbon atom has been removed by reaction, the two different

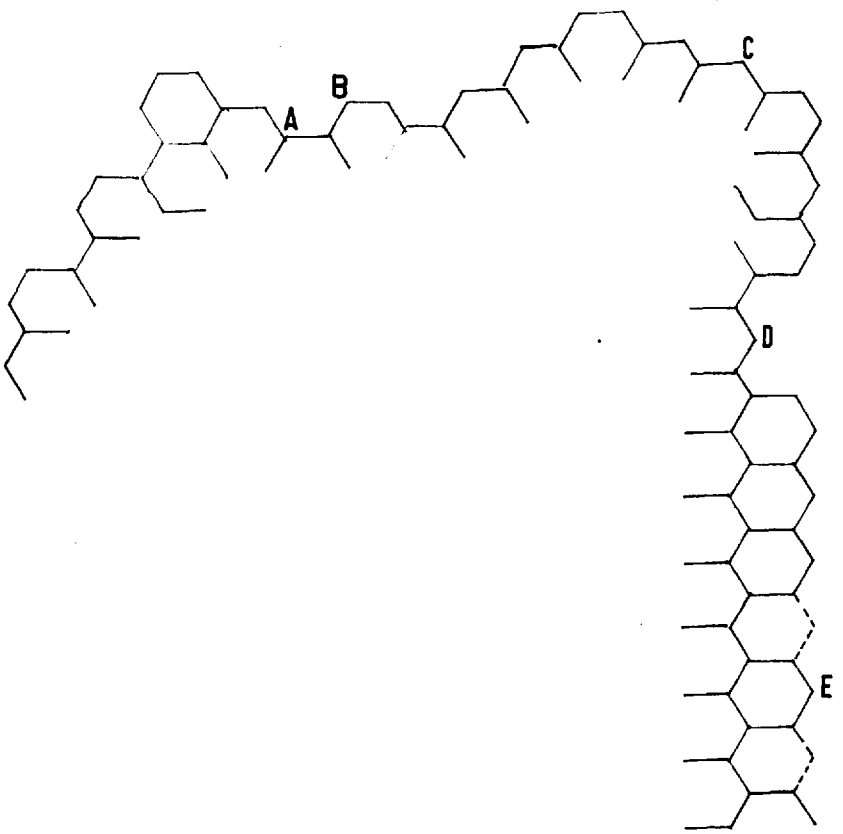

FIG. 6.1 Plan of graphite network

sites leave behind the network in different states of reactivity. In one case an extra edge site of type A/B could be formed. Under this idea the roughness factor of the filament would not change.

2. A second possible mechanism is that the non-ideal of the graphite is such that attack at certain edge atoms could uncover further edge atoms on other crystallites, or increase the area by a similiar mechanism. Considering the hypothetical case of reaction in direction Y, along edge atoms where two crystallites lie at an angle with one another. Attack along Y will not only leave edges in direction Y, but will also uncover additional edge atoms at points X where further reaction can proceed. Other possibilities exist with other defects.

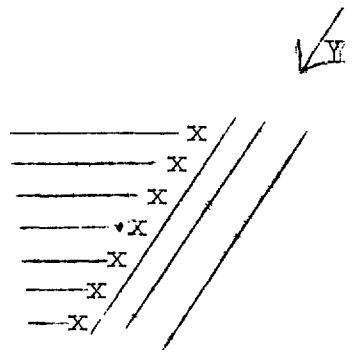

If the mechanism is similiar to the second one considered it is likely the the true area of the filament would change with reaction. The fact that at 0.76μ no such increase was detectable is explainable by the small part Process 3 plays at this pressure, as can be seen in Table A.6.4.

Considering the pressure dependance found for Process 3 and the fact that it can be related to one rate constant, suggests that there is some connection with the A sites in the Nagle and Strickland-Constable theory. As already stressed this would not affect the x in the Nagle theory since this would be instantaneously adjusting. Process 3 in this case would become;-

$$\text{rate} = K_3 P^y nx$$

There appears to be no fundamental reason why an expression of this form , with the other two processes, should not also fit the data.

B. Duval[3] found that at 0.76μ a hysteresis effect could be produced by merely heating in vacuum. This effect was about the same order of magnitude as the reaction hysteresis. This effect is consistent with the idea of thermal annealing taking place.

In the present work at 50μ, however, only a slight deactivation was produced by heating in vacuum. In the case where a black filament could be turned silvery by heating at 2000°C in vacuum, showing surface alteration on quite a large scale, it is thought that vaporisation plays an important part.

The fact that merely heating in vacuum appeares to cause very little hysteresis for reaction at 50μ, requires

further examination. This does suggest that another process is also responsible for the removal of A/B sites, in addition to the annealing. This process can be associated with the least satisfactory aspect of the theory, whereby at 50u n is greater than N. (Table A.6.5.)

As mentioned earlier attempts to include another removal process directly in the theory did not give satisfactory fits. A possible explanation , concerning Process 2, is that when n is small the chances of an oxygen molecule 'reacting' with a C site to give a A/B site are large. On the other hand the chances of an oxygen molecule 'reacting'with an A/B site and remove its activity is much greater when n is large. Process 2 therefore could represent two different mechanisms but both of which have almost identical rate constants. If this is so it suggests that the controlling reaction constant is the adsorption of oxygen, and the probability of whether an A/B site is removed or created depends on the probability of whether oxygen is adsorbed on a A/B or C site.

In addition to the other model mentioned in Section 6.3.2., the only other model which was found to fit the data satisfactorily was obtained by making Process 3 responsible for the creation of additional C sites. The equivalent

equation to Equation 6 (page 226) was then:-

$K_1 n = K_2 ((K_3 P^{x'} + N') - n) P.$ where N' is another constant related to the maximum possible number of C sites.

The equation for n becomes:-

$$n = \frac{(N' + K_5' P^{x'})}{(K_4 / P + 1)}$$

For this equation to fit the data at 0.76μ and 50μ it was necessary to put x' equal to 0.25 which is difficult to justify.

6.4.5. Results with other oxidising gases.

Boulangier and Duval[12] found a constant burnoff of about 3×10^{-7} g. atoms / cm^2 removed the hysteresis effect for O_2, CO_2, and H_2O. However since the roughness factor of filaments reacted in these gases varied in the order 25, 100, and 40, the total burnoff is by no means constant relative to the actual area.

As already mentioned Strickland-Constable found that filaments only burnt black in oxygen; a result confirmed in this work. It is therefore suggested that this blackening is related to Process 3, and that Process 3 only occurs for reaction in oxygen. For other gases it is suggested that only Processes 1 and 2 are applicable, but although the basic mechanisms may be the same, the rates of Process 1 and,

particularly Process 2, may alter from one gas to another because;-

a) If different active sites are involved for different gases, the annealing rate may alter because the different sites may be closer or further from a more stable state.

b) Creation of sites by Process 2 cannot be expected to be the same for different gases.

The main result of these suggestions is that with only two mechanisms applying, the hysteresis cannot change sense. Further the sense of the hysteresis will be as found for reaction in oxygen at 0.76μ. Both these conclusions are as found experimentally by Strickland-Constable[11] and Boulangier.[12]

SECTION 7. DISCUSSION OF RESULTS.

7.1. Untreated Filament Results.

The main results on untreated filaments show that the hysteresis is in the opposite sense to that observed by Duval[3] under reaction conditions of temperature and pressure. Other experiments showed that the explanation of the differences in their results was not due to different filaments used, nor to differences in the quantity burnt off.

The fact that the low burn off runs were no different and that a cold trap in the reactor did not affect the results supports the view that secondary reactions do not take place.

The hysteresis was found to change sense at a high temperature; the temperature of this change over decr asing with decreasing pressure. In general the results support the earlier work of Strickland-Constable, and the CO_2/CO ratio, while remaining small, increased with temperature as found by Shivonen[83].

The explanation of these hysteresis results is given and discussed in Section 6 together with a discussion on the nature of the active sites.

Certain results were found in the examination of the hysteresis which were against the general trend. Several results showed a hysteresis over an initial burn off of

less than 5 x10^{-7} gr atoms/cm^2 sec, which was contrary to the expected sense. The possibility that the hysteresis results was different at low burn offs can be discounted because of the low burn off runs, Graph 4.7, and also because most of the hysteresis results did not show this trend at low burn offs. It is thought most likely that these initial points were caused by desorption from the filament mounts and possible contamination of the surface of the filament. It was noticeable during any series of runs that if the filament was left standing in vacuum overnight the rate the following day was significantly lower. Duval[3] who observed the same effect showed that the contamination appeared to come from the grease, Apiezon L, replacing all his greased taps with Hg cut offs eliminated the effect.

The fact that filaments did not burn black in N_2O and black filaments were not turned silvery by extended burn off in N_2O strongly suggests that reaction for N_2O and O_2 occur on different sites. Additional evidence for this conclusion is given by the results which showed that reaction in one gas had a very small effect on subsequent reaction in the other.

Generally the reaction rate in N_2O was much less than observed by Strickland-Constable[11] and only a very small hysteresis effect was noticeable. A possible explanation for the activity of Strickland-Constable's filaments is that his extended reaction at high pressures caused pits to be formed

and also completely removed the less active pyrolytic carbon layer. The results for N_2O do however show the same effect of increasing rates at high temperatures and this is thought due to dissociation of N_2O as suggested by Strickland-Constable.

No pitting was found on the filament surface following reaction in oxygen and microphotographs showed very little difference in the surfaces for filaments burnt at different temperatures, both showing prominent cones. As expected the black filaments were rougher on the surface than silvery filaments but no deep pores could be seen.

The order of reaction as shown on Graph 4.6 shows an order of 1.5 between 20 and 150μ. Since our results and those of Strickland-Constable at 20μ were carried out on the same type of filaments these results can be considered fairly reliable. The order is also consistent with the Nagle Strickland-Constable theory which predicts an order greater than one in this region[21].

The same curves, however, show an order of 1 between 5μ and 0.65 μ which is neither consistent with Duval's results nor the mentioned theory. Two factors however make the order found in this region unreliable. The 0.65μ results were carried out on different filaments and this can cause a considerable difference in observed rates. The actual rates found by Duval for graphitized filaments showed quite a

variation for different filaments. The second factor is that the results at 5μ showed the effects of the glow discharge enhanced reaction at high temperatures.

This glow discharge was associated with blackening of the reactor walls suggesting vaporisation of carbon was taking place. The use of a cold trap did not eliminate the discharge, which suggests Duval's proposition that the discharge is caused by Hg vapour to be incorrect. In general the use of a cold trap on the reactor had no effect on the reaction.

7.2. Tentative explanation of rate maximum from electronic viewpoint.

The variation of the Hall effect with heat treatment found by Pacault et al[84] can be related to the maximum in the rate-temperature curve. The variation is shown below. A positive Hall coefficient is given by π band electrons while a negative one is given by positive holes. The Hall effect is seen to go through a minimum at about 1500°C and a maximum at about 1900°C; and also go from negative to positive.

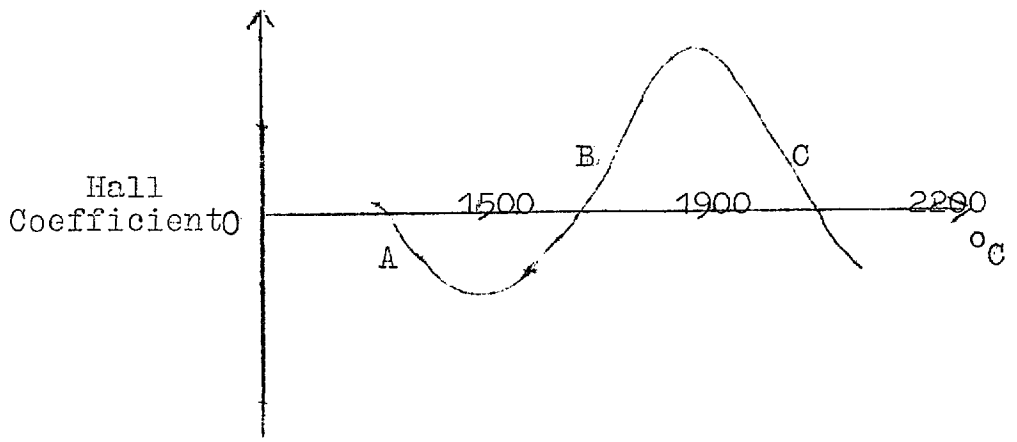

For part A the hole formation increases, and hence the number of traps for π electrons increase. This will tend to give Long and Sykes structure (b) [Fig.2.1] and hence increase the rate. After this first minimum the π band begins to fill up again and there is a greater tendency for the less reactive form (a) [Fig.2.1] of chemisorbed oxygen with consequently less reaction. After this maximum the number of electrons in the π band decreases due to thermal excitation of these fairly localised π electrons into the conductance band, as was suggested in the work reviewed in Section 2.5.5. As the π electrons decrease again the likelihood of structure (b) increases and consequently the rate once more speeds up.

Ubbelohde et al[85] related the formation of holes for curve A to loss of hydrogen. Volkenstein[63] has suggested that the hole formation can be related to solid defects, and interaction between defects. It seems likely that some mechanism other than evolution of hydrogen is responsible. Ubbelohde related the reduction in the number of holes in curve B to the knitting up of broken networks which accompany crystal growth. This is the same mechanism proposed in the 2 site annealing theory and these two ideas arise out of the same physical process. But in one the reaction is taken to occur actually on the broken bonds while in the other the reaction could occur elsewhere, the bonds just acting as electron traps.

This is only a very tentative explanation but it is useful in that it suggests a tie between various electronic data and the reactivity of carbon filaments. It also helps to bridge the gap between the uncatalysed and catalytic work on carbon described from the electronic viewpoint.

7.3. Catalytic reactions.

The fact that Zn and Pb did not affect the reaction was undoubtedly due to none of the particular substances remaining on the filament. Our results also showed that boron and silicon did not affect the rate although several previous workers have found an inhibiting effect[57,61,68].

The substances which catalysed the reaction, W, Fe, Zr, Pt, U, and Mo, were all able to exist on the filament, although W and Fe were slowly driven off at high temperatures. At low temperatures all these substances have been found to be catalysts[60] but it has also been reported that Zr can inhibit the high temperature reaction[88]. In the latter case a 35% Zr content was used which suggests that oxide formation at the high pressures used shielded the reaction of graphite.

From the oxygen balances there appeared in most cases to be some oxide formation, but also higher oxides appeared to decompose. This was particularly well shown in the results on Zr and U where heating in vacuum caused CO to be evolved. Further reaction in oxygen then caused a

net up take of oxygen. At first sight this suggests an intermediate mechanism but the quantity and speed of appearance of the CO cannot alone account for the increased rate. The other catalysts gave very little CO when heated in vacuum, while Pt would be expected to form no oxides. The fact that Pt is a catalyst again is evidence against an intermediate explanation.

The exact heat treatment and degassing procedure appeared to alter the activity of all the substances used. A similar effect was found by Gallagher et al with iron as reviewed in Section 2.7.4. Generally the results of low temperature catalysis and high temperature catalysis are not thought to be comparable. Not only is the basic mechanism for the uncatlysed reaction different, but the form of the catalyst on the surface would be very different.

Thermodynamic considerations show that most of the substances can exist as either carbides or oxides depending on the intimacy of contact with the carbon. This supports the experimental evidence, and it is interesting to note that in the case of zirconium on large particles a white surface characteristic of the dioxide was visible.

The thermodynamic calculations are of limited use for several reasons. Not only is there a lack of data on many compounds which might be involved, but the exact intimacy of contact between the metal and carbon is not known.

This can be further complicated by the possibilities of solid solutions being formed. To completely eliminate the possibility of the catalyst acting as an intermediate it would be necessary to know the relative speeds of the intermediate steps which of course must be faster than the uncatalysed reaction. In addition to the lack of fundamental thermodynamic data there is also a lack of vaporisation data, this again being complicated in not knowing the exact composition of the additive on the surface.

For most additions the CO_2/CO ratio was normal. In the case of iron an initial high CO_2 ratio was found possibly due to decomposition of the oxide. If it was due to catalytic oxidation of CO, the CO_2 quantity would be expected to be continuously high. A similar decomposition mechanism appears likely in the case of Uranium where the quantity of CO_2 went through a peak at about 1300°C and then decreased with decreasing oxygen balances. The fact that most substances, including Pt after the initial runs, gave predominantly CO adds evidence to the idea that the basic mechanism is not changed.

The most important results of the catalytic work show that the basic reaction mechanism is not changed. The reaction still exhibits a maximum in the rate; particularly well defined in the case of Fe, W, U, Mo and Pt.

The catalytic results also appeared to exhibit hysteresis effects. It is not possible to say whether the hysteresis is fundamental hysteresis due to the carbon oxidation, or hysteresis because the impurities alter their activity due to alternations in chemical form at different temperatures. The rates observed on the rate-temperature curves often returned to the same values at low (and high) temperatures which is indicative of it being a fundamental hysteresis. This was shown in the case of Pt although the magnitude of the hysteresis appeared to alter.

The above fact that the basic mechanism does not appear to change with catalysis is strong evidence of an electronic interpretation. An outline of the Long and Sykes theory is given in Section 2.7.2. The idea of Strickland-Constable[20] that the uncatalysed reaction occurs through a chemisorbed complex is compatible with the electronic theory. The complex can be considered to be adsorbed on active sites of types (a), a certain number of these sites being of, or becoming (b) with subsequent evolution of CO. The idea of a chemisorbed gas able to exist between two states of bonding 'weak' and 'strong' has been analysed by Volkenstein[63] from both an electronic view, and interaction at defects. The ideas were based largely on the localisation and delocalisation of electrons and holes, the relative rates depending on impurities and defects.

Apart from Pt those substances which catalysed the reaction could exist in various oxide states and also be reduced to the carbide. If a metal can exist between two oxide states two mechanisms are possible. One as suggested by Amargilio[66] is continuous oxidation and reduction of the oxides, and in this case the mechanism of the catalysed reaction is different from the uncatalysed reaction. The other mode of operation is that non stoichiometric oxides are formed which can accept electrons giving structure (b) by accepting an electron.

It was proposed by Long and Sykes that it was the conditions at the surface of a non stoichiometric oxide which enabled it to accept electrons. Semiconductor research has shown that p type oxides which tend to have excess oxygen in the lattice can give rise to a series of electron holes (traps) near the surface which will readily accept electrons[59]. This may be the case at low temperatures where conduction is by positive holes and not the actual iron, but our temperatures, with reducing conditions at the interface and low oxygen pressures, could be expected to give metal excess n type oxides[89]. At low temperatures n type oxides will not accept electrons but at high temperatures, as explained by Hauffe[59] the metal ions can migrate to the surface of the oxide and hence accept electrons. This is thought the

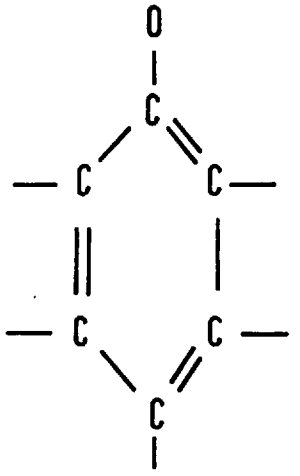

(a)

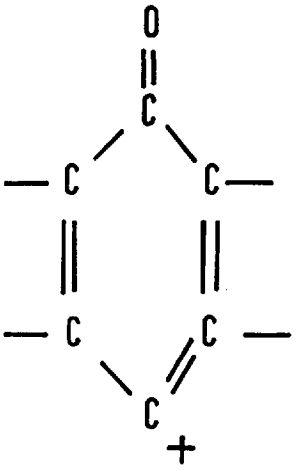

(b)

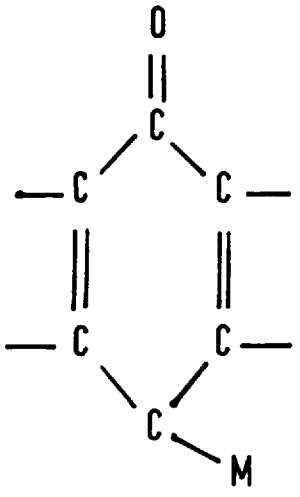

(c)

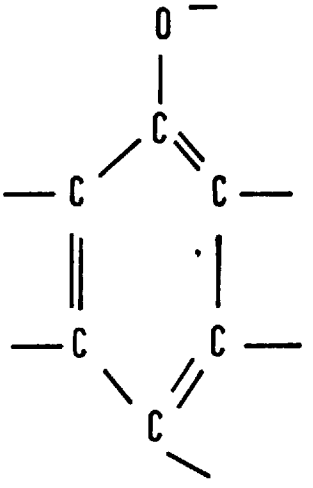

(d)

(Copy of) FIG 2.1 Long and Sykes distribution of bonds
(57)

possible mechanism in our case whereby the metal ions in the non stoichiometric oxide accept electrons giving structure (b). It is also likely that the free metal forming bonds with the π electrons again giving an active structure of type (c).

The activity appears in our results to be a function of temperature, oxygen pressure and time of heat treatment. The different activities are suggested due to different amounts and mixtures of non stoichiometric oxide formed and/or differences in the amount of free metal and carbide forming bonds of type (c). In the case of Pt no such oxides or carbides are formed, and it is thought that Pt merely accepts electrons.

Evidence has been forwarded by several authors that there exists an optimum particle size for catalysis [See Section 2.7.3]. This may be tied up with grain boundaries as suggested by Koblev. In our work no analysis of optimum particle size was carried out but the very large particles of Zr and U appeared to be very active. Even if there does exist an optimum size for the catalytic particles it does not necessarily discount the electronic interpretation. A particle at a grain boundary would be expected to have more influence since it could extract electrons from a greater number of graphite layers than a particle simply sitting on the basal plane.

The best catalysts appeared to cause considerable pittings on the surface which supports earlier workers, and suggests a certain localised action. The quantity of catalyst on the surface also appeared to affect the activity. This was particularly evident in the case of iron where depletion of the iron at high temperatures caused a decrease in the rate. It has been suggested that both these factors of localised action, and variation with quantity of catalyst are against the idea of an electronic interpretation. They are however completely compatible with the electronic approach in the case of graphite, because the solid is not continuous from the viewpoint of the electrons involved. It is for this reason that Band theory considerations as often applied to heterogeneous catalysis are not applicable to graphite[90]. Under the Long and Sykes mechanism the interaction in the C direction* would also be negligible. This is possibly the reason why putting iron and uranium in a filament and then coating with pyrolytic carbon had very little effect on the rate and why Mukuibo [Section 2.7.3] found vanadium had no effect inside graphite.

(* Perpendicular to the basal plane.)

APPENDICES.

APPENDIX 1.

Sample Run .

All pressures are in μ [10^{-3} mm Hg]

Run 1274.

Pressure of oxygen 5 minutes after introduction	52.0
Filament at 1290°C for 15 seconds	
Pressure after 5 minutes	55.9
Tap between reactor and McLeod section closed	
Cold trap in	
Pressure after 3 minutes	54.6
Tap to Hopcalite opened	
Pressure after 2 minutes	47.2

Cold trap removed and apparatus evacuated for at least 10 minutes.

For this run:-

Increase in pressure from reaction :- 3.9 μ

CO_2 pressure :- 1.3 μ corrected 0.5 μ

CO pressure :- 7.4 μ

Rate of reaction $= \frac{PA}{t} = 0.9127 \times 10^{-7}$ gr atoms of C reacted per sec. cm^2

$= \frac{7.4}{15} = 0.9127 \times 10^{-7}$

$= 4.80 \times 10^{-8}$

$r = CO_2/CO = 0.5/7.4 = 0.068.$

Oxygen accounted for = Final pressure + CO_2 pressure + 1/2CO pressure.

In this case the uncorrected CO_2 pressure is used since the final pressure is also uncorrected and the error cancels out.

∴Oxygen accounted for = 47.2 + 1.3 + 1/2 x 7.4 = 52.2

∴Oxygen balance = 52.2/52.0 = 100%

Calculation of R.

Assuming the ideal gas law applies to the system, which is a reasonable assumption since oxygen is used at low pressures Then $P_A V = N_A . RT$

where P_A is pressure of CO_2 and CO in mm Hg

N_A is no. of moles of CO_2 + CO; which is equivalent to number of gr atoms of carbon reacted.

Let time of reaction be t secs.

Area of filament be A cm^2. Based on Geometric area.

Then $NA = R = \frac{PA}{t} [\frac{V}{RAT}]$ gr atoms/cm^2 sec

where V = volume of apparatus in litres,

T = absolute temperature ^oC,

R = Gas constant = 62.36

The bracketed term is constant. All the experimental readings are assumed to be taken at 293^oK. The area of the filament will vary slightly because of burn off, but the effect is negligible.

Diameter of filaments 0.3 mm. Length 12.7 cm.

Volume of apparatus 1996 cc.

$\therefore$ R A T = 2.187×10^4

$\therefore$ $\underline{R = PA/t = 0.9127 \times 10^{-7}}$ for PA in μ t in secs.

APPENDIX 2.

List of Filaments.

Filament No.	Run Nos.	Treatment
1	Unreacted	
2	Unreacted	
3	Unreacted	
4	38 - 83	
5		Fe treated.
6	235 - 242	Sn evaporated from Pt coil.
7	243 - 252	Cu evaporated from Pt coil.
8	253 - 269	Granular Fe evaporated from W basket.
9	270 - 288	" "
10	Unreacted	Granular Fe evaporated from W basket while filament at 1200°C.
11	289 - 293	Zn heated in W basket at 870°C in 50μ of O_2.
12	294 - 297	"
13	298 - 300	Granular Fe evaporated from W basket.
14	301 - 325	W filament at 1500°C while carbon filament at 1200°C in 50μ of O_2.
15	329 - 358	Pt at 1050°C in 50μ of O_2 for 30 secs.
16	360 - 412	W treated, W filament at 1600°C in 50μ of O_2.
17	416 - 453	Fe wire at 1300°C in vacuum.
18	457 - 459	Fe wire in vacuum then coated with pyrolytic carbon.
19	460 - 464	Fe wire heated while coating with pyrolytic carbon.
20	465 - 485	Crystalline boron ground up in pestle and mortar.
21	456 - 502	" "
22	503 - 510	Crystalline boron in acetone.
23	511 - 531	Boric acid powder suspension in acetone

Filament	Run Nos.	Treatment
24	532 ; 556	Boric oxide evaporated from Pt coil.
25	557 - 567	Untreated.
26	570 - 580	Untreated to 579, coated with boric acid at 580.
27	592 - 615	Untreated.
28	616 - 633	Amorphous boron suspension in water.
29	634 - 643	Amorphous boron then coated with pyrolytic carbon.
30A	644 - 663	Amorphous suspension in acetone
30B	664 - 684	Zr suspension in acetone.
31	685 - 704	Zr suspension in acetone.
32	706 - 722	Zr suspension in acetone.
33	723 - 740	Mo powder in acetone.
34	741 - 751	Mo powder in acetone.
35	752 - 764	MoO_3 suspension in water.
36	770 - 788	Suspension of silicon powder in water.
37	781 - 790	Suspension of silicon powder in water.
38	791 - 794	Silica suspension in water.
40	795 - 796	Sodium silicate solution.
41	797 - 829	UO_3 suspension in water.
42	830 - 841	UO_3 treated then coated with pyrolytic carbon.
43	842 - 959	O_2 and N_2O hysteresis, untreated.
44	-	Reacted in N_2O, untreated.
45	960 -1003	Reacted in N_2O, untreated.
46	1004 -1029	Reacted in N_2O, treated with UO_3 after 1028.
47	1030 -1046	N_2O reacted. UO_3 suspension.
48	1049 -1076	Filament prepared from CCl_4.
49	-	Filament heated at 1270°C for total of 6 mins. in O_2 only.
50	-	Filament heated at 2000°C for total of 6 mins. in O_2 only.
51	-	Filament heated at 950°C for total of 6 mins. in O_2 only.

Filament No	Run Nos.	Treatment
52	1079 - 1174	Reacted in N_2O and O_2.
53	-	Reacted 2000°C to 950°C. Then 2 minutes at 950°C.
54	1175 - 1232	Reacted in O_2 at 50 μ.
55	1233 - 1251	Pt treated.
56	1255 - 1365	Composite curve at 50 μ untreated.
57	1366 - 1396	Pt treated.
58	1413 - 1498	O_2 hysteresis Runs.
59	1499 - 1587	Mo treated, from Mo filament.

APPENDIX 3.

Thermodynamic Calculations.

Method of Calculation.

1. Consider $ZrO_2 \longrightarrow Zr + O_2$

ΔF_R reaction at 1500°K = 193,900 k cals/gr mole

But $\Delta F_R = - RT \ln K_R$

where K_R = equilibrium constant

$$\therefore \quad \underline{\log_{10} K_R = - 1/4.579 \ \frac{F_R}{T}}$$

In this case $\log_{10} K_R = - 28.261$

For this reaction $K_R = P_{O_2}$ in atm.

$$\therefore \quad P_{O_2} = < 10^{-28} \text{ atm.}$$

Since under r action conditions $P_{O_2} \approx 10^{-6}$ the ZrO_2 will not decompose under reaction conditions.

2. Consider $ZrO_2 + 4CO \longrightarrow ZrC + 3CO_2$

ΔF_R reaction = $\Delta F(ZrC) + 3\Delta F(CO_2) - \Delta F(CO) - \Delta F(ZrO_2)$

= + 98, 530 $\therefore \log_{10} K_R = -14.361$

In this case $\log_{10} K_R = (P_{CO_2})^3 / (P_{CO})^4$

P_{CO} will vary between about 0 and 15μ during reaction. Taking P_{CO} = 7.6 u is $10^{-}5$ atm.

$$\therefore \quad (P_{CO})^4 = 10^{-20} \text{ atm.}$$

$$\therefore \quad \log_{10} K_R (P_{CO_2})^3 = -14.361 - 20.000 = 34.361$$

$$\therefore \quad \log_{10} (P_{CO_2}) = -11.451 = \bar{1}2.546$$

$$\therefore \quad P_{CO_2} = 3.5 = 10^{-12} \text{ atm.}$$

P_{CO_2} normally about 10^{-6} atm., and therefore this reaction is not feasible.

Free energies for formation of CO_2 and CO are

	1200°K	1500°K	2000°K
CO	-47,950	-58,400	-68,750
CO_2	-95,900	-116,800	-137,500

Data from:

(91) Kubaschewski, O., and Evans, E.Ll.
Metallurgical Thermodynamics, Perganon Press, (1958).

(92) Wicks, C.E. and Black, F.E.
Thermodynamic Properties of 65 Elements.
U.S.Bureau of Mines, B.605.

(93) Schick, H.L.
Thermodynamics of Certain Refractory Compounds.
Vol.2. Academic Press (1966).

(94) Remy, L.
Treatise on Inorganic Chemistry. Longmans (1964).

Table A.3.1.

Zinc

Zn B.Pt. 1181°K ZnO M.Pt 2248°K

Free energies	1200°K	1500°K	2000°K
ZnO	-53,400	-45,100	-131,000

Reaction

$2ZnO \longrightarrow 2Zn + O_2$	P_{O_2} atm	$<10^{-9}$	2.7×10^{-7}	4.1×10^{-4}

Platinum M.Pt 1769°C. B.Pt 4100°C.

No oxide of Pt is stable in oxygen under 1 atm. pressure above 500°C.

Tin M.Pt. 232°C. B.Pt. 2590°C. No stable oxides under reaction conditions.

Table A.3.2. Boron.

B M.Pt. 2050°C.		B_2O_3 B.Pt 2300°C	M.Pt. 450°C.
Free energies	1200°K	1500°K	2000°K
B_2O_3	-234,000	-219,300	-195,000
B_4C	- 12,750	- 12,500	- 12,200
Reactions.			
$B_2O_3 \rightarrow B_2 + 3/2\ O_2$	P_{O_2}	$< 10^{-21}$	$< 10^{-14}$
$B_2O_3 + 7C \rightarrow B_4C + 6CO$	P_{CO_2}	8.2×10^{-6}	1.5×10^{-1}	$> 10^{-2}$
$2B_2O_3 + 4C \rightarrow B_4C + 3CO_2$	P_{CO_2}	$<10^{-10}$	1.3×10^{-7}	1.9×10^{-3}
$2B_2O_3 + 8CO \rightarrow B_4C + 7CO_2$	P_{CO_2}	1.6×10^{-10}	3.1×10^{-11}	1.5×10^{-10}
$B_2O_3 + C \rightarrow B_2 + 3Co$	P_{CO}	3.4×10^{-6}	2.5×10^{-4}	4.0×10^{-1}
$2B_2O_3 + 3C \rightarrow B_2 + 3CO_2$	P_{CO_2}	$< 10^{-11}$	3.2×10^{-8}	1.5×10^{-4}
$2B_2O_3 + c \rightarrow B_4C + 3O_2$	P_{O_2}	$<10^{-27}$	$< 10^{-20}$	$<10^{-13}$
$B_2O_3 + 3CO \rightarrow B_2 + 3CO_2$	P_{CO_2}	$<10^{-23}$	$<10^{-23}$	$<10^{-16}$

Table A.3.3. Silicon.

Si M.Pt. 1413°C B.Pt. 2600°C.

SiO_2 M.Pt. 1900°K

SiC M.Pt. 2900°C.

Si formed when SiO_2 heated with charcoal will rapidly volatilize as low as 1300°C in vacuo. Carbide formed as low as 1600°C, above 2200°C silicon evaporates away.

Free energies.		1200°K	1500°K	2000°K
SiO_2		-158,450	-146,100	-123,800
SiC		- 10,700	- 10,200	- 9,200
Reactions.				
$SiO_2 \rightarrow Si + O_2$	P_{O_2}	$<10^{-28}$	$<10^{-21}$	$<10^{-13}$
$SiO_2 + 3C \rightarrow SiC + 2CO$	P_{CO}	1.9×10^{-5}	4.1×10^{-2}	19
$SiO_2 + 2C \rightarrow SiC + CO_2$	P_{CO_2}	2.1×10^{-10}	7.6×10^{-7}	5.6×10^{-3}
$SiO_2 + 4CO \rightarrow SiC + 3CO_2$	P_{CO_2}	$<10^{-10}$	$< 10^{-10}$	$< 10^{-10}$
$SiO_2 + C \rightarrow Si + CO_2$	P_{CO_2}	$<10^{-11}$	3.3×10^{-8}	7.1×10^{-4}
$SiO_2 + C \rightarrow SiC + O_2$	P_{O_2}	$<10^{-26}$	$<10^{-19}$	$<10^{-12}$
$SiO_2 + 2CO \rightarrow Si + 2CO_2$	P_{CO_2}	1.2×10^{-11}	$<10^{-10}$	1.3×10^{-9}
$SiO_2 + C \rightarrow Si + 2CO$	P_{CO}	2.0×10^{-6}	7.3×10^{-3}	5.6

Table A.3.4. Iron.

Fe M.Pt 1539°C.

Fe_3O_4 M.Pt 1378°C

Fe_2O_3 M.Pt 1597°C

$Fe_{0.95}O$ M.Pt. 1400°C.

Fe_3C M.Pt 1500°K Metastable above 2000°K

Free energies		1200°K	1500°K	2000°K
$Fe_{0.95}O$		-43,950	-39,050	-33,000
Fe_3O_4		-175,500	-154,000	-119,000
Fe_2O_3		-122,800	-105,400	- 76,000
Fe_3C		+200	+650	-3,500
Reactions.				
$2Fe_2O_3 \rightarrow Fe + 3O_2$	P_{O_2}	$<10^{-15}$	$<10^{-10}$	2.9×10^{-6}
$2Fe_2O_3 \rightarrow Fe_{0.95}O + O_2$	P_{O_2}	$<10^{-12}$	2.2×10^{-8}	6.5×10^{-3}
$Fe_3O_4 \rightarrow 3Fe + 2O_2$	P_{O_2}	$<10^{-15}$	$<10^{-11}$	3.1×10^{-7}
$Fe_3O_4 \rightarrow 6FeO + O_2$	P_{O_2}	$<10^{-15}$	$<10^{-10}$	4.2×10^{-5}
$2FeO \rightarrow 2Fe + O_2$	P_{O_2}	$<10^{-16}$	$<10^{-11}$	6.1×10^{-8}
$3FeO + 4C \rightarrow Fe_3C + 3CO$	P_{CO}	>1	$>10^2$	$>10^4$
$6FeO + C \rightarrow 2Fe_3C + 3CO_2$	P_{CO_2}	$>10^2$	$>10^2$	$>10^3$
$FeO + C \rightarrow Fe + CO$	P_{CO}	>1	$>10^2$	$>10^3$
$2FeO + C \rightarrow Fe + CO_2$	P_{CO_2}	>10	$>10^2$	$>10^3$
$3FeO + 5CO \rightarrow Fe_3C + 4CO_2$	P_{CO_2}	1.1×10^{-6}	3.6×10^{-8}	1.6×10^{-8}
$FeO + CO \rightarrow Fe + CO_2$	P_{CO_2}	5.4×10^{-5}	4.0×10^{-6}	1.8×10^{-6}
$Fe_3O_4 + C \rightarrow 3FeO + CO$	P_{CO}	>1	$>10^3$	$>10^5$
$Fe_2O_3 + C \rightarrow 2FeO + 3CO$	P_{CO}	$>10^6$	$>10^7$	10^7

Table A.3.4 (continued)

Reactions.		1200°K	1500°K	2000°K
$Fe_3O_4 + CO \rightarrow 3FeO + CO_2$	P_{CO_2}/P_{CO}	3.5	1.2	4.8
$Fe_2O_3 + CO \rightarrow 3FeO + CO_2$	"	10^2	3.4	60

The corresponding reactions 6-9 for Fe_2O_3 and Fe_3O_4 also give equilibrium pressures >1 atm.

Table A.3.5. Tungsten.

W. M.Pt. 3380°C
WO_3 M.Pt. 1473°C Volatilises above 1750°C
WC Decomposes 2900°K
WO_2 M.Pt. 1543°K Decomposes 2125°K
Intermediate oxides exist.

Free energies		1200°K	1500°K	2000°K
WO_3		-129,550	-112,850	-88,050
WO_2		- 87,600	- 75,400	-54,500
WC		- 7600	- 7100	- 6000
Reactions.				
$WO_2 \rightarrow W + O_2$	P_{O_2}	$<10^{-15}$	$<10^{-10}$	10^{-6}
$WO_2 + 3C \rightarrow WC + 2CO$	P_{CO}	>10	$>10^3$	$>10^4$
$WO_2 + 3C \rightarrow WC + CO_2$	P_{CO_2}	$>10^2$	$>10^2$	$>10^5$
$WO_2 + 3C \rightarrow W + 2CO$	P_{CO}	5.7	$>10^3$	$>10^4$
$WO_2 + C \rightarrow W + CO_2$	P_{CO_2}	>10	$>10^2$	$>10^4$
$WO_2 + 2CO \rightarrow W + 2CO_2$	P_{CO_2}	1.3×10^{-5}	6.9×10^{-6}	7.8×10^{-6}
$WO_2 + 4CO \rightarrow WC + 3CO_2$	P_{CO_2}	1.2×10^{-6}	3.0×10^{-8}	8.5×10^{-9}
$WO_2 + C \rightarrow WC + O_2$	P_{O_2}	$>10^{14}$	$>10^9$	$>10^5$
$2WO_3 \rightarrow 2WO_2 + O_2$	P_{O_2}	$<10^{-15}$	$<10^{-10}$	4.6×10^{-8}
$WO_3 \rightarrow 2W + 3\,O_2$	P_{O_2}	$<10^{-15}$	$<10^{-10}$	3.8×10^{-7}

Table A.3.6. Molybdenum.

Mo M.Pt. 2600°C

MoO_3 B.Pt. 1100°C Sublimes around 790°C. Cautious heating MoO_2

MoO_2 M.Pt. 2500°K

Mo_2C M.Pt. 2690°C

Various intermediate oxides exist.

Free Energies		1200°K	1500°K	2000°K
MoO_2		-87,500	-77,000	-60,000
MoO_3		-109,500	-98,000	-90,000
Mo_2C		-1,550	-3,000	-5,400

Reactions.

$MoO_2 \rightarrow Mo + O_2$	P_{O_2}	$<10^{-15}$	$<10^{-11}$	2.8×10^{-7}
$2MoO_2 + 3C \rightarrow Mo_2C + 4CO$	P_{CO}	7.0	$>10^3$	$>10^4$
$MoO_2 + 3C \rightarrow Mo_2C + 2CO_2$	P_{CO_2}	>10	$>10^2$	$>10^4$
$MoO_2 + C \rightarrow Mo + 2CO$	P_{CO}	5.8	$>10^2$	$>10^4$
$MoO_2 + C \rightarrow Mo + CO_2$	P_{CO_2}	>10	$>10^2$	$>10^3$
$MoO_2 + 2CO \rightarrow Mo + 2CO_2$	P_{CO_2}	3.4×10^{-5}	4.9×10^{-6}	4.0×10^{-5}
$MoO_2 + 6CO \rightarrow Mo_2C + 5CO_2$	P_{CO_2}	1.1×10^{-6}	4.1×10^{-8}	6.3×10^{-8}
$2MoO_2 + C \rightarrow Mo_2C + 2O_2$	P_{O_2}	$<10^{-15}$	$<10^{-10}$	4.3×10^{-7}
$2MoO_3 \rightarrow 2MoO_2 + O_2$	P_{O_2}	9.7×10^{-9}	7.6×10^{-7}	4.3×10^{-5}
$2MoO_3 \rightarrow 2Mo + 3O_2$	P_{O_2}	$<10^{-13}$	$<10^{-10}$	2.8×10^{-7}

Table A.3.7. Zirconium.

Zr	M.Pt.	2125°K.
ZrO_2	M.Pt.	2700°K.
ZrC	M.Pt.	3530°C.

Free Energies		1200°K	1500°K	2000°K
ZrO_2		-207400	-193900	-175000
ZrC		- 45426	- 44718	- 43676

Reactions.

$ZrO_2 \rightarrow Zr + O_2$	P_{O_2}	$<10^{-37}$	$<10^{-28}$	$<10^{-19}$
$ZrO_2 + 2C \rightarrow ZrC + CO$	P_{CO}	9.7×10^{-7}	4.4×10^{-3}	2.2
$ZrO_2 + C \rightarrow ZrC + CO_2$	P_{CO_2}	5.3×10^{-13}	1.2×10^{-8}	1.1×10^{-4}
$ZrO_2 + 4CO \rightarrow ZrC + 3CO_2$	P_{CO_2}	$<10^{-11}$	$<10^{-11}$	$<10^{-11}$
$ZrO_2 + C \rightarrow Zr + CO_2$	P_{CO_2}	$<10^{-20}$	$<10^{-14}$	$<10^{-9}$
$ZrO_2 + C \rightarrow Zr + 2CO$	P_{CO}	$<10^{-10}$	2.4×10^{-6}	8.9×10^{-3}
$ZrO_2 + C \rightarrow ZrC + O_2$	P_{O_2}	$<10^{-29}$	$<10^{-21}$	$<10^{-14}$
$ZrO_2 + 2CO \rightarrow Zr + 2CO_2$	P_{CO_2}	$<10^{-15}$	$<10^{-13}$	$<10^{-11}$

Table A.3.8. Uranium.

U	M.Pt.	1130°C	B.Pt.	3500°C
UO_2	M.Pt.	2500°C		
UC_2	M.Pt.	2500°C		

Other intermediate oxides are formed, but all reduce to UO_2 on heating.

Vapour pressure of Uranium at 1900°C = 0.026 mm Hg.

Free energies		1200°K	1500°K	2000°K
UO_2		-210000	-196700	-176000

Reactions

$UO_2 \rightarrow U + O_2$	P_{O_2}	-	-	$< 10^{-19}$
$UO_2 + C \rightarrow U + CO_2$	P_{CO_2}	-	$< 10^{-14}$	1.4×10^{-9}
$UO_2 + 2C \rightarrow U + 2CO$	P_{CO}	-	$< 10^{-20}$	$< 10^{-11}$

APPENDIX 4.

Experimental results on UNTREATED filaments not in main text.
(Graphs are before the Tables.)

GRAPH A.4.1 Rate-temperature curves in 50μ of oxygen

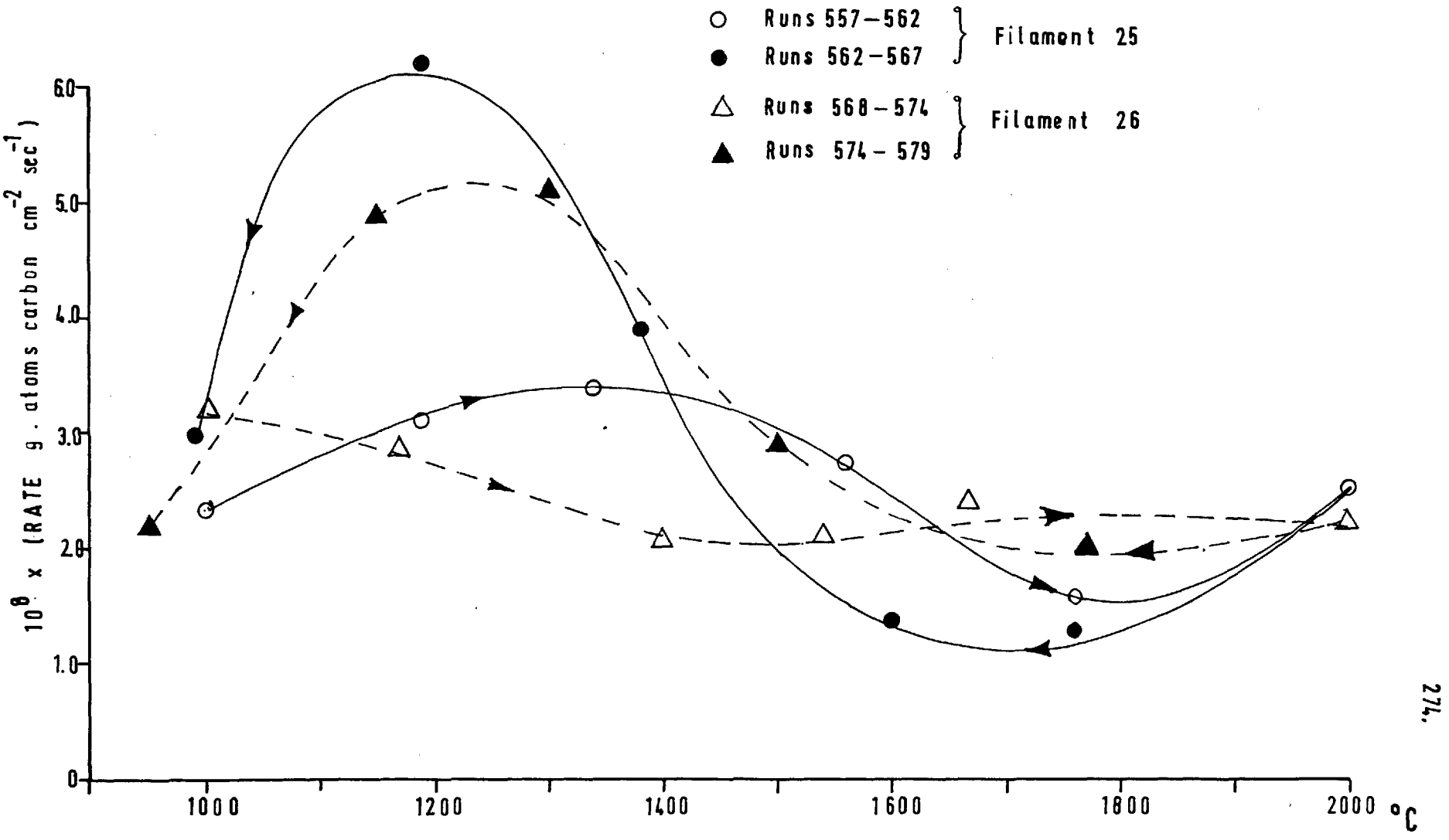

Table A.4.1. Oxidation of an untreated filament in oxygen at 50 μ pressure.

All reaction for 30 seconds. Filament No.27.

Run No.	T°C	Initial Pressure	CO formed μ	CO_2/CO ratio	O_2 balance	R x10^8 gm atoms/ cm^2/sec.
592	1100	50.4	8.9	0	99	2.7
593	1300	49.2	8.7	0.02	103	2.7
594	1450	49.6	8.5	0.03	101	2.7
595	1560	48.9	6.8	0.04	102	2.1
596	1800	48.4	6.8	0.10	100	2.3
597	2000	50.6	6.4	0.16	98	2.2
598	1740	49.3	5.0	0.02	100	1.5
599	1440	49.7	8.4	0.08	103	2.1
600	1370	50.7	12.3	0.04	108	3.9
601	1230	49.7	16.0	0	107	4.9
602	1000	48.5	9.1	0	102	2.7
603	1000	48.7	7.2	0	102	2.2
604	1260	50.9	10.1	0.02	102	3.1
605	1380	49.4	10.2	0.04	101	3.2
606	1520	50.2	7.8	0	101	2.4
607	1600	49.6	8.0	0.06	102	2.6
608	1700	51.3	6.4	0.06	100	2.1
609	2000	48.1	6.4	0.14	99	2.3
610	1700	50.2	5.1	0.14	101	1.7
611	1440	51.2	9.5	0.04	103	3.0
612	1440	50.0	9.2	0.03	105	2.9
613	1300	48.8	12.5	0.02	106	3.9
614	1150	49.0	11.2	0.04	108	3.6
615	950	50.0	6.8	0	101	2.1

Table A.4.2. Oxidation of an untreated filament in oxygen at 50 μ pressure. Reproducibility.

Filament No.25.

Run No.	T°C	Initial pressure μ	CO formed μ	CO_2/CO ratio	O_2 balance	R $\times 10^8$
557	1000	47.0	5.7	0.35	100	2.34
558	1190	50.1	10.2	0	98	3.10
559	1340	49.3	10.7	0.04	97	3.37
560	1560	49.9	8.8	0.02	99	2.73
561	1760	49.5	5.5	0.09	95	1.83
562	2000	47.2	7.0	0.06	91	2.25
563	1760	47.2	3.8	0.10	98	1.27
564	1600	50.1	4.4	0.02	98	1.37
565	1380	50.5	12.6	0.01	99	3.89
566	1190	49.7	20.4	0	102	6.20
567	990	50.0	9.6	0.04	98	2.98
Filament No.26						
568	1000	50.0	10.0	0.04	96	3.16
569	1170	49.2	9.0	0.04	93	2.86
570	1400	50.2	6.7	0	104	2.04
571	1540	53.6	7.1	0	106	2.1
572	1480	48.6	7.8	0.04	100	2.5
573	1670	50.0	7.3	0.11	101	2.4
574	2000	51.5	6.9	0.04	95	2.2
575	1770	51.0	5.2	0.29	103	2.0
576	1500	49.6	9.3	0.03	100	2.9
577	1300	49.7	16.5	0.02	103	5.1
578	1150	51.1	15.9	0.02	106	4.9
579	950	50.3	6.4	0.14	101	2.2

All reaction for 30 seconds except Run 573 where reaction was for 40 seconds.

Table A.4.3. Oxidation of an untreated filament in 50 μ of oxygen.

All reaction for 30 seconds. Filament No.43

Run No.	T°C.	Initial Pressure μ	CO formed μ	CO_2/CO ratio	Oxygen balance	R x10^8
853	1440	50.2	11.4	0.03	99	3.89
854	1540	52.0	10.2	0.06	95	3.28
855	1670	50.4	9.3	0.05	101	2.98
856	1760	49.3	7.5	0.03	96	2.34
857	1870	51.2	6.9	0.09	99	2.28
858	2030	50.4	8.1	0.10	98	2.71
859	1850	50.9	6.3	0.09	98	2.10
860	1690	49.6	5.9	0	99	1.79
861	1550	48.8	8.9	0.02	99	2.77
862	1440	49.3	16.9	0.02	97	5.23

Table A.4.4. Oxidation of an untreated filament in oxygen 150 μ. Filament No.4

Run No.	T°C	Secs. reaction	Initial pressure μ	Pressure CO formed μ	CO_2/CO ratio	Oxygen balance	R x10^8
38	1250	60	171.5	67.0	0.04	96	10.2
39	1250	60	147.5	59.0	0.02	98	8.97
40	900	60	187.5	11.8	0.50	108	1.98
43	1000	480	136.5	87.0	0.06	99	1.66
44	1100	240	172.0	76.0	0.04	100	2.89
46	1200	30	124.5	32.5	0.10	100	9.89
48	1300	60	129.5	80.0	0.03	100	12.2
49	1400	60	162.5	104	0.02	101	15.9
50	1500	30	150.0	42	0.10	105	12.8
51	1600	30	152.5	39	0.13	109	11.9
52	1700	30	141.0	41	0.06	104	12.5
53	1800	30	141.5	41.5	0.08	98	12.6
54	1700	30	141.5	58	0.06	101	17.6
55	1600	30	128.0	70	0.03	97	21.3
56	1500	30	155.0	77	0.05	99	23.4
57	1400	15	156.5	59	0.07	102	35.9
58	1300	30	160.5	115.5	0.03	101	35.1
59	1200	30	165.0	118.5	0.01	93	36.0
60	1100	30	150.5	105	0.03	99	31.9
61	1000	30	161.0	26.5	0.02	104	8.06
62	1300	30	155.0	140	0.02	98	42.6
63	1300	30	147.5	108	0.02	101	32.8

Table A.4.5. Oxidation of an untreated filament in oxygen at 5μ pressure.

Filament No.43.

Run No.	T°C	Initial Pressure μ	CO formed μ	CO_2/CO ratio	O_2 balance	R x10^{10}
886	840	4.86	0.27	0.11	100	0.91
887	890	4.96	0.42	0.28	100	0.82
888	1000	4.90	0.92	0.05	97	7.4
889	1120	5.07	2.29	0.04	98	18.3
890	1300	5.10	1.55	0	100	23.5
891	1400	5.07	0.80	0.14	96	13.8
892	1500	4.68	0.39	0.69	102	10.0
893	1660	4.88	0.63	0.38	101	13.2
894	1940	5.06	1.17	0.69	107	30.1
895	1940	4.84	1.03	0.36	104	21.3
896	1740	5.03	0.32	1.1	104	10.0
897	1580	4.90	0.19	0.74	101	5.0
898	1410	5.14	0.45	0.38	-	9.4
899	1260	4.78	0.81	0.36	-	16.7
900	1100	4.80	1.97	0.0	-	32.1
901	1010	5.18	1.51	0.01	-	25.2
902	950	4.74	0.43	0	-	8.5
903	940	4.96	0.57	0.17	-	12.1

Reaction for 1 min. except Runs 888,889 for 2 mins., 887 for 10 mins, and 886 for 5 mins.

Table A.4.6. Average rates at different temperatures and pressures.

Rates as gr. atom / cm^2 / sec.

T°C	0.65μ	5 μ	20μ	50μ	150μ
900	3.56×10^{-10}	-	-	-	-
1000	5.65	1.50×10^{-9}	4.22×10^{-9}	2.67×10^{-8}	0.45×10^{-7}
1100	5.80	2.40	7.24	3.58	1.72
1200	3.56	2.42	7.94	3.84	2.25
1300	2.08	1.87	6.46	3.76	2.52
1400	1.70	1.05	5.07	3.09	2.45
1500	1.59	0.75	4.00	2.42	1.97
1600	1.29	0.80	3.47	2.02	1.65
1700	1.50	1.11	2.92	1.82	1.45
1800	-	1.23	2.69	1.80	1.25
1900	-	2.02	2.58	1.99	-
2000	-	3.00	2.55	2.32	-

0.65μ results from Graph 8, Duval[3]; 20μ results from Strickland Constable[2].

Table A.4.7. Oxidation of an untreated filament in oxygen at 5μ pressure with low burn off.

Filament No.51.

Run No.	T°C	Initial pressure μ	CO pressure μ	R x 10^8
1077	2000	52.2	1.2	2.19
1078	1960	51.3	0.5	0.91
1079	1815	47.6	1.0	1.83
1080	1660	51.4	0.8	1.46
1081	1630	46.7	0.9	1.65
1082	1600	50.4	2.1	3.83
1083	1450	48.0	1.4	2.56
1084	1250	48.5	3.8	6.93
1085	1140	48.6	5.3	9.67
1086	1050	48.6	9.5	8.20
1087	950	50.7	1.0	1.83
1088	950	49.8	0.8	1.46
1089	1060	48.7	1.6	2.92
1090	1220	49.7	2.3	4.20
1091	1260	50.8	2.4	4.39
1092	1340	49.0	1.8	3.29
1093	1420	49.2	1.8	3.29
1094	1530	49.5	2.0	3.65
1095	1610	47.4	1.8	3.29
1096	1730	48.8	1.2	2.19
1097	1830	48.6	1.5	2.74
1098	2065	49.2	2.8	5.11

All reaction for 5 seconds.

After Run 1087 the filament was burnt twice for 2 mins. in 50μ of oxygen at 930°C.

Table A.4.8. Oxidation of a CCl_4 pyrolytic carbon filament at 50μ in oxygen.

Filament No.48.

Run No.	T°C	Initial Pressure μ	CO formed μ	CO_2/CO ratio	O_2 balance	R x10^8
1044	930	51.4	4.8	1.0	107	0.73
1050	1010	50.8	8.6	0.51	104	1.97
1051	1140	50.2	17.8	0.27	103	3.43
1052	1270	52.0	14.5	0.12	102	4.95
1053	1340	51.2	13.4	0.19	102	4.83
1054	1500	50.0	10.6	0.21	101	3.68
1055	1580	50.7	10.0	0.21	100	3.68
1056	1600	49.3	10.2	0.15	100	3.55
1057	1720	51.0	9.6	0.16	101	3.37
1058	1830	50.6	8.6	0.31	103	3.43
1059	2000	54.0	12.6	0.18	105	3.89
1060	2000	54.0	8.8	0.24	102	3.31
1061	2000	51.6	8.6	0.21	102	3.16
1062	2000	52.6	9.0	0.19	102	3.25
1063	1860	51.5	9.6	0.08	101	3.16
1064	1990	47.0	10.8	0.07	100	3.53
1065	1680	49.5	13.7	0.11	100	4.62
1066	1580	50.0	15.7	0.04	100	4.99
1067	1440	50.8	16.8	0.05	102	5.38
1068	1300	52.1	17.3	0.01	101	5.29
1069	1160	50.5	11.9	0.09	103	3.95
1070	1020	50.0	8.5	0.11	100	2.86
1071	980	52.8	5.8	0.21	103	2.16

Table A.4.9. Rate-temperature runs in 50μ pressure of N_2O.

Filament N_o.45.

Run No.	T°C	Initial Pressure μ	Pressure CO + N_2 μ	R x 10^9
971	2010	46.2	3.3	1.03
972	1800	46.0	2.3	0.68
973	1680	48.0	2.0	0.61
974	1590	48.4	1.8	0.55
975	1460	50.2	2.0	0.65
976	1320	50.0	2.1	0.69
977	1200	47.6	1.8	0.55
978	1110	48.0	1.5	0.45
979	950	50.0	1.1	0.35
980	1080	49.0	1.4	0.45
981	1210	48.6	2.1	0.65
982	1420	48.6	2.1	0.65
983	1310	47.0	1.7	0.51
984	1560	46.3	1.9	0.58
985	1700	45.2	2.3	0.68
986	1800	47.6	3.0	0.93
987	2010	48.6	4.4	1.39

All reaction for 120 seconds.

Table A.4.10. Rate-temperature runs in 50μ pressure of N_2O.

Filament No.43. Filament previously reacted in oxygen.

Run No.	T°C	Seconds reaction	Initial pressure μ	Pressure CO + N_2 μ	R x 10^9
915	2010	60	50.1	3.7	2.81
916	2010	60	48.0	2.4	1.75
917	2010	60	48.0	2.6	1.90
918	2010	60	54.0	2.8	2.28
919	2010	60	46.0	2.9	2.05
920	1800	60	52.4	2.2	1.75
921	1800	120	48.9	3.5	1.29
922	1800		48.4	3.5	1.29
923	1650		48.6	2.8	1.03
924	1650		50.2	2.6	0.99
925	1550		50.8	3.1	1.21
926	1550		47.6	2.2	0.80
927	1350		49.8	1.9	0.72
928	1350		51.8	3.7	1.45
929	1350		49.8	2.1	0.80
930	1200		55.0	3.6	1.52
931	1200		53.4	4.2	1.50
932	1200		48.0	5.0	1.83
933	1000		46.0	2.1	0.65
934	1000		46.4	1.7	0.61
935	1190		48.0	2.2	0.70
936	1190		47.6	3.0	1.07
937	1190		47.0	2.2	0.83
938	1190		49.4	3.0	1.14
939	1400		46.4	3.1	1.18
940	1400		47.4	3.3	1.25
941	1500		46.2	2.5	0.95

Table A.4.10 (continued).

Run No.	T°C.	Seconds reaction	Initial pressure μ	Pressure CO + N_2 μ	R x 10^9
942	1500		47.4	2.5	0.95
943	1640		47.6	3.1	1.18
944	1640		49.0	3.0	1.14
945	1800		51.0	4.6	1.75
946	1800		48.4	5.1	1.94
947	1800		48.6	5.0	1.90
948	2050		47.8	5.1	1.94
949	2050		47.6	4.9	1.86
950	2050		49.0	5.2	1.97
951	1960		47.0	3.1	1.18
952	1780		46.2	2.7	1.03
953	1630		48.0	2.7	1.03
954	1520		46.0	2.3	0.87
955	1370		47.4	2.3	0.87
956	1320		47.0	2.2	0.83
957	1190		47.0	1.9	0.72
958	1090		47.6	1.6	0.61
959	950		47.4	1.4	0.53

Table A.4.11. Duval type hysteresis curves for reaction in oxygen at 50μ pressure.

Filament No.43.

Filament initially reacted for a total of 15 mins at 910°C.

Run No.	T°C.	Secs. react	Initial pressure μ	Pressure CO μ	CO_2/CO ratio	Oxygen balance	$Rx10^8$	Total burn off $x10^7$
842	910	120	48.8	7.2	0.01	102	0.55	-
843	1530	15	49.2	3.2	0	98	1.95	2.92
844	1530	15	50.2	2.8	0	98	1.70	5.47
845	1530	30	49.9	5.0	0	99	1.52	10.7
846	1530	30	51.4	7.2	0	98	2.19	16.6
847	1530	30	50.4	10.2	0	97	3.10	25.9
848	1530	30	50.2	10.9	0.04	99	3.43	36.2
849	1530	30	51.4	12.6	0.02	97	3.89	47.9
850	1530	30	51.0	13.2	0.04	98	4.17	60.4
851	1530	30	51.0	13.7	0.08	97	4.50	73.9
852	1530	30	52.4	14.0	0.05	97	4.47	87.3
Filament reacted for a total of 10 mins at 930°C								
863	960	180	46.8	12.0	0.07	98	0.65	-
864	1350	15	48.0	4.3	0.12	99	2.92	4.4
865	"	"	48.8	5.4	0.08	98	3.53	9.7
866	"	"	48.6	6.2	0.03	98	3.89	15.5
867	"	"	49.8	6.9	0.04	98	4.38	22.1
868	"	"	49.7	7.8	0.08	98	5.11	29.7
869	"	"	48.0	7.6	0.01	98	4.69	36.8
870	"	"	49.4	8.3	0.04	98	5.23	44.6
871	"	"	50.4	8.3	0	98	5.05	52.2
872	"	"	52.0	8.8	0.01	98	5.41	60.3
873	"	"	48.8	8.4	0.01	98	5.17	68.1
874	"	"	49.2	8.6	0	98	5.23	75.9

Table A.4.11 (continued)

Run No.	T°C	Secs. react	Initial Pressure μ	Pressure CO μ	CO_2/CO ratio	Oxygen balance	$Rx10^8$	Total burn off $x 10^7$.
875	1680	15	50.8	5.6	0	96	3.41	81.1
876	"	"	50.9	4.8	0.08	97	3.16	85.8
877	"	"	51.4	5.0	0	99	3.04	90.1
878	"	"	49.6	4.4	0.09	107	2.92	94.5
879	"	"	48.6	4.5	0.02	98	2.80	98.7
880	"	"	48.8	5.2	0	96	3.16	103.4
881	"	"	50.8	4.9	0.04	99	3.16	108.1
882	"	"	52.2	5.0	0.08	98	3.29	113.1
883	"	"	49.4	4.9	0.06	99	3.16	117.8
884	"	"	52.7	5.0	0.04	98	3.16	122.6

Table A.4.12. Duval type hysteresis curves in oxygen at 50 μ. New pyrolytic filament.

Filament No.54.

Run No.	T°C	secs. react	Initial Pressure μ	Pressure CO μ	CO_2/Co ratio	Oxygen balance	Rx10^8	Total burn off x10^7
1175	1750	30	49.2	2.8	0.34	100	1.15	3.47
1176			51.2	3.3	0.24	100	1.25	7.2
1177			52.3	3.8	0.26	101	1.46	11.6
1178			52.0	4.0	0.17	101	1.43	15.9
1179			51.7	4.2	0.05	100	1.34	19.9
1180			51.4	4.6	0.02	100	1.43	24.2
1181	1100	15	49.6	12.5	0	101	7.60	35.6
1182			51.2	9.4	0.02	101	5.84	44.3
1183			52.6	6.1	0.07	101	3.95	50.3
1184			51.6	5.8	0.03	98	3.65	55.8
1185			52.5	4.3	0	97	2.61	59.7
1186			51.8	6.5	0.06	100	4.20	66.0
1187			49.8	5.7	0.09	100	3.77	71.6
1188			51.2	6.4	0.09	100	4.26	78.0
1189			52.2	5.9	0.12	98	4.01	84.1
1190			50.8	6.0	0	97	3.65	89.5
1191			49.6	7.2	0	98	4.38	96.1
1192			52.2	6.2	0	99	3.77	101.8
Filament heated in vacuum at 1100°C for 2 mins.								
1193	1100	15	50.8	5.0	0.08	100	3.28	106.7
1194			49.5	5.6	0	99	3.41	111.8
1195			50.0	6.5	0.01	100	4.01	117.8
1196			50.6	5.4	0	100	3.28	122.8
1197			49.2	5.4	0.11	100	3.65	128.2
1198		5	50.5	2.0	0.10	100	4.02	130.2
1199			50.6	2.3	0.13	100	4.75	132.6

Table A.4.12 (continued)

Run No.	T°C	secs react	Initial pressure μ	Pressure CO μ	CO_2/CO ratio	Oxygen balance	$Rx10^8$	Total burn off $x10^7$
Filament heated in vacuum at 1750°C for a total of 5 mins.								
1200	1100	5	48.1	1.2	0	102	2.19	133.7
1201			51.4	2.6	0	99	4.75	136.1
1202			52.0	2.0	0.10	100	3.65	137.9
1203			53.0	2.9	0.17	99	6.21	141.0
1204	1440	10	49.6	3.5	0	99	3.19	144.2
1205			50.4	4.5	0	99	4.11	148.3
1206			51.4	4.0	0.17	100	4.29	152.6
1207			50.2	5.0	0	99	4.56	157.2
1208			50.8	4.6	0	97	4.20	161.4
1209			50.0	4.2	0.14	100	4.38	165.7
1210			50.5	4.8	0.10	100	4.84	170.6
1211			51.0	5.4	0.09	100	5.38	176.0
1212			51.6	5.7	0.03	99	5.38	181.3
1213			51.7	5.8	0.05	100	5.57	186.9
1214			52.3	5.0	0.10	100	5.02	191.9
1215	1750	30	49.3	5.1	0.14	102	1.76	197.2
1216			47.6	5.8	0	100	1.76	202.5
1217			51.6	5.9	0	99	1.79	207.9
1218			50.0	5.6	0.05	101	1.79	203.3
1219	1380	10	49.2	6.2	0.03	100	5.84	219.1
1220			48.5	8.6	0.05	100	8.21	227.3
1221			50.0	8.2	0.02	100	7.67	235.3
1222			50.0	7.3	0	100	6.66	241.7
1223			50.2	5.9	0.03	100	5.57	247.2
1224			49.0	5.2	0.06	100	5.02	252.2
1225			51.1	5.7	0.02	100	5.29	257.6
1226			51.2	5.3	0	99	4.84	262.0

Table A.4.12 (continued)

Run No.	T°C	secs. react.	Initial pressure μ	Pressure CO μ	CO_2/CO ratio	Oxygen balance	$Rx10^8$	Total burn off $x10^7$
1227	1380	10	48.8	5.4	0.13	101	5.57	268.0
1228			50.2	5.6	0.11	101	5.66	273.6
1229	1000	10	50.0	3.3	0.18	101	3.56	277.2
1230			49.7	3.9	0	98	3.56	280.7
1231			52.0	3.5	0.03	101	3.29	284.0
1232			51.0	3.5	0.03	99	3.29	287.3

Table A.4.13.

Run No.	T°C	Initial pressure μ	Pressure CO μ	CO_2/CO ratio	Oxygen balance	$Rx10^8$	Total burn off $x10^7$
1252	850	49.2	0.7	0.09	98	0.099	1.19
1253		50.5	0.7	0.03	100	0.034	2.01
1254		50.5	1.8	0.22	100	0.084	4.02
1255		52.0	1.5	0.53	100	0.087	6.11
1256		49.4	1.5	0.33	100	0.076	7.94
1257	980	51.0	5.6	0.12	99	0.882	13.23
1258		52.7	5.5	0.04	99	0.866	18.44
1259		50.9	5.7	0.03	99	0.897	23.82
1260		50.7	6.3	0.03	100	0.988	29.95
1261		52.6	7.0	0.09	101	1.15	36.69
1262		53.2	7.0	0.06	99	1.12	43.44
1263		53.0	6.7	0.04	99	1.06	49.83
1264	1225	50.0	5.8	0.03	100	3.19	55.31
1265		51.3	8.3	0.02	100	3.88	63.07
1266		51.2	9.0	0.09	101	4.47	72.01
1267		50.9	8.9	0.03	99	4.20	80.41
1268		49.7	9.2	0.04	100	4.38	89.17
1269		52.7	9.4	0.08	100	4.65	98.48
1270		50.2	9.5	0.04	100	4.52	107.52
1271		51.3	9.4	0.05	101	4.52	116.55
1272	1290	51.6	7.0	0	97	4.26	122.94
1273		51.0	7.7	0	99	4.68	129.97
1274		52.0	7.4	0.07	100	4.80	137.18
1275		51.3	8.1	0.02	98	5.05	141.75
1276		51.7	8.1	0.04	98	5.11	152.42
1277		51.0	8.3	0.02	100	5.17	160.18
1278		51.6	8.1	0.02	99	5.05	167.75

Reaction at 850°C for 4 mins.
980°C for 1 min.
1225°C for 20 secs.
1290°C for 15 secs.

Table A.4.13 (continued)

Run No.	T°C	Initial pressure μ	Pressure CO μ	CO_2/CO ratio	Oxygen balance	$Rx10^8$	Total burn off $x10^7$
1279	1440	50.6	6.0	0.13	101	4.14	173.96
1280		50.8	6.7	0.07	99	4.38	180.53
1281		50.2	6.5	0.06	99	4.20	186.83
1282		51.8	7.7	0.05	100	4.93	194.22
1283		50.5	8.0	0.04	99	5.05	201.80
1284		51.6	7.8	0.03	99	4.87	209.10
1285	1500	51.8	6.9	0	98	4.20	215.40
1286		51.1	6.7	0.10	100	4.50	222.15
1287		51.3	7.0	0.03	98	4.38	228.54
1288		49.8	6.8	0.10	100	4.56	235.38
1289		50.0	6.0	0.05	98	3.83	241.13
1290		50.8	6.5	0.14	100	4.50	247.89
1291	1550	49.7	4.7	0.19	100	3.35	252.91
1292		50.4	4.6	0.17	100	3.28	257.84
1293		50.6	5.0	0.12	101	3.47	263.04
1294		49.5	4.8	0.08	100	3.16	267.79
1295		50.4	4.7	0.28	101	3.65	273.26
1296	1720	50.5	4.4	0.18	101	3.16	278.01
1297		51.0	3.8	0.26	101	2.92	282.39
1298		51.2	4.2	0.14	100	2.92	286.77
1299		51.2	3.8	0.10	100	2.55	290.60
1300		50.7	3.7	0.13	100	2.55	294.44
1301		50.8	4.2	0.10	101	2.80	298.63
1302		50.7	4.4	0.14	101	3.04	303.20
1303		50.3	4.5	0.13	100	3.10	306.03
1304		50.7	4.5	0.15	100	3.10	310.77
1305		50.7	4.4	0.14	101	3.04	315.34
1306	1850	51.3	4.4	0.11	100	2.98	319.81
1307		50.9	4.4	0	100	2.68	323.83

All reaction for 15 secs.

Table A.4.13 (continued)

Run No.	T°C	Initial pressure μ	Pressure CO μ	CO_2/CO ratio	Oxygen balance	R x10^8	Total burn off x10^7
1308	1850	50.6	3.7	0.05	100	2.37	327.38
1309		50.7	3.9	0.20	101	2.86	331.67
1310		51.3	4.0	0.25	101	2.28	336.24
1311		50.5	3.7	0.19	100	2.68	340.25
1312		50.3	4.2	0.10	100	2.80	344.45
1313		51.0	4.1	0	99	2.49	348.19
1314		51.4	4.0	0.10	100	2.68	352.21
1315	1660	51.1	3.8	0.10	99	2.55	356.04
1316		50.2	4.0	0.15	100	2.80	360.24
1317		50.4	3.6	0.11	101	2.43	363.89
1318		50.2	4.5	0.09	100	2.98	368.37
1319		50.5	5.1	0.10	100	3.35	373.37
1320		51.3	5.1	0.08	100	3.35	378.40
1321		50.4	5.3	0.09	100	3.53	383.70
1322		51.8	5.3	0.07	100	3.47	388.90
1323		50.8	4.5	0.22	101	3.35	393.92
1324		50.5	4.4	0.11	101	3.47	399.12
1325	1520	51.7	7.6	0.05	100	4.87	406.42
1326		50.7	8.1	0.09	99	5.35	414.46
1327		51.7	7.3	0.11	100	5.29	422.40
1328		51.5	7.5	0.12	100	5.11	430.06
1329		50.5	7.3	0.03	100	4.56	436.91
1330		51.0	7.1	0.08	100	4.68	443.93
1331		51.0	6.1	0.11	100	4.14	450.14
1332		49.5	6.2	0.11	100	4.20	456.64
1333		50.6	6.2	0.13	100	4.26	462.83
1334		51.7	6.0	0.12	100	4.08	468.94
1335	1330	50.4	10.8	0	100	6.57	478.80
1336		50.7	10.5	0.08	100	6.87	489.12
1337		49.6	8.2	0.08	101	5.41	497.24
1338		49.7	7.9	0.08	100	5.17	505.00

Table A.4.13 (continued)

Run No.	T°C	Initial pressure μ	Pressure CO μ	CO_2/CO ratio	Oxygen balance	$Rx10^8$	Total burn off $x10^7$
1339	1330	51.6	7.7	0.08	100	5.05	512.57
1340		52.0	7.8	0.05	100	4.99	520.06
1341		51.0	7.8	0.08	101	5.11	527.72
1342		50.4	7.1	0.04	100	4.50	534.48
1343		50.0	8.0	0.04	100	5.05	542.05
1344	1180	51.0	9.8	0.05	99	6.26	551.45
1345		51.4	8.0	0.05	100	5.11	559.12
1346		50.8	7.2	0.08	99	4.74	566.24
1347		49.3	6.0	0.08	99	3.95	572.17
1348		50.5	7.7	0	99	4.68	579.20
1349		49.8	7.2	0.10	100	4.80	586.41
1350		50.4	7.5	0.05	100	4.80	593.62
1351		49.0	7.1	0.03	99	4.44	600.28
1352		50.2	7.3	0.04	99	4.62	607.22
1353		50.0	7.3	0.08	101	4.80	614.43
1354	980	49.2	2.2	0	99	0.669	616.44
1355		48.7	2.5	0.08	100	0.821	618.90
1356		48.7	2.7	0.11	100	0.903	621.64
1357		49.6	3.6	0.17	100	1.28	625.47
1358		50.2	5.6	0.11	101	1.89	631.13
1359		49.3	7.0	0.04	99	2.22	637.79
1360		50.6	6.6	0.06	100	2.13	644.18
1361		50.4	6.3	0.02	100	1.95	650.02
1362		50.2	7.0	0.06	99	2.28	656.78
1363		51.5	7.6	0.13	100	2.62	664.63
1364		48.6	7.1	0.01	99	2.19	671.20
1365		50.6	8.7	0.08	99	2.86	679.78

Runs 1340-1353 reaction for 15 secs.
1354-1365 reaction for 30 secs.

Table A.4.14. Effect of increase burn off on rate of reaction in N_2O.

Filament 43. Previously reacted in oxygen, and degassed at at 1800°C by prolonged heating in vacuum.

Run No.	T°C	Initial pressure μ	Pressure CO + N_2 μ	R x10^{10}	Total burn off x 10^7
904	950	47.4	1.4	5.32	
905	1800	48.0	4.8	3.65	2.19
906		50.0	3.9	2.81	3.97
907		47.4	3.1	2.35	5.39
908		47.0	3.0	2.28	6.75
909		45.2	3.7	2.81	8.44
910		46.0	2.8	2.13	9.72
911		46.4	2.5	1.90	10.86
912		46.4	2.6	1.97	12.05
913		46.0	2.2	1.67	13.05
914		44.8	2.3	1.75	14.10

All reaction for 60 seconds except run 904 where reaction was for 120 seconds.

Filament No.43. Freshly coated, last treatment degassing at 2000°C.

All reaction at 1960°C for 2 minutes.

Run No.	Initial pressure μ	Pressure CO+N_2 μ	R x10^{10}	Total burn off x 10^7
1004	46.0	1.7	6.1	0.73
1005	50.0	1.7	6.5	1.51
1006	50.6	1.5	5.7	2.19
1007	49.2	1.4	5.3	2.83
1008	48.0	1.7	6.1	3.56
1009	49.0	1.6	6.1	4.29

Table A.4.15. Duval type hysteresis for CCl_4 pyrolytic carbon filament.

Filament burnt in 50μ of oxygen for 3' x 1 min. at 980°C following Run 1071.

Run No	Initial pressure μ	CO pressure μ	CO_2/CO ratio	Oxygen balance	R $x10^8$	Total burn off $x\ 10^7$
1072	50.8	6.0	0.17	100	4.27	6.39
1073	51.5	7.3	0.05	100	4.69	13.41
1074	53.3	7.3	0.12	101	4.93	20.81
1075	50.7	7.4	0.11	100	4.99	28.29
1076	49.0	7.4	0.10	100	4.93	35.69

All reaction for 15 seconds at 1550°C.

Table A.4.16 Effect of burning in oxygen then in Nitrous Oxide.

Filament 43. Last burnt in N_2O at 2010°C.

Reaction in oxygen at 1220°C for 60 seconds.

Run No.	Initial pressure μ	Pressure CO μ	CO_2/CO ratio	$Rx10^8$	Total burn off x 10^7	Oxygen balance
988	52.6	23.6	0	3.05	5.75	103
989	50.6	21.2	0	2.75	10.59	102
990	51.4	22.0	0	2.85	16.06	102
991	51.2	21.5	0	2.78	21.45	102
992	50.8	20.2	0	2.61	21.56	102
993	50.0	19.0	0	2.46	31.57	101
994	51.8	21.0	0	2.71	35.69	101
995	49.6	20.0	0	2.59	40.61	102

Reaction in N_2O for 120 seconds

Run No.	Initial pressure μ	CO + N_2 pressure μ	$R x10^9$	Total burn off x 10^7
996	48.4	1.6	0.51	0.727
997	48.8	1.5	0.49	9.41
998	53.2	2.8	0.91	2.69
999	45.2	1.6	0.51	3.42
1000	48.0	1.5	0.49	4.11

Filament burnt for a total of 210 min. in approx. 50μ of N_2O
8.73×10^{-5} g. atoms / cm^2 approx. burnoff. *

1001	45.0	2.8	0.91	

Filament burnt for a total of 120 min. in approx 50μ of N_2O
6.63×10^{-5} g. atoms / cm^2 approx. burnoff. *

1002	49.3	2.9	0.93	

* estimated.

Table A.4.17. Effect on reaction of alternatively burning filament in O_2 and N_2O.

Filament No.52.

Run No.	Initial pressure μ	Pressure CO μ	CO_2/CO ratio	Oxygen balance	$Rx10^8$	Total burn off x 107	
1099	53.8	23.4	0.08	101	1.91	23.0	
1100	51.3	13.1	0.12	101	1.12	36.4	
1101	47.1	-	-		1.14	50.1	O_2
1102	54.4	13.6	0.21	99	1.25	65.1	2 mins.
1103	54.0	12.6	0.33	102	1.27	80.4	at 970°C.
1104	49.3	12.3	0.39	103	1.30	96.0	
1105	52.5	12.7	0.39	101	1.34	112.1	
1106	53.5	9.3	0.45	101	4.11	124.4	
1107	54.7	12.4	0.35	101	5.11	139.7	
1108	48.8	13.2	0.26	100	5.05	154.9	O_2
1109	49.5	14.0	0.23	100	5.23	170.6	30 secs.
1110	47.6	13.8	0.19	100	4.99	185.5	at 1300°C.
1111	49.4	14.8	0.24	100	5.56	203.3	
1112	48.2	13.9	0.24	101	5.26	218.0	
1113	52.2	15.0	0.23	100	5.59	234.8	
1114	53.3	8.4	0.23	97	1.57	244.2	
1115	52.2	12.6	0.23	98	2.35	258.4	O_2
1116	51.2	12.2	0.26	101	2.34	272.4	60 secs.
1117	52.8	12.8	0.17	100	2.28	286.1	at 960°C
1118	51.3	11.6	0.31	100	2.31	300.0	
1119	51.3	11.2	0.34	100	2.28	313.7	

Table A.4.17 (continued)

Run No.	Initial pressure μ	$CO+N_2$ pressure μ	$Rx10^{10}$	Total burn off x10^7	
1120	47.6	1.76	6.67	315.28	
1121	46.2	1.44	5.47	316.61	
1122	50.2	1.51	5.74	317.98	
1123	47.3	1.44	5.47	319.29	N_2O
1124	46.7	1.61	6.12	320.77	4 mins.
1125	46.8	1.72	6.53	322.33	at 1300°C
1126	47.3	1.70	6.46	323.89	
1127	47.0	1.61	6.12	325.35	
1128	46.6	1.64	6.23	326.85	
1129	46.5	1.38	4.19	328.11	
1130	47.2	2.01	6.11	329.95	
1131	46.0	1.53	4.65	331.34	
1132	47.2	1.63	4.95	332.83	N_2O
1133	47.3	1.45	4.41	334.15	5 mins.
1134	50.8	1.55	4.71	335.57	at 970°C
1135	48.6	1.41	4.29	336.85	
1136	49.4	1.67	5.07	338.35	
1137	47.3	1.68	5.11	337.89	

Run No	Initial pressure μ	CO pressure μ	CO_2/CO ratio	Oxygen balance	$Rx10^8$	Total burn offx10^7	
1138	51.8	11.8	0.02	99	3.65	350.9	
1139	49.8	13.4	0.03	101	4.19	363.4	
1140	50.8	16.1	0.01	99	4.95	378.3	O_2
1141	53.4	17.0	0.01	99	5.20	393.9	30 sec
1142	53.0	16.4	0.02	100	5.11	409.3	at
1143	52.0	16.4	0.02	100	5.11	424.6	1300°C
1144	53.6	16.5	0	95	5.01	439.7	

Table A.4.17(continued)

Run No.	Initial pressure μ	CO_2+N_2 pressure μ	R x10^{10}	Total burn off x 10^7	
1145	50.8	1.60	4.87	441.10	
1146	50.0	1.29	3.92	442.28	
1147	47.5	1.34	4.07	443.50	N_2O
1148	47.0	1.27	3.86	444.66	5 mins.
1149	48.3	1.43	4.35	445.97	at
1150	51.0	1.53	4.62	447.36	970°C
1151	52.9	1.48	4.50	448.71	
1152	50.4	2.78	10.57	451.25	
1153	48.5	2.40	9.12	453.44	
1154	46.3	2.25	8.57	455.49	N_2O
1155	47.7	2.48	9.43	457.76	4 mins
1156	47.0	2.39	9.08	459.99	at
1157	47.5	2.23	8.47	461.97	1300°C
1158	52.5	2.45	9.31	464.21	
1159	46.0	2.22	8.43	466.23	
1160	47.4	2.29	8.70	468.33	

Run No.	Initial pressure μ	Pressure CO μ	CO_2/CO ratio	Oxygen balance	Rx10^8	Total burn off x 10^7	
1161	51.1	15.4	0.01	100	4.74	482.5	
1162	52.9	16.7	0.01	100	5.14	498.0	
1163	50.7	16.6	0.01	100	5.07	513.2	O_2
1164	50.8	16.2	0	101	5.05	528.4	30 secs
1165	51.3	17.7	0.01	99	5.44	544.7	at
1166	49.6	15.6	0.04	101	4.93	559.5	1300°C
1167	51.8	16.3	0.01	102	5.01	574.5	
1168	50.7	16.4	0.01	100	5.05	589.7	

Table A.4.17 (continued)

Run No.	Initial pressure μ	CO + N_2 pressure μ	R x10^{10}	Total burn off x 10^7	
1169	48.0	2.31	8.78	591.82	
1170	49.3	2.47	9.39	594.07	N_2O
1171	48.1	2.21	8.40	596.09	4 mins
1172	48.0	2.35	8.93	598.23	at
1173	47.0	2.31	8.75	600.34	1300°C
1174	47.2	2.31	8.75	602.45	

Table A.18

Run No.	Initial pressure μ	Pressure CO μ	CO_2/CO ratio	Oxygen balance	$Rx10^8$	Total burn off 10^7
At 950°C All reaction for 2 minutes except 1413 for 1 minute.						
1413 S	51.8	3.7	0	99	0.56	3.4
1414 S	52.6	8.7	0.01	100	0.67	11.4
1415 S	52.6	9.4	0.04	99	0.74	20.3
1416 S	52.2	8.8	0.11	99	0.74	29.3
1417 S	52.0	10.0	0.05	99	0.80	38.9
1418 S	52.8	10.6	0.04	100	0.84	48.4
1419 S	52.8	9.9	0.07	100	0.81	58.6
1420 S	51.0	7.7	0.16	101	0.68	66.7
1421 S	51.5	11.0	0.06	100	0.89	77.4
1422 S	51.0	11.0	0.03	100	0.86	87.7
1423 S	51.7	10.8	0.02	100	0.84	97.7
1424 S	50.8	11.8	0.06	102	0.95	109.2
1425 S	51.5	11.0	0.07	100	0.90	120.0
1426 S	50.8	No analysis				131.1
1427 S	53.4	12.1	0.04	99	0.96	142.6
1428 S	52.0	12.1	0.04	99	0.96	154.1
1429 S	52.6	11.7	0	100	0.89	164.8
1430 S	53.9	10.9	0.09	100	0.90	175.7
1431 S	52.6	12.1	0.07	101	0.98	187.5
1432 S	51.8	11.9	0.04	100	0.94	198.8
1433 S	50.2	No analysis				210.6
1434 S	52.2	12.1	0.07	100	0.98	222.3
1435 S	52.6	12.6	0.02	99	0.98	234.1

Table A.18 (continued)

Run No.	Initial pressure μ	Pressure CO μ	CO_2/CO ratio	Oxygen balance	$Rx10^8$	Total burn off x 10^7
<u>At 1270°C</u> All reaction for 30 secs. except 1436 for 15 secs.						
1436 S	51.7	5.2	0.06	100	3.34	239.1
1437 S	50.2	10.7	0	98	3.25	248.9
1438 B	52.2	14.4	0.06	101	4.62	262.8
1439 M	51.6	15.1	0	99	4.58	276.5
1440 M	52.0	14.6	0.05	102	4.65	290.5
1441 M	51.5	14.6	0.04	100	4.62	304.4
<u>At 950°C</u>. All reaction for 2 mins. except 1442 for 1 min.						
1442 B	52.0	9.2	0.07	100	1.49	313.3
1443 S	50.7	15.3	0.04	100	1.21	327.8
1444 S	51.0	11.7	0.03	100	0.92	338.9
1445 S	51.1	12.2	0.03	100	0.96	350.4
1446 S	51.2	13.0	0.04	101	1.03	362.7
1447 S	50.8	12.7	0.02	99	0.98	375.0
1448 S	51.4	13.0	0.04	100	1.03	387.3
1449 S	52.6	12.8	0.03	100	1.00	399.4
1450 S	50.0	13.2	0.02	99	1.03	411.7
1451 S	51.5	13.0	0.04	100	1.03	424.0
<u>At 1270°C</u>. All reaction for 30 secs except 1452 for 15 secs.						
1452 S	50.3	4.7	0.06	99	3.04	428.6
1453	52.0	10.9	0.07	99	3.56	439.3
1454 B	50.8	13.8	0.02	99	4.26	452.1
1455 M	50.5	14.3	0.03	99	4.47	465.5
1456 M	50.9	15.2	0.03	113 (Leak)	4.74	479.7
1457 M	51.9	14.0	0.03	100	4.65	493.7
1458 M	51.4	15.6	0	98	4.74	507.9
1459 M	51.3	14.9	0.05	100	4.74	522.2
1460 M	50.2	15.0	0.05	100	4.74	536.5

Table A.18 (continued)

Run No.		Initial pressure μ	Pressure CO μ	CO_2/CO ratio	Oxygen balance	$Rx10^8$	Total burn off x 10^7
At 950°C		All reaction for 2 mins. except 1461 for 1 min.					
1461	M	51.6	4.8	0.12	99	0.82	551.6
1462	B	50.0	16.2	0.02	99	1.26	567.3
1463	S	50.4	16.6	0.05	99	1.31	582.4
1464	S	51.4	15.7	0.05	100	1.25	596.4
1465	S	50.0	15.2	0.01	99	1.17	608.3
1466	S	50.0	12.5	0.04	99	0.99	620.2
1467	S	50.0	14.5	0.03	99	1.14	633.9
1468	S	50.4	14.9	0.02	99	1.15	647.7
1469	S	49.0	9.1	0.08	103	0.74	656.7
1470	S	50.0	13.6	0	101	1.03	669.1
1471	S	50.8	12.5	0.01	101	0.96	680.7
1472	S	51.2	13.0	0.01	100	1.00	692.7
1473	S	51.0	13.0	0.03	101	1.02	705.0
1747	S	50.1	13.2	0.03	101	1.03	717.4
1475	S	51.2	13.4	0.01	101	1.03	729.8
At 1270°C		All reaction for 30 secs except 1476 for 15 secs.					
1476	S	50.6	3.8	0.05	100	2.43	733.4
1477	S	49.8	8.1	0.05	101	2.59	741.2
1478	B	50.6	12.1	0.03	102	3.80	752.6
1479	M	50.6	12.0	0.02	100	3.74	763.8
1480	M	51.3	12.8	0.05	101	4.08	776.1
1481	M	49.4	12.3	0.08	100	3.77	787.4
1482	M	50.0	12.6	0.06	100	4.05	799.5
1483	M	50.3	No analysis				811.9
1484	M	49.7	13.4	0.05	101	4.29	824.8
1485	M	49.5	13.0	0.05	100	4.14	837.2
1486	M	50.8	14.0	0.04	101	4.26	850.0

Table A.18. (continued)

Run No.		Initial pressure μ	Pressure CO μ	CO_2/CO ratio	Oxygen balance	$Rx10^8$	Total burn off x 10^7
At 1270°C.							
1487	M	52.2	13.9	0.06	101	4.47	863.4
1488	M	51.7	No analysis				876.7
1489	M	49.4	14.0	0.04	100	4.44	890.0
1490	M	52.6	No analysis				903.4
1491	M	51.6	13.6	0.07	100	4.44	916.7

S = silvery filament
B = bronze filament
M = matt black filament
} after reaction

APPENDIX 5.

Experimental results on TREATED filaments not in main text.
(Graphs are before the Tables.)

GRAPH A.5.1 Rate-temperature curves for Amorphous Boron treatment

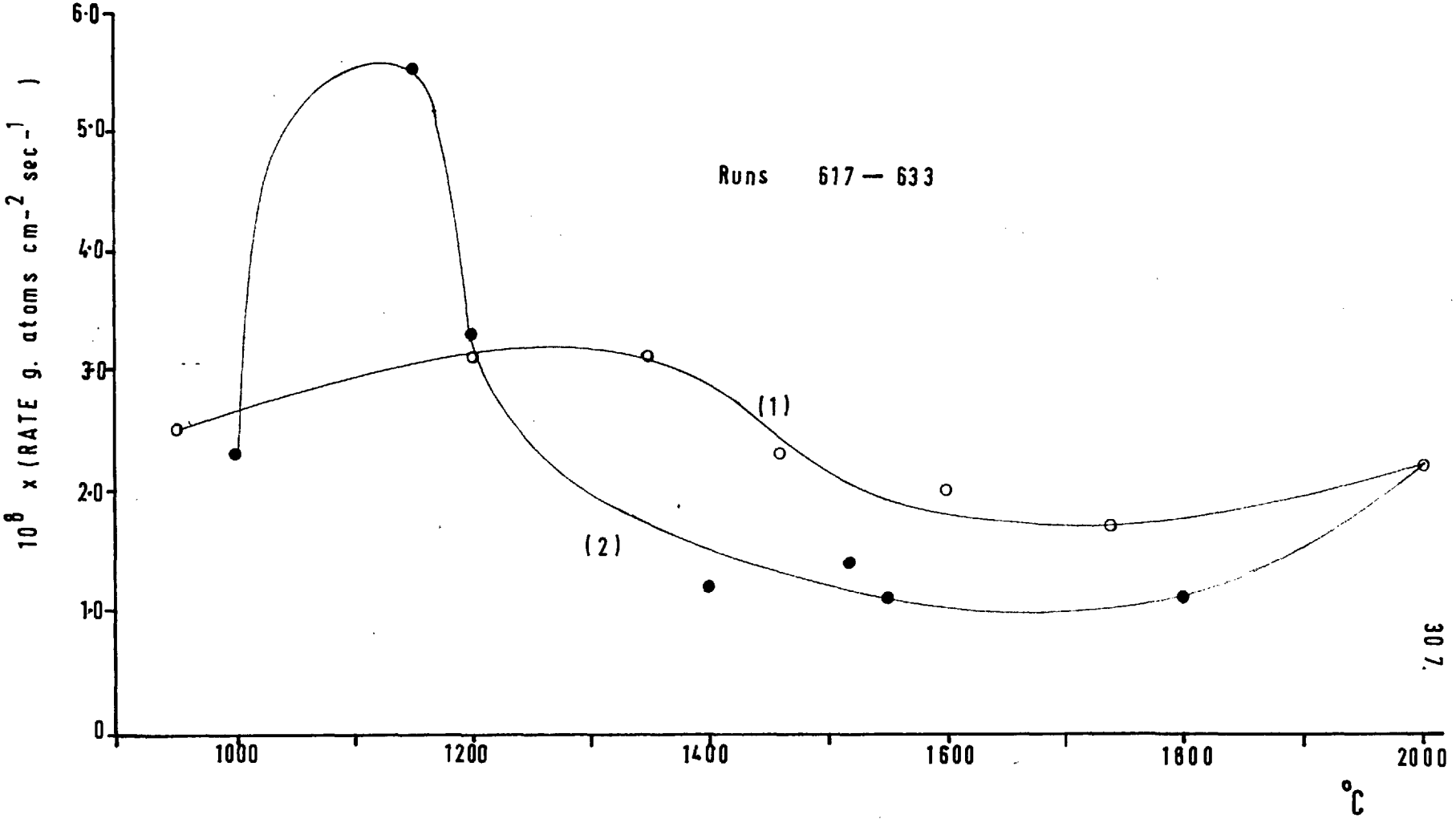

GRAPH A 5.2 Rate - temperature curves for Boric acid treatment

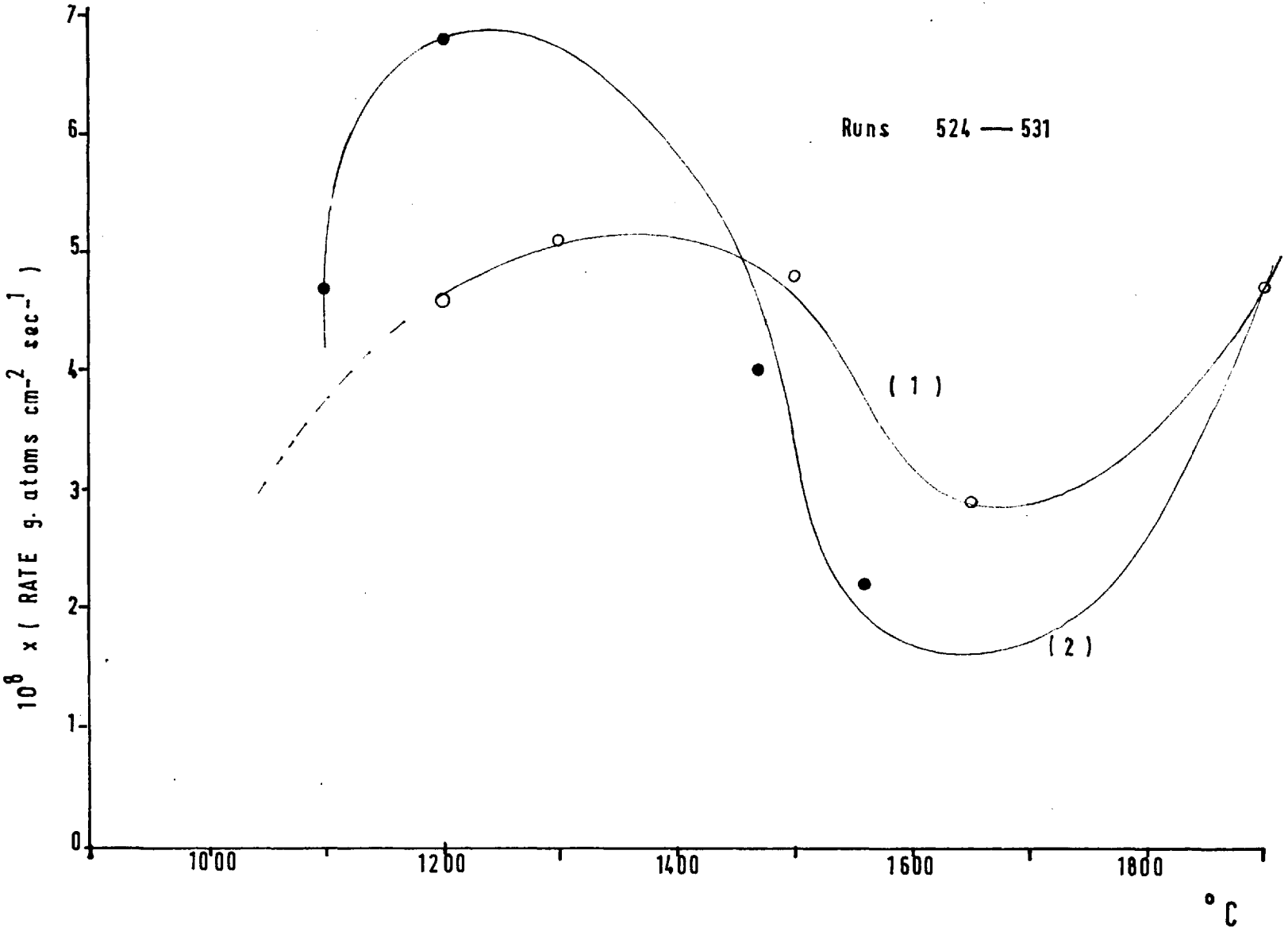

GRAPH A·5·3 Rate-temperature curves for a Silicon treated filament.

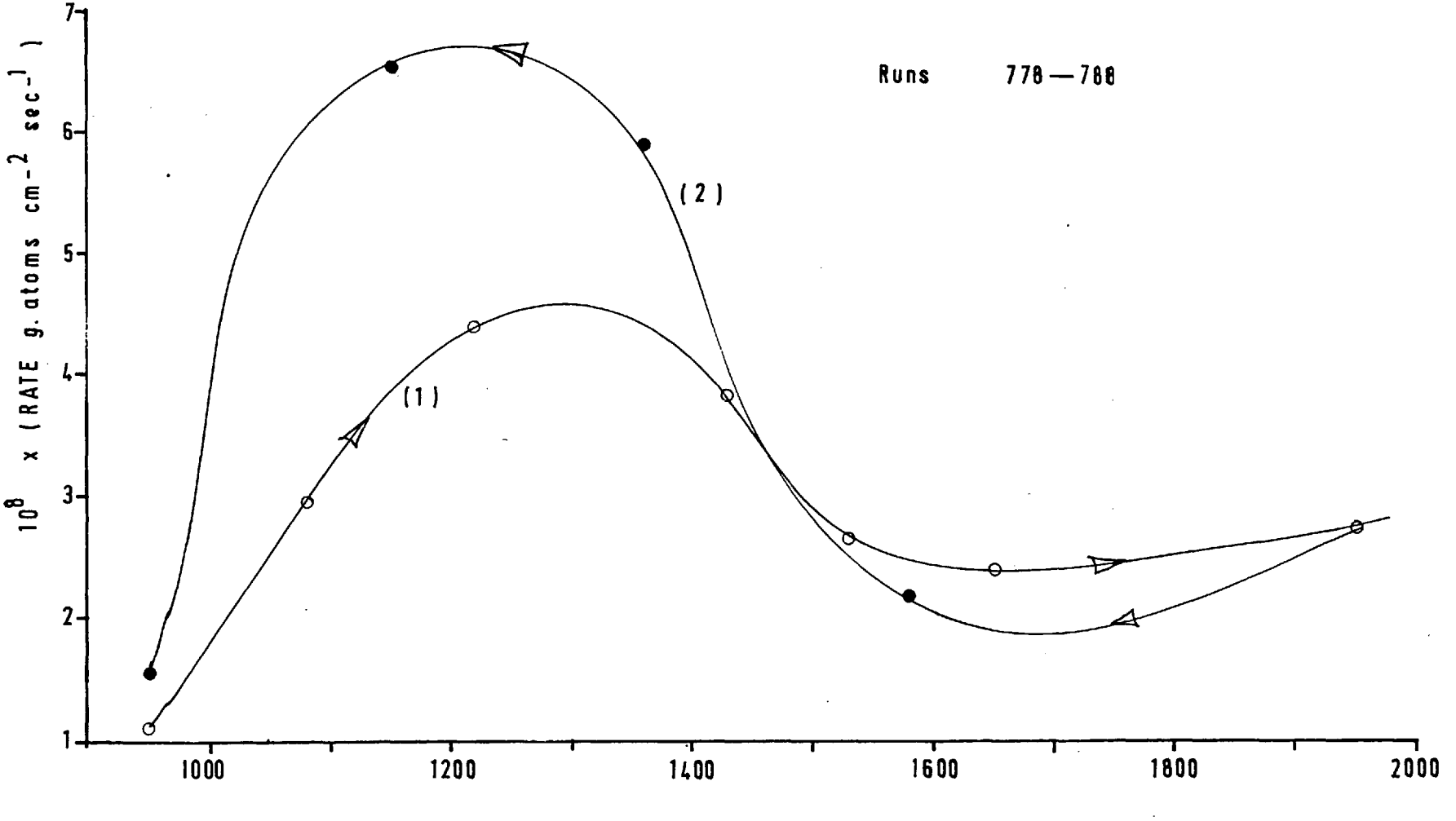

GRAPH A.5.4 Rate-temperature curves for a Zirconium treated filament.

NO Preheating at 2000°C

Runs 664—677

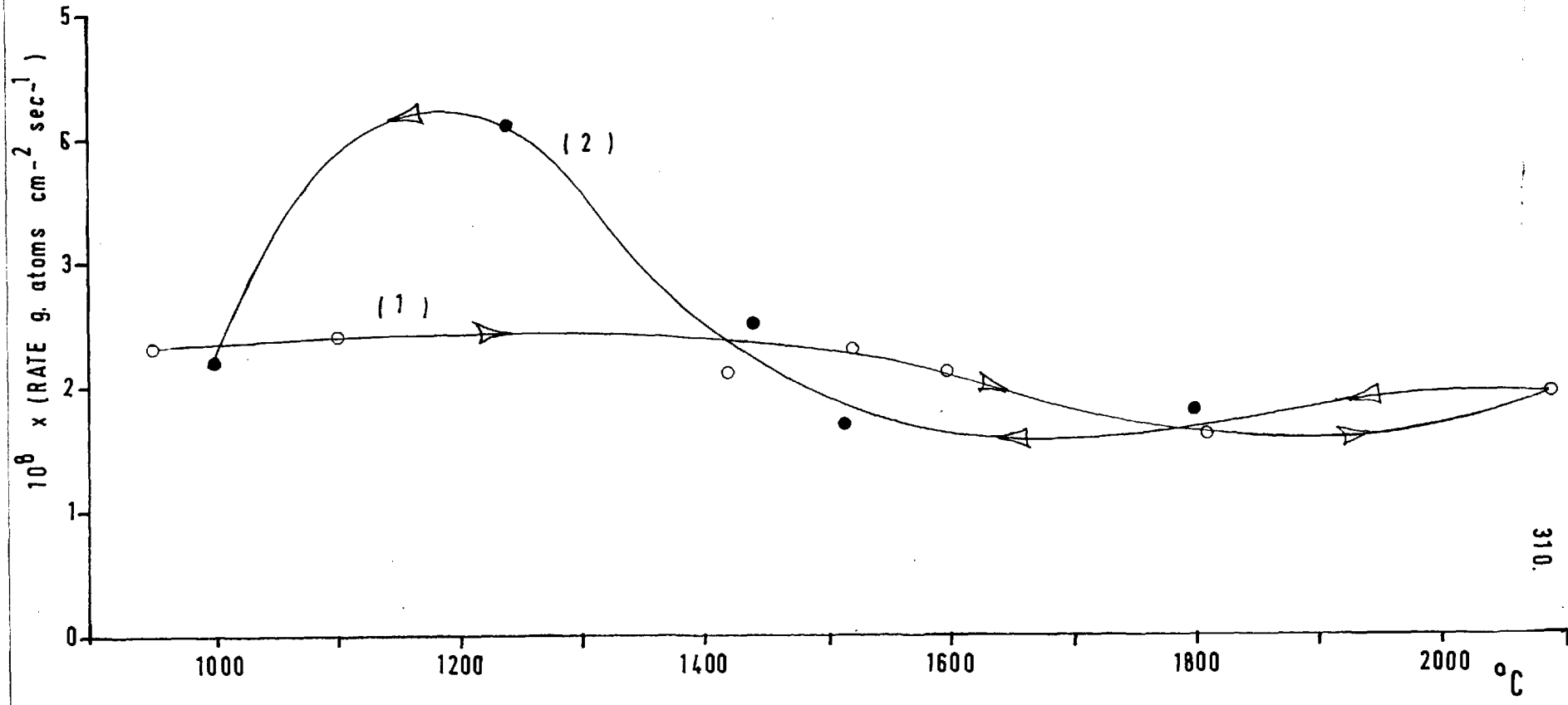

Table A.5.Q. Rate Runs at 1200°C in oxygen at 50μ pressure

Filament 4. Untreated filaments.

Run No.	T°C	Secs react	Initial Pressure μ	Pressure CO μ	R x10^8	Oxygen balance	CO_2/CO ratio
197	1200	30	50.5	11.7	3.74	101	0.05
198			52.8	12.7	4.11	99	0.06
199			50.8	12.8	4.17	100	0.07
200			50.4	12.4	3.98	100	0.04
201			53.2	12.9	4.14	101	0.06
202			50.8	9.4	2.98	101 Discounted	0.05
203			53.0	11.1	3.83	100	0.12
204			53.3	12.1	4.01	100	0.09
205			49.4	11.7	4.11	100	0.15
206			51.5	11.2	3.71	100	0.09
207			50.4	11.9	3.98	99	0.10
208			51.6	12.0	3.98	100	0.09
209			54.4	12.6	4.08	100	0.07
230	1800	60	53.6	16.5	2.80	103	0.11
231		60	49.8	15.5	2.69	103	0.15
232		60	53.5	17.3	3.02	102	0.15
233		30	53.4	8.6	2.98	101	0.14
234		30	50.4	9.0	2.89	103	0.05

Oxygen balance based on increase in pressure and CO formed.

Average rate: at 1200°C = 3.99 gr atoms/cm^2/sec

1800°C = 2.88

Table A.5.1. Zinc treated filament. Filament 11.

All reaction at 1200°C.

Run No.	Secs. react.	Initial pressure μ	Pressure CO μ	CO_2/CO ratio	R x 10^8	Oxygen balance
289	15	50.4	6.2	0.04	3.89	98
290	5	51.4	4.0	0.02	7.44	101
291	10	51.0	3.5	0.12	3.56	99
292	30	51.7	8.6	0.17	3.07	102
293	30	49.7	10.2	0.11	3.44	102
New carbon filament. Filament No.12. No previous burn off of filament						
294	30	47.8	6.5	0.02	1.99	99
295	30	50.7	11.6	0.05	3.53	99
296	30	47.4	12.5	0.25	3.80	97
297	30	52.2	14.1	0.23	4.29	98

For Runs 294-297 the pressure of CO was based on the increase in pressure due to the analysis by a Pt filament failing.

Table A.5.2. Filament 24.

Filament ~~treated~~ with boric acid from platinum filament.
Filament heated twice in 50μ of oxygen at 1200°C

Run No.	Initial pressure μ	Pressure CO μ	CO_2/CO ratio	Oxygen balance	R x10^8
Untreated filament					
532	49.0	14.3	0.03	98	4.5
Boric oxide heated on Pt filament for $2\frac{1}{2}$ minutes in vacuum					
533	48.5	15.4	0	97	4.7
534	48.4	12.7	0.02	98	3.9
535	48.4	13.7	0.02	97	4.3
Boric oxide heated on Pt filament for 3 mins in 50μ of oxygen					
536	49.7	12.8	0.04	99	4.1
Filament heated at 2000°C for 15 minutes in vacuum					
537	48.0	13.6	0.02	98	4.2
538	48.6	13.9	0.02	98	4.3

Table A.5.3. Filament heated with crystalline boron ground in a pestle and mortar.

Filament 20.

Run No.	Initial pressure μ	Pressure CO μ	CO_2/CO ratio	Oxygen balance	R $x10^8$
469	50.4	9.8	0.23	82	3.67
470	49.1	12.1	0.04	87	3.80
471	49.3	14.1	0.08	91	4.60
472	50.4	1.8	0.28	100	0.67
473	49.2	15.3	0.03	91	4.80
474	48.1	16.8	0.04	92	5.27
475	49.0	16.7	0.06	95	5.40
476	49.0	18.3	0	94	5.54
477	48.4	19.8	0.05	93	6.30
478	50.0	16.0	0.04	100	5.10
479	48.8	15.8	0.02	98	4.90
480	50.2	15.9	0.09	100	5.20
Filament heated at 2000°C for 5 minutes in vacuum					
481	49.7	16.0	0	97	4.9
482	49.6	18.5	0.01	97	5.7
483	48.0	19.1	0	96	5.8
484	49.8	20.2	0.01	97	6.2
485	49.4	17.7	0.03	98	5.5

All reaction for 30 seconds at 1200°C.

Table A.5.4. Filament 21.

Filament treated with crystalline boron suspension ground up in pestle and mortar. Filament first reacted twice.

Run No.	Initial pressure μ	Pressure CO μ	CO_2/CO ratio	Oxygen balance	$Rx10^8$	Total burn off $x10^7$
486	48.0	7.2	0.04	92	2.3	6.8
487	48.3	9.0	0.01	83	2.7	15.1
488	51.6	10.4	0.04	89	3.3	25.0
489	49.2	12.0	0.08	89	3.7	36.0
490	47.8	9.8	0.19	97	3.5	46.7
491	48.0	9.7	0.49	102	4.1	60.9
492	48.0	14.2	0.20	98	5.2	76.4
493	49.0	15.4	0.23	98	5.8	93.7
494	50.0	16.5	0.25	101	6.3	112.5
495	52.2	20.6	0.22	97	7.6	135.4
496	50.2	11.4	0.54	101	5.3	151.5
497	49.0	10.8	0.34	101	4.4	164.7
498	50.0	13.3	0.28	100	5.1	180.2
499	51.6	18.7	0.14	101	6.5	199.7
500	48.8	16.8	0.08	103	5.5	216.3

All reaction at 1300°C for 30 seconds

The following runs were carried out with a cold trap on the reactor

501	50.0	19.1	0.23	96	6.9	236.9
502	49.5	17.8	0.21	98	6.3	255.7

Table A.5.5. Filament 22.

Filament treated with boron hammered to pulverise.

Filament initially reacted three times in 50μ of oxygen at 1300°C for 30 seconds.

Run No.	Initial pressure μ	Pressure CO μ	CO_2/CO ratio	Oxygen balance	R x10^8
503	49.9	10.5	0.55	94	4.7
504	50.6	15.8	0.39	96	6.4
505	50.0	16.8	0.40	96	6.8
Filament heated at 2000°C for 15 minutes in vacuum					
506	46.4	21.7	0.03	93	7.1
507	48.4	19.1	0.01	96	5.9
508	49.6	16.2	0	97	4.9
509	50.4	17.1	0.02	96	5.3
510	49.8	16.2	0.05	98	5.2

All reaction at 1200°C for 30 seconds.

Table A.5.6. Filament 28.

Filament painted with suspension of amorphous boron.

Run No.	T°C	Initial pressure μ.	Pressure CO μ	CO_2/CO ratio	Oxygen balance	$Rx10^8$
617	1250	48.0	15.6	0	107	4.7
618	1250	50.0	11.4	0	108	3.9
619	1250	50.8	11.2	0	106	3.4
620	950	50.0	8.2	0.02	101	2.5
621	1200	47.8	10.0	0.02	101	3.1
622	1350	48.9	9.4	0.08	100	3.1
623	1460	48.0	7.0	0.09	100	2.3
624	1620	49.2	6.4	0.03	99	2.0
625	1840	47.6	5.2	0.08	100	1.7
626	2000	47.5	6.0	0.20	99	2.2
627	1800	48.4	3.4	0.06	99	1.1
628	1550	48.2	3.6	0	98	1.1
629	1520	49.7	4.6	0	99	1.4
630	1400	49.0	8.0	0.06	101	1.2
631	1200	50.2	10.5	0.29	106	3.3
632	1150	48.6	18.8	0.05	102	5.5
633	1000	48.0	7.1	0.07	101	2.3

All reaction for 30 seconds.

Table A.5.7. Filament 30A.

Filament painted with amorphous boron suspension and heated in vacuum at 2000°C for 30 minutes.

Run No.	T°C	Initial pressure μ	Pressure CO μ	CO_2/CO ratio	Oxygen balance	R $\times 10^8$
644	1200	49.0	10.5	0.02	97	3.3
645	1000	49.0	8.4	0	100	2.5
646	1000	51.6	8.2	0	101	2.5
647	1220	48.5	10.0	0.07	97	3.3
648	1350	49.4	8.4	0.04	85	2.7
649	1540	49.8	10.9	0.02	48	3.4
650	1710	50.7	9.0	0.09	41	3.0
651	2030	49.5	5.6	0.45	41	2.5
652	2010	49.5	4.5	0.08	96	1.5
653	1700	50.2	3.8	0.05	99	1.2
654	1530	48.6	7.1	0.10	100	1.5
655	1420	51.6	9.1	0.03	104	2.9
656	1260	50.0	14.9	0.02	112	4.6
657	1070	50.0	10.8	0.05	105	3.5
658	1000	49.5	6.6	0.03	102	2.1
659	1300	51.4	8.1	0.06	106	2.7
660	1460	51.0	6.9	0.06	103	2.2
661	1600	51.2	5.6	0.11	102	1.9
662	1720	51.4	5.1	0.02	101	1.6
663	2000	49.4	4.1	0.01	101	1.4

After Run 651 the filament was heated twice at 2030°C in 50 μ of oxygen for 30 seconds.

Table A.5.8. Filament 29.

Filament painted with amorphous boron suspension and then coated with pyrolytic carbon.

Run No.	T°C	Initial pressure μ	Pressure CO μ	CO_2/CO ratio	Oxygen balance	$Rx10^8$
634	950	46.7	3.8	0.05	97	1.2
635	1180	48.4	12.3	0.03	102	3.9
636	1300	49.5	12.2	0.01	104	3.7
637	1450	51.2	11.4	0.04	103	3.6
638	1660	50.7	9.4	0.03	102	2.9
639	1800	50.4	7.0	0.11	101	2.4
640	1600	49.6	12.1	0.03	103	3.8
641	1400	47.6	12.8	0.02	111	4.0
642	1150	48.9	14.6	0	113	4.5
643	1000	51.4	8.2	0.05	105	2.6

Table A.5.9. Filament 23.

Boric acid treated filament at increasing temperature

Run No.	T°C	Initial pressure μ	Pressure CO μ	CO_2/CO ratio	Oxygen balance	$R x10^8$
524	1300	49.0	14.5	0.15	101	5.1
525	1500	49.0	19.0	0.13	99	4.8
526	1650	47.4	8.4	0.12	99	2.9
527	1900	49.3	7.9	0.32	98	4.7
528	1560	48.8	6.4	0.14	98	2.2
529	1470	48.5	10.6	0.05	96	4.0
530	1200	50.4	22.0	0.01	100	6.8
531	1100	49.0	14.4	0.06	100	4.7

All reaction for 30 seconds except 527 which was for 20 secs.

Table A.5.10. Filament 26.

Rate-temperature runs for boric acid treated filament. Aqueous solution used, followed by heating filament in vacuum at 950°C for 45 minutes.

Run No.	T°C	Initial pressure μ	Pressure CO μ	CO_2/CO ratio	Oxygen balance	R x 10^8
580	970	50.3	7.1	0.07	96	2.3
581	1280	50.4	12.5	0.21	103	4.6
582	1420	50.9	13.3	0.24	104	4.3
583	1450	50.0	12.9	0.16	104	4.5
584	1600	50.5	10.5	0.11	105	3.5
585	1820	49.7	8.2	0.04	102	2.6
586	2000	49.5	8.9	0.16	96	3.1
587	1870	51.0	5.8	0.05	100	1.7
588	1600	50.2	8.0	0.04	102	2.5
589	1400	50.7	15.2	0.06	104	4.9
590	1200	50.0	40.8	0.01	104	12.7
591	950	49.5	11.1	0.01	105	3.4

Reaction for 30 seconds except Run 582 which was for 35 secs.

Table A.5.11. Filament 24.

Rate-temperature curve for filament painted with boric oxide suspension in acetone.

Filament heated at 1200°C in vacuum 4 times for 30 secs. each.

Run No.	T°C	Initial pressure μ	Pressure CO μ	CO_2/CO ratio	Oxygen balance	$Rx10^8$
547	1000	2.2	7.1	0.06	97	2.28
548	1170	4.0	11.3	0.03	97	3.53
549	1360	2.3	7.7	0.01	97	2.37
550	1520	4.9	12.5	0.04	97	3.83
551	2000	0.4	13.4	0.22	88	4.99
552	1680	2.0	4.6	0.13	99	1.58
553	1600	0.7	4.3	0.05	97	1.37
554	1450	2.0	5.6	0.11	98	1.89
555	1220	8.3	16.9	0.18	100	5.23
556	1090	11.9	22.3	0.27	102	6.66

All reaction for 30 seconds.

Table A.5.12. Silicon treated filament.

Filament No.37.

Run No.	T°C	Secs react.	Initial pressure μ	Pressure CO μ	CO_2/CO ratio	Oxygen balance	$Rx10^8$
770	1060	30	50.0	2.7	0.15	100	0.94
771	1060	60	50.6	8.9	0.11	99	1.51
772	1060	60	48.8	11.2	0.11	101	1.89
773	1600	5	49.0	3.0	0.20	73	6.58
774	1600	5	48.6	2.2	0.14	84	4.57
775A	1720	5	52.0	-	-	-	
775B	1720	10	51.8	2.2	0.27	99	2.55
776	1720	30	51.4	3.3	0.15	99	1.15
777	1720	60	50.0	6.4	0.25	102	1.21
778	950	60	51.5	6.8	0	98	1.07
779	1080	60	51.2	18.6	0.04	98	2.95
780	1220	30	48.5	14.0	0.03	97	4.38
781	1430	20	52.6	8.1	0.04	97	3.83
782	1530	30	48.3	7.5	0.16	101	2.65
783	1150	30	50.8	6.8	0.16	100	2.40
784	1950	35	49.0	8.3	0.26	102	2.73
785	1580	20	50.4	6.8	0.06	95	2.19
786	1360	30	52.6	18.6	0.03	98	5.90
787	1150	30	48.8	21.4	0.01	97	6.53
788	950	60	50.8	9.6	0.05	98	1.53

Table A.5.13. Tungsten treated. Filament 14.

All reaction at 1200°C for 3 secs. except 318 which was for 5 seconds.

Run No.	Initial pressure	Pressure CO μ	CO_2/CO ratio	Oxygen balance	R x10^7
W filament at 1500°C while reacting.					
305	55.4	10.4	0.05	100	3.8
306	54.5	11.3	0.09	97	4.6
307	54.0	14.6	0.04	85	3.0
W filament not on.					
308	51.0	9.0	0.10	103	3.0
309	55.2	9.4	0.04	100	2.9
310	57.6	9.0	0.06	101	2.9
311	48.6	1.9	0.28	107	0.7
312	54.5	7.1	0.07	102	2.3
313	54.0	2.4	0.17	104	0.8
314	51.2	7.8	0	101	2.4
W filament at 2000°C for 15 secs. in 50μ oxygen before runs.					
315	53.4	13.4	0.03	96	4.2
316	55.2	10.2	0.19	98	3.4
317	53.4	9.3	0.02	97	2.9
318	53.2	15.4	0.03	98	4.8
319	54.4	10.6	0.12	96	3.6
320	52.6	14.3	0.02	90	4.4
321	55.4	10.7	0.04	95	3.4
322	50.3	9.6	0.07	96	3.1
323	49.7	10.4	0.04	95	3.3
324	48.8	10.5	0.05	95	3.3
Filament heated in vacuum and then retreated with W					
325	55.4	10.4	0.03	98	3.2

Table A.5.14. Tungsten treated filament.

Tungsten wire heated in 50μ of oxygen. Filament 16.

Run 360 untreated filament.

Run No.	Secs. react.	T°C	Initial pressure μ	Pressure CO μ	CO_2/CO ratio	Oxygen balance	R x10^8
360	30	1200	46.0	9.41	0.11	98	3.13
361	15	800	49.0	-	-	-	-
362	10	1200	47.8	-	-	-	-
363	10	800	49.4	2.4	1.12	100	1.53
364	5	900	46.7	10.0	0.41	104	4.27
365	30	1000	46.7	9.6	0.22	100	3.53
366	11	1200	49.6	13.4	0	95	4.07
367	5	1400	50.6	5.9	0.20	96	2.13
368	6	1600	47.4	3.7	0.43	101	1.60
369	30	1800	49.6	6.0	0.02	98	1.87
370	10	1600	50.0	5.2	0	96	2.27
371	20	1400	45.4	8.2	0.05	96	3.93
372	30	1200	46.0	12.0	0	97	3.87
373	30	1000	46.2	5.0	0	100	1.73
374	300	800	49.5	0.9	0.9	101	0.51

Table A.5.15. Tungsten treated.

Filament coated between runs. Filament 16.

Run No.	T°C	$S_e$cs. react	Initial pressure μ	Pressure CO μ	CO_2/CO ratio	Oxygen balance	Rx10^8
375	800	600	48.6	1.8	0.33	98	0.37
376	1000	300	46.6	10.9	0.03	99	1.07
377	1200	5	46.8	9.0	0.07	100	17.5
378	1400	5	48.5	11.0	0.13	99	22.7
379	1600	5	49.6	11.4	0.09	98	22.7
380	1800	5	47.6	11.2	0.01	98	23.0
381	1600	5	45.3	18.4	0.05	98	35.5
382	1400	3	48.6	20.6	0.05	97	66.0
383	1200	3	49.5	12.2	0.05	98	38.9
384	1000	5	49.0	2.5	0.64	101	7.5
385	800	5	48.2	1.5	0.80	100	0.08

Table A.5.16. Tungsten treated.

Filament heated at 1800°C between reaction at 1200°C for 3 seconds.

Filament 16.

Run No.	Secs heating at 1800°C.	Initial pressure	Pressure CO μ	CO_2/CO ratio	Oxygen balance	$Rx10^7$
387	60	54.8	26.5	0.01	96	8.14
388	15	46.3	10.0	0	96	3.04
389	15	46.4	7.1	0	95	2.16
390	15	46.8	6.5	0.37	98	2.71
391	15	51.0	9.1	0.01	95	2.79
392	15	52.3	12.7	0.09	98	4.19
393	15	48.0	12.0	0.08	94	3.68
394	15	45.5	11.0	0.07	96	3.59
395	-	54.2	15.6	0.03	96	4.90
396	-	49.5	11.6	0.10	98	3.89
397	-	53.4	12.8	0.07	98	4.17

Run No.	Burn off gr atoms/cm^2
387	24.2 x 10^7
388	33.3
389	39.8
390	45.7
391	54.0
392	65.6
393	76.6
394	86.6
395	100.8
396	111.4
397	128.0

Table A.5.17. Tungsten treated.

Order runs at 1200°C for 3 seconds. Filament 16.

Run No.	Initial pressure μ	Pressure CO μ	CO_2/CO ratio	Oxygen balance	R x10 ^{8}
398	14.45	8.0	0.14	101	27.7
399	25.5	4.5	0.04	100	14.3
400	65.7	12.6	0	98	38.3
401	99.5	14.5	0.08	99	47.4
402	136.5	18.5	0	98	56.3
403	169.5	13.5	0.09	100	44.7
404	207.25	17.0	0.08	100	55.6
405	120.75	9.5	0.04	99	29.9
406	72.3	7.2	0.01	98	22.2
407	23.65	30.5	0.05	94	9.7
408	49.4	2.7	0	98	10.7
409	47.2	2.4	0.29	100	9.4
Filament heated at 1800°C for 15 seconds					
410	48.9	1.2	0.33	97	4.9
411	51.1	3.2	0.12	99	10.9
412	48.8	3.9	0.03	98	11.5

Table A.5.18. Mo Vacuum deposited runs.

Series 1. Mo oxides evaporated onto filament prior to each run.

Run No.	T°C	Secs. react.	Initial pressure μ	Pressure CO μ	CO_2/CO ratio	Oxygen balance	$Rx10^8$
1514	1000	15	48.9	13.8	0.01	100	8.52
1515	1120	10	50.5	23.5	0.04	101	22.3
1516	1240	15	50.4	27.0	0.01	101	16.7
1517	1450	10	51.0	16.4	0.02	101	15.3
1518	1570	10	49.2	9.4	0.04	99	8.94
1519	1680	15	49.6	8.5	0.06	102	5.47
1520	1790	15	49.4	11.5	0.04	100	7.30
1521	2000	15	51.5	7.6	0.12	100	5.17
1522	2000	15	51.4	6.1	0	99	3.71
1523	1780	15	50.4	6.2	0.06	99	4.01
1524	1650	15	51.3	9.8	0.06	105	6.33
1525	1480	10	49.8	15.1	0.04	100	14.2
1526	1360	10	51.5	33.0	0.03	103	30.9
1527	1170	10	50.0	37.0	0.02	104	34.4
1528	1000	15	50.5	32.8	0.02	102	20.3
1529	1000	12	50.0	23.3	0.04	102	18.5
1530	1220	10	51.7	31.9	0.03	105	30.0
1531	1390	10	49.8	24.0	0.02	103	22.4
1532	1530	10	52.0	15.4	0.04	100	14.6
1533	1690	15	51.5	11.2	0.04	100	7.06
1534	1900	15	50.3	6.9	0.10	100	4.62
Series 2. No treatment prior to Runs.							
1535	1900	20	49.5	4.8	0.10	100	2.37
1536	1720	20	48.0	5.2	0.08	100	2.51
1537	1550	20	48.0	5.5	0.06	103	2.60
1538	1400	20	47.8	18.5	0.04	102	8.76

Table A.5.18 (continued)

Run No.	T°C	Secs. react.	Initial pressure μ	Pressure CO μ	CO_2/CO ratio	Oxygen balance	$Rx10^8$
1539	1180	15	48.8	26.6	0.04	104	16.5
1540	1050	15	50.3	26.3	0.02	101	16.2
1541	980	20	51.5	13.3	0.01	101	6.39
1542	1080	15	51.0	18.4	0.05	99	11.5
1543	1230	15	49.5	16.0	0.03	99	9.98
1544	1430	15	50.8	8.1	0.04	101	5.11
1545	1640	20	48.6	5.9	0.07	100	2.87
1546	1950	15	51.4	3.8	0.18	99	2.74
1547	1750	15	50.1	3.8	0.16	101	2.68
1548	1520	15	50.7	5.5	0.11	100	3.71
1549	1430	15	52.2	6.6	0.06	101	4.21
1550	1300	15	50.6	11.4	0.02	101	7.06
1551	1100	15	49.2	11.0	0.06	101	7.06
1552	990	20	51.5	11.0	0	102	5.02
Series 3. Mo oxides evaporated onto filament prior to each run, and filament then heated to 1500°C in vacuum							
1553	980	15	48.8	17.7	0.04	99	11.2
1554	1100	10	49.4	35.7	0.03	102	33.7
1555	1260	10	51.0	51.8	0.01	101	47.9
1556	1350	10	50.0	52.2	0.01	101	48.4
1557	1510	10	50.5	46.0	0.03	101	43.1
1558	1620	5	49.8	25.0	0.01	99	46.0
1559	1750	5	49.8	18.6	0.02	99	34.7
1560	1910	5	49.6	13.0	0.03	100	24.5
1561	1930	5	49.4	10.8	0.05	102	20.8
1562	1780	5	48.8	16.7	0.02	100	31.2
1563	1610	5	50.6	28.9	0.01	99	55.0
1564	1500	5	50.0	36.2	0.05	104	107
1565	1350	3	49.6	34.9	0.03	101	109

Table A.5.18 (continued)

Run No.	T°C	Secs. react.	Initial pressure μ	Pressure CO μ	CO_2/CO ratio	Oxygen balance	$Rx10^8$
1566	1120	3	48.9	15.2	0.03	99	47.4
1567	990	10	51.0	26.0	0.04	101	24.7
1568	1020	10	49.2	28.6	0.02	101	26.6
1569	1120	3	49.1	14.0	0	99	42.6
1570	1300	3	50.4	26.6	0.02	101	82.7
1571	1480	3	50.2	36.7	0.02	101	113.
1572	1580	6	49.0	30.2	0.01	100	68.4
1573	1800	6	51.0	22.2	0.01	101	50.6
1574	2000	10	50.8	12.8	0.03	100	12.0
Series 4. No treatment prior to Runs.							
1575	2000	10	49.8	11.8	0.02	99	10.9
1576	1750	10	50.2	28.6	0.01	101	26.3
1577	1630	3	51.8	27.3	0.02	102	84.6
1578	1510	3	50.3	37.5	0	100	115
1579	1310	3	50.2	36.4	0.01	103	112.
1580	1130	5	52.0	32.4	0.01	101	59.9
1581	980	10	52.2	22.2	0.01	98	20.4
1582	1170	3	49.7	17.3	0.01	99	52.9
1583	1390	3	49.5	23.6	0.02	105	73.0
1584	1510	3	48.0	23.5	0	102	71.5
1585	1610	3	49.8	15.3	0.03	100	48.1
1586	1720	3	49.8	17.0	0.02	99	52.9
1587	2010	10	50.0	10.0	0.06	100	5.11

Table A.5.19. Zirconium Runs.

Filament No.30B.

Run No.	T°C	Secs react.	Initial Pressure μ	Pressure CO μ	CO_2/CO ratio	Oxygen balance	$Rx10^8$
664	1060	30	49.2	6.7	0.06	103	2.1
665	950	30	50.0	6.2	0.21	80	2.3
666	1100	30	48.9	6.6	0.18	101	2.4
667	1420	30	51.0	6.8	0.03	99	2.1
668	1420	30	50.2	7.1	0.17	102	2.5
669	1520	30	51.1	6.9	0.07	100	2.3
670	1600	30	51.4	6.3	0.13	101	2.1
671	1810	30	53.0	4.7	0.13	100	1.6
672	2150	30	49.8	5.2	0.21	101	1.9
673	1800	30	51.4	5.5	0.07	100	1.8
674	1520	30	52.4	5.3	0.08	101	1.7
675	1440	30	48.8	8.1	0.02	101	2.5
676	1240	30	53.0	13.1	0.03	112	4.1
677	1000	30	49.1	6.4	0.16	105	2.2

Table A.5.20. N_2O catalyst runs. Uranium trioxide treated filament No.47.

Run No.	T°C	Secs. react	Initial pressure μ	Pressure CO μ	Oxygen balance	N_2 balance	$Rx10^8$	N_2/CO ratio
1029	1850	15	46.2	3.2	98	103	1.95	1.87
1030	1850	30	45.0	5.6	91	103	1.70	1.4
1031	1850	30	46.4	4.2	97	101	1.27	1.6
1032	1850	30	48.8	3.2	97	102	0.97	1.9
1033	1850	30	51.8	3.3	98	101	1.00	1.6
1034	1720	30	49.6	1.7	95	102	0.52	3.2
1035	1560	30	48.6	4.1	97	101	1.25	1.6
1036	1450	30	50.0	10.2	94	102	3.10	1.4
1037	1340	30	49.8	15.2	97	105	4.68	1.2
1038	1100	30	52.0	1.0	95	100	0.42	5.0
1039	950	30	51.4	0.6	96	99	0.24	5.0
1040	1090	30	50.8	1.3	95	99	0.52	3.6
1041	1330	15	50.6	19.2	97	102	11.7	1.2
1042	1710	35	49.2	21.3	99	103	5.76	1.2
1043	1500	30	46.8	15.6	97	105	4.74	1.3
1044	1640	30	47.0	11.0	95	99	3.35	1.2
1045	1770	30	48.6	11.4	101	103	3.47	1.2
1046	1920	30	47.0	8.7	99	101	2.71	1.3

Table A.5.21. Platinum. Rate-Temperature Runs.

Run No.	T°C	Secs. react.	Initial pressure μ	Pressure CO μ	CO_2/CO ratio	Oxygen balance	$Rx10^8$
1366	1130	10	48.3	8.7	1.29	99	18.2
1367	900	10	49.2	1.8	4.55	99	9.13
1368			49.1	1.1	6.30	100	7.30
1369			50.2	1.2	5.17	100	6.75
1370			51.2	1.6	3.37	100	6.39
1371			50.6	1.4	3.71	101	6.02
1372	1030	5	40.9	3.8	1.68	97	18.6
1372	1230		50.7	22.1	0.64	116	66.1
1374	1360		51.2	23.2	0.21	102	51.5
1375	1290		50.0	21.1	0.75	100	48.2
1376	1530		51.0	17.8	0.21	102	39.3
1377	1620		51.2	10.6	0.21	101	23.4
1378	1700		51.1	9.6	0.06	98	18.6
1379	1700		49.0	6.0	0.10	100	12.1
1380	1880		50.3	3.7	0.08	100	7.31
1381	2030		49.8	14.4	0.50	60	39.5*
1382	2030		51.0	13.0	0.63	75	38.7*
1383	1860		49.8	3.6	0	100	6.58
1384	Not done						
1385	1700		49.4	3.4	0.06	100	6.58
1386	1520		49.8	3.8	0.10	101	7.67
1387	1370		50.8	5.8	0.03	99	11.0
1388	1280		51.7	9.4	0.02	99	17.5
1389	1100		50.0	11.0	0.05	99	21.2
1390	980	10	50.8	8.4	0.11	99	8.49
1391	900		50.0	2.3	0.09	100	2.28
1392	1040	5	51.4	6.5	0.03	99	12.2
1393	1290		49.8	12.0	0.08	100	22.1
1394	1460		51.5	7.1	0.04	100	13.5
1395	1630		50.7	5.0	0.04	100	9.50
1396	1800		52.0	3.6	0.05	99	6.09

* Glow discharge

APPENDIX 6.1. CALCULATION OF EXPERIMENTAL STEADY SITE DISTRIBUTION AT 50μ.

For the purposes of determining the variation of the equilibrium site concentration n/n_{ref} with temperature the results obtained on the single filament, No.56, were used. Results obtained on different filaments did not show good reproducibility.

The method of obtaining n/n_{ref} was based on the equation used by Duval[3] rate = r.n where r is the fundamental rate of reaction.

If T_1 is the previous temperature of reaction, at a temperature T_2 the initial rate at zero time will be characterised by a site concentration n_1, where n_1 is the equilibrium site concentration corresponding to T_1. When equilibrium site concentration is reached at T_2, the surface will be characterised by a site concentration n_2.

Hence Initial rate = $r.n_1$

Final rate = $r.n_2$

Therefore

$$\log(n_2/n_1) = \log(\text{Final Rate}) - \log(\text{Initial Rate}) \quad [1]$$

Also it follows if equilibrium conditions are reached

$$n_3/n_1 = n_3/n_2 \cdot n_2/n_1 \quad [2]$$

and

$$-\log n_2/n_1 = \log n_1/n_2 \quad [3]$$

The values of R were obtained from Table A.4.13 and the

logarithms plotted against time of reaction. These plots are shown in Graphs A.6.1 to A.6.3. The results going from 1180°C to 980°C were not plotted as the filament showed abnormal behaviour (Section 4).

From these graphs $\log(n_2/n_1)$ was obtained by extrapolating back to zero time to get the initial rate. Then using equations [2] and [3] values of $n/n_{980^\circ C}$ were obtained at various temperatures as shown on Graph 6.1. The calculation of $n/n_{980^\circ C}$ is shown in Table A.6.1.

From the curve on Graph 6.1 the values of $n/n_{1150^\circ C}$ were obtained which were used in Section 6.

The accuracy of the $\log_{10} n/n_{850}$ curve shown on Graph 6.1 depends largely on the accuracy of the initial rate, which in turn is largely governed by the first rate determined.

For example considering reaction at 1225°C after 980°C. Graph A.6.1. The rate after 15 seconds was 3.19×10^{-8} If this was 10% too high, i.e. the rate was 2.87×10^{-8}, $\log_{10}R = 8.4579$. This point, X, is shown on the graph and gives a value of $\log_{10}R_{initial}$ of 8.320.

Hence $\log n_{1225}/n_{980}$ now = 0.330 as against 0.235 before, which is an error of near 30%. An initial error, therefore, in the first rate determined experimentally, is increased by a factor of about 3 when calculating the site concentration curve.

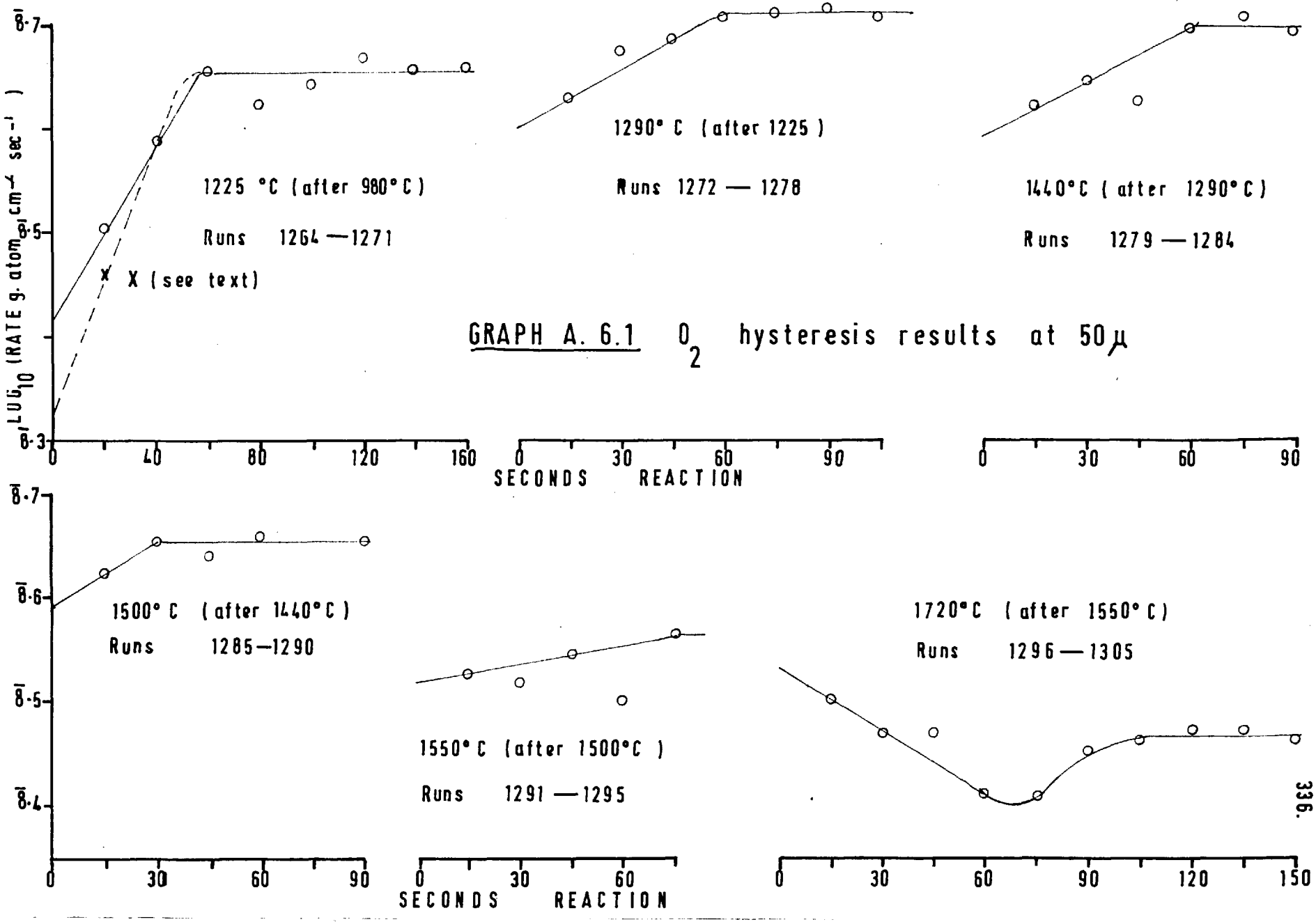

GRAPH A. 6.1 O_2 hysteresis results at 50μ

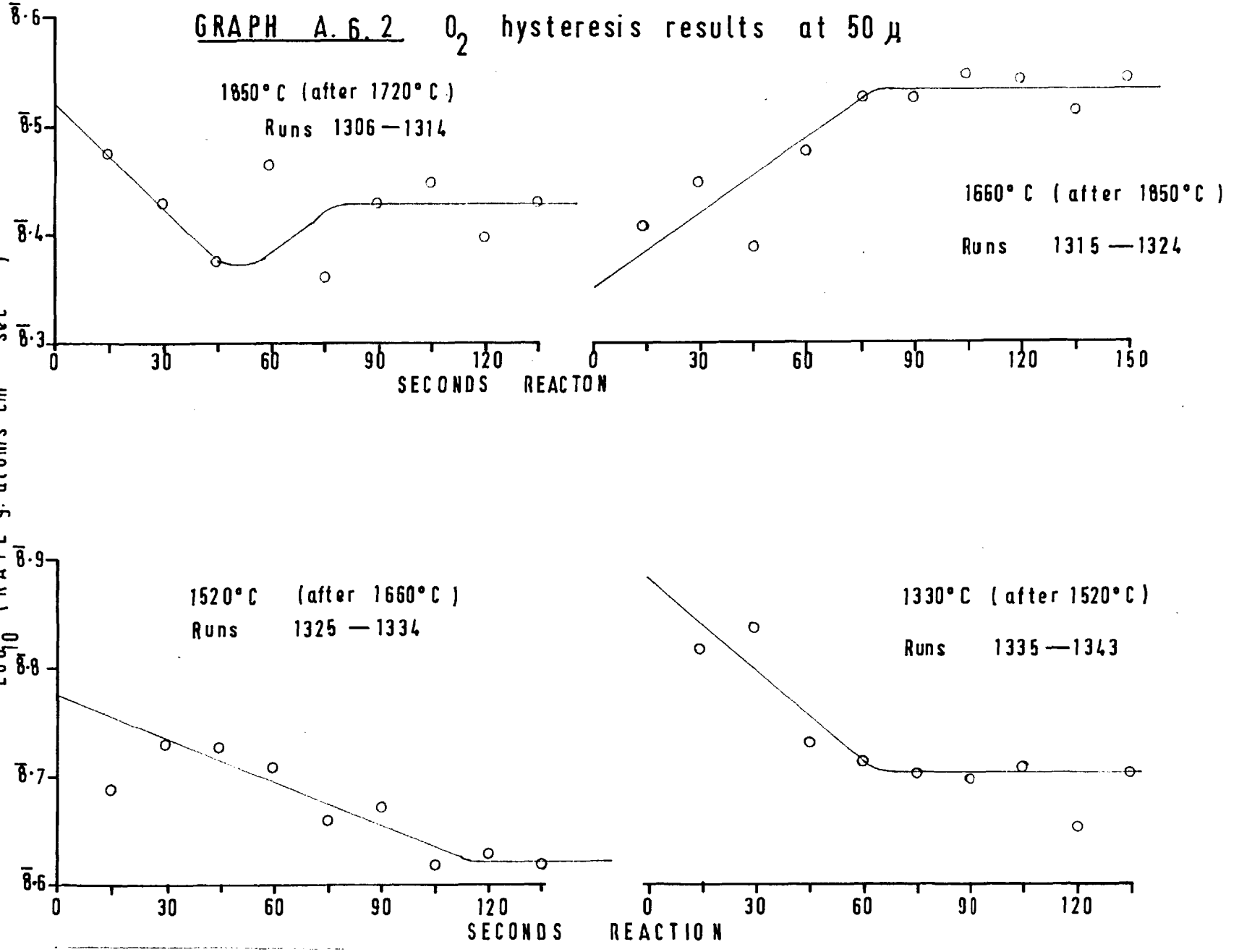
GRAPH A.6.2 O_2 hysteresis results at 50 μ
1850° C (after 1720° C)
Runs 1306 — 1314
1660° C (after 1850° C)
Runs 1315 — 1324
1520° C (after 1660° C)
Runs 1325 — 1334
1330° C (after 1520° C)
Runs 1335 — 1343
LOG10 (RATE g. atoms cm-2 sec-1)
8·6
8·5
8·4
8·3
8·9
8·8
8·7
8·6
0
30
60
90
120
150
SECONDS REACTON
SECONDS REACTION

GRAPH A.6.3 O_2 hysterisis results at 50μ

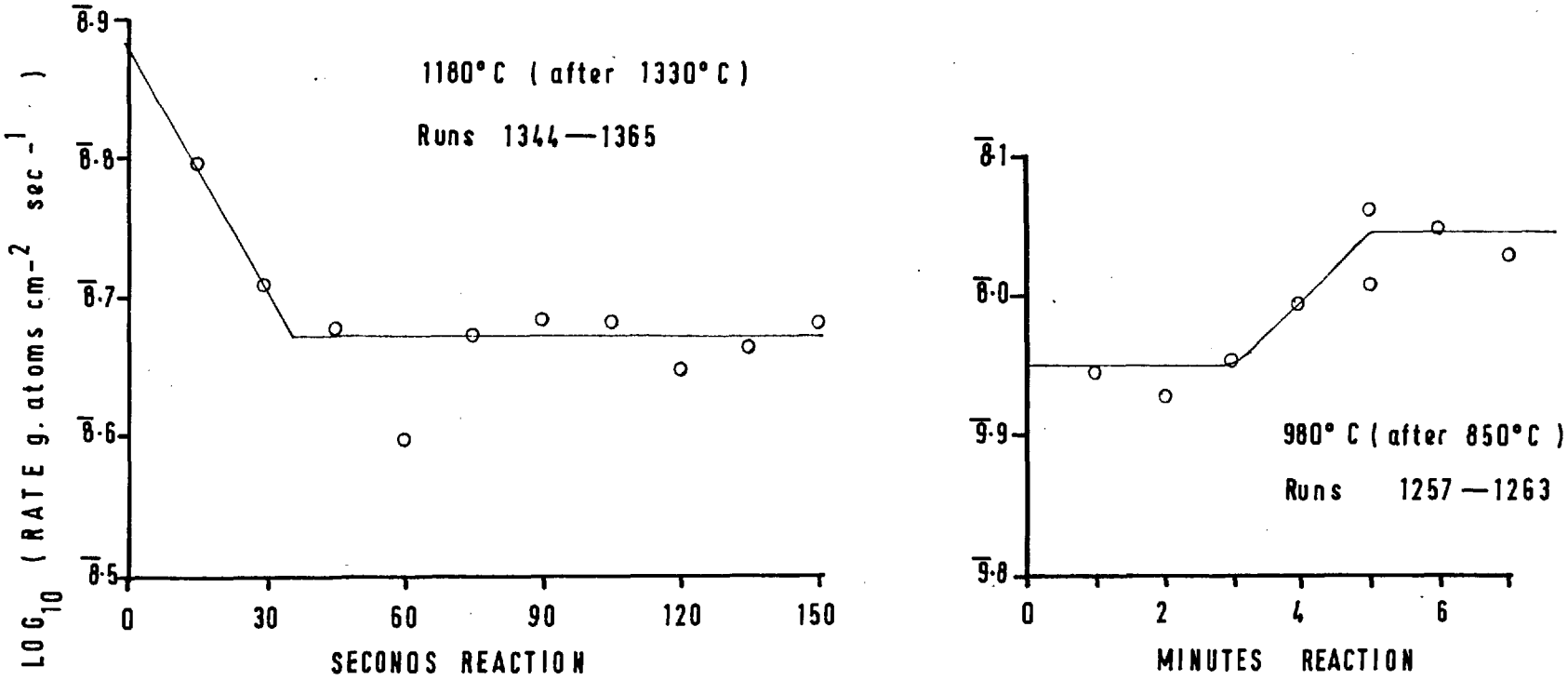

APPENDIX 6.2. Calculation of experimental fundamental rate r

1. Method of calculating rate from Duval's Results[3].

Duval's results were in terms of F , where

$$F = \frac{\text{oxygen reacted}}{\text{oxygen striking surface}} \quad \text{units in } cm^2 \text{ and } \mu m\ Hg$$

$$= \frac{\text{oxygen reacted}}{3.5 \times 10^{-2} P}$$

Assuming each oxygen gives 2CO i.e. no CO_2 formed

$$CO \text{ formed} = 2F \times 3.5 \times 10^{-2} P\ cm^{-2}\ min^{-1}$$

$$= 1.17\ F.P \times 10^{-3} \text{ gr moles/cm}^2 \text{ sec.}$$

$$= g \text{ atoms of carbon reacted/cm}^2 \text{ sec.}$$

The results given by Duval for the variation of F with ^{o}K for graphitised filaments were between 0.6 and 0.7μ. For the purposes of comparison with the Nagle theory, F was taken to be the same at 0.76μ.

Calculation of r.

$$R = rn'^{r} \quad \text{where } n' = n/N.$$

For 0.76μ $n_{1200} = 0.951N$ where N is a constant, see section 6.3. The values of F are obtained from Duval's results for graphitised filaments, Ref(3), Fig.8 as are the values of n/n_{1200}. (Fig.17).

For 50μ n/N, i.e. n', is obtained from Table A.6.5. In fact here the calculated values of n/N are used but as can be seen in Table A.6.5 and on Graph 6.4 these values are very close to the experimental values.

The calculations relevant to this section are shown in Table A.6.2.

Table A.6.1.

$T^{\circ}C$ reaction	$T^{\circ}C$ reaction	$Log_{10}R$ initial	$Log_{10}R$ final	$Log_{10} n_{T_2}/n_{T_1}$	$Log_{10} n_{T_2}/n_{950^{\circ}C}$
980	850	$\bar{9}.950$	$\bar{8}.046$	0.096	0.096
1225	980	$\bar{8}.415$	$\bar{8}.650$	0.235	0.331
1290	1225	$\bar{8}.600$	$\bar{8}.710$	0.110	0.441
1440	1290	$\bar{8}.590$	$\bar{8}.695$	0.105	0.546
1500	1440	$\bar{8}.592$	$\bar{8}.654$	0.062	0.608
1550	1500	$\bar{8}.520$	$\bar{8}.562$	0.042	0.650
1720	1550	$\bar{8}.530$	$\bar{8}.485$	-0.045	0.650
1850	1720	$\bar{8}.520$	$\bar{8}.427$	-0.093	0.512
1660	1850	$\bar{8}.350$	$\bar{8}.533$	0.183	0.695
1520	1660	$\bar{8}.775$	$\bar{8}.622$	-0.153	0.542
1330	1520	$\bar{8}.883$	$\bar{8}.703$	-0.180	0.362
1180	1330	$\bar{8}.882$	$\bar{8}.673$	-0.209	0.151

$T^{\circ}K$	$\ln_e n/n_{1150}$ from Graph 6.1
1150	0
1200	0.058
1300	0.207
1400	0.426
1500	0.737
1600	1.036
1700	1.324
1800	1.497
1900	1.554
2000	1.451
2100	1.267
2200	1.059

Table A.6.2. Calculation of r. At 0.76μ

^{o}K	$Fx10^{4}$	$Rx10^{10}$	$Log_{10}R$	$Log_{10}\ n_{1200}/n$	Log_{10} N/n	$Log_{10}R\ \frac{N}{n}$ $=log_{10}r$
1100	1.65	1.47	$\bar{1}\bar{0}.167$	0		
1200	5.8	5.16	$\bar{1}\bar{0}.713$	0	-0.022	$\bar{1}\bar{0}.691$
1300	7.45	6.62	$\bar{1}\bar{0}.821$	0.075	0.055	$\bar{1}\bar{0}.876$
1400	7.45	6.62	$\bar{1}\bar{0}.821$	0.195	0.173	$\bar{1}\bar{0}.994$
1500	4.05	3.60	$\bar{1}\bar{0}.556$	0.355	0.333	$\bar{1}\bar{0}.889$
1600	2.65	2.36	$\bar{1}\bar{0}.373$	0.55	0.528	$\bar{1}\bar{0}.901$
1700	2.25	2.00	$\bar{1}\bar{0}.301$	0.775	0.752	$\bar{9}.053$
1800	1.9	1.69	$\bar{1}\bar{0}.228$	1.05	0.928	$\bar{9}.156$
1900	1.65	1.47	$\bar{1}\bar{0}.167$	1.195	1.172	$\bar{9}.339$
2000	1.5	1.34	$\bar{1}\bar{0}.127$	1.30	1.278	$\bar{9}.405$

At 50 μ

^{o}K	$Rx10^{8}$	$Log_{10}R$	n/N	$r = R.N/n\ x10^{9}$	$Log_{10}r$
1150	0.30	$\bar{9}.477$	1.479	2.03	$\bar{9}.307$
1200	0.70	$\bar{9}.845$	1.575	4.44	$\bar{9}.648$
1300	1.7	$\bar{8}.230$	1.848	9.20	$\bar{9}.964$
1400	3.1	$\bar{8}.491$	2.217	14.0	$\bar{8}.146$
1500	4.7	$\bar{8}.672$	2.833	16.6	$\bar{8}.220$
1600	5.27	$\bar{8}.723$	3.610	14.6	$\bar{8}.164$
1700	5.15	$\bar{8}.712$	4.808	10.7	$\bar{8}.030$
1800	4.05	$\bar{8}.607$	6.329	6.40	$\bar{9}.806$
1900	3.47	$\bar{8}.540$	8.000	4.34	$\bar{9}.637$
2000	3.10	$\bar{8}.491$	7.246	4.28	$\bar{9}.631$
2100	2.70	$\bar{8}.431$	5.000	5.40	$\bar{9}.732$
2200	2.30	$\bar{8}.362$	3.413	6.74	$\bar{9}.829$

APPENDIX 6.3. Calculauion of Nagle-Strickland-Constable Theory.

From Section 2

$$\text{Rate} = \frac{k_A P}{1+k_Z P} x + k_B P(1-x) \text{ gr atoms/cm}^2 \text{ sec}$$

$$\text{where} \quad x = \frac{1}{1+K_T/(K_B P)}$$

Using the constants calculated by Nagle[14] namely

$$K_A = 20 \exp [-30,000/RT]$$

$$K_B = 0.0046 \exp [-15,200/RT]$$

$$K_T = 1.51 \times 10^5 \exp [-97,000/RT]$$

$$K_Z = 21.3 \exp [+4100/RT]$$

the calculated values of $\text{Log}_{10}R$ at 0.76 and 50μ are shown in Table A.6.3.

Table A.6.3. Calculation of R from Nagle-Strickland Constable Theory.

at 0.76μ

^{o}K	K_T/K_BP)	x	K_APxx10^{10}	K_Bx10^5	$K_B(1-x)$ P $x10^{11}$	$Rx10^{10}$	$\log_{10}R$
1200	0.044	0.967	0.732	-	-	0.73	$\bar{1}\bar{1}$.863
1300	0.479	0.690	1.10	1.2	0.37	1.1	$\bar{1}\bar{0}$.041
1400	4.68	0.176	1.27	1.8	1.48	1.43	$\bar{1}\bar{0}$.155
1500	33.9	0.029	0.269	2.7	2.62	0.53	$\bar{1}\bar{1}$.724
1600	19.0	0.005	0.090	3.8	3.74	0.46	$\bar{1}\bar{1}$.663
1700	871	0.001	0.003	5	5	0.5	$\bar{1}\bar{1}$.699
1800	-		0	8	8	0.8	$\bar{1}\bar{1}$.903
1900	-		0	12	12	1.2	$\bar{1}\bar{0}$.079
2000	-		0	16	16	1.6	$\bar{1}\bar{0}$.207

at 50μ.

^{o}K	K_t/K_BP	x	K_ZPx10^3	$\frac{K_AP}{1+K_ZP}$	$K_BP(1-x)$	$Rx10^9$	$Log_{10}R$
1200	0	1	8	4.70	0	4.7	$\bar{9}$.672
1300	0.008	0.995	7	19.8	0	19.8	$\bar{8}$.297
1400	0.074	0.931	6	41.9	0.08	42.0	$\bar{8}$.633
1500	0.527	0.651	6	37.7	0.62	38.3	$\bar{8}$.583
1600	2.75	0.267	5	29.0	1.69	30.7	$\bar{8}$.487
1700	13.8	0.068	5	12.8	3.07	15.9	$\bar{8}$.201
1900	138	0.007	4	3.43	5.24	5.7	$\bar{9}$.756
2100	1445	0.001	4	1.01	7.9	8.9	$\bar{9}$.949
2300			3	0	10.6	10.6	$\bar{8}$.025

A.6.4. Calculation of Constants for proposed Hystereis Theory.

Table A.6.4. Calculations for Sections 6.3.5.

Calculation of K_5

T^oK	$1/Tx10^4$	$e^{-\frac{1.67x10^4}{T}}$	$9.0x10^4 e^{-\frac{0.76\mu}{(\ )}}$	$1.36x10^3 e^{-\frac{50\mu}{(\ )}}$
1150	8.696	$4.80\ x10^{-7}$		$6.53\ x10^{-4}$
1200	8.333	$8.83\ x10^{-7}$	$7.95\ x10^{-2}$	$1.20\ x10^{-3}$
1300	7.692	$2.57\ x10^{-6}$	$2.31\ x10^{-1}$	3.49
1400	7.143	6.46	$5.81\ x10^{-1}$	8.79
1500	6.617	$1.56\ x10^{-5}$	1.40	$2.12\ x10^{-2}$
1600	6.250	2.87	2.58	3.90
1700	5.882	5.27	4.74	7.17
1800	5.556	9.14	8.23	$1.24\ x10^{-1}$
1900	5.263	$1.51\ x10^{-4}$	13.59	2.05
2000	5.000	2.34	21.1	3.18
2100	4.762	3.53	-	4.80
2200	4.545	5.02	-	6.83

Calculation of K_4

T^oK	$e^{-\frac{0.35x10^4}{T}}$	$2.38\ e^{-\frac{0.76\mu}{(\ )}}$	$6.8\ e^{-\frac{50\mu}{(\ )}}$
1150	$4.78\ x10^{-2}$		0.325
1200	5.39	$1.28\ x10^{-1}$	0.366
1300	6.79	1.62	0.462
1400	8.21	1.95	0.558
1500	9.83	2.34	0.668
1600	$1.12\ x10^{-1}$	2.66	0.762
1700	1.27	3.02	0.864
1800	1.42	3.38	0.966
1900	1.59	3.78	1.08
2000	1.74	4.14	1.18
2100	1.88	-	1.28
2200	2.04	-	1.39

Table A.6.4 (continued)

50μ	= 6.6×10^{-5} atm	$(6.6 \times 10^{-5})^{0.25}$	= 9.014×10^{-2}
0.76μ	= 10^{-1} atm.	$(10^{-6})^{0.25}$	3.162×10^{-2}

Table A.6.5. Calculation of n/n_{ref} at 50μ. Graph 6.4.

$T^{\circ}K$	$(1+K_5/P-K_4P^{0.25})$	$\frac{(\quad)1150}{(\quad)}$	$\frac{(\quad)1150}{(\quad)}$	ln n/n_{1150} exptl.
1150	0.676	1.000	0	0
1200	0.635	1.065	0.063	0.058
1300	0.541	1.249	0.223	0.207
1400	0.451	1.500	0.405	0.426
1500	0.353	1.915	0.650	0.737
1600	0.277	2.440	0.892	1.036
1700	0.208	3.250	1.179	1.324
1800	0.158	4.278	1.453	1.497
1900	0.125	5.408	1.690	1.554
2000	0.138	4.893	1.589	1.451
2100	0.200	3.380	1.218	1.267
2200	0.293	2.307	0.837	1.059

Experimental values from Appendix 6.1.

Table A.6.6. Calculation of n/n_{ref} at 0.76μ. Graph 6.5.

$T^{\circ}K$	$(1+K_5/P-K_4P^{0.25})$	$\frac{(\quad)1200}{(\quad)T}$	$-\ln\frac{(\quad)}{(\quad)T}$	$-\ln n/n_{1200}$ experimental
1200	0.951	1.000	0	0
1300	1.069	0.890	0.116	0.173
1400	1.386	0.686	0.377	0.449
1500	2.166	0.439	0.823	0.819
1600	3.314	0.287	1.248	1.267
1700	5.438	0.175	1.743	1.785
1800	8.892	0.107	2.345	2.418
1900	14.21	0.067	2.703	2.752
2000	21.69	0.044	3.120	2.994

$\ln n/n_{1200}$ experimental from Duval Ref. (3) Fig 17.

Table A.6.7. Non equilibrium results for reaction at 1700°K after 1200°K at 0.76μ.

$Log_{10}(F-F_1)$ data, and $F_1 = 2.3 \times 10^{-4}$ from Duval[3] Fig.12.

t secs.	$Log_{10}(F-F_1)$	$F \times 10^3$	$F/F_1 = n/n_\infty$
0	$\bar{3}.775$	9.26	4.026
20	$\bar{3}.600$	6.28	2.730
40	$\bar{3}.300$	4.29	1.865
60	$\bar{3}.030$	3.37	1.465
80	$\bar{4}.687$	2.79	1.212
110	$\bar{4}.375$	2.54	1.103
140	$\bar{4}.200$	2.46	1.067

Steady value F_1 only reached after several minutes [3].

Using $\theta = 3.0 \times 10^{-2}$ and $n_o/n_\infty = 4.026$

Equation 13 becomes $n/n_\infty = 1 + 3.026\ e^{-3.0 \times 10^{-2} t}$

t secs	$e^{-\theta t}$	$3.026\ e^{-\theta t}$	n/n_∞ calc.
0	1.000	3.026	4.026
20	0.549	1.661	2.661
40	0.301	0.911	1.911
60	0.165	0.500	1.500
80	0.091	0.274	1.274
110	0.037	0.112	1.112
140	0.015	0.045	1.045

Table A.6.8. Non equilibrium results for reaction at 1508°K after 1153°K at 50μ.

Run No.	t secs.	R x10^8	$r/R_{final} = n/n_\infty$
Graph	0	1.97	0.438
1264	15	2.74	0.609
1265	30	3.88	0.862
1266	45	4.47	0.993
1267	60	4.20	0.933
1268	75	4.38	0.973
1269	90	4.65	1
1270	105	4.52	1
1271	120	4.52	1

R_{final} also from Graph 4.15 = 4.50 x10^{-8}

Using $\theta = 3.48 \times 10^{-2}$ and $n_o/n_\infty = 0.438$

Equation 13 becomes $n/n_\infty = 1 - 0.562^{-3.48 \times 10^{-2}t}$

t secs.	$e^{-\theta t}$	$0.562\ e^{-\theta t}$	n/n_∞ calc.
0	1.000	0.562	0.438
15	0.594	0.333	0.667
30	0.353	0.198	0.802
45	0.208	0.117	0.883
60	0.124	0.070	0.930
75	0.073	0.041	0.959
90	0.044	0.024	0.976
105	0.026	0.015	0.986
120	0.015	0.008	0.992

APPENDIX 6.5. CALCULATION OF NUMBER OF CARBON ATOMS ON FILAMENT SURFACE.

Considering a hexagonal graphite ring :-

Assuming the intermolecular C-C bond distance is 1.415 $\mathring{A}$ [85]

The area of the hexagonal ring = $3/2\ (2.451 \quad 1.415)\ \mathring{A}^2$

$= 5.202\ \mathring{A}^2$

If for this approximation the surface is considered a perfect network with very few edge atoms, and therefore the number of atoms shared for each ring is 6, giving 3 atoms per ring for the equivalent area

$\therefore$ Area associated with each atom = $1/3 \times 5.202\ \mathring{A}^2$

$\therefore$ No. of atoms per cm^2 = $3/5.202 \times 10^{16}$

$= \underline{5.767 \times 10^{15}} = N$

Using Avagadro's number = no. of atoms per gr atom = 6.02×10^{23}

No. of gr. atoms per cm^2 = $\dfrac{5.767 \times 10^{15}}{6.023 \times 10^{23}} = 9.6 \times 10^{-9}$

$\therefore$ <u>No. of gr atoms per cm^2 = 10^{-8}</u> of actual carbon surface.

REFERENCES.

1 Berkowitz-Mattuch,J.B; Büchler,A; Engelke,J.L; and Goldstein,S.N. J. Chem. Phys. 39 2722 (1963)

2. Strickland-Constable,R.F. Trans. Far. Soc. 40 333 (1944)

3. Duval,X. Ann. de Chimie. 10 903 (1955)

4. Langmuir,L. J. Am. Chem. Soc. 37 1139 (1915)

5. Martin,H; & Meyer,L. Zeit für Electrochem. 41 136 (1935)

6. Meyer,L. Zeit. für Chem. 17 385 (1932)

7. Meyer,L. Trans. Far. Soc. 34 1056 (1938)

8. Meyer,L. J. Chim. Phys. 47 328 (1950)

9. Eucken,A. Zeit für Angew. Chem. 43 987 (1930)

10. Arthur,J.R; & Bowring,J.R. J. Chem. Soc. 1949 (1951)

11. Strickland-Constable,R.F. Trans. Far. Soc. 43 769 (1947)

12. Boulangier,F; Duval,X; & Letort,M. Proc. 3rd Carb. Conf. 257 (1959)

13. Rosner,D.E; & Allendorf,H.D. Carbon 3 153 (1965)

14. Nagle,J; & Strickland-Constable,R.F. Proc. 5th Carb. Conf. 1 154 (1962)

15. Walls,J.R. Ph.D. Thesis London (1964)

16. Evans,T; & Phaal,C. Proc. 5th Carb. Conf. 1 147 (1962)

17. Meyer,L; & Gomer,G. Proc. 3rd Carb. Conf. 425 (1959)

18. Strickland-Constable,R.F. D.Phil. Thesis. Oxford

19. Bonnetain,L; Duval,X; & Letort,M. Proc. 4th Carb. Conf. 107 (1960)

20. Blyholder,G;Binford,J.S; & Eyring,H. J. Phys. Chem. 62 263 (1958)

21. Strickland-Constable,R.F. 2nd. Ind. Carb. Conf. London (1965)

22. Antonowicz,K. Proc. 5th Carb. Conf. 1 46 (1962)

23. Polley,M.H; Schaffer,W.D; & Smith,W.R. J. Phys. Chem. 57 469 (1953)

24. Mizushima,S. Proc. 4th Carb. Conf. 417 (1960)

25. Mizushima,S. Proc. 5th Carb. Conf. 2 439 (1963)

26. Ong,J. Carbon 2 281 (1964)
27. Long,F.J; & Sykes,K.W. Proc. Roy. Soc. 193A 377 (1948)
28. Hennig,G.R. J. Chim. Phys. 58 12 (1961)
29. Deitz,N.R; & McFarlane,E.F. Proc. 5th Carb. Conf. 2 219 (1963)
30. Laine,N.R; Vastola,F.J; & Walker,P.L. Proc. 5th Carb. Conf. 2 211 (1964)
31. Duval,X. J. Chim. Phys. 58 3 (1961)
32. Bonnetain,L. J. Chim. Phys. 56 486 (1959)
33. Heuchamps,C; Duval,X; & Letort,M. Compt. Rendu. 260 1160 (1965)
34. Hoyant,C; Duval,X; & Letort,M. Compt. Rendu. 259 2827 (1964)
35. Diefendorf,R.J. Proc. 4th Carb. Conf. 489 (1960)
36. Nagle,J. Ph.D. Thesis London (1961)
37. Heuchamps,C; & Duval,X. Carbon 4 243 (1961)
38. Hedden,K; & Wicke,E. Proc. 3rd Carb. Conf. 249 (1959)
39. Pallmer,P.G. Carbon 4 145 (1966)
40. Blackman,L.C.F. Carbon 5 196 (1967)
41. Lewis,J.C. 2nd. Ind. Carb. Conf. London (1965)
42. Hennig,G.R. Proc. 3rd Carb. Conf. 265 (1959)
43. Hennig,G.R. Proc. 5th Carb. Conf. 1 143 (1962)
44. Hennig,G.R; & Kanter,M.A. Proc. 4th Carb. Conf. 141 (1960)
45. Williamson,G.K; & Baker,C. Proc. 5th Carb. Conf. 2 521 (1963)
46. Follett,E.A.C. Carbon 1 329 (1964)
47. Antonowicz,K. J. Chem. Phys. 36 2046 (1962)
48. Harker,H; Jackson,C; & Wynne Jones,W.F.K. Proc. Roy. Soc. A262 328 (1961)
49. Harker,H; Gallager,J.T; & Parker,A. Carbon 4 401 (1966)
50. Mrozowski,S; & Andrew, J.F. Proc. 4th Carb. Conf. 207 (1959)
51. Mrozowski,S; Proc. 5th Carb. Conf. 2 79 (1963)
52. Antonowicz,K. J. Chem. Phys. 37 204 (1962)

53. Yokozawa,Y. J. Chem. Phys. 37 204 (1962)
54. Vastola,F.J; Hart,P.J; & Walker,P.L. Carbon 2 65 (1964)
55. Hart,P.J; Vastola,F.J; & Walker,P.L. Carbon 5 303 (1967)
56. Redmand,J.P; & Walker,P.L. J. Phys. Chem. 64 1093 (1960)
57. Long,F.J; & Sykes,K.W. Proc. Roy. Soc. A215 (1952)
58. Long,F.J; & Sykes,K.W. J. Chim. Phys. 47 361 (1950)
59. Hauffe,K. Adv. in Catalysis 7 218 (1957)
60. Heintz,E.A; & Parker,W.E. Carbon 4 473 (1966)
61. Rakszawski,J.F; & Parker,W.E. Carbon 2 53 (1964)
62. Berkmann,S; Morrell,J.C; & Egloff,G. Catalysis
63. Volkenstein,F.F. Electronic Theory of Catalysis on Semiconductors. Pergammon Press 1963
64. Baker,M.McD; & Jenkins,G.I. Adv. in Catalysis 7 (1957)
65. Thomas,J.M; & Thomas,W.J. Introduction to Principles of Heterogeneous Catalysis. Pergammon Press 1967
66. AMarglio,H; & Duval,X. Carbon 4 323 (1966)
67. Toplim et al. Adv. in Catalysis 5 217 (1953)
68. Thomas,J.M; & Roscoe,C. 2nd. Ind. Carb. Conf. London (1965)
69. Hennig,G.R. Proc. 4th Carb. Conf. 145 (1960)
70. Hennig,G.R. J. Inorg. Nucl. Chem. 24 1129 (1962)
71. Mukeibo,T; & Yamauchi. Carbon 3 87 1965)
72. Rakszawski,J.F; Rusinko,F; &Walker,P.L. Proc. 5th Carb. Conf. 2 243 (1963)
73. Gallagher,J.T; & Harker,A. Carbon 2 163 (1964)
74. Madley,D.G; & Strickland- Constable,R.F. Analysis 78 122 (1953)
75. Diefendorf,R.J. J. Chim. Phys. 57 815 (1960)
76. Nishiyana,Z. Zeit für Physick 71 600 (1931)
77. Holland,L. Vacuum Deposition of Thin Films. Chapmann and Hall London 1958
78. Schissel,P.O; & Trulson,O.C. J. Chem. Phys. 43 737 (1965)
79. Busso,R.H. J. Chim. Phys. 47 533 (1950)
80. Feldman,M. J. Appl. Phys. 23 1200 (1952)

81. Dienes,G.J. J. Appl. Phys. 23 1194 (1952)
82. Taylor,H.H; & Thon,T. J. Am. Chem. Soc. 74 4169 (1952)
83. Shivonen,V. Trans. Far. Soc. 34 1062 (1938)
84. Pacault,A. J. Chim. Phys. 57 892 (1960)
85. Ubbelohde,A.R; & Lewis,F.A. Graphite and its crystal compounds. Clarendon Press. 1960
86. Boudart,M. J. Am. Chem. Soc. 74 1531 (1952)
87. Hennig,G.R; & Smaller,C. Proc. 2nd Carb. Conf. 113 (1955)
88. Goldstein,E.M; Carter,E.W; Kluz,S. Carbon 4 273 (1966)
89. Libowitz,G.G. Progress in Solid State Chemistry. Vol 2 Pergammon Press. (1965)
90. Harker,H. Proc. 4th Carb. Conf. 125 (1959)
91. Kubaschewski,O; & Evans,E.LL. Metallurgic Thermochemistry. Pergammon Press. (1958)
92. Wicks,C.E; & Block,F.E. U.S. Bureau of Mines Bulletin 605
93. Schick,H.L. Thermodynamics of certain refractory compds. Vol.2 Academic Press (1966)
94. Remy,L. Treatise on Inorganic Chemistry. Longmanns. 1964.
95. Bangham,D.H. J. Chim. Phys. (Disc.) 47 327 (1950)
96. Horton,W.S. Proc. 5th Carb. Conf. 2 233 (1963)
97. Tuddenham,W.M; & Hill,G.R. Ind. Eng. Chem. 47 2129 (1955)